Surface
Science Western

CONTRACT REPORT NUMBER 79037-01-SS
REQUISITION NUMBER 23440-7-9037
CONTRACTOR: University of Western Ontario

ION PROBE MICROANALYSIS OF GOLD IN COMMON SULPHIDE MINERALS AND IMPLICATIONS FOR ENHANCED RECOVERY FROM REFRACTORY GOLD ORES (UP-W6-015)

(DSS FILE # 50SS.23440-7-9037)

A Research Report prepared for:

CANMET- MSL Division
Energy Mines and Resources Canada
555 Booth Street
Ottawa Ontario
K1A 0G1

Attn: Dr. Louis J. Cabri
Scientific Authority

by:

Stephen L. Chryssoulis
Principal Investigator
Process Mineralogy
Surface Science Western
University of Western Ontario
London, Ontario N6A 5B7.

319 pp

SSW/PMS/89/10

MICROMEDIA

April 30 1989

PREFACE

The existence of chemically bound gold in sulphides has been debated since the early work of Burg (1935) who introduced the term **invisible gold** to characterize both solid solution and colloidal-size gold. Since then, numerous studies have been performed both on synthetic and natural sulphides, without being able to confirm beyond any doubt the presence of chemically bound gold in the sulphide structure. Of note is the ^{195}Au Mössbauer spectroscopy study by Wagner et al. (1986) which was the first technique to prove the presence of chemically bound gold in sulphides. However, this technique is bulk in nature and the minimum detection limit is high (200 g/t).

Ion probe microanalysis, or secondary ion mass spectrometry (SIMS) is a sensitive microbeam technique enabling the analysis of indiviual sulphide grains with a minimum detection limit of 0.5 ppm or better per mineral grain. Therefore, it is the ideal tool to solve the long standing problem on the presence of invisible gold.

The present report is the result of a collective effort to demonstrate in a quantitative way, the presence of invisible gold in sulphides from several Canadian refractory gold ores, as well as in the copper anodes from the four Canadian refineries. With the exception of the introductory chapter, each chapter corresponds to an individual report to the corresponding mining company. Therefore, some repetition was unavoidable.

In presenting the material, it was decided to emphasize the metallurgical implications in each case, since the aim of the study was also to demonstrate the potential in optimizing gold recoveries by characterizing the distribution and association of the refractory gold.

The completion of this work would have been impossible without the help and encouragement of many friends and colleagues. Although they can not all be mentioned here, they are none the less remembered and thanked for their kindness. Special thanks are due to my co-investigator Dr. N.J. Cook. Messers C. Weisener and G. Mount assisted with the operation of the ion microprobe. Dr. N.S. McIntyre and Mr. R. Davidson made every possible effort to provide instrument time and review parts of the report in draught form. Valuable critical comments were made by Dr. J.D. Scott (Kidd Creek), Mr. J. Toohey (Canamax) and Mrs. M. Sizgoric (INCO), who reviewed respective parts of the report. Mr. D. Ferguson assisted in the preparation of the diagrams and the final typing of the manuscript.

Financial support for this study was made possible through CANMET, the GSC and the participating mining companies. The support of Mr. L.L. Sirois, Director of MSL; Dr. F.R. Campbell, Manager of MPL, Mr. M.C. Campbell, Manager of EML, all at CANMET,

and of Dr. A.G. Plant at the GSC is acknowledged. The insight, contribution of information and encouragement from the mining industry personnel involved, is greatly appreciated.

Finally, I am most thankfull to Dr. L.J. Cabri, the scientific authority on this project, for his continuous encouragement and support, throughout this study and his joyful way of looking at things even when they are bleak.

LIST OF CONTENTS PAGE

CHAPTER 1 **ION PROBE MICROANALYSIS OF SULPHIDE MINERALS** 1

1.1.0 Introduction 8

1.2.0 Methodology 10
1.2.1 Sampling 10
1.2.1.1 Sample Preparation 10
1.2.2 Microscopy 12
1.2.2.1 Image analysis 12
1.2.3 Chemical Assays 17
1.2.4 Cyanide Leach Testing 17
1.2.5 Scanning Electron Microscopy (SEM) and Electron Probe Microanalysis (EPMA) 17
1.2.6 Ion probe microanalysis 18
1.2.6.1 Methodology 18
1.2.6.2 Standardization 18
1.2.6.3 Accuracy 28
1.2.6.4 Precision 28

CASE STUDIES

CHAPTER 2 **DETERMINATION OF INVISIBLE GOLD WITHIN SULPHIDE MINERALS IN FLOTATION TAILINGS FROM TROUT LAKE MINE, MANITOBA.**
Hudson Bay Mining and Smelting Company Ltd. 30

2.1.0 Introduction 34

2.2.0 Methodology 36

2.3.0 Results 36
2.3.1 Chemical assays 36
2.3.2 Mineralogy 36
2.3.3 Invisible gold 38
2.3.4 Cyanidation tests 42

2.4.0 Discussion 42

2.5.0 Conclusions 44

CHAPTER 3 **DIRECT DETERMINATION OF THE INVISIBLE GOLD CONTENT OF PYRITE AND IMPLICATIONS ON THE CYANIDATION OF THE AUDREY RESOURCES TAILINGS.**
Ressources Audrey Inc. 64

3.1.0 Introduction 68

3.2.0 **Methodology** 68

3.3.0 **Results** 69

3.3.1 Chemical assays 69
3.3.2 Mineralogy of ore samples 69
3.3.3 Mineralogy of tailings 73

3.4.0 **Discussion** 79

3.5.0 **Conclusions** 79

CHAPTER 4 **DIRECT DETERMINATION OF INVISIBLE GOLD IN THE ELMTREE COMPOSITE ORE #1. IMPLICATIONS FOR GOLD RECOVERY FROM OXIDISED AND NON-OXIDISED ORES.**
Lacana Mining Corporation. 86

4.1.0 **Introduction** 90

4.2.0 **Methodology** 91

4.3.0 **Results** 92
4.3.1 Chemical assays 92
4.3.2 Mineralogy of ore samples 92
4.3.3 Mineralogy of composite ore #1 92

4.4.0 **Discussion** 100

4.5.0 **Conclusions** 104

CHAPTER 5 **DETERMINATION OF THE MINERALOGICAL DISTRIBUTION OF GOLD IN A COMPOSITE ORE FROM THE HOWARD ZONE, CONGRESS MINE, B.C.**
Levon Resources Ltd. 111

5.1.0 **Introduction** 116

5.2.0 **Methodology** 117

5.3.0 **Results** 117
5.3.1 Chemical assays 117
5.3.2 Mineralogy 119
5.3.3 Invisible gold 122

5.4.0 **Discussion** 126

5.5.0 **Conclusions** 127

CHAPTER 6 **DETERMINATION OF THE DISTRIBUTION OF GOLD IN THE LARA DEPOSIT, VANCOUVER ISLAND, B.C.**
Abermin Corporation. 129

6.1.0 **Introduction** 131

6.2.0 **Methodology** 131

6.3.0 Results 132
6.3.1 Chemical assays 132
6.3.2 Mineralogy of ores 135
6.3.2.1 Visible gold 136
6.3.2.2 Invisible gold 145

6.4.0 Discussion 149

6.5.0 Conclusions 152

CHAPTER 7 GOLD MINERALOGICAL DISTRIBUTION IN COMPOSITES CBE-QP-1 AND CBW-87-1 FROM THE GOLDEN POND PROPERTY, QUEBEC.
INCO Gold Ltd. 156

7.1.0 Introduction 161

7.2.0 Methodology 161

7.3.0 Results 163
7.3.1 Chemical assays 163
7.3.2 Mineralogy 163
7.3.2.1 Sulphide minerals 163
7.3.2.2 Visible gold 165
7.3.2.3 Invisible gold 165

7.4.0 Discussion 168

7.5.0 Conclusions 172

CHAPTER 8 DETERMINATION OF INVISIBLE GOLD IN FLOTATION PRODUCTS AND FOUR ORE TYPES FROM THE HW MINE, B.C.
Westmin Resources Ltd. 179

8.1.0 Introduction 184

8.2.0 Methodology 184

8.3.0 Results 186
8.3.1 Chemical assays 186
8.3.2 Mineralogy of ores and millfeed 186
8.3.2.1 Bornite-rich ores 190
8.3.3 Mineralogy of products 194
8.3.3.1 Zinc concentrate 194
8.3.3.2 Copper concentrate 194
8.3.4 Invisible gold 199
8.3.5 Diagnostic cyanidation tests 202
8.3.6 Normative mineralogy and image analysis 207

8.4.0 Discussion 207

8.5.0 Conclusions 209

CHAPTER 9 DETERMINATION OF INVISIBLE GOLD IN SULPHIDE MINERALS FROM THE ESTRADES DEPOSIT, QUEBEC. Teck Corporation. 224

9.1.0 Introduction 228

9.2.0 Methodology 228

9.3.0 Results 230
9.3.1 Chemical assays 230
9.3.2 Mineralogy 230
9.3.2.1 Sulphide mineralogy 230
9.3.2.2 Gold mineralogy 234

9.4.0 Discussion 238

9.5.0 Conclusions 241

CHAPTER 10 DIRECT DETERMINATION OF THE INVISIBLE GOLD AND COMPLETE GOLD MINERALOGICAL DISTRIBUTION IN THE MASSIVE SULPHIDE ORE FROM KETZA RIVER (Y.T.) CANAMAX Resources Inc. 247

10.1.0 Introduction 251

10.2.0 Methodology 252

10.3.0 Results 252
10.3.1 Visible gold 252
10.3.2 Invisible gold 255

10.4.0 Discussion 261

10.5.0 Conclusions 268

CHAPTER 11 PROCESS MINERALOGICAL STUDY OF THE PEEL ZONE HIGH GRADE AND AB COMPOSITES AND THE LAB ZONE COMPOSITE FROM THE KETZA RIVER MINE, YUKON TERRITORIES. CANAMAX Resources Inc. 282

11.1.0 Introduction 291

11.2.0 Methodology 291

11.3.0 Results 293
11.3.1 Mineralogy 293
11.3.2 Visible gold 295
11.3.2.1 Peel zone high grade composite 295
11.3.2.2 Peel zone composite AB 300
11.3.2.3 LAB zone composite 302

11.4.0 Discussion 304

11.5.0 Conclusions 312

CHAPTER 12 QUANTIFICATION OF GOLD IN COPPER ANODES BY ION PROBE MICROANALYSIS 339

12.1.0 **Introduction** 341

12.2.0 **Methodology** 341
12.2.1 Sample procurement and prparation 341
12.2.2 Analytical 342
12.2.2.1 Standardization 342

12.3.0 **Results** 342

12.4.0 **Discussion** 347

12.5.0 **Conclusions** 352

CONCLUSIONS 368

REFERENCES 369

CHAPTER 1

ION PROBE MICROANALYSIS OF SULPHIDE MINERALS

SUMMARY

Ion probe microanalysis was used to quantify the 'invisible' gold concentration in common sulphide, sulpharsenide and sulphantimonide minerals. The minimum detection limit (3σ) for gold in pyrite is 0.3 ppm and in arsenopyrite 0.2 ppm. Internal and external standardization were both used to quantify the results. With internal standardization, the accuracy at the one part per million (weight) concentration level is better than 15% and the precision is 20%. With external standardization however, results may be less accurate due to matrix effects or charging. Invisible gold may occur either in solid solution or within the crystal structure as a colloidal dispersion in the sulphide and sulpharsenide minerals. The in-depth profiling capability of the ion microprobe enables the discrimination of colloidal gold down to 100-200 Å in size, depending on operating conditions and the matrix analysed. Differentiation of finer colloidal gold would require high resolution transmission electron microscopy.

In the ten refractory, or partially refractory gold ores investigated, the invisible gold concentrates preferentially in the arsenopyrite, where it reaches its maximum concentration of 1.1 wt. %. The invisible gold concentration in pyrite only becomes significant beyond a threshold value of 0.7-1.0 wt. % arsenic. A positive correlation between gold and arsenic concentration has been documented for the arsenian pyrites. The following concentration ranges for 'invisible' gold in common sulphides and related minerals were determined: arsenopyrite <0.2 - 11,000 ppm; pyrite <0.3 - 104 ppm; pyrrhotite <0.3 - 1.8 ppm; marcasite <0.5 - 4.1 ppm; chalcopyrite <0.3 - 20 ppm; tetrahedrite-tennantite <0.2 - 78 ppm and galena <0.1 to 3.4 ppm.

Invisible gold in sulphides, sulpharsenides and sulphantimonides is not recoverable by direct cyanidation. Major sulphides in some gold deposits have been shown to carry invisible gold in minor amounts, but because of their abundance have accounted for the bulk of the refractory gold (Audrey, Ketza River). In other deposits the gold-carrier sulpharsenide, although a minor constituent of the ore, has accounted for most of the refractory gold because of its high gold concentration (Congress, Golden Pond, Estrades). In the Elmtree deposit, both the arsenian pyrite and arsenopyrite are equally accountable for the refractory fraction of gold. Determination of the invisible gold distribution, apart from permitting calculation of complete gold mineralogical balances, and establishing the maximum recoverable gold by direct cyanidation, also provides the neccessary information for the preconcentration of the invisible gold; information which cannot be obtained otherwise.

In the Golden Pond and the Congress deposits, the invisible gold concentration in the arsenopyrite is inversely related to crystal size. This is an important consideration to bear in mind when flotation is the favoured method of preconcentration.

Process mineralogical studies of refractory gold ores, integrated with diagnostic metallurgical testing have led to an improved understanding of the cause for their refractoriness. This, in turn, has given direction to metallurgical flowsheet development.

With the ion microprobe it was possible to detect and quantify the invisible gold concentration in anode samples from four Canadian copper refineries. The determined concentrations compare closely with published bulk analytical data. In the Kidd Creek anodes, it was determined that the gold concentration in the rim of the anode is significantly lower than in the core.

SOMMAIRE

La microanalyse par sonde ionique a été employé pour quantifier les concentrations d'or "invisible" dans des sulphures, sulpharséniures et sulphoantimoniures communs. Le seuil de détection (3σ) pour l'or dans la pyrite est de 0.3 ppm et de 0.2 ppm dans l'arsénopyrite. Des étalonnages interne et externe furent employés pour quantifier les résultats. Par étalonnage interne, le niveau d'exactitude pour une concentration d'une partie par million (en poids) est de 15% et le degré de précision est de 20%. Par étalonnage externe le degré de précision est comparable, toutefois les résultats peuvent être plus inexacts due à des effets de matrice ou de charge. L'or "invisible" peut se présenter soit en solution solide, à même la structure cristalline, ou en dispersion colloïdal dans les sulphures ou sulpharséniures. L'obtention de profil en profondeur avec la microsonde ionique rend possible la discrimination d'or colloïdal j'usqu'à une granulométrie de 100-200 Å, dépendant des conditions d'opération et de la matrice analysée. La différentiation de particules d'or colloïdal plus fines, requerrait une étude par microscope électronique à transmission à haute résolution.

Des dix minerais d'or réfractaires ou partiellement réfractaires étudiés, l'or "invisible" se concentre de préférence dans l'arsénopyrite, où il atteint une concentration maximale de 1.1% en poids. Le niveau de concentration d'or "invisible" dans la pyrite prend de l'importance à partir d'un seuil de 0.7 - 1.0% en poids d'arsenic. Une correlation positive entre la concentration en or et en arsenic a été documentée pour les pyrites arsénifères. Les variations de concentration suivantes en or "invisible" furent déterminées dans les sulphures communs: arsénopyrite, <0.2 - 11,000 ppm; pyrite, <0.3 - 104 ppm; pyrrhotite, <0.3 - 1.8 ppm; marcasite, <0.5 - 4.1 ppm; chalcopyrite, <0.3 - 20 ppm; tétrahédrite-tennantite, <0.2 - 78 ppm et la galène, <0.1 - 3.4 ppm.

L'or "invisible" présent dans les sulphures, sulpharséniures et sulphantimoniures n'est pas récupérable par cyanuration directe. Les sulphures principaux de certains gisements d'or ont démontrés contenir de l'or "invisible" en quantités mineures, mais vue leur abondance, ces minéraux renferment la majorité de l'or réfractaire (Audrey, Ketza). Dans d'autres gisements le sulpharséniure porteur-d'or, même s'il s'agit d'un constituent mineur du minerais, s'est montré responsable pour la plus grande partie de l'or réfractaire à cause justement de sa haute teneur en or (Congress, Golden Pond, Estrades). Pour ce qui est du gisement d'Elmtree, la pyrite arsénifère de même que l'arsénopyrite sont également responsables en ce qui concerne l'or réfractaire. La détermination de la distribution de l'or "invisible", en plus de permettre le calcul de balance minéralogique de l'or, et d'établir un rendement maximum de l'or récupérable par cyanuration directe, elle fournit également l'information nécessaire pour la préconcentration de l'or "invisible", information qui ne peut être obtenu autrement.

En ce qui concerne les gisements Golden Pond et Congress, la teneur d'or "invisible" dans l'arsénopyrite est inversement reliée à la dimension des cristaux. Il s'agit ici d'un point important si le procédé de flottation est considéré comme méthode de préconcentration.

Les études de traitements minéralogiques des minerais d'or réfractaire combinées à l'analyse de tests métallurgiques ont conduit à une meilleure compréhension sur le pourquoi de leur pouvoir réfractaire; ce qui en retour a conduit au dévelopement de schéma métallurgique.

La microsonde ionique a également permit de détecter et de quantifier la teneur de l'or "invisible" présent dans des échantillons d'anodes, de quatre raffineries canadiennes de cuivre. Les teneurs obtenues se comparent avantageusement avec les valeurs analytiques publiées. Il a également été possible de déterminer, pour les anodes de Kidd Creek, que la teneur en or à la bordure de l'anode est passablement moins élevée qu'en son centre.

LIST OF TABLES

Table 1 List of refractory gold ores studied.

Table 2 Reproducibility of image analysis of visible gold.

Table 3 Reproducibility of modal determination of mineral proportions.

Table 4 instrumental operating conditions for the ion microprobe.

Table 5 Accuracy of ion probe microanalysis.

LIST OF FIGURES

Figure 1 Reproducibility of visible gold concentration by image analysis.

Figure 2 Schematic diagram of the CAMECA IMS-3f ion microprobe.

Figure 3 Schematic diagram of the Pelletron heavy mass ion separator.

Figure 4 Schematic diagram of Faraday cup assembly.

Figure 5 Characteristic distribution of implanted gold ions with depth.

Figure 6 Backscattered electron image indicating the destructive character of ion probe microanalysis.

Figure 7 Diagram indicating depth of crater produced by ion probe microanalysis.

Figure 8 Calibration curve for external standardization.

1.1.0 Introduction

Many types of gold ores exist, differing in geological association, genetic environment and in mineralogy. An important type in Canada and elsewhere are sulphide-bearing where gold may be the only pay-metal being extracted or it is a by-product of base metal extraction. Commonly, gold occurs within these ores as discrete minerals, of which native gold and electrum are the most commonly encountered. In many ores, mineralogical determinations of the amount of gold present as these minerals is in close agreement with the amount of gold in the ore as determined by chemical assay. In other ores, however, the amount of gold accounted for as discrete minerals is considerably less than the total gold assay. Such unaccounted gold has been called by Burg (1935) **"invisible gold". The invisible gold may either be in solid solution or in colloidal dispersion within the sulphides. The invisible gold cannot be detected either with the optical microscope or on the electron microscope.**

The invisible gold is not amenable to direct cyanidation. In order to become recoverable, the sulphide must decompose. Solid solution gold typically concentrates in one, or two at the most sulphide minerals allowing preconcentration. However, colloidal gold may be hosted in several minerals, including gangue minerals, therefore preconcentration is frequently impossible.

Successful metallurgical treatment of the refractory gold ores depends upon knowledge of the mineralogical balance for the gold, both visible and invisible, since a fuller understanding of the gold mineralogy can lead to the development of adapted flowsheets aiming to optimize gold recovery. For such refractory gold ores, where a significant proportion of the gold is "invisible", knowledge of the gold content of sulphide minerals is an important link in the development of a metallurgical treatment strategy. Knowledge of the gold mineralogical balance also permits the establishment of the maximum recoverable gold by a given process.

Estimates of invisible gold had, in the past, been made by selective dissolution or by combining quantitative measurements of the visible gold with bulk chemical assays. However, these methods cannot, because of their very nature, be definitive (Boyle, 1979). Indeed, considerable debate evolved as to whether gold may actually enter solid solution (Gasparrini, 1983). Little data existed on the gold concentrations in sulphide minerals, since, although invisible gold may be determined by a variety of microanalytical techniques, including the electron microprobe (Aubert et al., 1964; Swarts, 1988) and by micro-PIXE (Cabri, 1988), the gold content of sulphide minerals is normally appreciably lower than the minimum detection limit (MDL) of these techniques. The use of ion probe microanalysis or Secondary Ion Mass Spectroscopy (SIMS) as a technique to determine the gold content of sulphide minerals has been developed at Surface Science Western (Chryssoulis, 1987). The ion microprobe has been calibrated to detect gold in sulphides at ppm concentrations and lower, with a MDL (3σ) of 350 ppb for gold in pyrite and 200 ppb for gold in arsenopyrite. This technique is at present the most sensitive in-situ microanalytical technique for the determination of gold in sulphides. The MDL offered by the ion microprobe is three orders of magnitude less than that of the electron microprobe (200 ppm) and at least two orders of magnitude more sensitive than the proton microprobe.

The development of this technique, to determine invisible gold contents of sulphide minerals, is an important link in being able to give a complete mineralogical balance for gold in each of the ores studied. Coupled with chemical assaying and diagnostic metallurgical testing, the data on invisible gold contents give a complete picture on the balance between visible (mostly recoverable) and invisible (mostly refractory to direct cyanidation) gold in each ore tested. Optical microscopy and electron probe microanalysis are used to determine the size distribution, association and composition of the visible gold. Gold mineralogical balances thus acquired are of paramount importance in the flowsheet development for challenging gold ores, with a view of reaching optimum gold recovery and minimizing both cost and time of the laboratory metallurgical testing. It is a lot easier to design the appropriate flowsheet for metallurgical testing of a difficult gold ore based on quantitative data on the various forms of gold.

Diagnostic cyanidation testing using excess of cyanide on three grinds, a coarse (80% minus 150 or 200 mesh), a fine grind (80% minus 400 mesh) and on a pulverised sample, has been shown to be the most effective way of determining the visible gold concentration and the effect of grinding upon recovery. In the event gold is in the form of tellurides or aurostibite, a higher than normal pH is required. Coupled with optical microscopy and electron probe microanalysis of the visible gold, a complete picture of the visible gold can be obtained which is more accurate and precise than automated image analysis of the gold minerals alone. Ion probe microanalysis is, at present the only accurate means of obtaining quantitative data on the distribution of the invisible (refractory to direct cyanidation) gold. When considering the preconcentration of the refractory gold for further treatment by either pressure oxidation, bioleaching, the Nitox or the Arseno-process, ion probe microanalysis proves valuable.

Nine ores, all sulphide bearing, but varying greatly in genetic type and geological setting, mineralogy and Au content have been tested. A complete mineralogical balance for gold has been derived for each. Invisible gold has also been determined in four copper anode samples. When different ores are compared, considerable differences in the relative significance of the invisible gold content of each ore and in the concentration of gold found in each mineral phase were found.

The objectives of this study are:

1) to determine the invisible gold concentration in common sulphides from refractory Canadian gold ores (Table 1)

2) to calculate the invisible gold distribution in these ores

3) to obtain a complete mineralogical balance for those ores, and,

4) to generate a data base on the gold contents of common sulphide minerals.

The aim of this study was to assist in the optimization of the gold recovery from difficult ores. Selected ores were subjected to metallurgical testing, to demonstrate how the information obtained in the present study can lead to improved gold recovery from the ore.

1.2.0 Methodology

1.2.1 Sampling

Each sample received from the participating mining companies was considered to be representative of the ore, mill feed or product to be investigated. Generally, at least 5 kg of sample was supplied for the process mineralogical study and for cyanidation tests.

1.2.1.1 Sample Preparation

Ore samples received from the participating mines were minus 1/8". Seiving was carried out using nylon sieves to produce the following size fractions: plus 500 µm (35 mesh), 500-202 µm (35-70 mesh), 202-90 µm (70-170 mesh), 90-53 µm (170-270 mesh), 53-37 µm (270-400 mesh) and -37 µm (400 mesh). Grain mounts to be used in ion probe microanalysis were of a +90 µm size fraction. In most cases, the sieving was performed dry, in order to minimize surface oxidation of the sulphide grains. Wet sieving with soaping agent was used on copper and zinc concentrate samples.

TABLE 1

LIST OF SAMPLES STUDIED

Participating Mine	Sample type(s)
ABERMIN RESOURCES Lara property, B.C.	6 rock chip samples Concentrate samples
RESSOURCES AUDREY INC. Mobrun Mine, Quebec	Pyritic ore chip samples Tailings sample
CANAMAX RESOURCES Ketza River Mine, Yukon	Composite ore Peel zone composite High grade composite LAB zone composite
HUDSON BAY MINING & SMELTING Trout Lake Mine, Manitoba	Flotation tailings
INCO Gold Ltd. Golden Pond, Quebec.	Sulphide concentrates of composites CBE-QP-1 and CBW-87-1
LACANA MINING CO. Elmtree property, N.B.	Composite ore #1
LEVON RESOURCES Congress property, B.C.	Composite ore (Howard zone)
TECK CORPORATION Estrades property, Quebec.	Composite ore 4-C
WESTMIN RESOURCES HW Mine, B.C.	4 distinct ore types Mill Feed sample Copper concentrate Zinc concentrate

Sulphides were concentrated using heavy liquid separation. A Sodium Polytungstate solution with a working density of 3.0 $g.cm^{-3}$ was used. Size fractions coarser than 50 µm separated well. In finer grained size fractions, the separation was poorer. The mass split between heavy and light fractions was calculated for each sample.

Ground samples, and in a few cases, rock chips were mounted in epoxy resin to produce blocks of 1" in diameter. The epoxy was evacuated to remove ether, which outgasses under the high vacuum used in the ion probe analysis. About 15 Wt. % of pulverised carbon per mount was added to provide bulk conductivity. The added carbon minimized particle charging during the analysis to 0-10 V. However, this procedure did not work with grain mounts of the zinc concentrates. To date it has been impossible to analyze sphalerite particles for gold with the ion probe.

Standard polishing procedures were followed to produce polished grain mounts. Every effort was taken to eliminate scratches and pits. This is because they affect the implantation range by introducing tails (Davies and Howe, 1980). Polishing was accomplished using 6, 3, 1, 1/2, 1/4 µm medium grade diamond paste. The mounts were sonicated and cleaned using acetone.

1.2.2 Optical Microscopy

Reflected light microscopy was used to determine the major ore minerals, select particles for ion probe microanalysis and to identify and measure the size of the visible gold. Sulphide particles for ion probe microanalysis were selected using 80X and 320X magnifications. Image analysis of the visible gold was performed using higher magnifications, 800x and 2000x. Oil immersion was used at 800x and 2000x. The entire surface of each polished mount was studied at 800 X magnification under oil immersion to determine the presence of native gold, electrum and other gold minerals.

The grains selected for ion probe microanalysis were larger than 70 µm in diameter and were free of inclusions, pits and scratches. For each polished section composite micrographs showing the location of marked paticles for ion probe microanalysis were taken. This facilitated the location of the preselected particles in the ion microprobe using the attached microscope.

1.2.2.1 Image Analysis

The size of each gold grain was determined on the reflected light microscope. Image analysis is commonly used to estimate the gold content and association of visible gold. The problem encountered in such estimation is **How many polished sections should be examined to give a reliable estimation?**

This will depend upon the following factors: (1) the head grade of the sample and (2) the size distribution and size uniformity of gold particles. The second factor is the most important and will critically affect the total number of gold particles observed and the reliability of estimations (nugget effect).

The **reproducibility** of optical examination has been tested by comparing two sets of data from the optical examination of an ore. This ore has a visible gold content of 10.4 ppm (from diagnostic cyanidation leaching) and a total of 169 grains of native gold were observed in twenty 1" polished blocks. This data was divided into two sets of ten mounts. The reproducibility between the two sets of data was acceptable, with relative errors of 25% for the total number of gold grains and 26% for the concentration of gold. Reproducibility for the number of grains associated with arsenopyrite (the major association) was also good (Table 2). However, the reproducibility between the two sets for other mineralogical associations decreases as the total number of grains in that association decreases. However, this does not take place uniformly since **each association is a distinct population with its own size distribution** (Figure 1).

In the case of an ore assaying 10 g/t visible gold, with an average gold size of 23 μm^2, 65% of the grains within the range from 1 to 81 μm^2 and 95% of the grains in the range 1 to 139 μm^2, it was established that a **minimum** of 6 mounts (about 50 grains) would have to be observed in order to obtain a precise estimate of the visible gold content reproducible within 25%. This number would increase if either the grade was lower or the grains were coarser in size.

Both modal and normative analysis were used to determine the major sulphides content in the samples studied. Modal analysis was used to determine two distinct types of the same mineral, for example coarse and fine grained arsenopyrite, and in some ores where scorodite is present.

A series of three standards were prepared to test the accuracy of this method. Known amounts of four different sulphide minerals (pure samples of pyrite, sphalerite, arsenopyrite and galena, which had been ground to less than 200 µm in size) were prepared in 1" mounts. Area measurement of these mounts shows that precision was better than 10% (Table 3).

TABLE 2

Reproducibility of estimation of visible gold by optical microscopy

Ore: LAB zone composite, Ketza River deposit

Head grade: 11.8 ppm,

Total cyanidable Au: 10.4 ppm

	Ist set	2nd set	Total	Average
Number of mounts	10	10	20	
Number of gold grains	95	74	169	
Modal concentration of Au (ppm)	**8.73**	**6.75* (24.4)**		**7.74 ± 1.98**
# grains associated with arsenopyrite	50	55	105	
# grains associated with non-magnetic minerals	68	61	129	
Concentration of Au associated with non-magnetic minerals	7.12	6.32*		6.72 ± 0.80
# grains associated with pyrrhotite	27	13	40	

---

* excluding one anomalously large grain

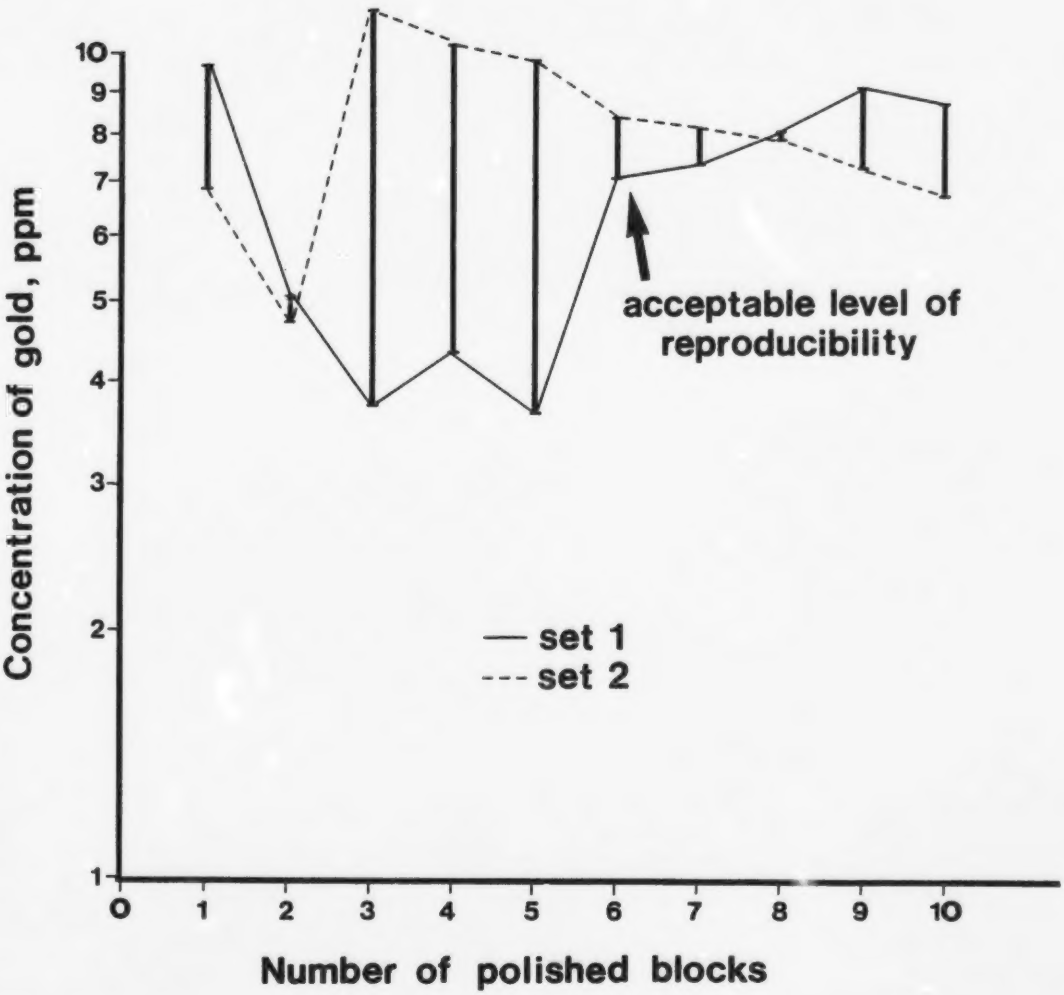

FIGURE 1. Reproducubility of visible gold concentration by image analysis.

TABLE 3

AREA MEASUREMENT

STANDARDS

					KNOWN PROPORTIONS				MEASURED PROPORTIONS				PRECISION (1)			
STD. #	# OF AREAS MEASURED	TOTAL AREA MEASURED (mm^2)	TOTAL # OF GRAINS	AREA COVERED BY GRAINS %	Py	Aspy	Sph	Gal	Py	Aspy	Sph	Gal	Py	Aspy	Spy	Gal
S1	8	173.2	2313	30.03	62	4	30	4	62.8 ±3.8	6.9 ±1.1	25.6 ±3.6	4.6 ±1.5	+1%	+73%	-15%	+15%
S2	8	173.2	2081	27.2	48	43	4	5	44.3 ±3.0	41.4 ±3.3	7.4 ±2.3	6.9 ±1.5	-8%	-4%	+85%	+52%
S3	8	173.2	3046	30.8	36	0	56	8	38.6 ±2.0	-- --	53.8 ±4.3	7.6 ±2.6	+7%	--	-4%	-5%

(1) precision = $\left(\dfrac{\text{measured proportion}}{\text{known proportion}}\right) \times 100$

1.2.3 Chemical Assays

Chemical assays were carried out at the analytical laboratories of Lakefield Research, under the supervision of Mr. A.E. Carr. Analytical methods were as follows:

Au: Fire assay with Atomic absorption or ICP finish

Te: X Ray Fluorescence Spectroscopy
Sb: X Ray Fluorescence Spectroscopy
Bi: X Ray Fluorescence Spectroscopy
As: X Ray Fluorescence Spectroscopy
S: Atomic Absorption Spectroscopy
Organic C: Atomic Absorbtion Spectroscopy

Typically, gold was assayed several times to obtain a better estimate and to establish a confidence interval.

1.2.4 Cyanide Leach Testing

Cyanide leach testing was carried out at the metallurgical laboratories of Lakefield Research, under the supervision of Mrs. R. Jackman. The test were performed on three grinds, a coarse (80% minus 100 or 75 µm), a fine grind (80% minus 53 µm) and a pulverised sample (80% minus 20 µm or less). The cyanide concentration was maintained at 1 g/l, but in several cases dropped to 0.5 g/l, at a pH of 10.5 to 11.0, and for a 48 hour period.

The objective of the cyanide testing was to obtain a reliable estimate of the visible gold from the pulverised sample and to determine the effect of grinding upon recovery. Invariably the visible gold estimated from the recovery from the pulverised samples was more accurate and reproducible than automated image analysis (Chryssoulis, 1988; Petruk, 1989).

1.2.5 Scanning Electron Microscopy (SEM) and Electron Probe Microanalysis (EPMA)

Phases whose identity could not be verified using the reflected light microscope were identified using the ISI DS 130 Scanning Electron Microscope equiped with an X-ray energy dispersive analyser (EDX) at Surface Science Western.

Quantitative electron probe microanalysis of native gold, electrum and arsenian pyrite was performed on a JEOL EXA-8600 superprobe in the Department of Geology, U.W.O. Instrumental conditions for EDX determinations were the following: 20 KV, 1.8 nA, constant beam current. Gold and silver were determined using the $M\alpha$ and $L\alpha$ spectral lines respectively. Raw data were corrected using the ZAF correction program. Standards of pure Ag and pure Au were used in the determination of electrum and native gold compositions. The precision of analysis was generally better than 2%.

The arsenic content of pyrite was determined using the wavelength dispersive X-ray analyzer (WDX) and employing arsenopyrite and arsenic-free pyrite as standards. The electron probe arsenic determinations were used to calibrate the ion microprobe for arsenic in pyrite.

1.2.6 Ion Probe Microanalysis

1.2.6.1 Methodology

Ion probe microanalysis of the major sulphides in each sample was carried out on the CAMECA IMS-3f ion microprobe at Surface Science Western. The instrument (Figure 2, schematic diagram), mode of operation and instrumental operating conditions (Table 4) have been previously describe by Chryssoulis et al. (1987). An incident Cs+ ion beam was found to give high ion yields for gold. Preselected particles were located using the optical microscope attached to the instrument. The beam was rastered over an area of 150 µm by 150 µm, and the secondary ion image was examined to confirm that the beam was centered over the particle of interest. The area that was analyzed was a circle of 60 µm in diameter in the centre of the rastered area, as determined by a field aperture in the secondary column and was confined to a single mineral particle. Gold (197) was monitored together with sulphur (33) and arsenic (75). Sulphur was used to monitor instrumental stability.

1.2.6.2 Standardization

Both internal and external standardization were used to quantify results in this project. The main difference between the two methods of calibration is that in the internal standard, both the unknown quantity of gold and the standard quantity reside within the same microvolume analysed. Most of the calibration had to be done by internal standardization because of the lack of suitable mineral standards. Closely matching standards have been advocated by Morrison (1981) as the most accurate way of quantifying the ion microprobe data.

Internal standards are prepared by doping the mineral grain mount with gold 197, the only natural isotope of gold. Doping of the grain mount is achieved by ion implantation using the heavy mass ion separator (Pelletron, Figure 3, schematic diagram). Details on gold ion implantation have been discussed by Chryssoulis et al. (1987). The implant dose or fluence (F)

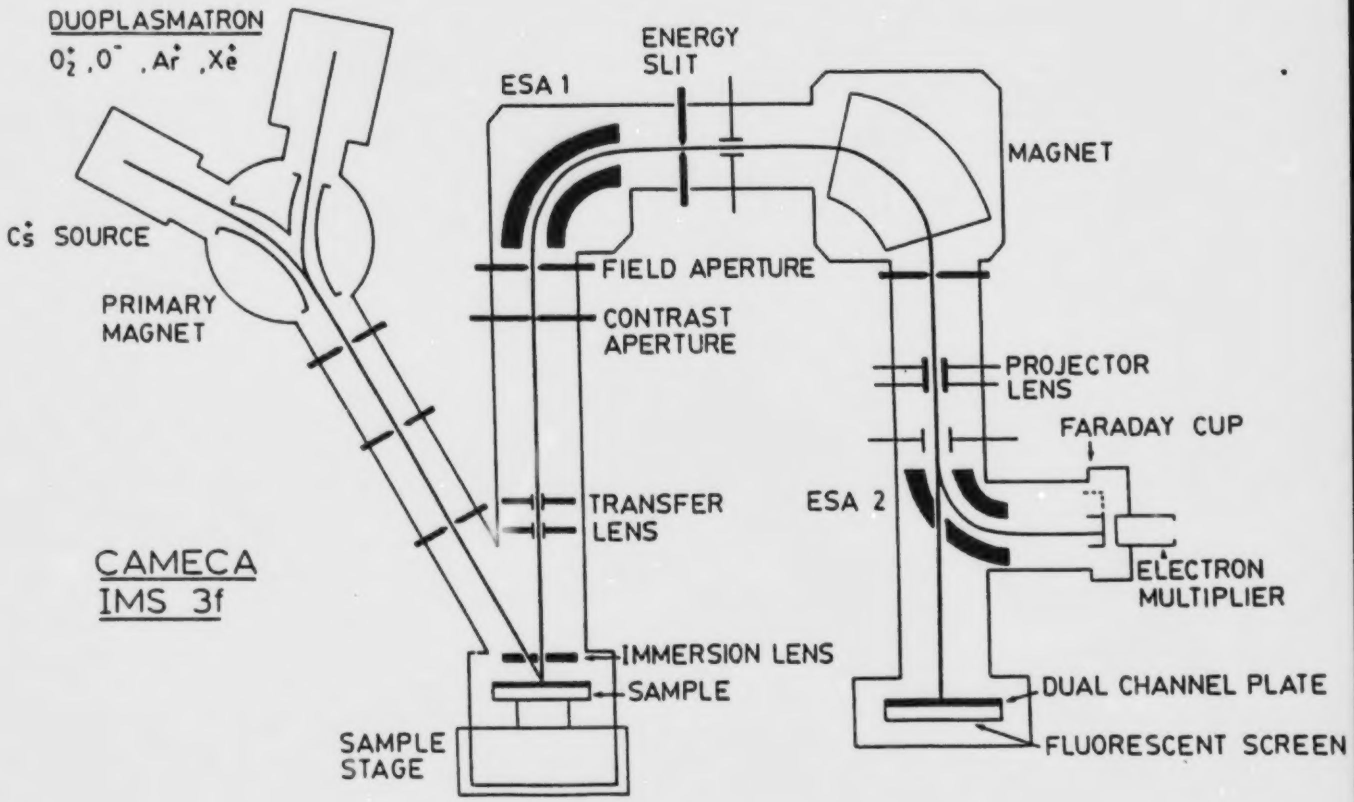
DUOPLASMATRON
O_2^+, O^-, Ar^+, Xe^+
ENERGY SLIT
ESA 1
MAGNET
Cs^+ SOURCE
FIELD APERTURE
PRIMARY MAGNET
CONTRAST APERTURE
PROJECTOR LENS
FARADAY CUP
TRANSFER LENS
ESA 2
CAMECA IMS 3f
ELECTRON MULTIPLIER
IMMERSION LENS
SAMPLE
DUAL CHANNEL PLATE
SAMPLE STAGE
FLUORESCENT SCREEN

FIGURE 2. Schematic diagram of the CAMECA IMS-3f ion microprobe.

TABLE 4 **Operating conditions**

Beam	Cs^+
Isotopes monitored	$^{197}Au^-$, $^{33}S^-$, $^{75}As^-$, $^{63}Cu^-$, $^{80}Se^-$
Rastered area	250 x 250 µm or 150 x 150 µm (Cu)
Analysis area	10 - 60 µm
Analysis time	4 - 12 min.
Depth of analysis	1 - 4 µm
External standardization	NBS, CANMET standards
Internal standardization	ion implanted standards
Energy offset	125 - 200 V
Energy window	50 eV

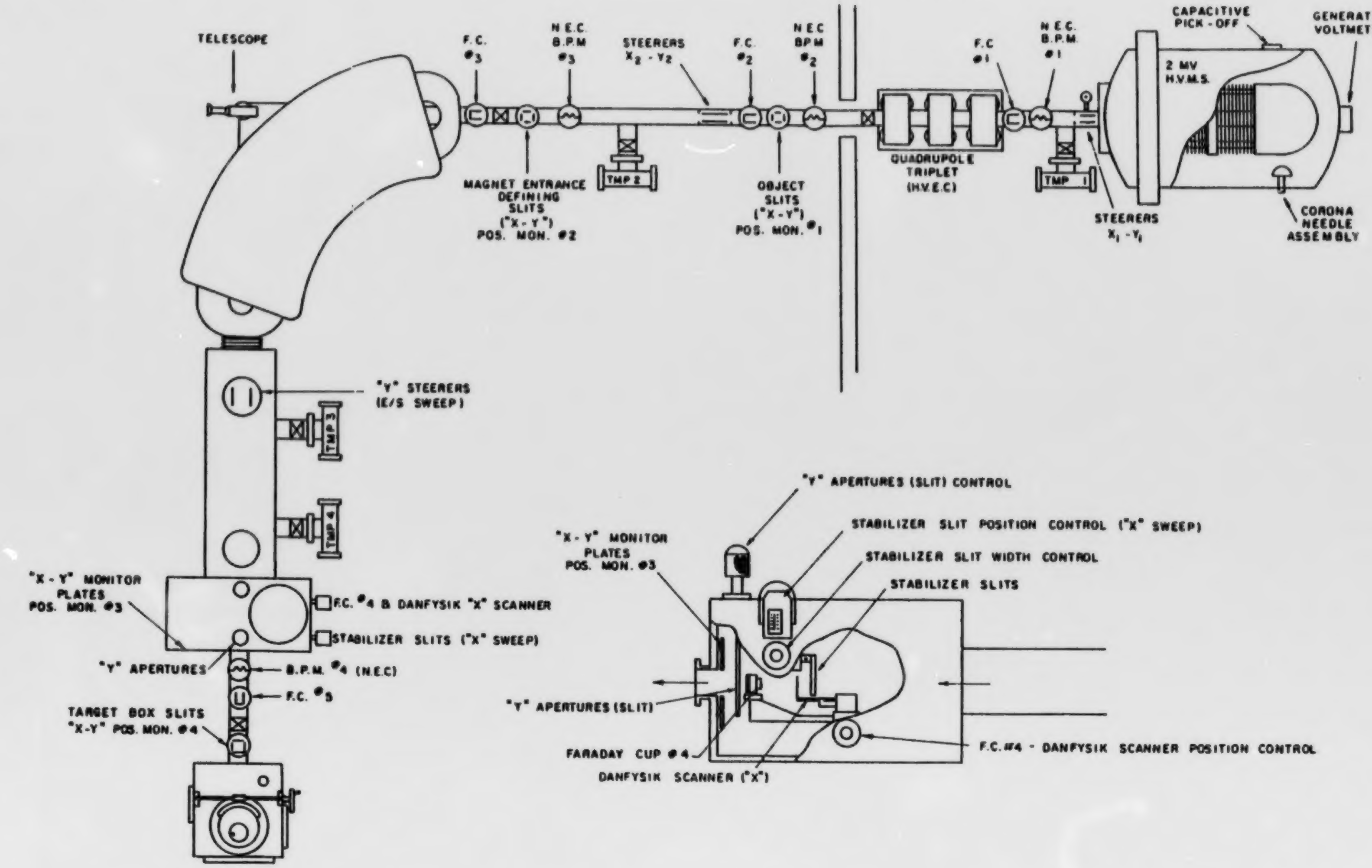
TELESCOPE
F.C. #3
N.E.C. B.P.M #3
STEERERS X2 - Y2
F.C. #2
N.E.C BPM #2
F.C #1
N.E.C. B.P.M. #1
CAPACITIVE PICK - OFF
GENERATING VOLTMETER
2 MV H.V.M.S.
MAGNET ENTRANCE DEFINING SLITS ("X - Y") POS. MON. #2
TMP 2
OBJECT SLITS ("X - Y") POS. MON. #1
QUADRUPOLE TRIPLET (H.V.E.C)
TMP 1
STEERERS X1 - Y1
CORONA NEEDLE ASSEMBLY
"Y" STEERERS (E/S SWEEP)
TMP 3
TMP 4
"X - Y" MONITOR PLATES POS. MON. #3
F.C. #4 & DANFYSIK "X" SCANNER
STABILIZER SLITS ("X" SWEEP)
"Y" APERTURES
B.P.M. #4 (N.E.C)
F.C. #5
TARGET BOX SLITS "X-Y" POS. MON. #4
"Y" APERTURES (SLIT) CONTROL
STABILIZER SLIT POSITION CONTROL ("X" SWEEP)
STABILIZER SLIT WIDTH CONTROL
STABILIZER SLITS
"X - Y" MONITOR PLATES POS. MON. #3
"Y" APERTURES (SLIT)
FARADAY CUP #4
DANFYSIK SCANNER ("X")
F.C.#4 - DANFYSIK SCANNER POSITION CONTROL

FIGURE 3. Schematic diagram of the Pelletron heavy mass ion separator.

is intitially measured in atoms per cm², by the current delivered to the specimen which forms the bottom of a deep Faraday cup (Figure 4). The implanted gold ions come to rest within the first one micrometer and have a characteristic distribution with depth (Figure 5).

The implant concentration C_i, is converted into atoms per cm² by employing the in-depth profiling capabilities of the ion microprobe. Ion probe microanalysis, being a destructive microanalytical technique (Figure 6) analyzes progressively deeper layers into the particle with time. The depth D of the crater produced (Figure 7) in order to recover the implant is measured using a surface profilometer. Therefore, $C_i = F/D$.

The total signal from the implanted gold S_i, is determined by integration of the implant counts. Likewise, the signal from the intrinsic gold S_o, is determined by extrapolation to the surface of the signal level established beyond the implant and integration of the intinsic gold counts. The intrinsic gold concentration C_o, is calculated from the equation

$$C_o = \frac{S_o}{S_i} C_i \qquad \text{or,} \qquad (1)$$

$$C_o = \frac{F.S_o}{D.S_i} \quad (\text{atoms. cm}^{-3}) \qquad (2)$$

The concentration is converted into parts per million (ppm) weight by taking into consideration the gramatom weight of gold, 197 $g.mol^{-1}$; the Avogadro number, N, and the specific gravity of the mineral analyzed.

Chryssoulis and Cabri (1989) used the secondary ion yield ratios of gold to a matrix ion to read from a calibration curve the gold concentration in ppm. A series of standards with different concentrations of gold was used to produce the curve, which is mineral and element specific and applies to a given set of operating conditions (Figure 8). The standards can be synthetic homogeneously doped with gold or ion implanted particles of natural minerals containing invisible gold in varying amounts. Copper-gold alloys with minor to trace amounts of gold were used to quantify the invisible gold in copper anodes (Chapter 12). Invisible gold in pyrite, arsenopyrite and other sulphides was quantified using calibration curves produced from implanted sulphide particles.

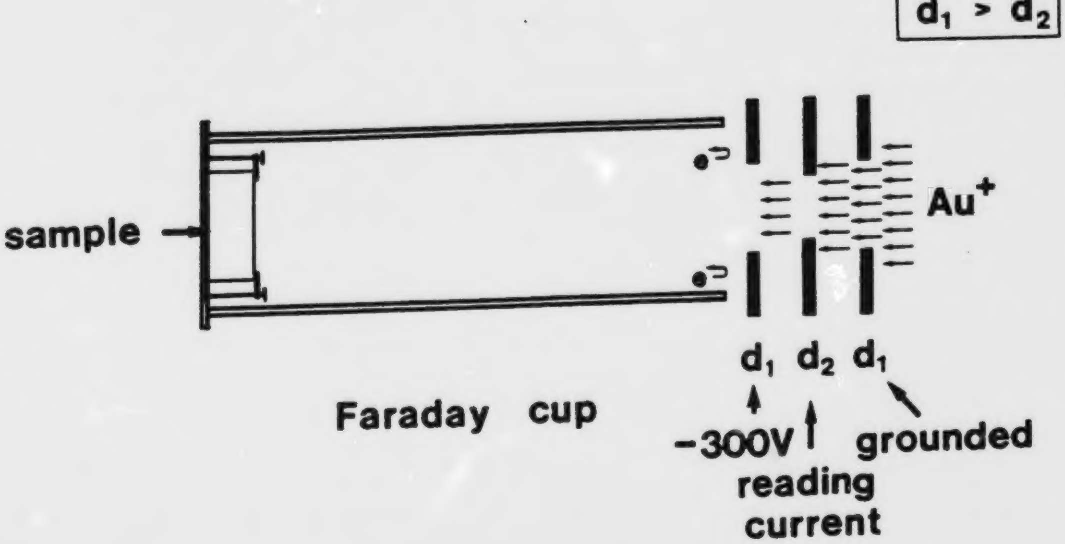
$d_1 > d_2$
sample
e^-
e^-
Au^+
d_1 d_2 d_1
Faraday cup
-300V
reading current
grounded

FIGURE 4. Schematic diagram of Faraday cup assembly.

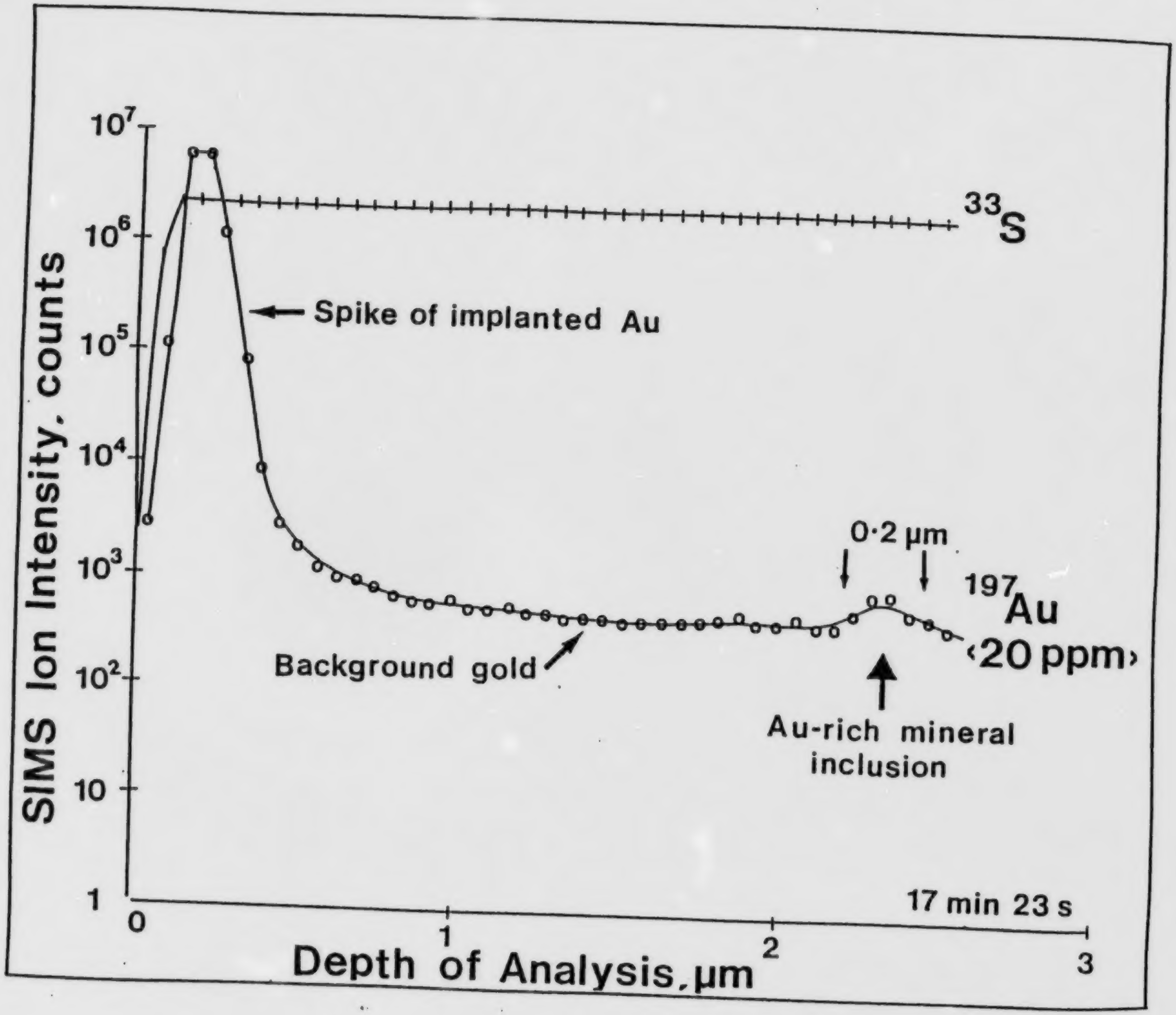

FIGURE 5. Characteristic distribution of implanted gold ions with depth.

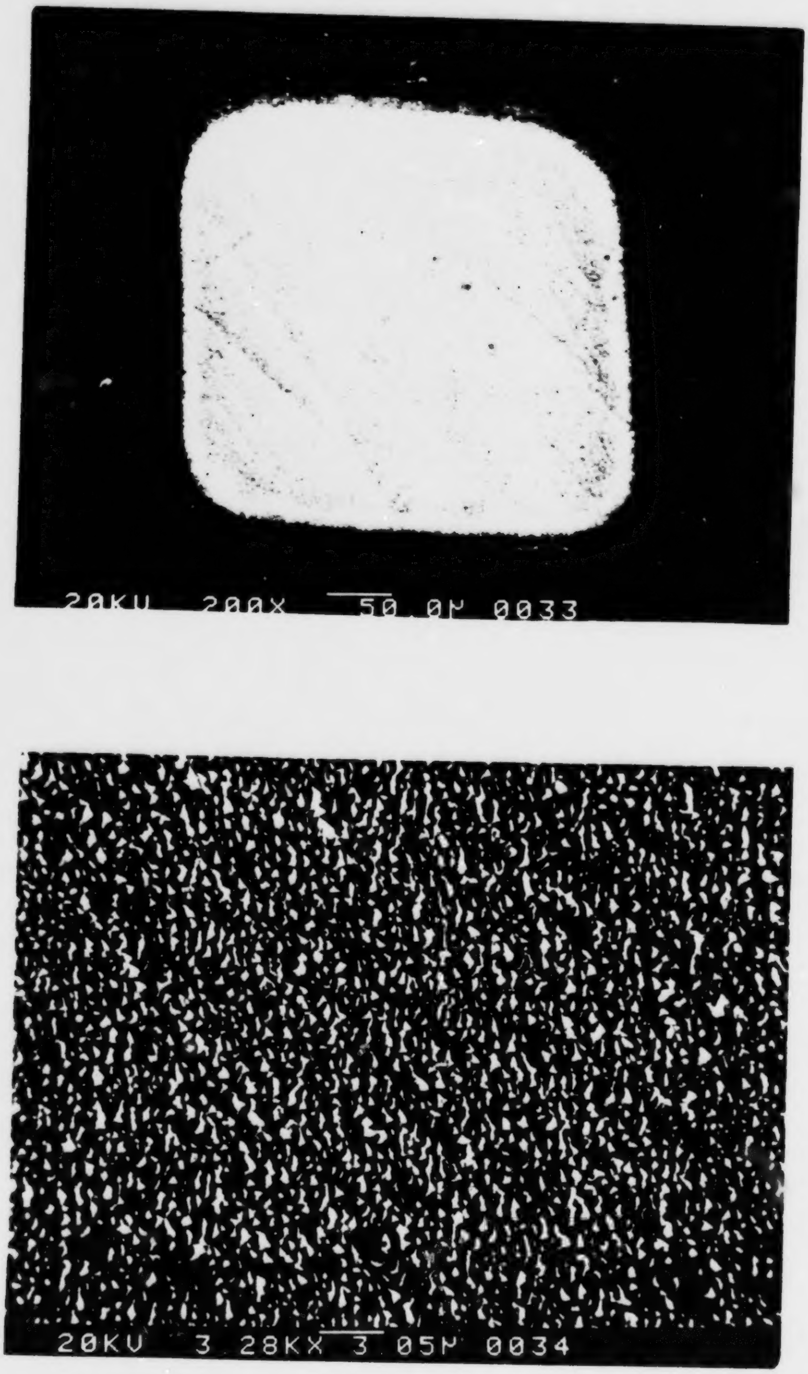
20KV 200X 50.0µ 0033
20KV 3.28KX 3.05µ 0034

FIGURE 6. Backscattered electron image indicating the destructive character of ion probe microanalysis. SIMS crater in galena under low and high magnifications.

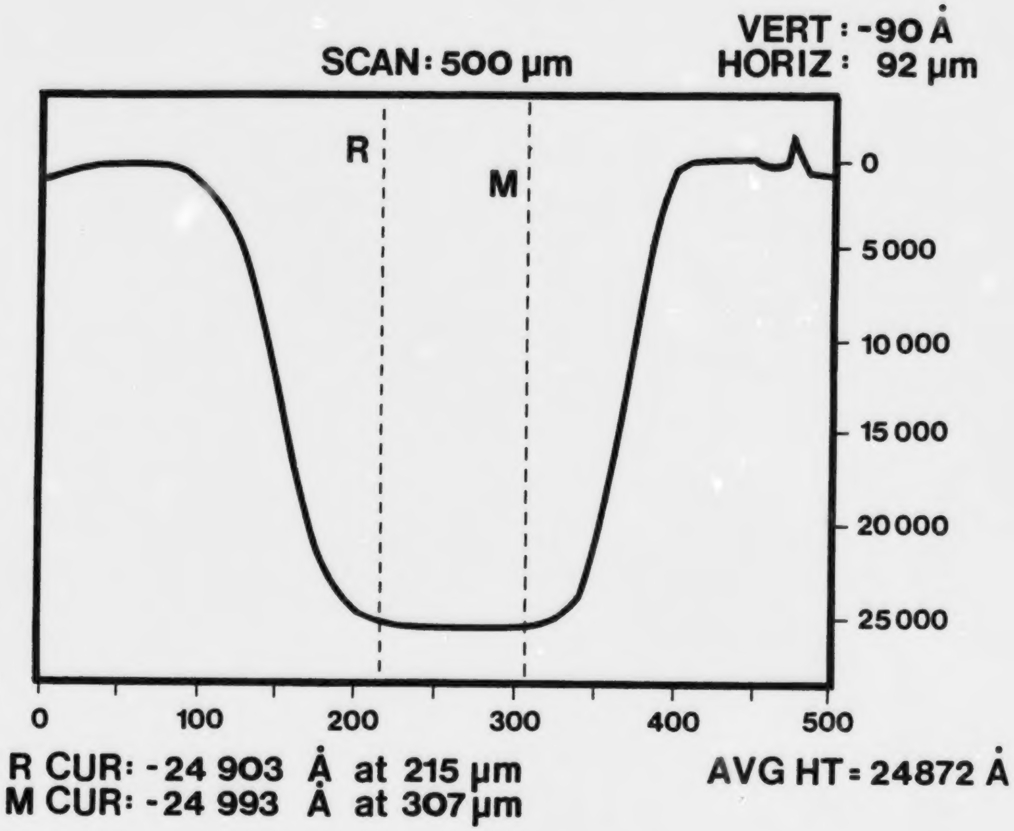

FIGURE 7. Diagram indicating depyh of crator produced by ion probe microanalysis.

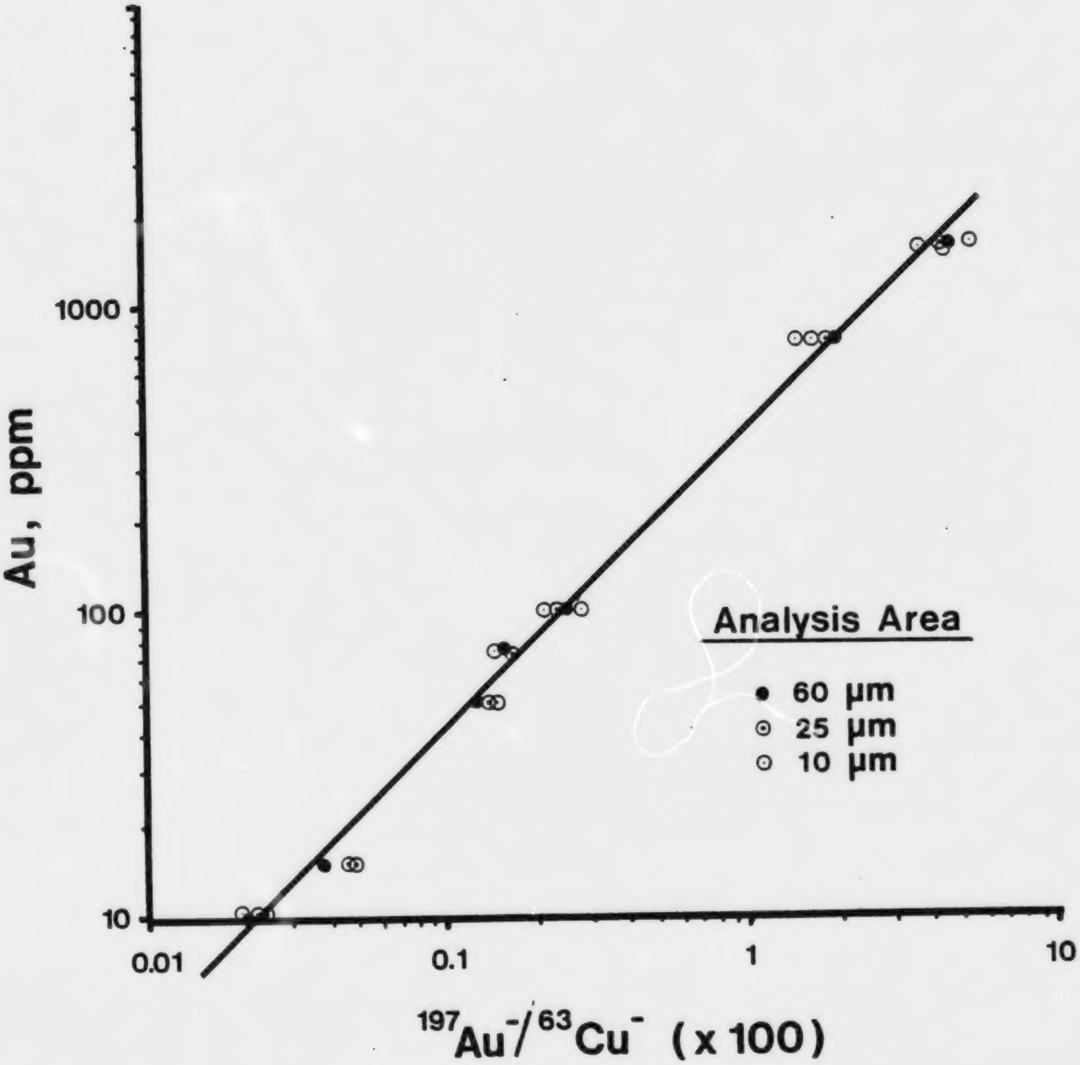

FIGURE 8. Calibration curve for external standardization.

1.2.6.4 Accuracy

The accuracy of the ion probe microanalyses for gold in sulphides was determined by comparing ion probe data with neutron activation results in two synthetic pyrrhotite standards homogeneously doped with gold. For the ion probe microanalysis the pyrrhotites were ion implanted with gold. The accuracy, expressed as relative error in terms of concentration ratios determined by the two methods, is better than 15% at the 1 ppm concentration level (Table 5).

The accuracy in internal standardization depends on the purity of the implantation beam, the current integration, and the lateral homogeneity of the implant. The large radius of the Pelletron magnet ensures good isotope separation. Rutherford backscattering and ion probe microanalysis of gold implanted in silicon confirmed that gold was the only ion implanted. The same techniques were used to determine the lateral homogeneity of the gold implants in silicon and the sulphides. Lateral homogeneity measured as variation in the implant density is 5.2 percent. The specifically designed Faraday cup specimen holder ensures good current integration, by minimizing 'escaping electrons'.

The accuracy with external standardization depends on standard homogeneity and matching of the standard and unknown matrices, as well as operating conditions. Internal standardization is believed to provide more accurate determinations (Chryssoulis and Cabri, 1989).

2.6.5 Precision

The precision of the ion probe microanalysis for gold in the sulphides using internal standardization is a function of the precision for each measured parameter in equation (2). For silver, it was determined to be 20% (Chryssoulis et al, 1986). The precision using external standardization depends on the scatter of the data points used for regression of the calibration curve. In most matrices, precision is better than 20% and in several, better than 10%, as determined by the Thompson and Howarth method (1978).

TABLE 5

ACCURACY

SAMPLE	NOMINAL VALUE (ppb)	ANALYSIS TECHNIQUE	SIMS ANALYSIS (ppb)	PERCENT ERROR
641 synthetic pyrrhotite	430,486	INNA	570,470	13.5
644 synthetic pyrrhotite	1420	INNA	1400,1360 1420,1510	0.2
Arsenopyrite Goldenville, NS	1115,1210	INNA	1660,1080*	42.7

*inhomogeneous gold distribution

CHAPTER 2

DETERMINATION OF INVISIBLE GOLD WITHIN SULPHIDE MINERALS IN FLOTATION TAILINGS FROM TROUT LAKE MINE, MANITOBA

SSW/PMS/88/11

SUMMARY

Invisible gold has been determined to be present within both pyrite and arsenopyrite. The average gold concentration in pyrite is 0.72 ± 0.38 g/t, and accounts for 26.7 ± 14.8 % of the total gold in the tailings. The average concentration of invisible gold in arsenopyrite is 30.2 ± 8.6 g/t. Arsenopyrite is a minor component of the tailings (0.199 ± 0.035% by volume), and the invisible gold in arsenopyrite accounts for 8.9 ± 3.0% of the total gold in the tailings. Direct cyanidation of the tailings gave a gold recovery of 64.4%. Thus the total gold accounted for in the Trout Lake tailings is 100 ± 8.9%.

FIGURE 1

MINERALOGICAL DISTRIBUTION OF GOLD

(Trout Lake, final tailings)

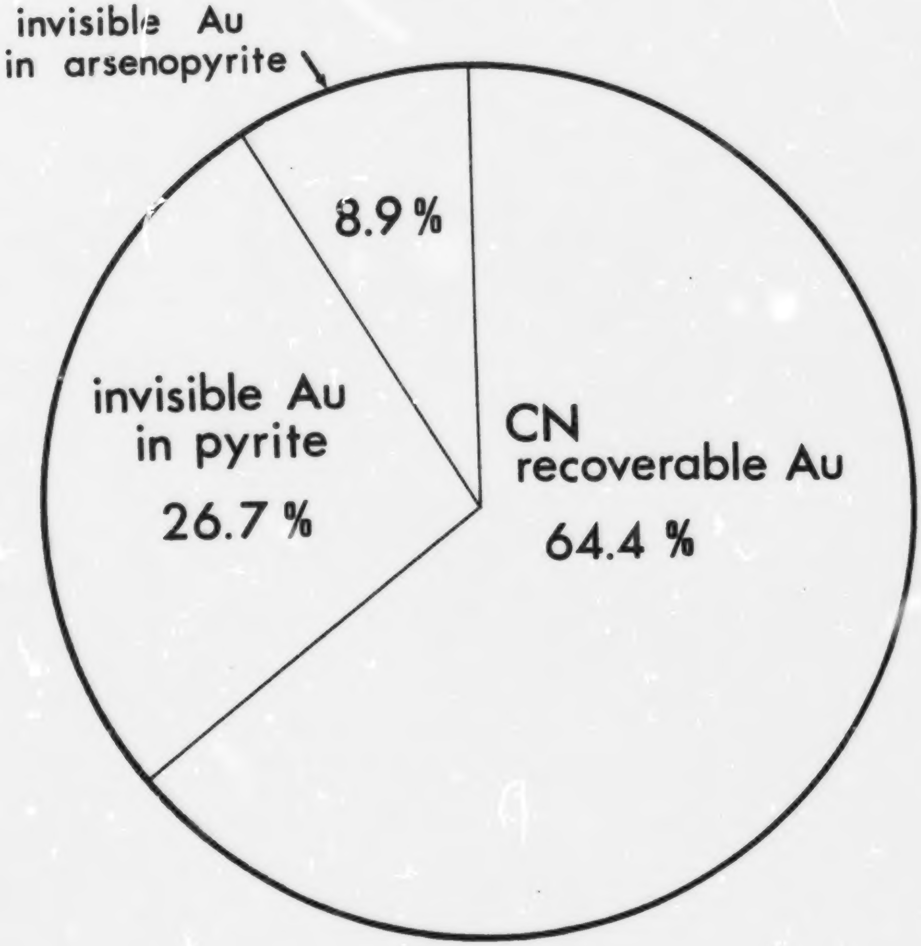

TABLE 1

MINERALOGICAL DISTRIBUTION OF GOLD IN FLOTATION TAILINGS

	Assay	Distribution %	Precision
Assayed Au	0.675 + 0.088	100.0	± 13.0
CN- recoverable Au (K_{80} = 18 μm)	0.435 ± 0.030	64.4	± 4.4
Invisible gold in arsenopyrite (concn. 30.2 ± 8.6 ppm) (0.199 ± 0.040 % by mode)	0.06 ± 0.02	8.9	± 3.1
Invisible gold in pyrite (concn. 0.72 ± 0.38 ppm) (24.7 ± 2.2 % by mode)	0.18 ± 0.10	26.7	± 14.8
TOTAL	0.675 ± 0.06	100.0	± 8.9

LIST OF TABLES

Table 1 Mineralogical distribution of gold in flotation tailings

Table 2 Chemical assays

Table 3 Cyanidation tests

LIST OF FIGURES

Figure 1 Mineralogical distribution of gold

Figure 2 Distribution of invisible gold in arsenopyrite

Figure 3 Distribution of invisible gold in pyrite

Figure 4 Distribution of arsenic in pyrite

LIST OF PLATES

Plate 1 Sphalerite - arsenopyrite intergrowths

APPENDICES

A1 Ion probe microanalytical data

A2 Assays and distribution of invisible gold in heavy and light fractions

OBJECTIVES

1. Determine the gold concentration in the **pyrite** and **arsenopyrite**.
2. Obtain the gold mineralogical distribution in the flotation tailings.
3. Determine the arsenic concentration in the pyrite by ion probe microanalysis.

2.1.0 INTRODUCTION

Flotation tailings from Trout Lake were supplied by N.C. McEachern, Supervisor in Process Technology with Hudson Bay Mining and Smelting Co. Ltd., for determination of the distribution of gold. It was suspected that part of the gold in the sample was "invisible", i.e. present in solid solution within the crystal lattice of the sulphide minerals.

Gold contents of the deposit are low (head grade 1.25 g/tonne). Sixty percent of the gold is recovered in the Cu-concentrate. A further 7 % is recovered in the Zn-concentrate. A total of 33 % of the gold reports to the tailings, which have a sulphide content of about 20 %, mostly pyrite.

Previous mineralogical studies(1) have shown that the only gold mineral present is mercurian electrum. The electrum was most commonly present associated with chalcopyrtie and as inclusions within, and in fractures between, pyrtie grains. No association of Au and As was noted, either geochemically ore paragenetically.

In previous testing (Appendix A1), direct cyanidation of the tailings gave a Au recovery of only 35 %, which could be increased to 44 %, by regrinding. Production of a pyrite concentrate by flotation gave a 72 % Au recovery. Direct cyanidation of this concentrate gave a recovery of only 40 % of the gold, leading to the conclusion that invisible gold in pyrite represented a significant portion of the total gold.

TABLE 2

CHEMICAL ASSAYS

Au :	0.60 0.60 0.73 0.77	
$\hat{x} \pm \lambda$:	0.675 ± 0.10	g/t
Au (HBM):	0.63	g/t

S :	13.2 ± 1.2	%
Te :	< 3	ppm
Bi :	< 20	ppm
Sb :	< 20	ppm
As :	1040 ± 120	ppm
C (organic):	< 0.05	%

2.2.0 METHODOLOGY

A sample of Trout Lake circuit tailings was received from HBM. The sample was sieved into the size fractions -53 µm, 53-90 µm, and +90 µm. The +90 µm fraction (11.5 % of the total sample) was separated using heavy liquid techniques. The heavy liquid represented 21 % of the total +90 µm fraction. Nine one inch polished grain mounts were prepared from the heavy +90 µm fraction for ion probe microanalysis.

Optical microscopy was used to determine the gold minerals size and association. The invisible gold in the sulphide minerals was determined by ion probe microanalysis (2). The arsenic concentration in pyrite was determined by ion probe microanalysis.

2.3.0 RESULTS

2.3.1 CHEMICAL ASSAYS

A series of chemical assays were determined on the bulk tailings sample. Results are given in Table 2.

2.3.2 MINERALOGY

The following minerals were identified in the sample:

Pyrite, sphalerite, chalcopyrite, arsenopyrite, galena, cassiterite, native antimony.

Pyrite: The pyrite grains are generally fresh and clean in appearance. Inclusions of silicates and of other sulphides (chalcopyrite, pyrrhotite and sphalerite) are widespread. Intergrowths of pyrtie with other grains are rare.

Arsenopyrite: is present intergrown with pyrite and also forms fine grained intergrowths with sphalerite (Plate 1). Spalerite-arsenopyrite composite grains had been previously noted (1) within the massive sphalerite and banded pyrite-sphalerite ore types.

Other minerals: Sphalerite contains chalcopyrite disease (inclusions of chalcopyrite), and is commonly intergrown with chalcopyrite and pyrrhotite. Trace galena and native antimony are noted.

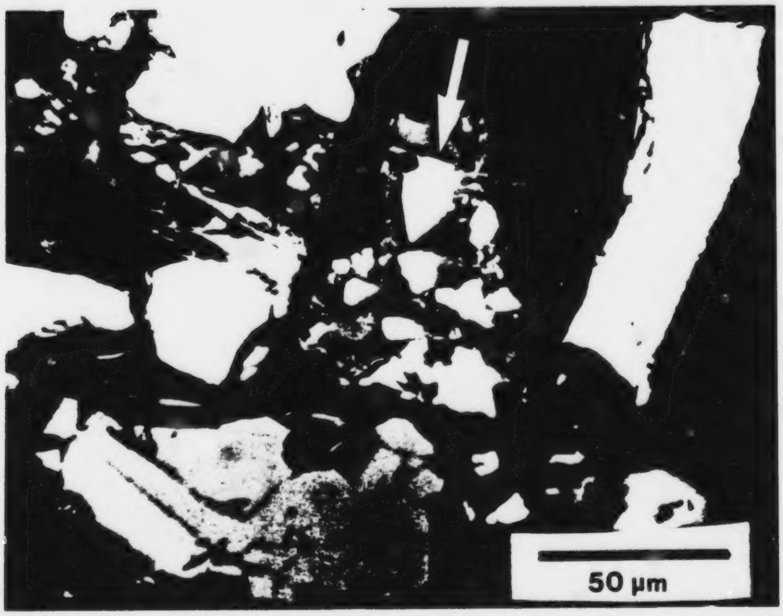

Plate 1 Fine-grained arsenopyrite combined with sphalerite.

Gold minerals: No grains of native gold or electrum were recognised in the investigated samples.

2.3.3 INVISIBLE GOLD

Invisible gold is the gold which is invisible under the optical or scanning electron microscopes. It may either be in the crystal lattice of the sulphide minerals or fine, sub-micron scale inclusions of native gold or electrum (< 0.1 µm). The invisible gold is not recoverable by direct cyanidation, and requires prior oxidation of the host sulphides in order for the gold to be recovered. Invisible gold was found to be present in both pyrite and arsenopyrite. Concentrations in the arsenopyrite are **40 times** higher than in the pyrite.

The average concentration of the gold in 44 arsenopyrite particles, as determined with the ion microprobe was 30.2 parts per million (g/t). with a confidence interval of 8.6 g/t, at a 95% significance level. This means that 95 out of 100 arsenopyrite particles would have a gold concentration in the range from 21.6 to 38.8 g/t. Measured concentrations in the sampled population ranged from 2 to 112 g/t. The distribution of invisible gold is shown as a histogram in Figure 2.

The average concentration of the gold in 46 pyrite particles, as determined with the ion microprobe was 0.72 parts per million (g/t), with a confidence interval of 0.38 g/t, at a 95 % significance level. Measured concentrations in the sampled population ranged from 0 to 6.80 g/t. The distribution of invisible gold in pyrite is shown as a histogram in Figure 3.

The arsenic contents of the pyrite grains were also measured (Figure 4). The average As content of pyrite in the 47 pyrite particles was 500 ± 247 ppm. The measured analyses ranged from less than 10 ppm to 4100 ppm (0.41%). There was no correlation between the As and Au content of pyrite in these As-poor pyrites. A positive correlation has been observed in arsenian pyrites from other ores.

The ion probe microanalysis data is presented in Appendix A1.

FIGURE 2

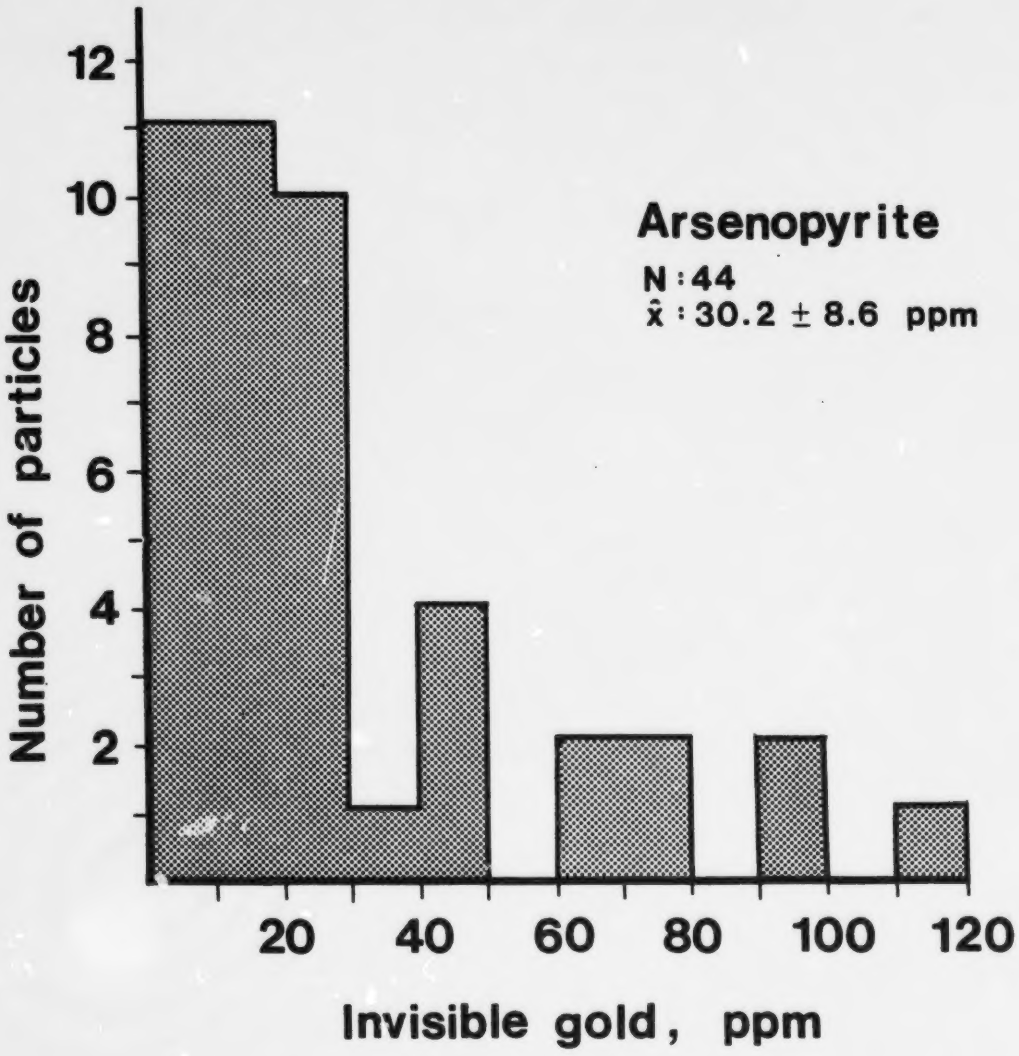
12
10
8
6
4
2
Number of particles
20
40
60
80
100
120
Invisible gold, ppm
Arsenopyrite
N : 44
x̂ : 30.2 ± 8.6 ppm

FIGURE 3

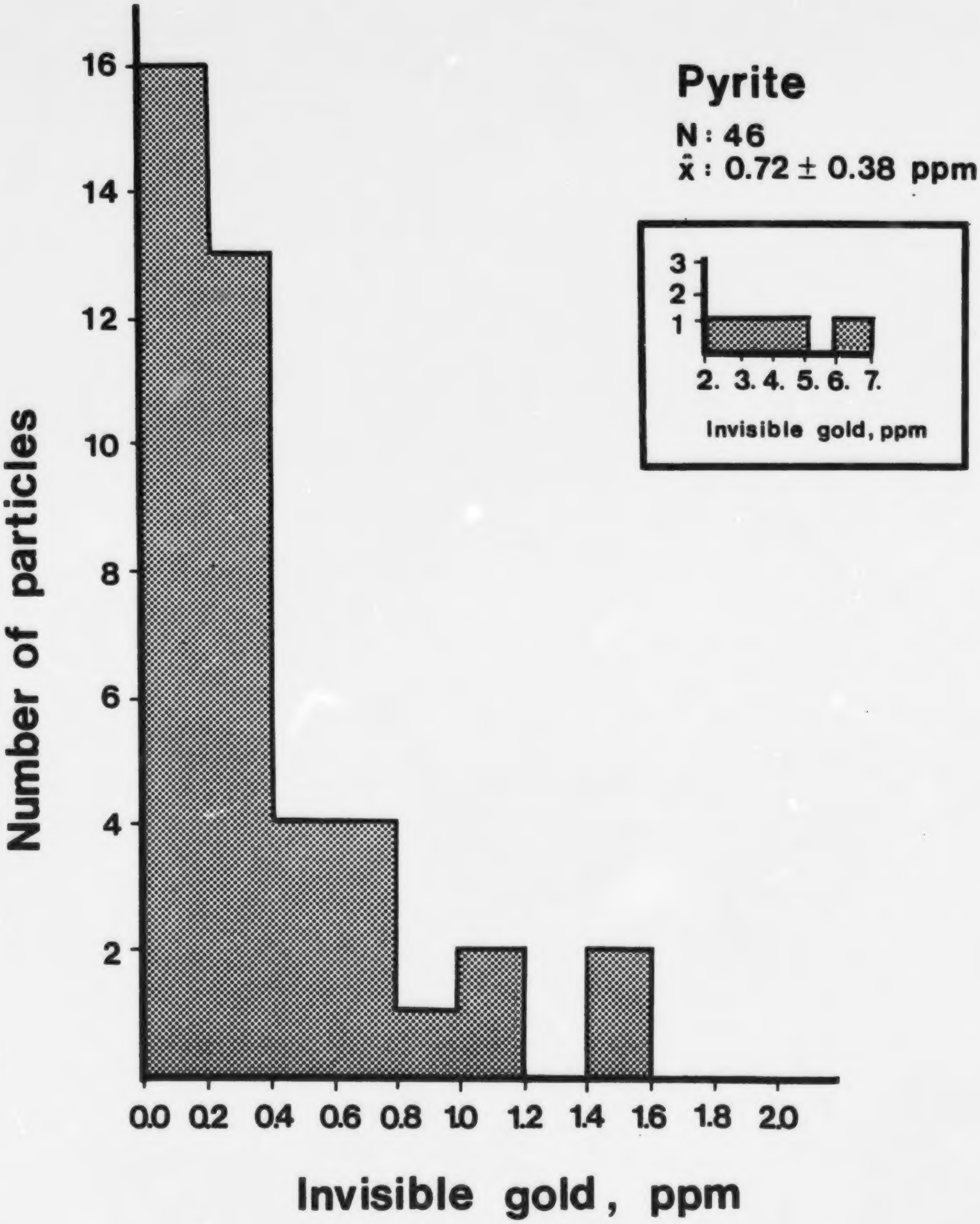
Pyrite
N: 46
x̂: 0.72 ± 0.38 ppm
3
2
1
2. 3. 4. 5. 6. 7.
Invisible gold, ppm
16
14
12
10
8
6
4
2
Number of particles
0.0 0.2 0.4 0.6 0.8 1.0 1.2 1.4 1.6 1.8 2.0
Invisible gold, ppm

FIGURE 4

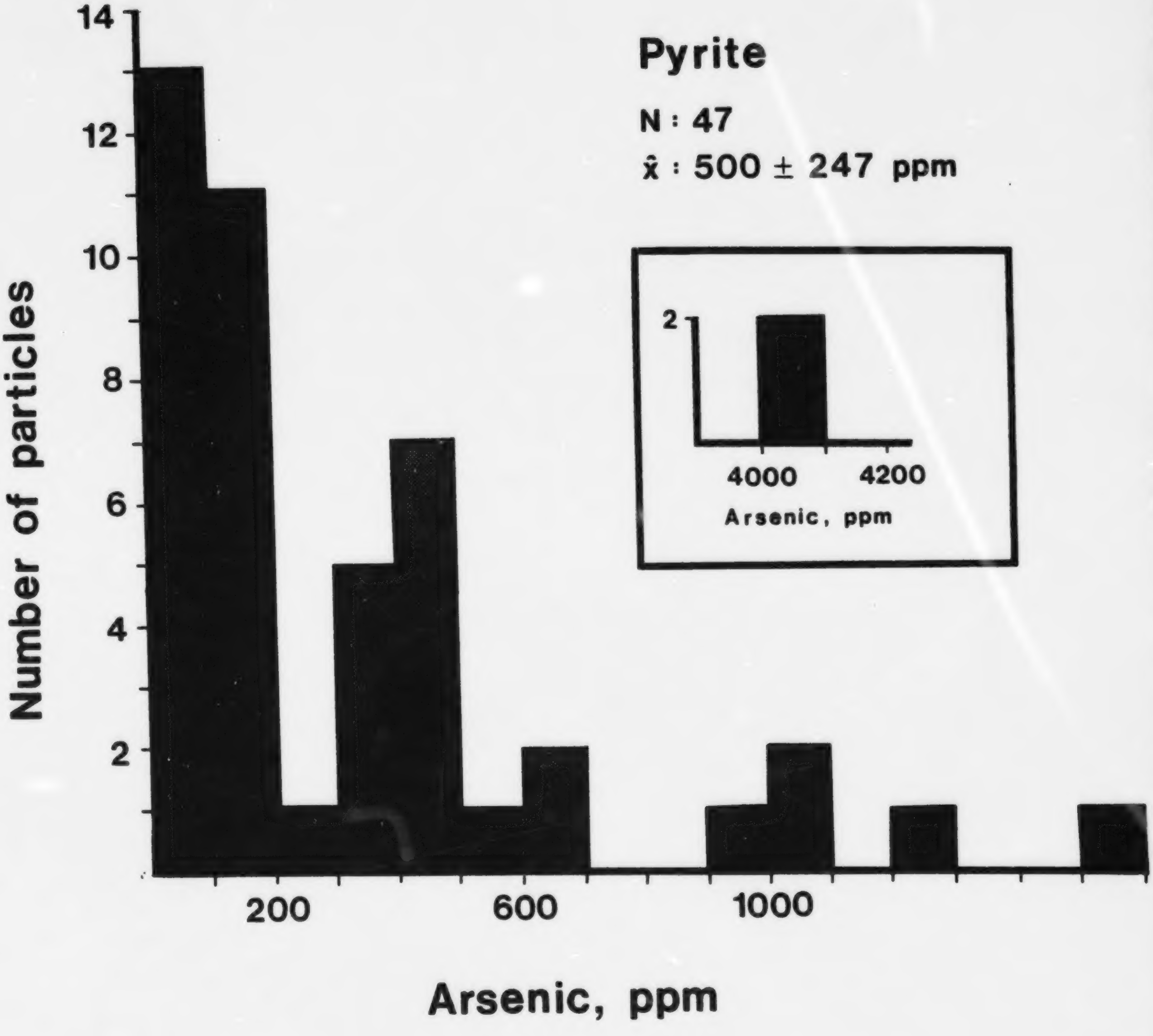
Pyrite
N : 47
x̂ : 500 ± 247 ppm
Number of particles
14
12
10
8
6
4
2
200
600
1000
Arsenic, ppm
2
4000
4200
Arsenic, ppm

2.3.4 CYANIDATION TESTS

Three cyanidation tests at progessively finer grinds (K_{80} = 50 µm; 23 µm; 18 µm) were carried out in order to determine the amount of gold recoverable by direct cyanidation and to obtain an idea of its size distribution. Exposed native gold and electrum are amenable to cyanidation, however, sub-micron gold and gold in solid solution in the pyrite and arsenopyrite are not recoverable. Conditions were: 33% solids, 1 g/l NaCN, pH 10.5 - 11.0, 48 hours. Increasing the fineness of grind increased Au recovery from 57% at K_{80} = 50 µm to 64.4% at K_{80} = 18 µm. Results are given in Table 3.

2.4.0 DISCUSSION

Cyanidation testing of the tailings showed that at a finest grind of K_{80} = 18 µm, 64.4% of the total gold (0.675 ± 0.088 g/t) could be recovered by direct cyanidation. The difference between the gold recovery at a similar grind (K_{80} = 50 µm) from previous testing, 57% versus 34.5% Au can be explained by the higher cyanide concentration, longer duration of test, and lower pulp density used in the present study. The objective of these cyanide tests was to determine a maximum value for the cyanide recoverable (visible) gold, rather than to evaluate cyanidation for processing the flotation tailings.

The remaining 35.6% of the gold is present in solid solution within the crystal lattices of pyrite and arsenopyrite. In order to calculate the amounts of invisible gold in the two minerals, it is neccessary to know the proportions of pyrite and arsenopyrite in the sample.

The proportion of pyrite can be calculated from the sulphur assay (13.2 ± 1.2%). Since other sulphides account for less than one per cent of the sample, it is reasonable to calculate all sulphides as pyrite. The proportion of pyrite is calculated to be 24.7 ± 2.2 %. The proportion of arsenopyrite may be calculated from the As assay (1040 ± 120 ppm) by subtracting the average As solid solution in pyrite (500 ± 247 ppm) which has been measured with the ion microprobe. Thus the proportion of arsenopyrite is calculated to be 0.199 ± 0.040%.

TABLE 3

CYANIDATION TESTS

				HEAD		
Test #	K_{80} (µm)	% Extrn Au	Residue g/t Au	x Direct g/t	Calc. g/t	Yield %
1	50	34.9	0.29	0.675 ± 0.08	0.45	57
2	23	43.2	0.23		0.40	66
3	18	43.8	0.24		0.43	64.4

$$\text{Yield} = \frac{(\text{Direct head}) - (\text{Residue})}{(\text{Direct head})}$$

Knowing the concentration of gold in arsenopyrite to be 30.2 ± 8.6 g/t, it can be shown that 0.06 ± 0.02 g/t, or 8.9 ± 3.1% of the total gold is present within solid solution in arsenopyrite.

The concentration of gold in pyrite is 0.72 ± 0.38 g/t, so it can similarly be calculated that 0.18 ± 0.10 g/t, or 26.7 ± 14.8 % of the total gold can be accounted for within solid solution in pyrite. Thus 100% of the gold can be accounted for, with an error of 8.9%. The mineralogical distribution for gold is given in Table 1 and is presented as a pie diagram in Figure 1. The distribution of gold can also be calculated for the heavy and light fractions (Appendix A2).

2.5.0 CONCLUSIONS

Pyrite is the principal carrier of invisible gold in the tailings. The average gold concentration of pyrite is 0.72 ± 0.38 g/t. Invisible gold in solid solution within the crystal lattice of pyrite accounts for 26.7 ± 14.8% of the total gold in the tailings.

Arsenopyrite contains significant concentrations of gold. The average concentration was 30.2 ± 8.6 g/t. However, arsenopyrite is only a volumetrically minor constituent of the sample (0.199 ± 0.040 % by volume). The amount of invisible gold in the pyrite is three times greater than the amount in arsenopyrite in the tailings.

This study supports the validity of earlier data, and confirms that approximately one third of the gold in the tailings is invisible, and that two thirds of the gold is recoverable by cyanidation.

APPENDIX A1

ION PROBE MICROANALYTICAL DATA

INVISIBLE GOLD CONCENTRATION IN SULPHIDES
(HBM, Trout Lake, Man.)

Arsenopyrite

Particle #	Au, g/t	Particle #	Au, g/t
1	68.	37	3.
2	19.	38	7.8
3	112.	39	10.
4	50.	40	100.
7	17.5	41	6.
8	9.7	42	33.
9	18.6	47	25.
14	26.1	5	2.8
16	3.7	59	28.8
17	80.	63	17.5
18	14.9	66	27.3
19	4.5	67	26.4
20	17.2	70	49.
22	23.	71	42.
23	65.	72	104.
26	9.5	73	16.
28	23.4	80	12.
31	30.	84	26.
31α	18.	85	80.
34	16.	95	11.
35	44.	97	23.
36	6.	100	2.

n = 44

x = 30.2 ± 8.6 g/t Au

Pyrite

Particle #	Au, g/t	Particle #	Au, g/t
6	0.07 < MDL	57	0.52
10	0.02 < MDL	58	3.49
11	3.00	60	0.31 < MDL
12	0.02 < MDL.	61	0.38 < MDL
13	0.00	62	0.28 < MDL
15	1.18	64	0.05 < MDL
21	0.03 < MDL	65	0.00 < MDL
24	0.00	68	0.65
25	0.00	69	0.44 < MDL
27	0.10 < MDL	74	0.00 < MDL
29	0.55	79	0.35
29α	0.34 < MDL	81	0.76
30	0.16 < MDL	83	0.46
31	0.27 < MDL	86	1.52
44	0.28 < MDL	87	1.50
45	0.00 < MDL	88	1.08
46	0.00 < MDL	89	0.98
49	0.00 < MDL	90	0.24
50	0.01 < MDL	91	0.32
51	0.21 < MDL	92	6.80
52	0.22 < MDL	93	0.76
53	0.62	94	0.29
54	4.49	98	0.22

n = 46

x = 0.72 ± 0.38 g/t Au

Arsenic in pyrite

Particle #	Arsenic (ppm)	Particle #	Arsenic ppm)
6	84	57	14
10	54	58	4100
11	150	60	50
12	54	61	39
13	340	62	1600
15	125	64	145
21	42	65	500
24	640	68	470
25	105	69	72
27	200	74	115
29	570	79	4100
30	490	81	96
33	260	83	< 10
23D	630	86	< 10
30D	500	87	190
44	1000	88	25
45	58	89	420
46	460	90	200
49	110	91	1050
50	350	92	410
51	370	93	1300
52	170	94	320
53	330	98	130
54	1100		

N = 47

x = 500 ± 247 ppm As

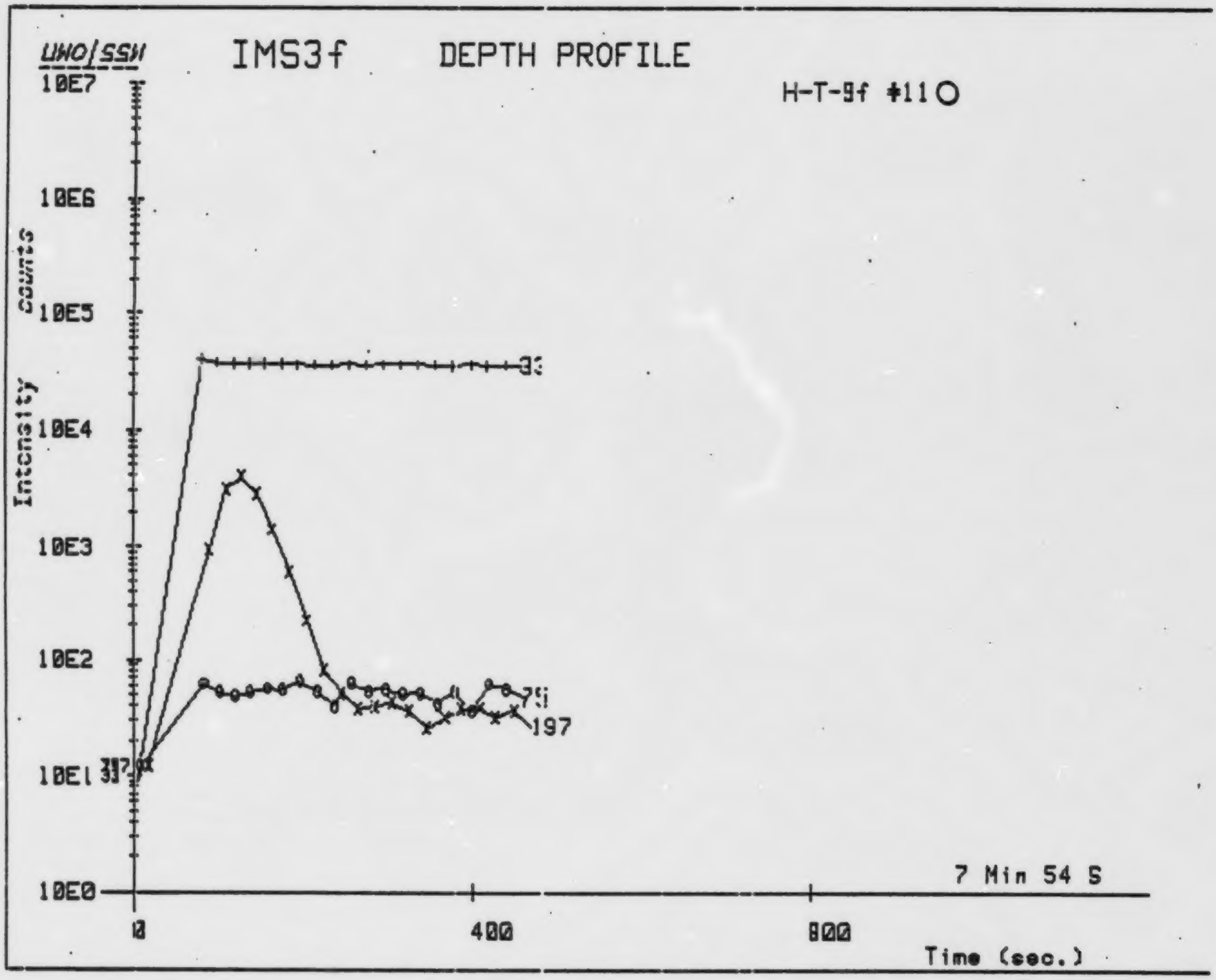

```
    SAMPLE:H-T-9f #11 O
    DATE:
    PRIMARY IONS :       CS            +
    SECONDARY IONS :                   -
       DEAD TIME: 500.00E-10 sec.

    PRIMARY CURRENT :     379 NANO AMP
    HIGH VOLTAGE :
156.65 DD.D
 <ILOVOLTS
    RASTERING :            250 MICRONS
    TRANSFER OPTICS :      150 MICRONS
    FIELD APERTURE :   1  2  3
    CONTRAST APERTURE :  4  3  2  :
```

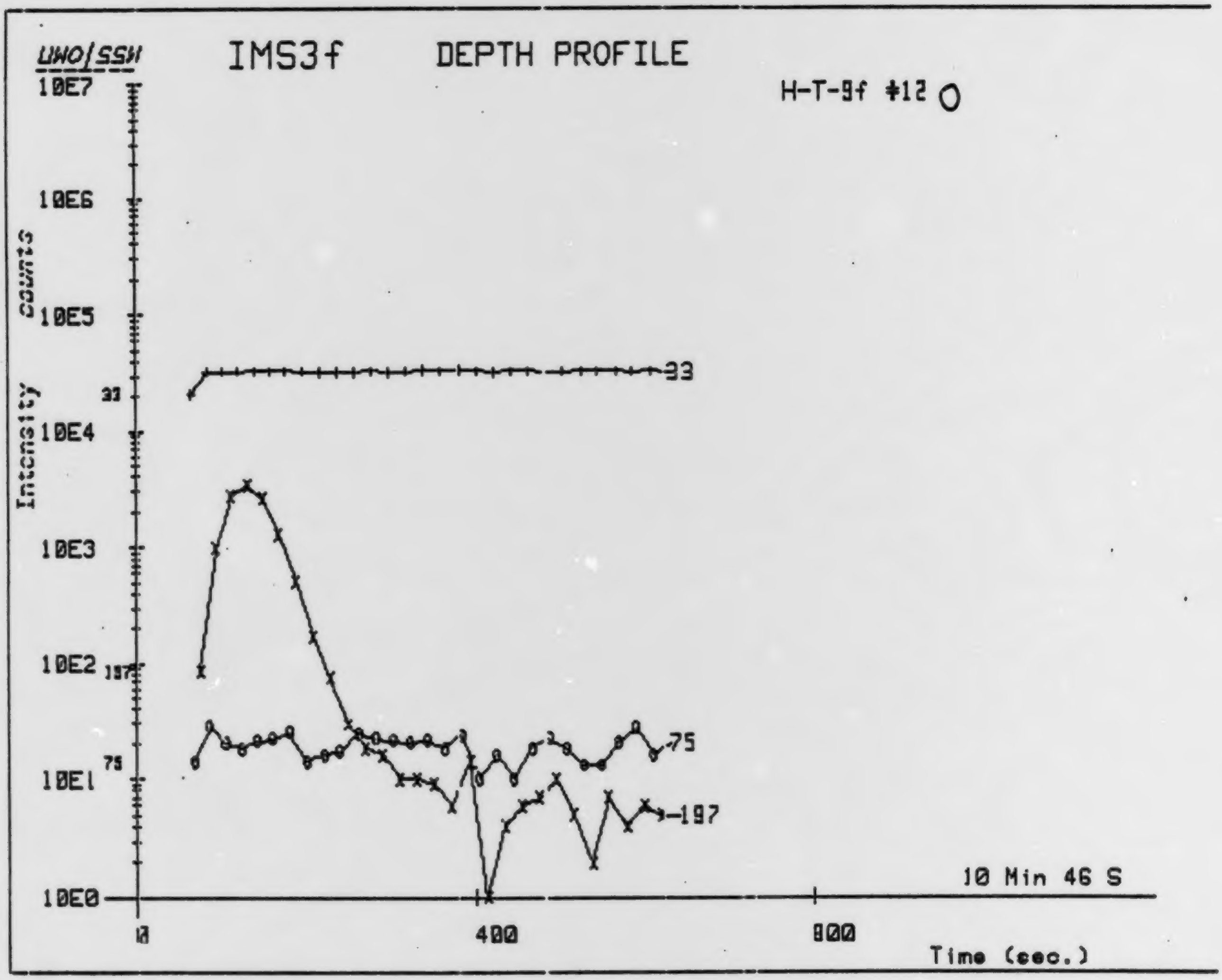

```
    SAMPLE:H-T-9f #12 O
    DATE:
    PRIMARY IONS :       CS          +
    SECONDARY IONS :                 -
       DEAD TIME: 500.00E-10 sec.

    PRIMARY CURRENT :    354 NANO AMP
    HIGH VOLTAGE :
156.65 DD.D
 <ILOVOLTS
    RASTERING :           250 MICRONS
    TRANSFER OPTICS :     150 MICRONS
    FIELD APERTURE :  1  2  3
    CONTRAST APERTURE :  4  3  2  :
```

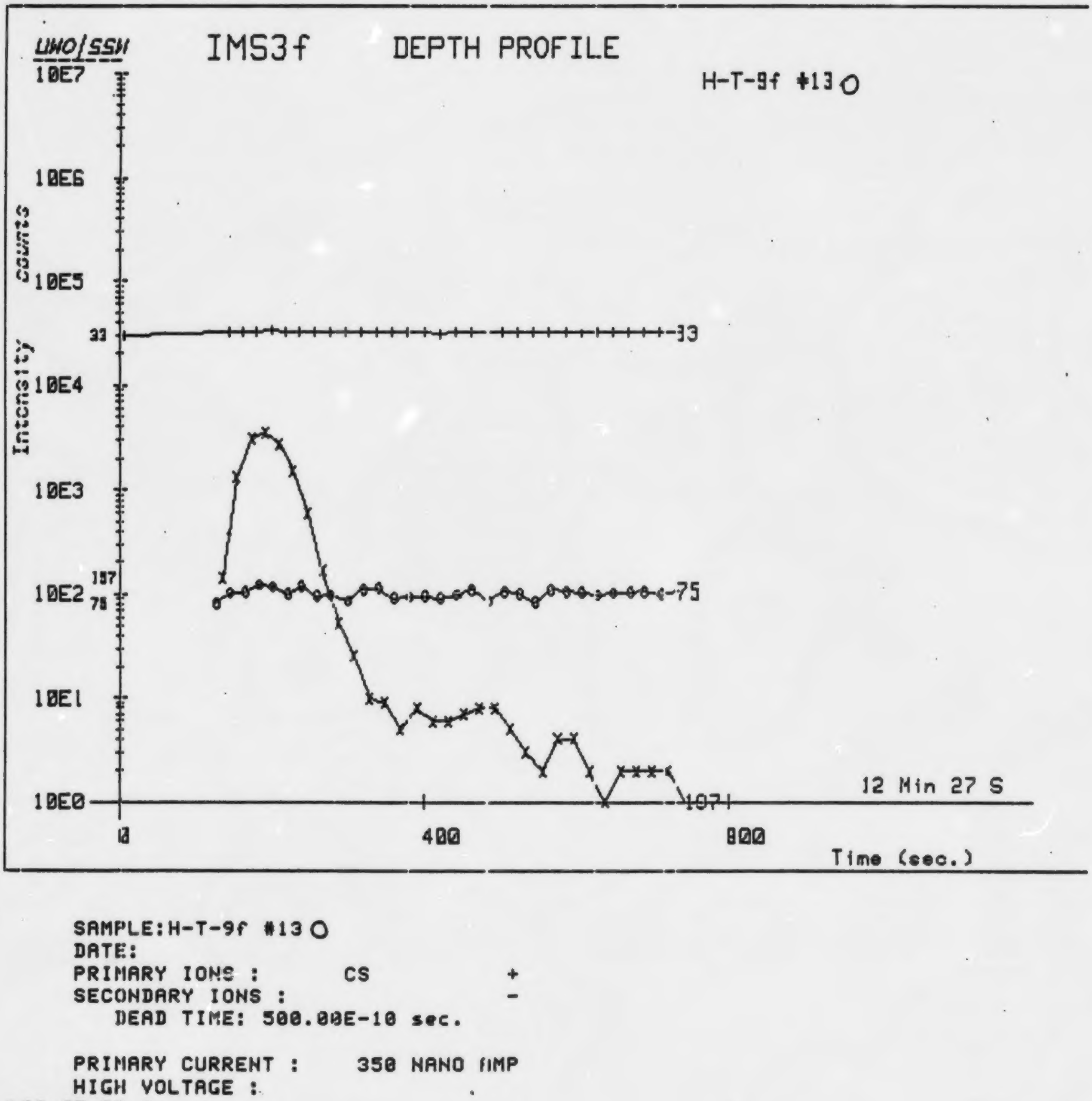

```
SAMPLE:H-T-9f #13 O
DATE:
PRIMARY IONS :       CS          +
SECONDARY IONS :                 -
   DEAD TIME: 500.00E-10 sec.

PRIMARY CURRENT :    350 NANO AMP
HIGH VOLTAGE :
156.65 DD.D
KILOVOLTS
RASTERING :            250 MICRONS
TRANSFER OPTICS :      150 MICRONS
FIELD APERTURE :   1  2  3
CONTRAST APERTURE :  4  3  2  :
```

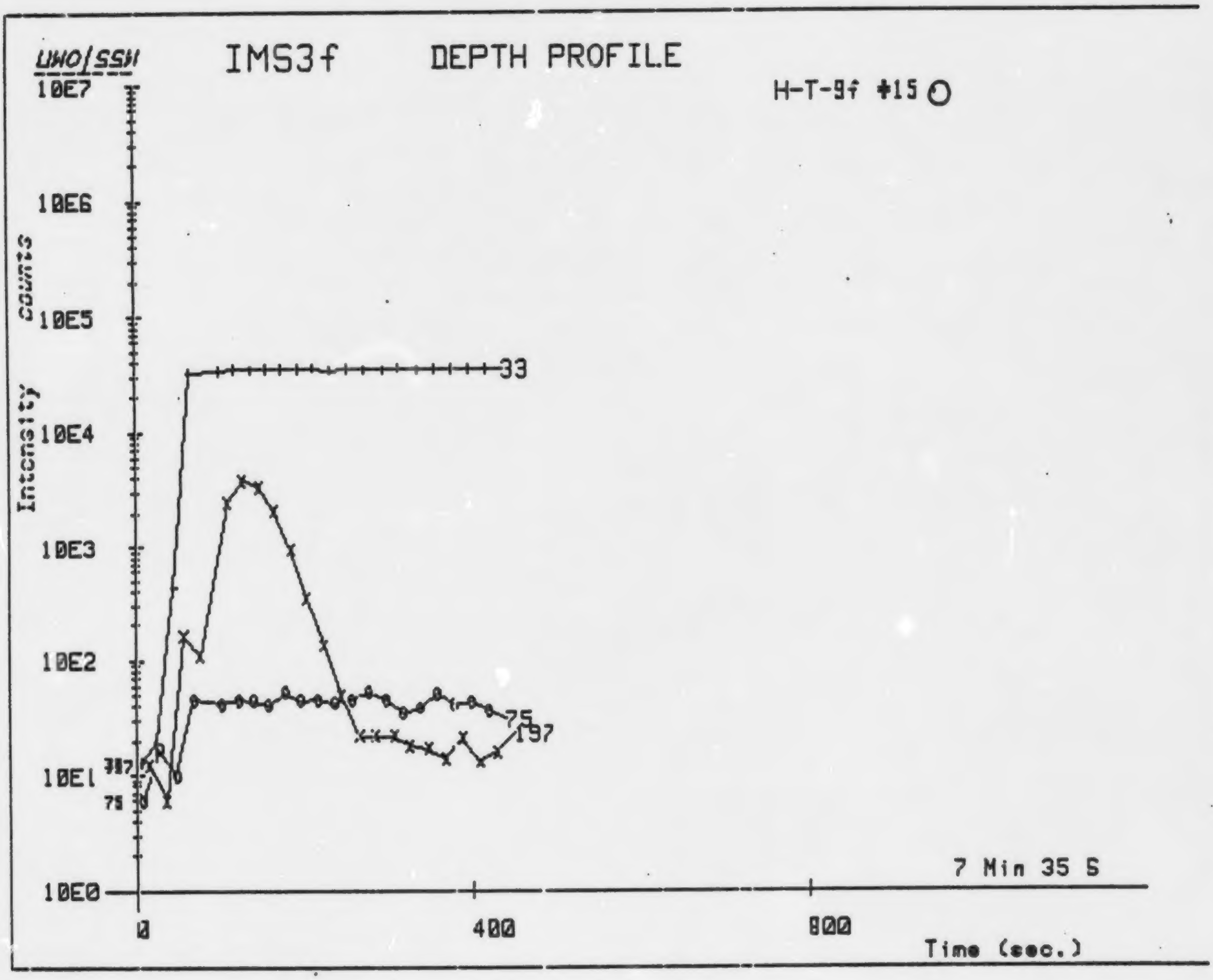

```
    SAMPLE:H-T-9f #15 O
    DATE:
    PRIMARY IONS :       CS          +
    SECONDARY IONS :                 -
       DEAD TIME: 500.00E-10 sec.

    PRIMARY CURRENT :    343 NANO AMP
    HIGH VOLTAGE :
156.65 DD.D
 <ILOVOLTS
    RASTERING :           250 MICRONS
    TRANSFER OPTICS :     150 MICRONS
    FIELD APERTURE :.  1  2  3
    CONTRAST APERTURE :  4  3  2  :
```

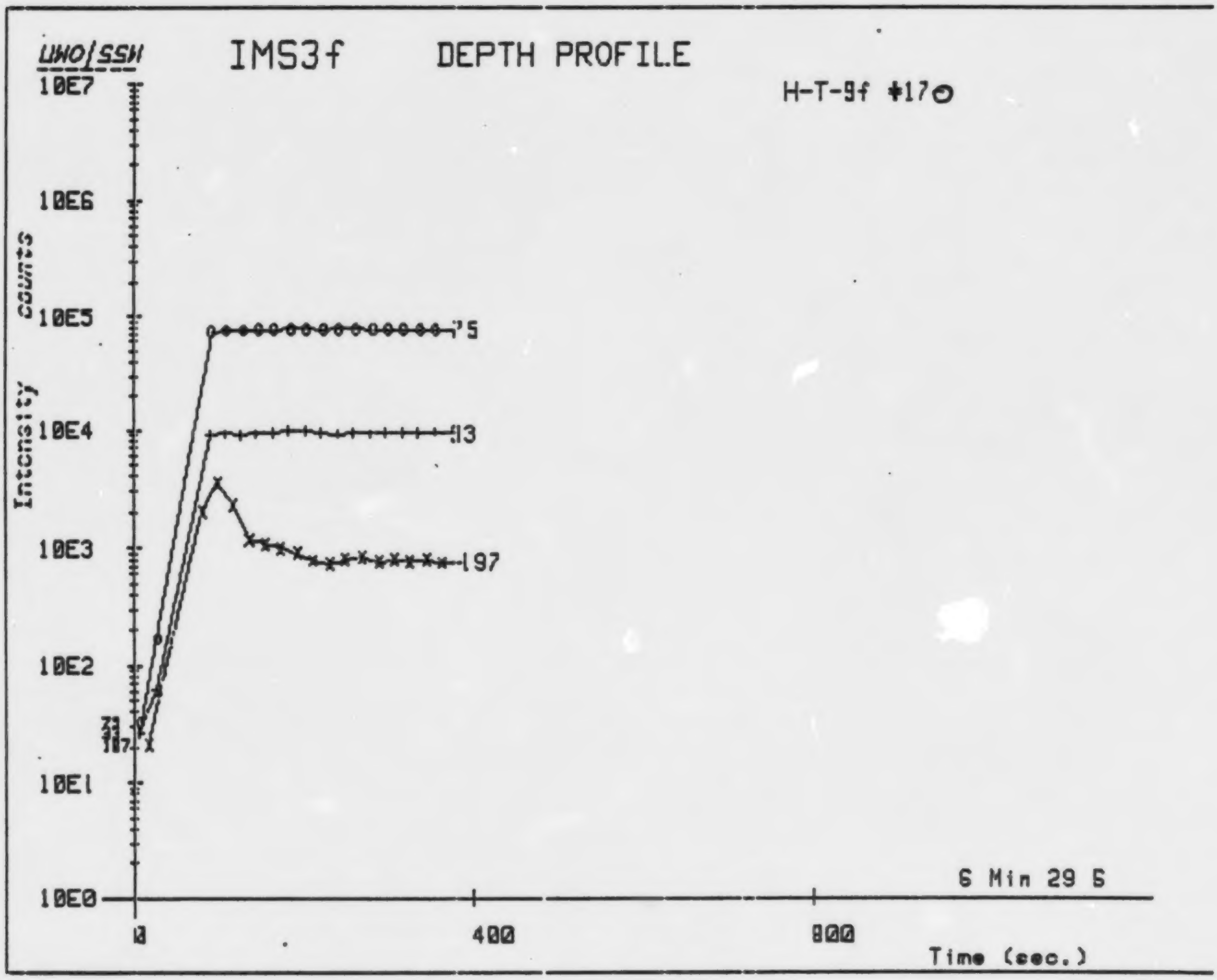

```
SAMPLE:H-T-9f #170
DATE:
PRIMARY IONS :       CS          +
SECONDARY IONS :                 -
   DEAD TIME: 500.00E-10 sec.

PRIMARY CURRENT :    332 NANO AMP
HIGH VOLTAGE :
156.65 DD.D
 <ILOVOLTS
RASTERING :          250 MICRONS
TRANSFER OPTICS :    150 MICRONS
FIELD APERTURE :   1  2  3
CONTRAST APERTURE :  4  3  2  :
```

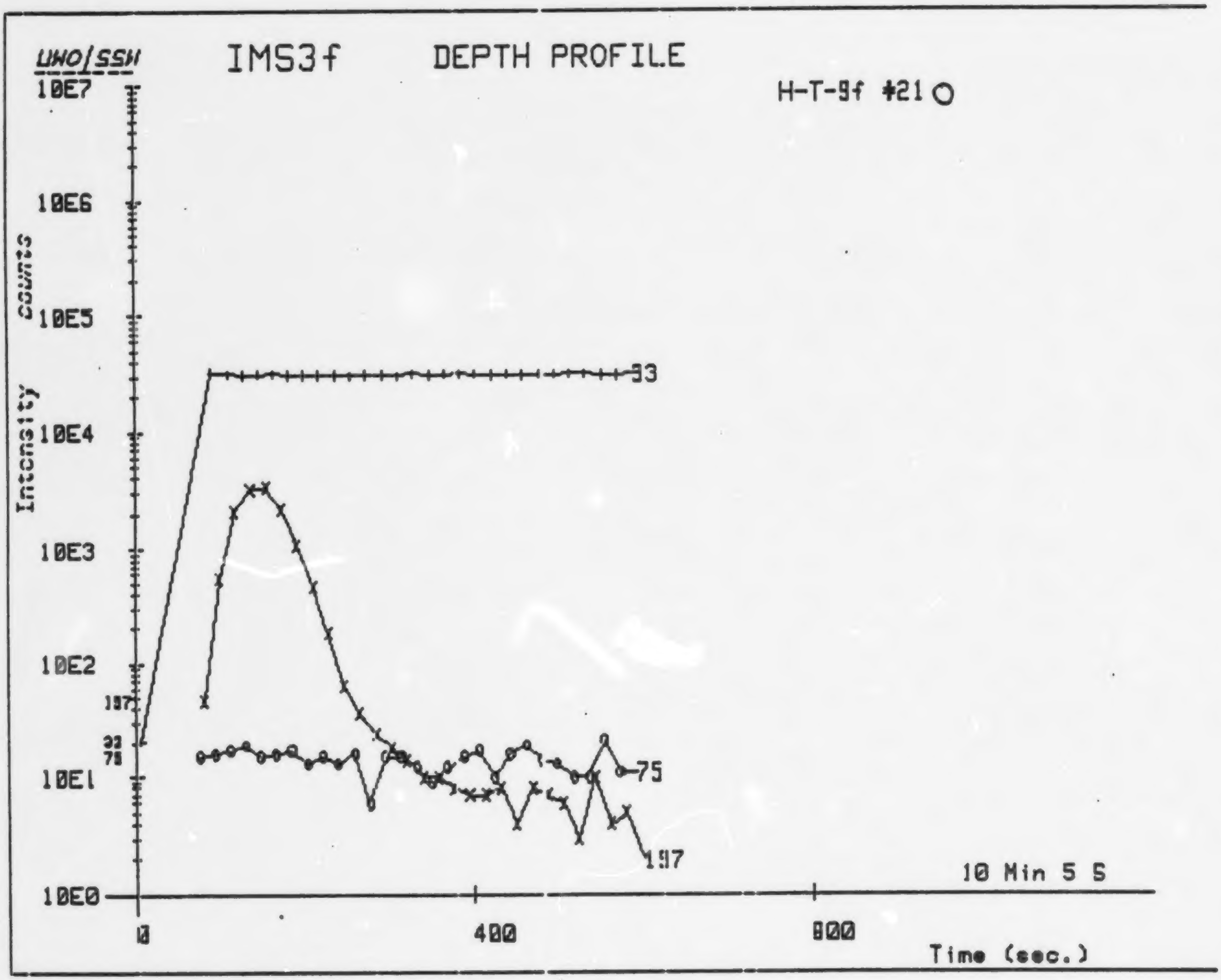

```
SAMPLE:H-T-9f #21 O
DATE:
PRIMARY IONS :       CS           +
SECONDARY IONS :                  -
   DEAD TIME: 500.00E-10 sec.

PRIMARY CURRENT :    325 NANO AMP
HIGH VOLTAGE :
156.65 DD.D
 <ILOVOLTS
RASTERING :            250 MICRONS
TRANSFER OPTICS :      150 MICRONS
FIELD APERTURE :   1  2  3
CONTRAST APERTURE :  4  5  6  .
```

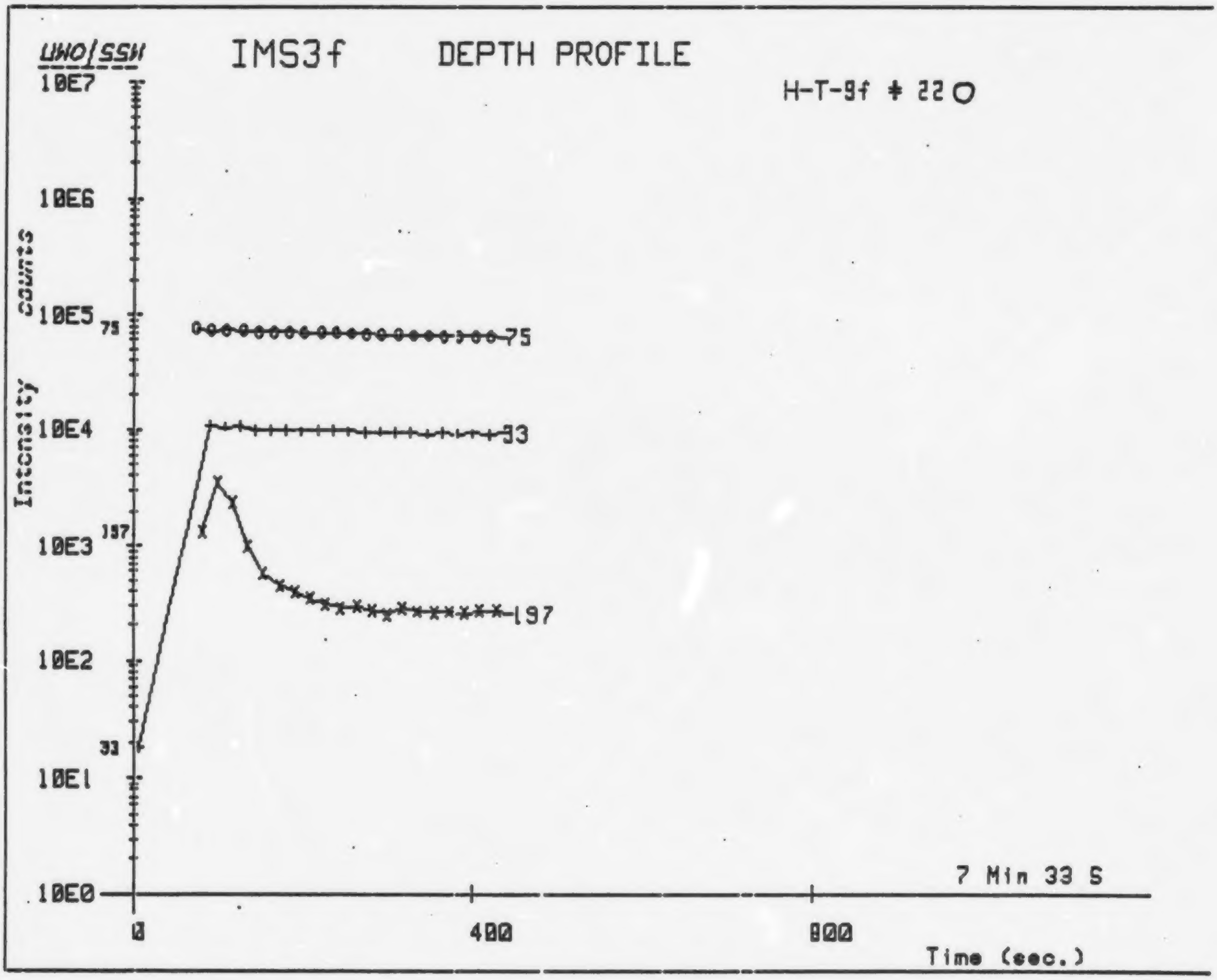

```
    SAMPLE:H-T-9f # 22○
    DATE:
    PRIMARY IONS :       CS          +
    SECONDARY IONS :                 -
       DEAD TIME: 500.00E-10 sec.

    PRIMARY CURRENT :    330 NANO AMP
    HIGH VOLTAGE :
156.65 DD.D
 <ILOVOLTS
    RASTERING :           250 MICRONS
    TRANSFER OPTICS :     150 MICRONS
    FIELD APERTURE :  1  2  3
    CONTRAST APERTURE :  4  3  2
```

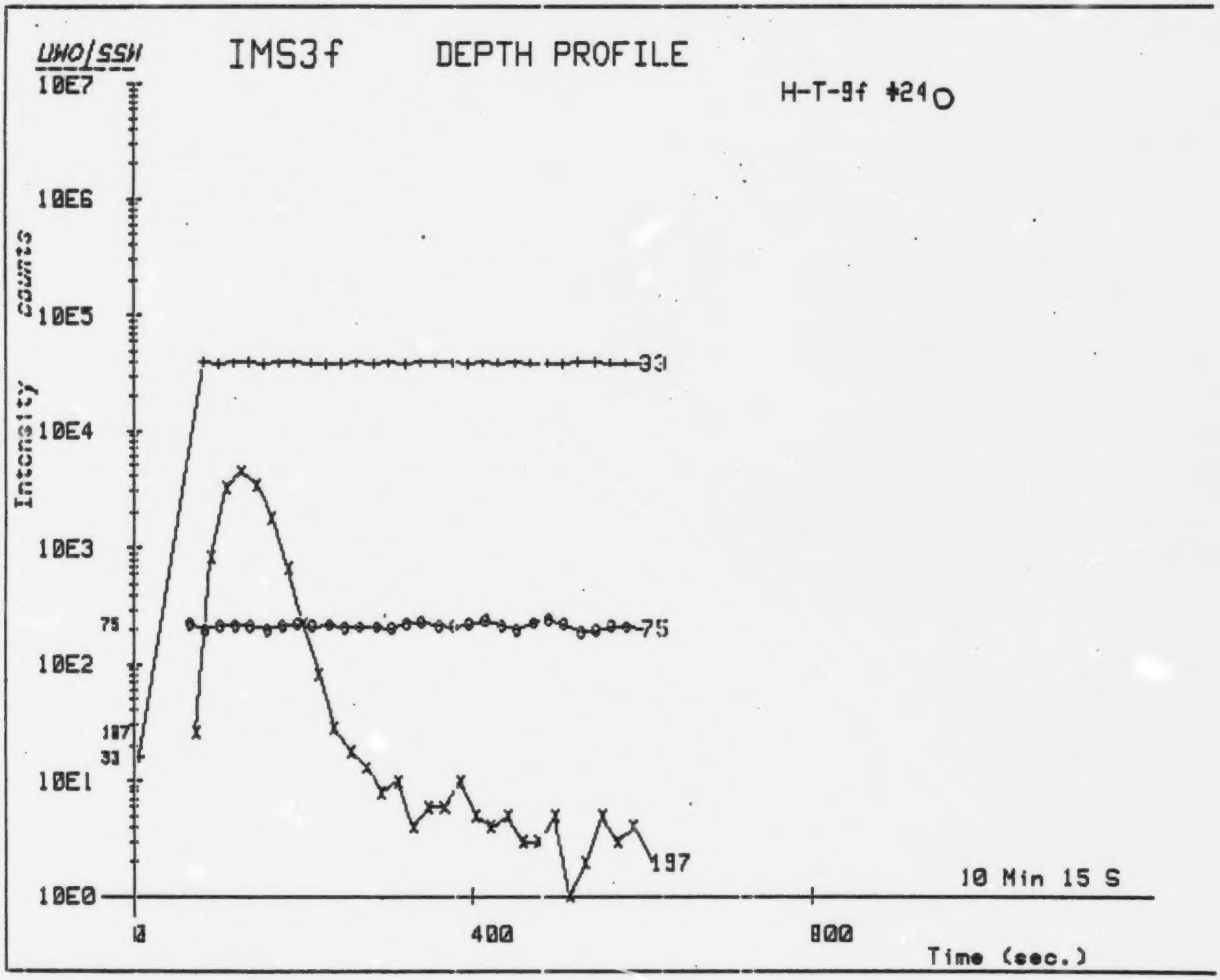

```
    SAMPLE:H-T-9f #24O
    DATE:
    PRIMARY IONS :        CS          +
    SECONDARY IONS :                  -
       DEAD TIME: 500.00E-10 sec.

    PRIMARY CURRENT :     387 NANO AMP
    HIGH VOLTAGE :
156.65 DD.D
 <ILOVOLTS
    RASTERING :           250 MICRONS
    TRANSFER OPTICS :     150 MICRONS
    FIELD APERTURE :   1  2  3
    CONTRAST APERTURE :  4  3  2  :
```

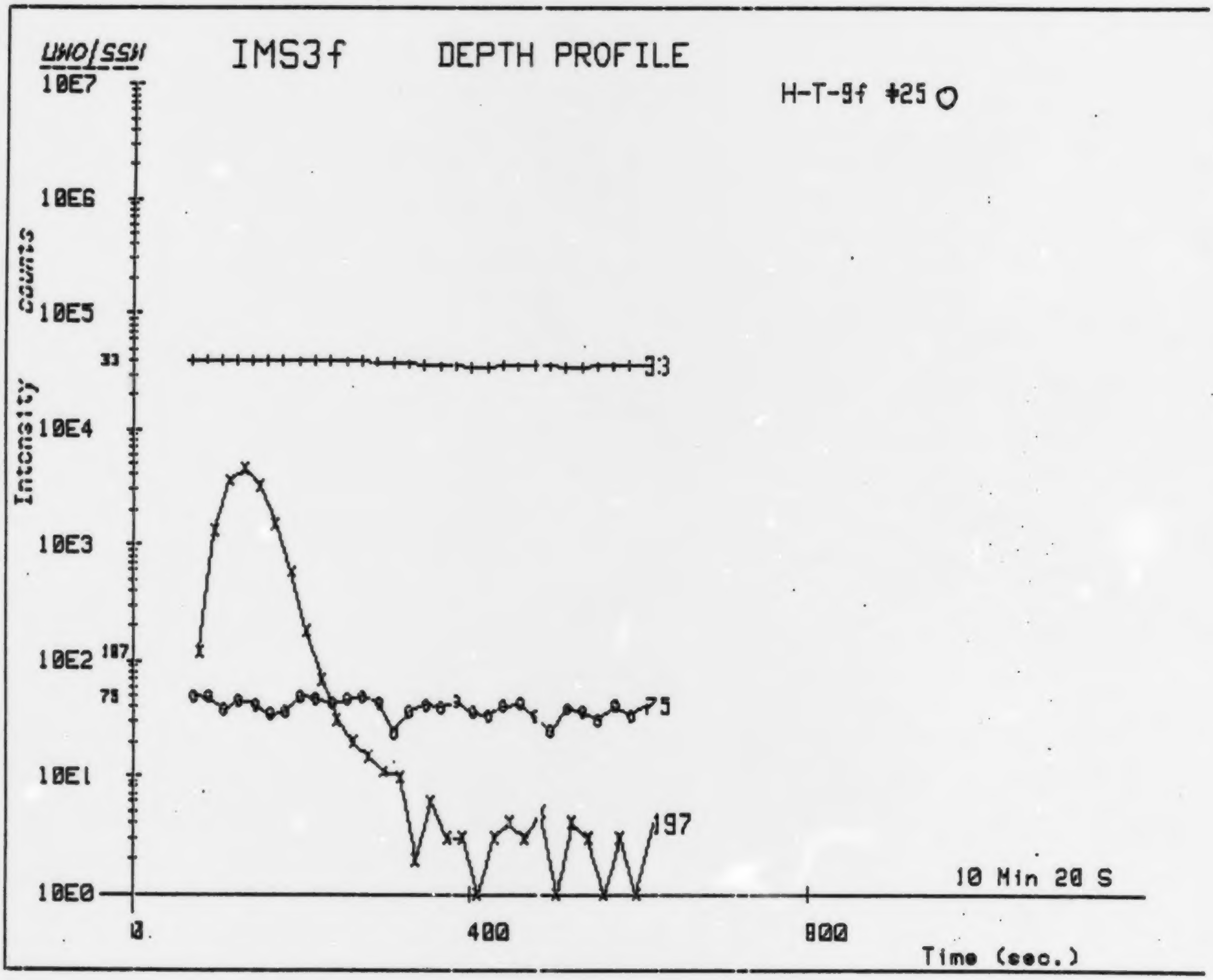

```
    SAMPLE:H-T-9f #25 O
    DATE:
    PRIMARY IONS :       CS           +
    SECONDARY IONS :                  -
       DEAD TIME: 500.00E-10 sec.

    PRIMARY CURRENT :    388 NANO AMP
    HIGH VOLTAGE :
156.65 DD.D
 <ILOVOLTS
    RASTERING :           250 MICRONS
    TRANSFER OPTICS :     150 MICRONS
    FIELD APERTURE :   1  2  3
    CONTRAST APERTURE :  4  3  2
```

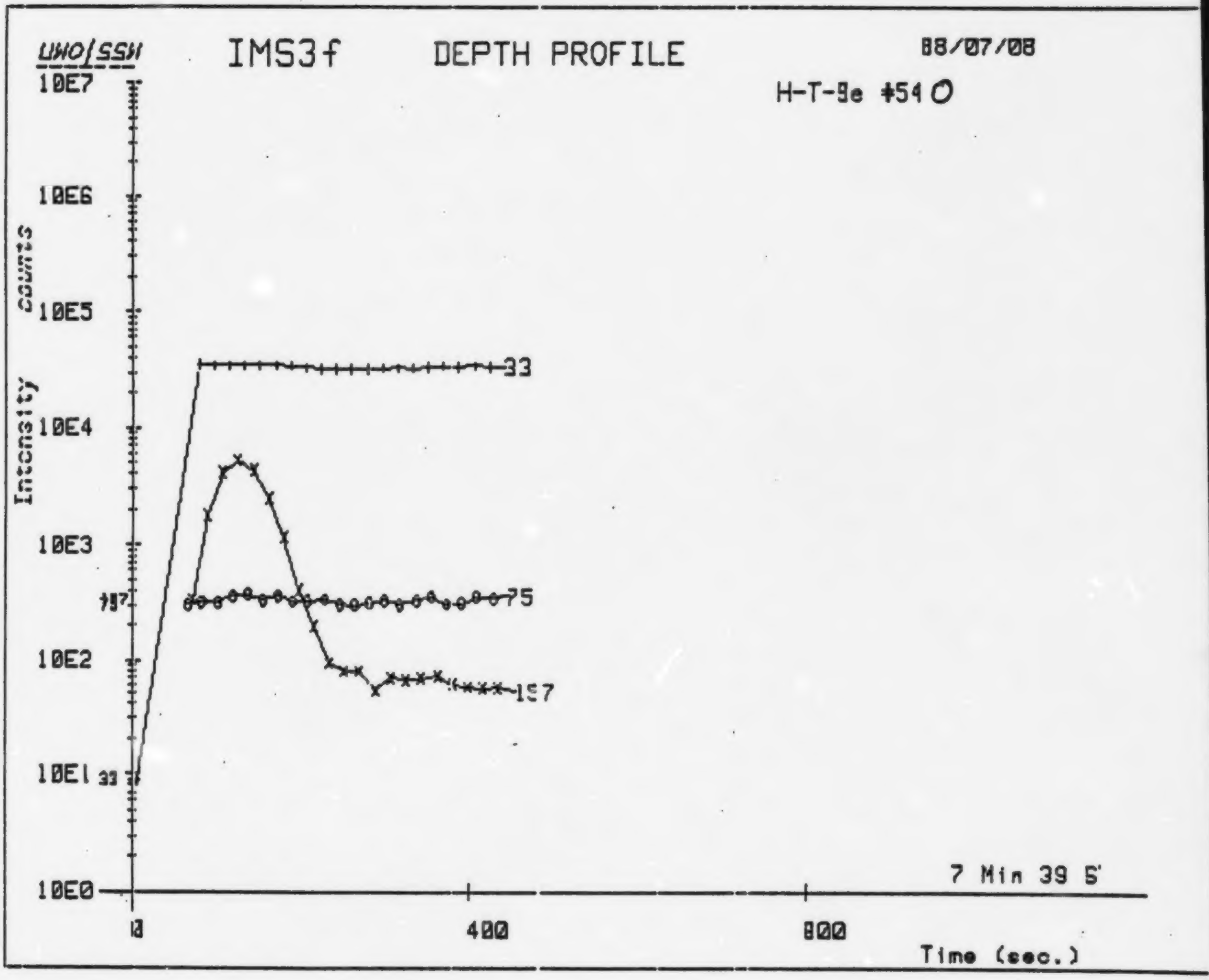

```
    SAMPLE:H-T-9e #54 O
    DATE:88/07/08
    PRIMARY IONS :      CESILM      +
    SECONDARY IONS :                -
       DEAD TIME: 500.00E-10 sec.

    PRIMARY CURRENT :    375 NANO AMP
    HIGH VOLTAGE :
156.65 DD.D
 <ILOVOLTS
    RASTERING :           250 MICRONS
    TRANSFER OPTICS :     150 MICRONS
    FIELD APERTURE :   1  2  3
    CONTRAST APERTURE :  4  3  2  :
```

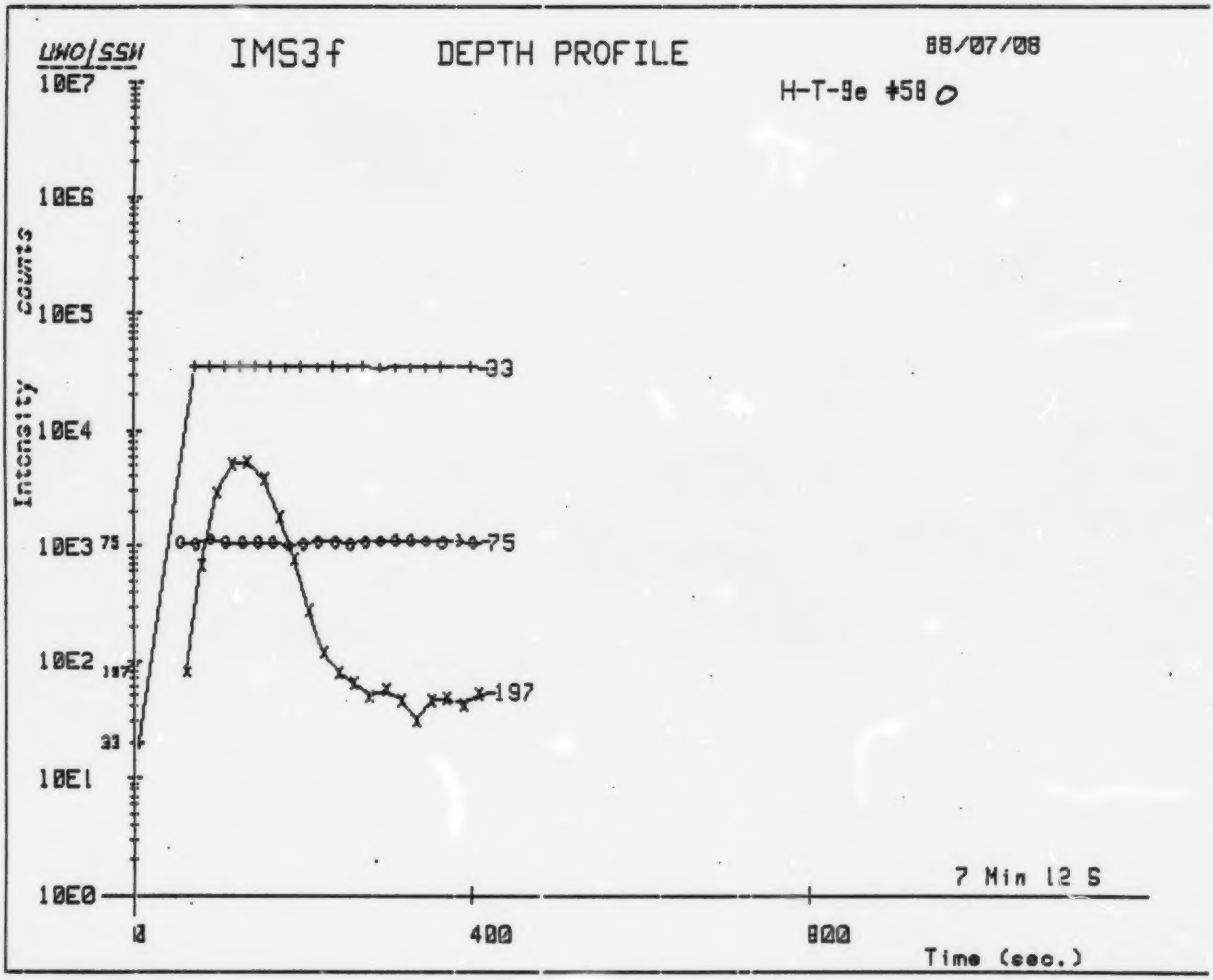

```
    SAMPLE:H-T-9e #58 O
    DATE:88/07/08
    PRIMARY IONS :        CESIUM      +
    SECONDARY IONS :                  -
       DEAD TIME: 500.00E-10 sec.

    PRIMARY CURRENT :     373 NANO AMP
    HIGH VOLTAGE :
156.65 DD.D
 KILOVOLTS
    RASTERING :             250 MICRONS
    TRANSFER OPTICS :       150 MICRONS
    FIELD APERTURE :    1  2  3
    CONTRAST APERTURE :  4  3  2  :
```

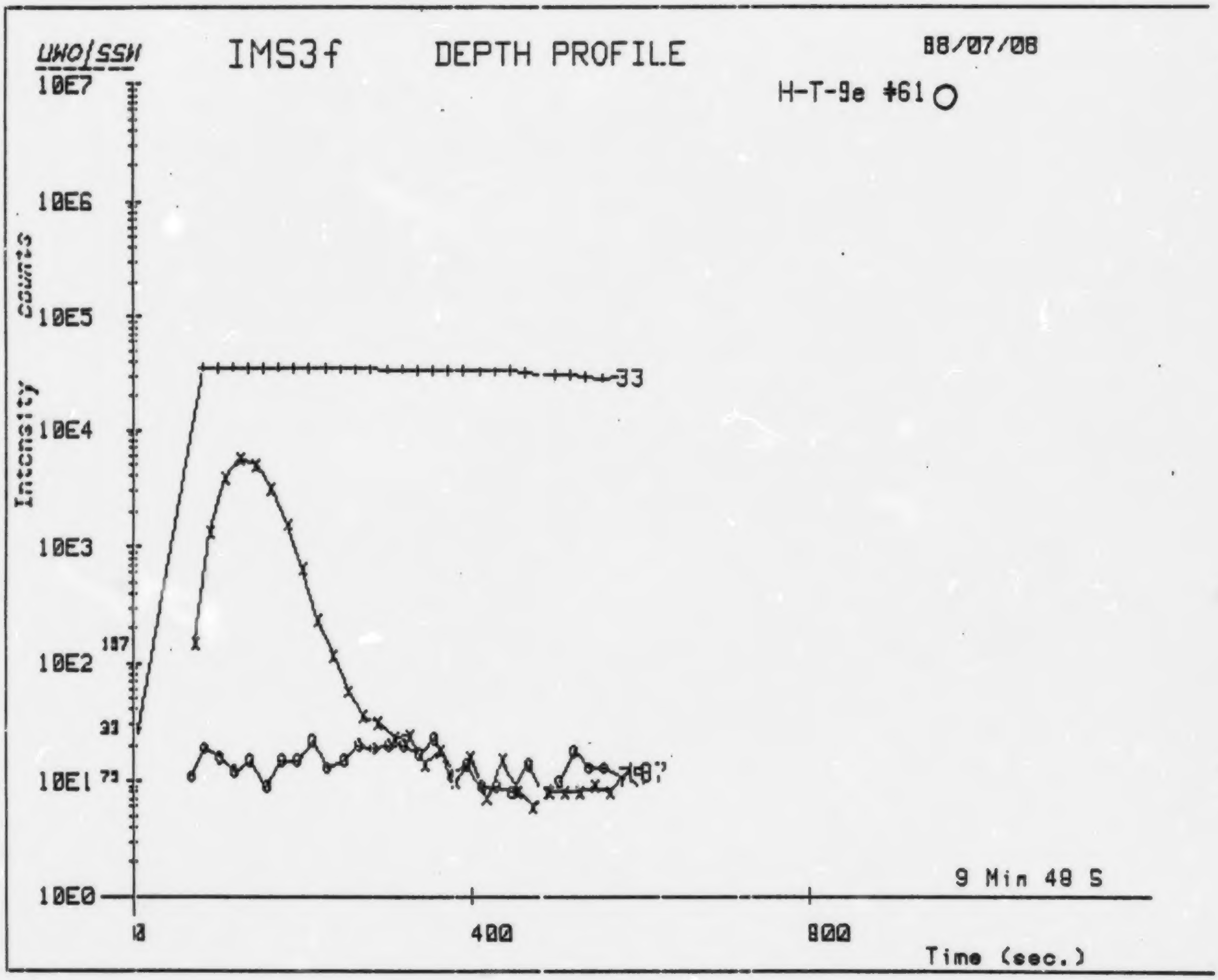

```
    SAMPLE:H-T-9e #61O
    DATE:88/07/08
    PRIMARY IONS :       CESILM      +
    SECONDARY IONS :                 -
       DEAD TIME: 500.00E-10 sec.

    PRIMARY CURRENT :     370 NANO AMP
    HIGH VOLTAGE :
156.65 DD.D
 <ILOVOLTS
    RASTERING :           250 MICRONS
    TRANSFER OPTICS.:     150 MICRONS
    FIELD APERTURE :   1  2  3
```

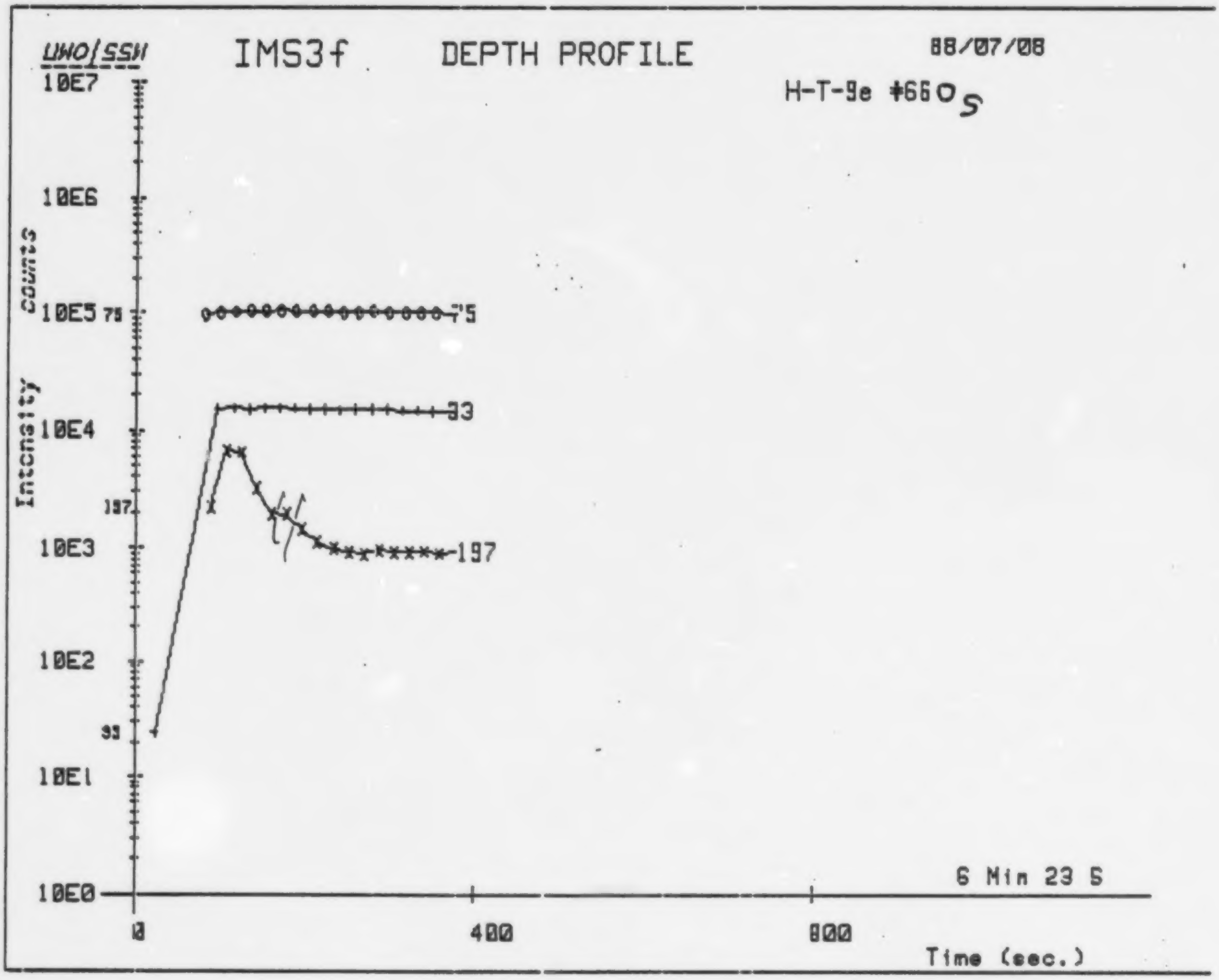

SAMPLE:H-T-9e #66 O
DATE:88/07/08
PRIMARY IONS : CESILM +
SECONDARY IONS : -
DEAD TIME: 500.00E-10 sec.

PRIMARY CURRENT : 369 NANO AMP
HIGH VOLTAGE :
156.65 DD.D
<ILOVOLTS
RASTERING : 250 MICRONS
TRANSFER OPTICS : 150 MICRONS
FIELD APERTURE : 1 2 3
CONTRAST APERTURE : 4 3 2

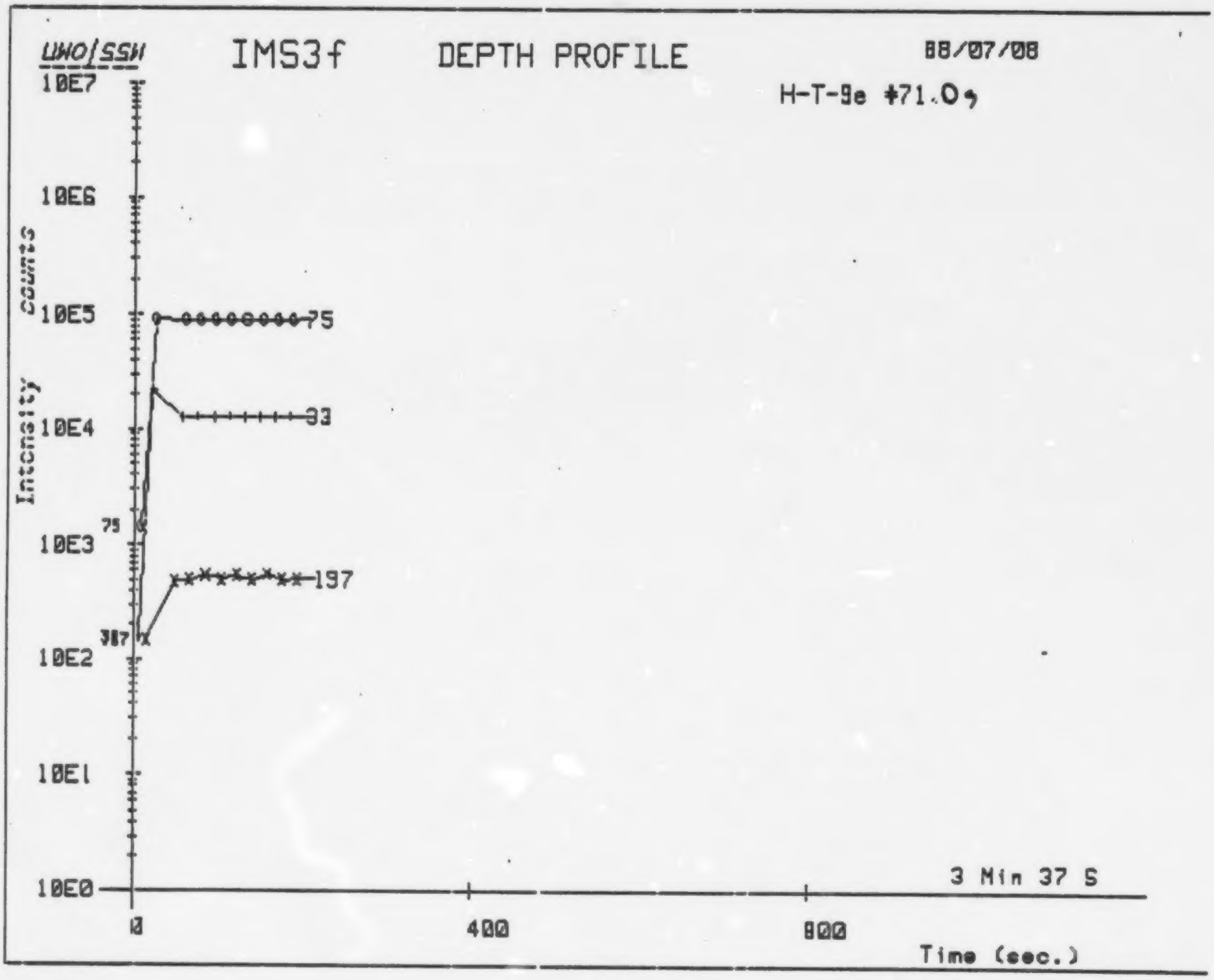

```
    SAMPLE:H-T-9e #71 09
    DATE:88/07/08
    PRIMARY IONS :       CESILM      +
    SECONDARY IONS :                 -
       DEAD TIME: 500.00E-10 sec.

    PRIMARY CURRENT :     381 NANO /IMP
    HIGH VOLTAGE :
156.65 DD.D
 <ILOVOLTS
    RASTERING :            250 MICR(INS
    TRANSFER OPTICS :      150 MICR(INS
    FIELD APERTURE :   1  2  3
    CONTRAST APERTURE :  4  3  2  :
```

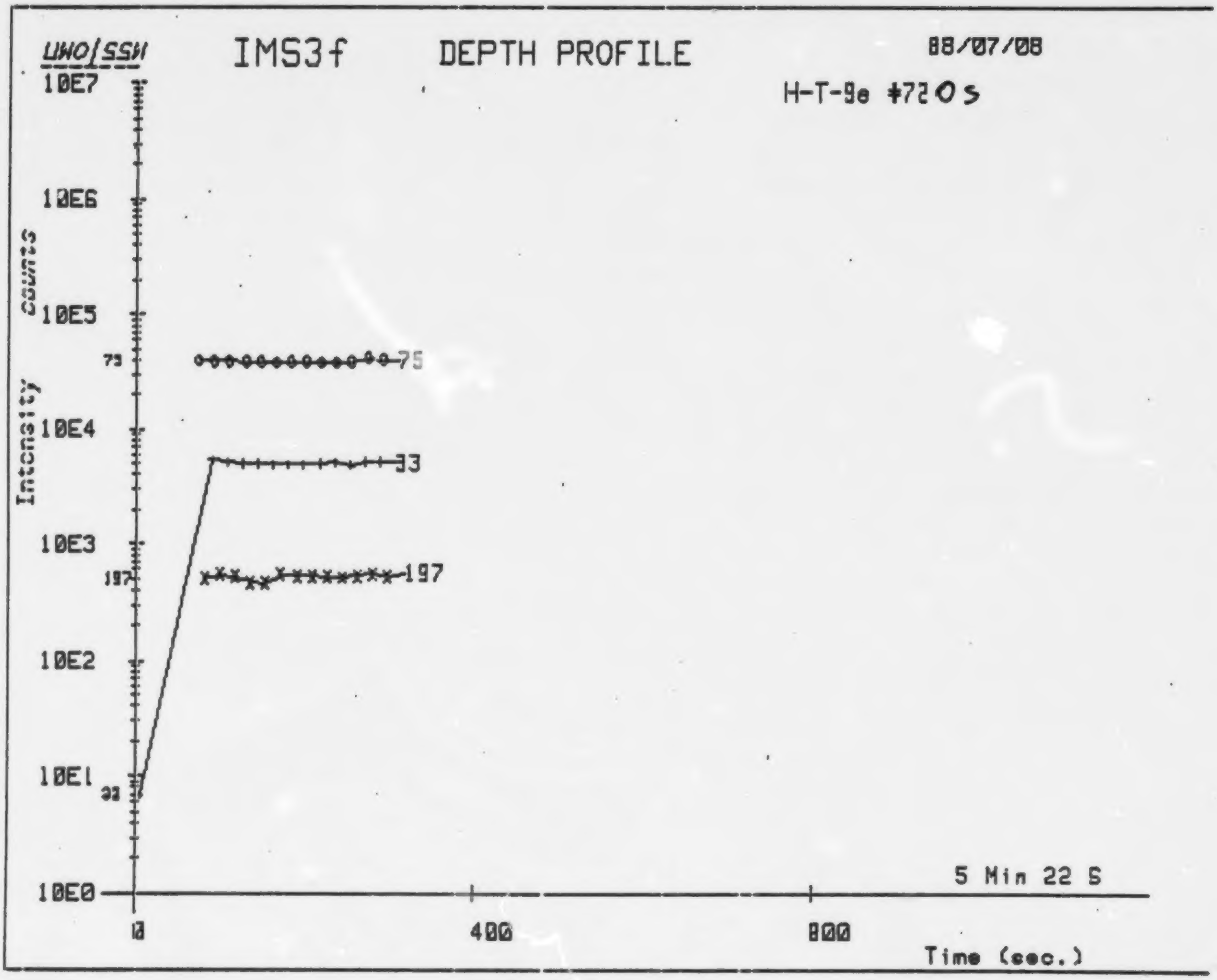

```
    SAMPLE:H-T-9e #72 0s
    DATE:88/07/08
    PRIMARY IONS :      CESILM       +
    SECONDARY IONS :                 -
       DEAD TIME: 500.00E-10 sec.

    PRIMARY CURRENT :    375 NANO AMP
    HIGH VOLTAGE :
156.65 DD.D
 <ILOVOLTS
    RASTERING :           250 MICRONS
    TRANSFER OPTICS :     150 MICRONS
    FIELD APERTURE :   1  2  3
    CONTRAST APERTURE :  4  3  2  :
```

APPENDIX A2

ASSAYS OF HEAVY AND LIGHT FRACTIONS

	Mass Split	Au g/t	Au Distribution	As ppm	S %
Tailings	100	0.675 ±0.10	100	1040 ± 120	13.2 ± 1.2
Light fraction	79	0.15	17	120	0.65
Heavy fraction	21	2.67 (calc)	83	4500 (calc)	53 (calc)

DISTRIBUTION OF INVISIBLE GOLD IN HEAVY AND LIGHT FRACTIONS

	HEAVY FRACTION		LIGHT FRACTION	
	assay	distrib. %	assay	distrib. %
Assayed Au	2.67 (calc)	100.0	0.15	100.0
Invisible gold in arsenopyrite (30.2 ± 8.6 ppm) (0.87 % of heavy 0.025 % of light)	0.26 ±0.07	9.7 ±2.6	0.008 ±0.002	5.3 ±1.5
Invisible gold in pyrite (0.72 ± 0.38 ppm) (100 % of heavy 1.22 % of light)	0.72 ±0.38	26.9 ±14.2	0.009 ±0.005	6.0 ±3.1
Total invisible gold	0.98	36.6 +16.8	0.017	11.3 ± 4.6

CHAPTER 3

DIRECT DETERMINATION OF THE INVISIBLE GOLD CONTENT OF PYRITE AND IMPLICATIONS ON THE CYANIDATION OF THE AUDREY RESSOURCES TAILINGS.

SSW/PMS/88/13

SUMMARY

Electrum, with 13% silver is the only gold mineral observed in the final tailings sample from the Norberc concentrator, when processing a gold bearing copper/zinc massive sulphide ore of Ressources Audrey Inc. All eight electrum grains observed were enclosed or associated with pyrite and had an average size of 8 µm². Thirty two percent of the gold in the tailings is recoverable by direct cyanidation at a grind of K_{80} = 14 µm. Fine grinds did not significantly increase the recovery.

Of the remaining 68% of the total gold which reported to the cyanide leach residue, all may be accounted for as 'invisible' gold in the pyrite with a precision of 11.6 %. Pyrite is the principal gold bearing mineral in the final tailings. The average 'invisible' gold concentration of the pyrite is 1.41 ± 0.23 g/t. Pyrite is the only major sulphide in the tailings, accounting for 69.7% by weight.

FIGURE 1

MINERALOGICAL DISTRIBUTION OF GOLD

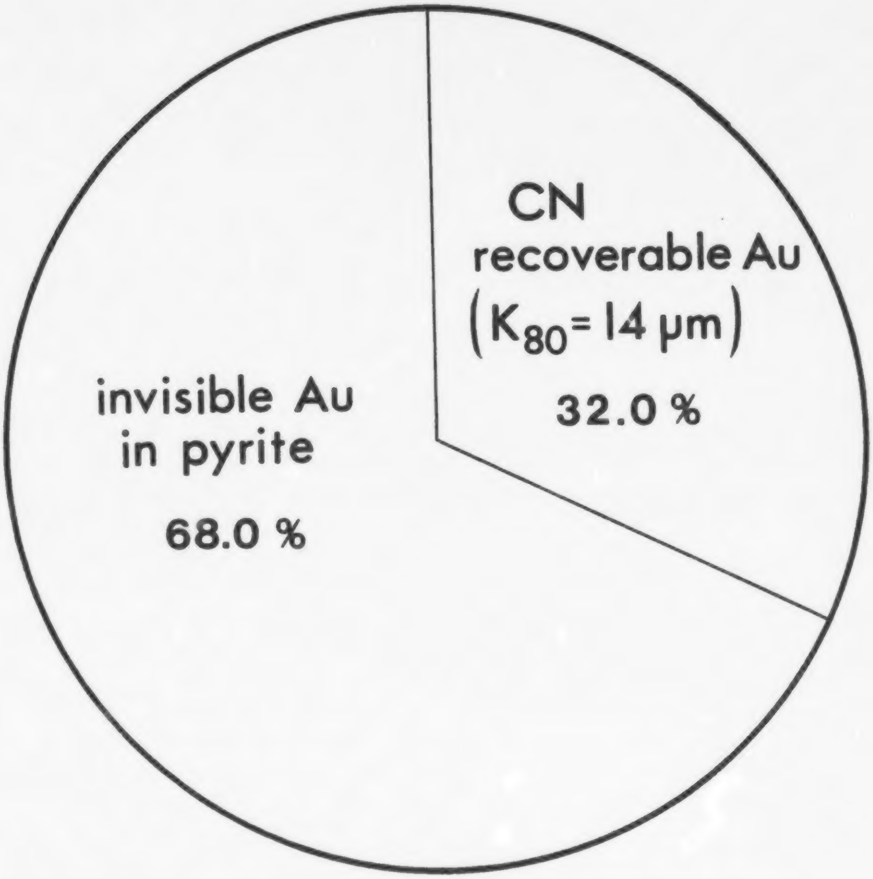

TABLE 1

MINERALOGICAL DISTRIBUTION OF GOLD IN TAILINGS

	Au g/t	Distribution %	Precision
Tailings	1.44 ± 0.05	100.0	± 3.5
CN- recoverable Au (K_{80} = 14 µm)	0.46 ± 0.02	32.0	± 1.5
Invisible gold in pyrite (69.7 ± 4.8% normative Wt. %)	0.98 ± 0.17	68.0	±11.6
Total accounted gold	1.44 ± 0.49	100.0	+11.7

LIST OF TABLES

Table 1 Mineralogical distribution of gold in tailings
Table 2 Results of cyanidation testing
Table 3 Results of sieve testing and heavy liquid separation
Table 4 Chemical assays of tailings
Table 5 Image analysis and normative mineralogy of tailings and heavy and light fractions
Table 6 Statistical analysis of visible gold grains in the tailings
Table 7 Electron probe microanalysis of electrum grains
Table 8 Invisible gold concentration in sulphides

LIST OF FIGURES

Figure 1 Mineralogical distribution of gold in tailings
Figure 2 Distribution of invisible gold in pyrite.

LIST OF PLATES

Plate 1 Photograph of gold grain in chip samples
Plate 2 Photograph of gold grain in chip sample

APPENDICES

A1 Image analysis of gold grains in the chip samples
A2 Image analysis of gold grains in the tailings
A3 Calculation of visible gold in the tailings

3.1.0 INTRODUCTION

Mr. Michel Bouchard, vice president and exploration manager with Ressources Audrey Inc. requested the determination of the invisible gold concentration in the sulphides from the Mobrun Mine, Que., as part of the general project on the characterisation of Canadian refractory gold ores by ion probe microanalysis. The aim of this major project is to assist in improving the gold recovery by providing detailed information on the gold mineralogical distribution. The approach followed is that of a process mineralogical study coupled with metallurgical testing (Chryssoulis, 1987).

The objective of this particular study was the determination of the nature of the gold in the final tailings of the Norberc concentrator; in order to (i) assess the amenability to direct cyanidation and (ii) assist in the optimization of the process.

At present, approximately 40% of the gold is lost to the final tailings. On the basis of the detailed gold mineralogical distribution, the size and association of the gold-bearing minerals, the gold recovery by direct cyanidation from the flotation tailings is discussed.

The study was financed by Ressources Audrey Inc., CANMET, the Geological Survey of Canada and the Department of Supply and Services (DSS contract no 23440-7-9037/01 SS)

3.2.0 METHODOLOGY

Chip samples of massive fine-grained pyrite ore from the Mobrun Mine and samples from the final tailings (August 1987) and the copper concentrate (March 1988) from the Norberc concentrator were recieved for this study. Six polished blocks were prepared for a general microscopic study.

The sample of the final tailings, where 40% of the gold is lost was used for the detailed process mineralogical study and metallurgical testing. The procedure followed is described in Chapter 1. Cyanidation tests were performed

---

footnote: 'invisible gold' is a general term including both gold in solid solution in the sulphide crystal lattice and sub-micron, less than 0.1 µm, gold inclusions dispersed in the sulphide.

on three 500 g charges using progressively finer grinds to determine the cyanide recoverable gold and the effect of grinding upon recovery. Conditions are given in Table 2. A sub-sample was sieved into the following size fractions +90 µm, 90-53 µm, 53-37 µm and -37 µm. Mass splits are given in Table 3. The +90 µm fraction comprising 4.3 % of the weight was separated using sodium polytungstate (S.G. 3.0 $g.cm^{-3}$). The heavy to light fraction split was in the ratio 2.6:1.7. Nine polished blocks were prepared from the +90 µm sink fraction for ion probe microanalysis of gold in pyrite, (Chryssoulis et el, 1987). These samples and an additional eighteen blocks from the 37-53 µm and 53-90 µm sink fractions were examined by optical and scanning electron microscopy to determine the size and association of the visible gold. The silver content of electrum was determined by electron probe microanalysis (EPMA).

The pyrite content of the tailings, required for the calculation of the fraction of total gold present as invisible gold in pyrite, was determined from the sulphur assay by attributing all sulphur to FeS_2. The error introduced by ignoring all other sulphur-bearing species which are present only in trace amounts, is well within the relative error of the sulphur assay, 1.8 % versus 7% (see Tables 4 and 5).

The sample of the copper concentrate was examined optically to determine the size, distribution and association of the recovered visible gold.

3.3.0 RESULTS

3.3.1 Chemical Assays

Chemical assays of the final tailings as received, are given in Table 4. Also reported is the assay of the light fraction and the calculated assay of the heavy fraction.

3.3.2 Mineralogy of Ores

Major minerals: Pyrite, chalcopyrite, sphalerite

Minor minerals: Pyrrhotite, galena, arsenopyrite, electrum, native bismuth, cassiterite, stannite.

TABLE 2

CYANIDATION TEST RESULTS

				HEAD		CONSUMPTION	
Test No.	K_{80} µm	% Extrn Au	Residue g/t Au	Calc. g/t Au	Direct g/t Au	NaCN Kg/t	CaO Kg/t
1	70	10.1	1.15	1.27	1.39	2.9	3.2
2	24	22.9	1.04	1.35	1.45	5.2	2.3
3	14	25.1	0.98	1.31	1.47	4.7	2.6

Test No.	Au recovery, %	Au recovered, g/t
1	20	0.29
2	28	0.32
3	32	0.46

$$\text{Au recovered} = \frac{(\text{Mean direct head}) - (\text{Residue})}{(\text{Mean direct head})}$$

Mean direct head: 1.44 ± 0.05 g/t Au

Au non-recoverable by direct cyanidation =

1.44 - 0.46 = 0.98 g/t

Conditions: 33% solids, 1 g/l NaCN, pH 10.5-11.0, 48 hours.

TABLE 3

RESULTS OF SIEVE TESTING AND HEAVY LIQUID SEPARATION

FRACTION	MASS SPLIT %	SINK	FLOAT
-37 µm	71.8	63.3 (88.2%)	8.5 (11.8%)
37 - 53 µm	8.9	7.7 (86.5%)	1.2 (13.5%)
53 - 90 µm	13.0	11.0 (84.6%)	2.0 (15.4%)
+ 90 µm	4.3	2.6 (60.0%)	1.7 (40.0%)
TOTAL	98.0	84.6	12.4

TABLE 4

CHEMICAL ASSAYS

	mass split%	Au (g/t)	Au distrib.	S %	Te ppm	As ppm	Bi ppm	Sb ppm
Tailings	100	1.44 ±0.05	100.0	37.2 ±2.6	9	610	<20	<20
Light fraction	21	0.17	2.5	-	-	-	-	-
Heavy fraction	79	1.78(calc)	97.5	-	-	-	-	-

* 69.6 ± 4.9 % normative pyrite, assuming all the sulphur is present as pyrite.

The massive ores feature closely packed small aggregated grains of pyrite, generally less than 50 μm in size. Minor chalcopyrite and sphalerite are present in the matrix between the pyrite grains. Small scale quartz veining through the ores carries the majority of the chalcopyrite and sphalerite grains, which are of larger size than the pyrite. Also present in the micro-veining are very small grains of arsenopyrite and galena. Additionally, the micro-veinlets carry larger euhedral grains of pyrite, up to 100 μm in size, which genetically belong to a discrete later generation. The pyrite contains ubiquitous tiny inclusions of both silicate minerals and of other sulphides (chalcopyrite, sphalerite, galena and pyrrhotite in decreasing order of importance). Inclusions of chalcopyrite are widespread in the sphalerite, which also contains inclusions of pyrite.

Gold Minerals

Seven grains of electrum have been identified in the six chip samples (Appendix A1). Five were present as inclusions within chalcopyrite. These were small and had sizes of 4, 5, 2, 2, and 5 μm^2 respectively. Two much larger grains were observed. These were present at the interface between chalcopyrite and sphalerite in the ore matrix between pyrites. Grain size was 3750 μm^2 and 2746 μm^2. No gold minerals occuring as inclusions within pyrite grains were seen, and no telluride minerals were noted. A photograph of a larger grain is shown in Plate 2. A smaller electrum grain, included in pyrite is shown in Plate 1 (from the tailings). The total area of electrum in the chip samples was 6514 μm^2.

3.3.3 Mineralogy of Tailings

Pyrite

Three texturally distinct types of pyrite particles are recognised in the final tailings. The first is coarser grained and relatively free of inclusions. The second is also coarse grained but with abundant cavities and inclusions of both gangue and of sulphide minerals, giving the pyrite a spotted appearance. The last type is that of aggregates of fine-grained pyrite, less than 10 μm in diameter. The gold inclusions in the tailings appear to be located within the coarser grained type of pyrite.

Plate 1

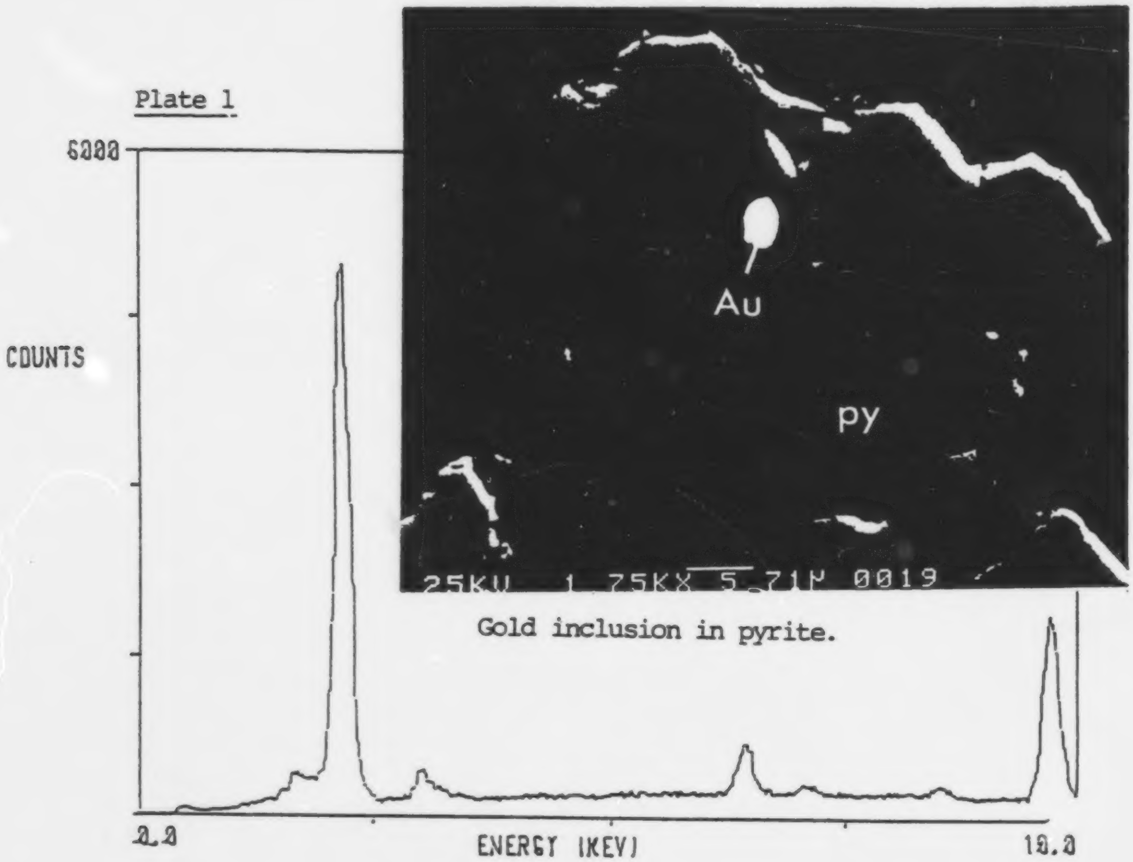

Gold inclusion in pyrite.

Plate 2

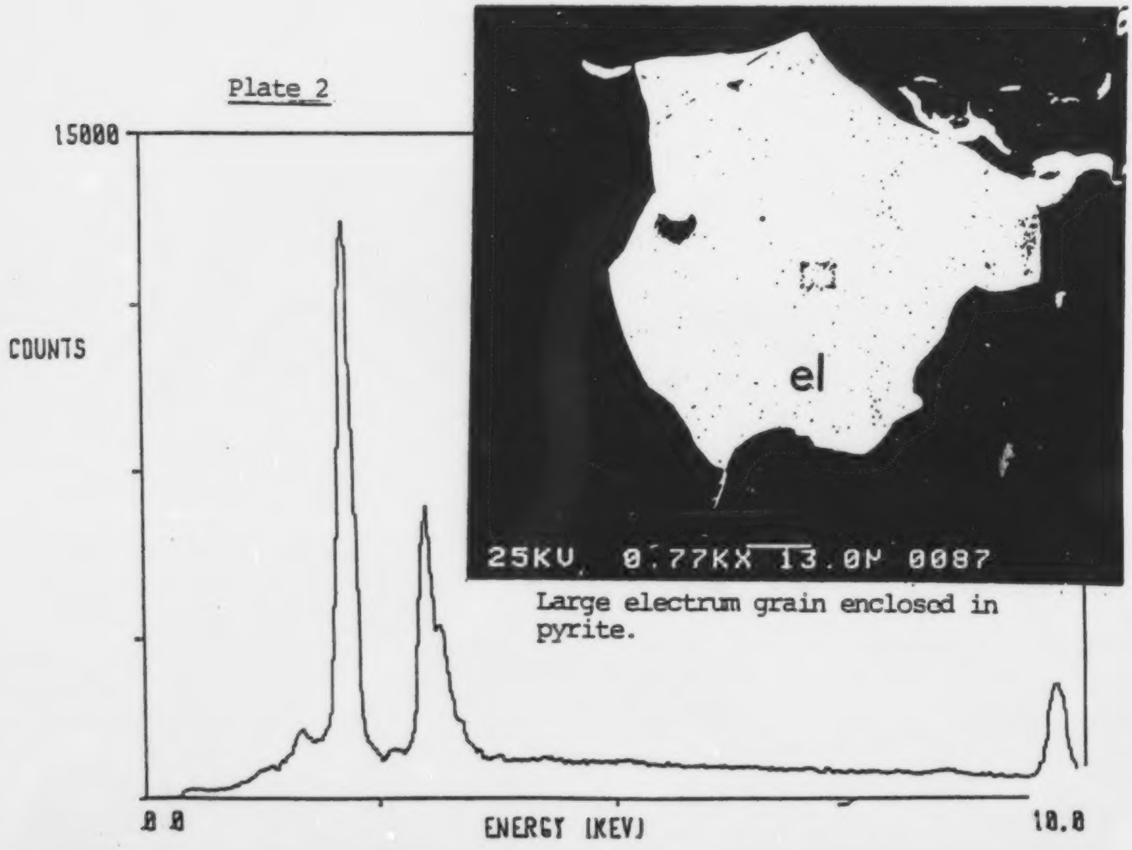

Large electrum grain enclosed in pyrite.

In the tailings, normative pyrite was calculated to be 69.7% and the proportions of pyrite in the heavy and light fractions were estimated at 86.7% and 10.5% respectively. There is a close agreement between calculated normative and measured pyrite (Table 5).

Visible Gold

Electrum was the only gold mineral identified in the 16 sections investigated. A total of eight grains of electrum were observed (Appendix A2). All except one was located as an inclusion within pyrite. The total surface area of the electrum was 67 μm^2. Only one single grain was greater than 10 μm^2 in size (41 μm^2). The mean grain size was 8.4 μm^2. A statistical analysis of the population is given in Table 6. The standard deviation (σ) was 13.4 μm^2 and the confidence interval of the mean (λ) was 9.5 μm^2. The calculation for the amount of visible gold in the sample is given in Appendix A3.

Results of conventional direct cyanidation tests in Table 2, indicate that only a small part of the gold in the tailings is recoverable and that fine grinds do not significantly increase the recovery.

The mean silver content of electrum grains in the tailings was 13.1 % ± 0.23. Details are given in Table 7. The larger electrum grains identified in the chip samples were more silver rich (17.67 %).

Invisible Gold

'Invisible' or submicroscopic gold is the gold which is below the minimum detection limit of the scanning electron microscope, of 0.1 µm (=1000 Å). The invisible gold is dispersed in the crystal lattice of the host mineral as extremely fine but discrete inclusions in the size range from 50 to 1000 Å, only visible by high resolution transmission electron microscopy (Bakken et al, 1988) or is in solid solution in the sulphide. Whichever of these two forms the gold is in, it is below the lower size limit of the field of conventional cyanidation.

Pyrite, the only major sulphide phase in the final tailings is gold-bearing. The average concentration of gold in 104 pyrite particles, as determined with the ion microprobe is 0.41 parts per million (g/t), with a confidence interval of 0.23 g/t at a 95% significance level. This means that the average gold concentration in 95 out of 100 cases should fall in the range from 1.18 to 1.64 g/t.

TABLE 5

AREA MEASUREMENT AND NORMATIVE MINERALOGY OF TAILINGS AND HEAVY AND LIGHT FRACTIONS

	Area measurement	Calculated Normative Mineralogy		
	Heavy fraction	Heavy	Light	Tailings
Pyrite	93.2 ± 1.9	86.7	10.5	69.7
Sphalerite	1.8 ± 1.3			
Chalcopyrite	0.3 ± 0.6			
Galena	0.9 ± 1.2			
Pyrrhotite	0.2 ± 0.6			
TOTAL SULPHIDE	96.4			
Gangue	3.6 ± 4.5			
TOTAL	100.0			

TABLE 6

STATISTICAL ANALYSIS OF GOLD GRAINS IN TAILINGS

Total gold area = 67. μm^2

Mean grain size (x) = 8.4 μm^2

Standard deviation (σ) = 13.4 μm^2

Confidence interval of mean(λ) = 9.5 μm^2

Association of grains:

	N	x	Σarea	% of total
Enclosed in pyrite	7	9.3	65.0	97
Combined with pyrite	1	2.0	2.0	3

$$\lambda = \frac{2\sigma}{\sqrt{N}}$$

TABLE 7

ELECTRON PROBE MICROANALYSIS OF ELECTRUM GRAINS

	WEIGHT %		
Grain #	Au	Ag	Total
ORE CHIP SAMPLE			
1	82.68	16.96	99.64
2	81.89	18.39	100.82
TAILINGS			
1 x (N=2)	85.85	12.99	98.84
3	86.84	13.16	100*
4 x (N=2)	85.53	12.77	98.30
Mean (x)	**86.90**	**13.10**	**100.00**

* Normalised to 100%. Low total (92%) due to small size of grain.

Measured gold concentrations range from 0.0 to a maximum of 5.6 g/t. The distribution of invisible gold in pyrite is depicted in Figure 2. The ion probe data are given in Table 8.

The average concentration of gold in 14 chalcopyrite particles was 1.1 g/t, with a confidence interval of 0.8 g/t at a 95% significance level (Table 8).

3.4.0 DISCUSSION

Cyanidation testing showed that only up to a third of the gold in the final tailings is recovered by direct cyanidation. Fine grinds did not significantly improve the recovery. With 80% of the ore finer than 14 µm, only **32%** of the gold could be recovered. The amount of visible gold identified after a detailed study of 16 one inch in diameter polished blocks accounted for 7% of the total gold. The short fall is attributed to a few coarser gold particles which were not encountered during the microscopic study. The chances of missing 1 grain of electrum 240 μm^2 in size, that would account for the difference of 25% or 0.36 g/t are 37%.

The 'invisible' gold content of the pyrite is 1.41 ± 0.23 g/t, accounting for **68%** of the gold in the final tailings. Since the 'invisible' gold is in the pyrite, which represents 69.7% of the tailings by weight, the economics of recovering this gold by any of the presently availiable processes at the current gold prices ($410.00/ oz) are not there.

Approximately **25%** of the gold can be recovered by conventional direct cyanidation from the final tailings without additional grinding.

The mineralogical distribution of gold is given in Table 1 and depicted as a pie diagram in Figure 1.

3.5.0 CONCLUSIONS

Electrum is the only gold mineral that was identified in the ores, final tailings and the copper concentrate. The average size of the eight gold grains in the tailings was 8.4 μm^2, and the average silver content was determined to be 13.1 ± 0.23 %. All of the visible gold in the tailings occured associated with pyrite.

FIGURE 2 Distribution of invisible gold in pyrite

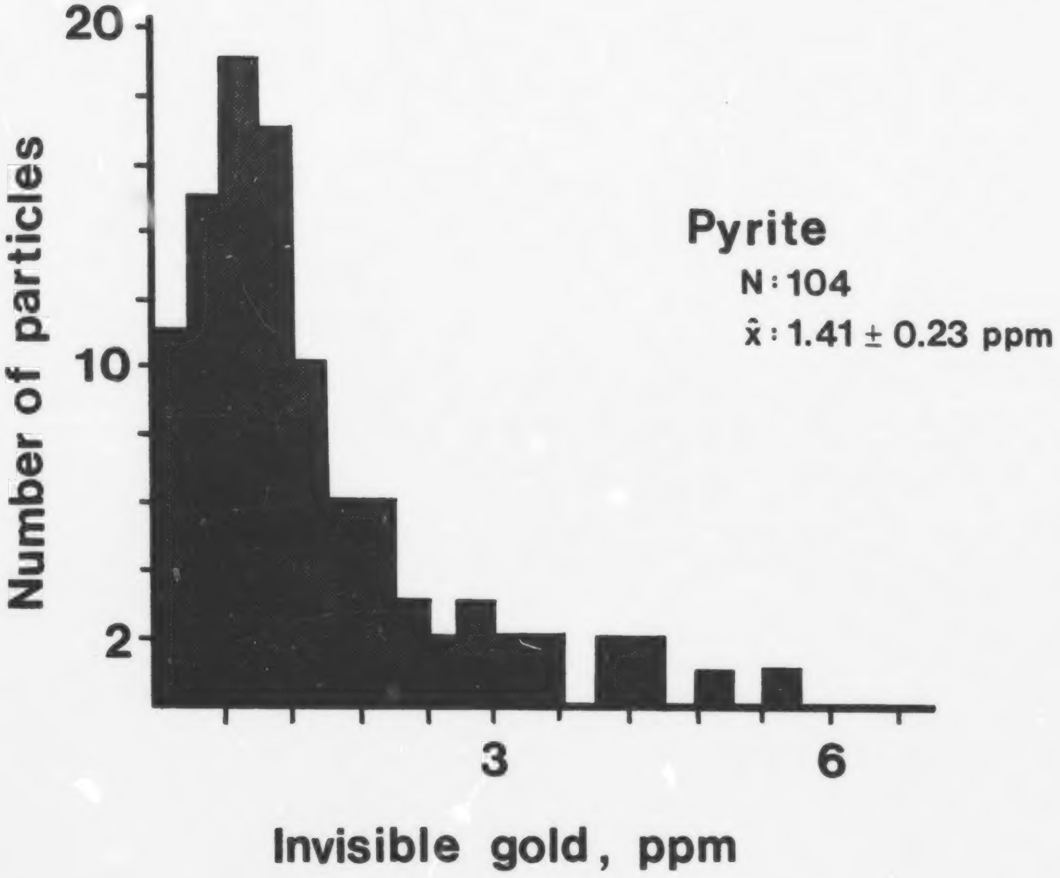

Table 8

INVISIBLE GOLD CONCENTRATION IN SULPHIDES
(Moburn Mine, Audrey Resources)

Pyrite

particle #	Au, g/t	particle #	Au, g/t	particle #	Au, g/t
1a	1.5	23	0.7	61	0.7
2a	1.2	24	0.8	62	0.85
3a	2.4	25	3.1	63	1.9
4a	0.7	26	0.9	64	1.3
7a	0.0 < MDL	27	1.6	65	0.3 < MDL
1b	0.0 < MDL	28	4.0	66	1.2
2b	0.3 < MDL	29	0.6	67	1.8
3b	0.8	30	1.2	68	0.7
4b	0.7	31	4.1	69	1.0
5b	1.5	32	0.8	70	1.9
6b	1.5	33	0.4 < MDL	71	0.3
7b	2.0	34	1.4	72	1.0
1	1.1	35	1.8	73	0.6
2	0.4 < MDL	36	0.6	1'	1.1
3	0.4 < MDL	37	1.4	2'	0.84
4	3.2	38	0.7	3'	1.36
5	1.1	39	2.8	4'	0.70
6	2.5	40	1.1	5'	0.41
7	4.6	41	2.6	6'	4.5
8	1.2	42	3.4	7'	0.8
9	0.8	43	1.2	8'	4.5
10	1.7	44	1.7	9'	2.9
11	2.4	45	1.0	10'	5.1
12	2.3	46	1.0	11'	1.7
13	0.0	47	3.5	12'	0.36 < MDL
13c	0.4	48	3.0	13'	1.7
14	0.54	49	2.1	14'	0.44
15	0.2	50	1.9	15'	0.75
16	0.6	52	1.1	16'	0.89
17	0.3	55	0.8	17'	5.61
18	1.4	56	0.3 < MDL	18'	0.81
19	1.0	57	0.3 < MDL	19'	0.12 < MDL
20	2.0	58	0.6	20'	0.13 < MDL
21	1.4	59	0.4 < MDL	21'	0.85 < MDL
22	1.9	60	1.0		

N = 104

$\hat{x} = 1.41 \pm 0.23$ (16%)

Chalcopyrite

particle #	Au, g/t
1	0.46
16	0.25
2	0.55
51	2.20
1'	0.53
2'	1.08
3'	1.94
4'	0.84
5'	0.24
6'	0.22
7'	1.00
8'	0.38
9'	6.00
10'	0.15

N = 14

$\hat{x} = 1.1 \pm 0.8$

Pyrite is the principal gold-bearing mineral in the tailings. The average gold concentration of the pyrite is 1.41 ± 0.23 g/t. Invisible gold within the crystal lattice of pyrite accounts for 68. ± 11.6 % of the total gold in the tailings.

Cyanidation testing showed that 32% of the gold was present as visible gold and could be recovered by direct cyanidation. Both Te (9 ppm) and Sb (<20 ppm) are in trace amounts, making the presence of gold tellurides or aurostibite, minerals which are sparingly soluble in cyanide, rather unlikely.

APPENDIX A1

ELECTRUM GRAINS IN THE ORE SAMPLES

Grain #	Association	Size (sq µm)
1	Enclosed in chalcopyrite	4
2	"	5
3	"	2
4	"	2
5	"	5
6	Combined with ccp + sph	3750
7	"	2746
	TOTAL	6514

Number of sections: 6

APPENDIX A2

ELECTRUM GRAINS IN THE TAILINGS

Grain #	Association	Size (sq µm)
1	Enclosed in pyrite	41
2	"	2
3	"	4
4	"	9
5	Combined with pyrite	2
6	Enclosed in pyrite	4
7	"	4
8	"	1
	TOTAL	67

Number of sections: 16

APPENDIX A3

CALCULATION OF VISIBLE GOLD IN TAILINGS

Sample area investigated (16 x 4.91 cm^2) = 78.56 cm^2

Sample coverage = 28 %

Total sample area covered = 22.00 cm^2

Total sample weight (unit depth: 10^{-4} cm, average sp grav.; 5.0 $g.cm^{-3}$) = 110.00 x 10^{-4}g

---

Total gold area = 67 μm^2 ± 10

= 6.7 x 10^{-8} cm^2

Average Au content of electrum = 86.9 %

Total gold weight (unit depth: 10^{-4} cm, average sp. grav.; 19.3 $g.cm^{-3}$) = 11.4 x 10^{-10}g

Total gold concentration relative to sulphide (visible gold) = 0.10 ppm (7.2%) ± 0.02

CHAPTER 4

DIRECT DETERMINATION OF INVISIBLE GOLD IN THE ELMTREE COMPOSITE ORE #1. IMPLICATIONS FOR GOLD RECOVERY FROM OXIDISED AND NON-OXIDISED ORES.

SSW/PMS/88/14

SUMMARY

The Elmtree composite sample #1 is a partially oxidised sulphide ore assaying 11.0 g/t Au, 4.15% S and 2.91 % As. Sixty percent of the gold is recoverable by direct cyanidation. Fine grinds have insignificant effects upon the recovery. A significant fraction of the cyanide recoverable gold is in the form of sub-microscopic inclusions in scorodite and in iron oxides and hydroxides, which are the oxidation products of the gold-bearing arsenopyrite and pyrite, but also of the pyrrhotite of unknown gold content. The remainder of the cyanide recoverable gold is fine grained and associated with silicates and to a lesser extent sulphides.

The refractory gold (40%) is submicroscopically distributed in the lattices of arsenopyrite and pyrite in the ratio 2:1. The invisible gold content of the arsenopyrite is 123 ± 61. g/t and that of the arsenian pyrite is 24.1 ± 5.3 g/t.

In the disseminated sulphide ore, the percentage of the cyanide recoverable gold is significantly lower because none of the invisible gold in the sulphides became availiable to cyanidation by supergene oxidation.

FIGURE 1

MINERALOGICAL DISTRIBUTION OF GOLD

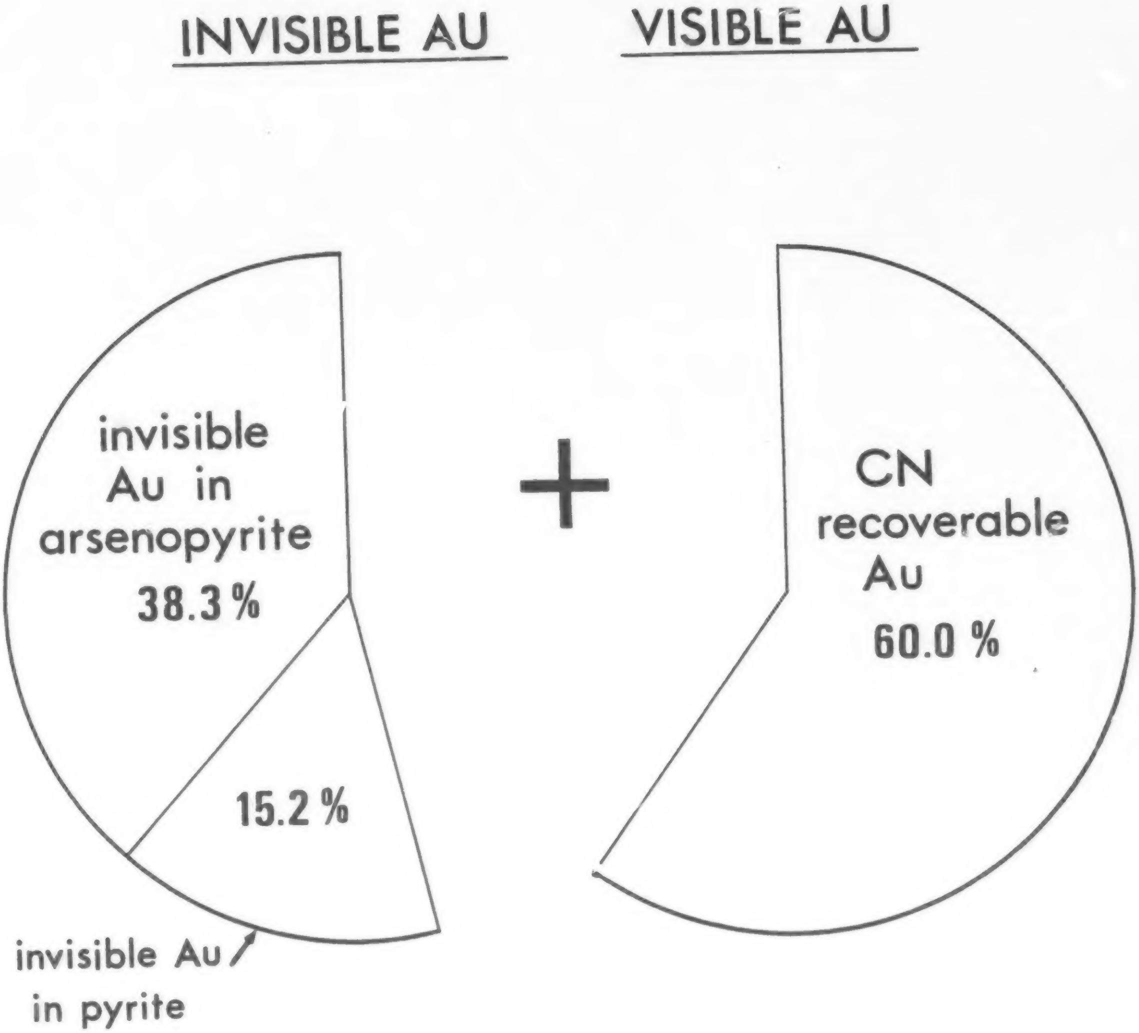

TABLE 1

MINERALOGICAL DISTRIBUTION OF GOLD

	Au g/t	Au %	Precision
Assayed Au	11.07	100.0	-
CN- recoverable Au (K_{80} = 13 µm)	6.6 ± 0.3	60.0	± 2.7
Invisible gold			
In pyrite (6.96 ± 1.1 Wt.%, conc. 24.1 ± 5.3 ppm)	1.68± 0.45	15.2	± 4.1
In arsenopyrite (3.45 ± 1.0 Wt.%, conc. 123 ± 61 ppm)	4.24± 2.45	38.3	±22.2
Total	12.52± 3.2	113.5	±28.9

LIST OF TABLES

Table 1 Mineralogical distribution of gold
Table 2 Chemical assays
Table 3 Invisible gold in sulphides
Table 4 Cyanidation tests
Table 5 Invisible gold in scorodite and iron oxides

LIST OF FIGURES

Figure 1 Mineralogical distribution of gold
Figure 2 Distribution of As in pyrite
Figure 3 Distribution of invisible gold in arsenopyrite
Figure 4 Distribution of invisible gold in pyrite
Figure 5 Correlation between As and Au in pyrite

LIST OF PLATES

Plate 1 Two textural types of pyrite
Plate 2 Back-scattered image showing inhomogeneities of As within pyrite particle
Plate 3 Coating of arsenopyrite by scorodite

APPENDICES

A1 Arsenic content of pyrite
A2 Image analysis

4.1.0 INTRODUCTION

Mr. Barker, chief geologist with Lacana Mining Corporation requested the determination of the gold mineralogy in the Elmtree deposit, N.B., as part of the general project on the characterisation of Canadian refractory gold ores by ion probe microanalysis. The aim of this project is to provide the basic information that will lead to improved gold recoveries.

The Elmtree gold-bearing deposit exhibits secondary zoning due to oxidation that has resulted in two distinct ore types from a metallurgical point of view: a partially oxidised ore with a gold recovery by direct cyanidation ranging from 53.1 to 59.0 % (Lakefield Research, 1985); and a disseminated sulphide ore with a gold recovery in the range from 13 % (Thibault, 1987) to 25% (Lakefield Research, 1985). The fact that fine grinds failed to significantly improve the leachability, and that flotation test #1A (Lakefield Research, 1985) on a composite of the underground drillcore samples gave a high recovery of both sulphide and gold, led Tucker (1987) to conclude that gold is intimately associated, finely disseminated and locked in solid solution in the sulphides. Pyrite and arsenopyrite are the main sulphide minerals in the partially oxidised ore. In the underlying disseminated sulphide ore, pyrrhotite is also important (Harris, 1986 and Chryssoulis and Coleman, 1987). It was recommended by Mortimer (1986), based on the results of selective flotation test #14 of arsenopyrite, which yielded an arsenopyrite rougher concentrate containing 16.93% of the weight of the original sample, 94.9% of the gold and assaying 29.5 g/t, that production of a selective arsenopyrite concentrate is the most viable option. However, the Lakefield testwork does not clearly show complete association of the gold with the arsenopyrite fraction, which is corroborated by the bioleach results reported by Hackl (1987). Bacilli suited to arsenopyrite preferentially attack this portion of the material. The nearly complete sulphur removal required to achieve gold recoveries in excess of 90% indicate that a significant fraction of the gold is associated with the pyrite (Tucker, 1987).

Harris (1986) determined that gold occurs mostly as fine grains, generally from 2 to 5 µm, with a maximum of 10-14 µm in the silicate gangue, attached to pyrite and arsenopyrite and rarely as inclusions in arsenopyrite, pyrite or pyrrhotite. No attempt was made to balance the visible gold.

The objectives of this study are as follows: (i) to determine directly the concentration of gold dispersed in the crystal lattice of the pyrite and arsenopyrite; (ii) to calculate the gold carried by leach sulphide as a fraction of the total; (iii) to balance cyanide recoverable gold with the invisible gold and (iv) to recommend metallurgical testwork to improve gold recovery,based on the complete mineralogical balance of gold and its size and association.

This study was sponsored by Lacana Mining Corporation, CANMET, the Geological Survey of Canada and Department of Supply and Services (DSS).

4.2.0 METHODOLOGY

A series of ore (chip) samples were received from Lacana Mining Corporation. Polished blocks were prepared from the following six ore samples: 8/ 607, 17/ 604, 87-26/1163, 87-23/1699, G/5 and 13/ 609.

A crushed sample from composite ore #1 representing a partially oxidised ore from the surface was received from Lakefield Research. Metallurgical tests were conducted by Lakefield in 1985 and 1986. This sample was used to obtain a complete mineralogical balance for gold. The approach followed is described in the section on methodology in the general report to DSS. Firstly, cyanidation tests were carried out on three 500g charges, using progressively finer grinds, to determine the cyanide recoverable gold and the effect of grinding upon recovery. A sub-sample was sieved into the following size fractions: -90 µm, 90-560 µm, and +560 µm. The 90-560 µm fraction, comprising 32% of the total weight was separated using sodium polytungstate (S.G. 3.0 g.cm^{-3}). The heavy fraction represented 11.7 % and six polished sections were prepared for further examination.

Optical microscopy was used to determine the gold minerals, their size and association. Ion probe microanalysis was used to determine the gold content of the pyrite and arsenopyrite. The polished blocks of the composite ore were implanted with a known amount of gold for internal standardization of the sulphide mineral particles analysed with the ion probe according to the technique described by Chryssoulis et al (1987). The relative proportions of pyrite, arsenopyrite and iron oxides in the samples for the gold mineralogical distribution were determined by image analysis. The arsenic content of pyrite was determined by both electron and ion probe microanalysis.

4.3.0 RESULTS

4.3.1 Chemical Assays

Chemical analyses of the composite ore sample were carried out. Details are given in Table 2. Also given are the Au, As and S assays of the light fraction and the calculated assays of the heavy fraction.

4.3.2 Mineralogy of ore samples

Major minerals: Pyrite, arsenopyrite, pyrrhotite.

Minor minerals: Sphalerite, chalcopyrite, galena, tetrahedrite.

Each of the ores was different in mineralogy and although pyrite is always the dominant sulphide mineral, the other sulphides vary considerably in their relative abundances from one ore sample to the next. Grain size and textures of the ores also seems to vary considerably.

Pyrite grains are generally small and subhedral. Inclusions of gangue silicate phases and of other sulphides (pyrrhotite, chalcopyrite and sphalerite) are widespread. In the ores, only a single generation of pyrite appeared to be present. Blastic **arsenopyrite** occurs throughout the ores, grain size is typically smaller than the pyrite. Inclusions of silicate minerals are widespread. **Sphalerite**, **chalcopyrite** and **pyrrhotite** compose the matrix of the ores and are often intergrown with one another. **Galena** and **tetrahedrite** are very minor constituents.

Gold minerals

A single grain of gold was noted in the chip samples. The small grain (25 µm) was present as an inclusion in pyrite.

4.3.3 Mineralogy of Composite Ore #1

Major minerals: Pyrite, arsenopyrite, marcasite.

Minor minerals: Chalcopyrite, sphalerite, pyrrhotite, galena, tetrahedrite.

TABLE 2

CHEMICAL ASSAYS

	mass split%	Au g/t	Au distrib	S %	As %	Sb ppm	Bi ppm	Te ppm
Composite Ore	100.0	11.07	100.0	4.15	2.91	60	<20	<3
Light fraction	88.3	7.95	63.8	1.41	2.39			
Heavy fraction	11.7	(34.68)	(30.6)					

* parentheses indicate calculated values.

Pyrite

Two texturally distinct types of pyrite were recognised. They are approximately equal in abundance in the sections investigated. The first type features rounded grains with numerous inclusions of silicate minerals and other sulphide species. The second type contains fewer silicate inclusions, although inclusions of pyrrhotite, chalcopyrite and sphalerite (in that order of significance) are widespread. Plate 1 illustrates the typomorphic character of the two pyrite types. Iron oxides coat and fill fractures in the pyrite particles.

Electron probe microanalysis revealed the presence of arsenic-poor and arsenic-rich pyrite. The average arsenic concentration of the arsenian pyrite, based on 61 spot analyses from eight grains is 1.79 ± 0.40 Wt. % As. The arsenic-poor pyrites have less than 0.1 Wt. % arsenic. Results are graphically depicted in Figure 2, with details given in Appendix A1. The arsenian pyrite appears to be in the form of irregular patches and growth zones, within the arsenic-poor pyrite. Since they are closely intergrown, they are not separable by grinding. Small euhedral arsenopyrites are frequently observed within the arsenic-rich zones (Plate 2).

The pyrite content of the composite ore sample was determined by image analysis to be 7.7 ± 3.4 Wt. % (Appendix A2).

Arsenopyrite

Two types of arsenopyrite are also distinguishable. They are approximately equal in abundance. The first type is, in general, more coarse and rounded, with numerous silicate inclusions. Inclusions of sulphides are rare. The second type of arsenopyrite is more euhedral, smaller in size and has fewer inclusions. Inclusions of pyrrhotite, pyrite and chalcopyrite are present. The arsenopyrite particles are frequently partially oxidised, having a sizable coating and fractures filled with scorodite ($FeAsO_4.2H_2O$) and iron-oxides and hydroxides.

Other Sulphide Minerals

Grains of chalcopyrite, pyrrhotite, sphalerite, galena and tetrahedrite account for a few percent of the composite ore by volume. Pyrrhotite is in general inclusion-free, as is chalcopyrite. Sphalerite grains carry chalcopyrite disease. Galena is a very minor constituent, as is

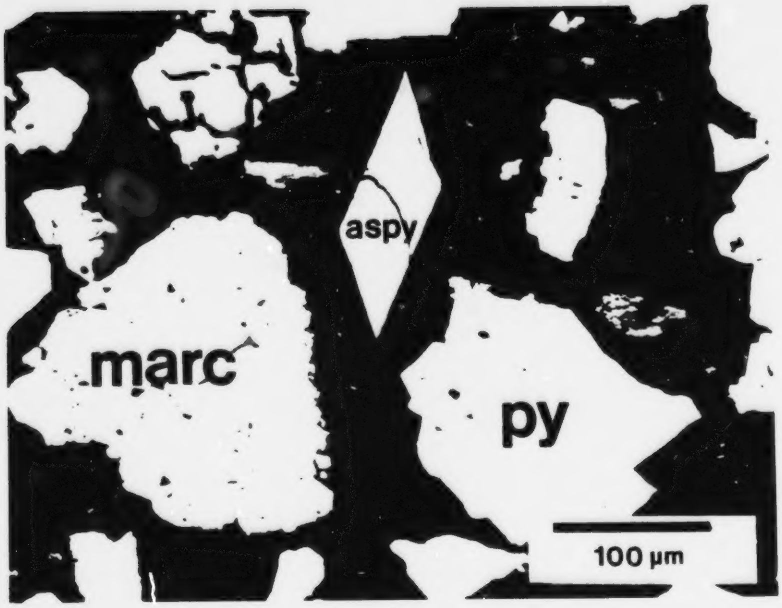
aspy
marc
py
100 µm

Plate 1 Pyrite (py), arsenopyrite (aspy) and pyrite almost completely replaced by marcasite (marc).

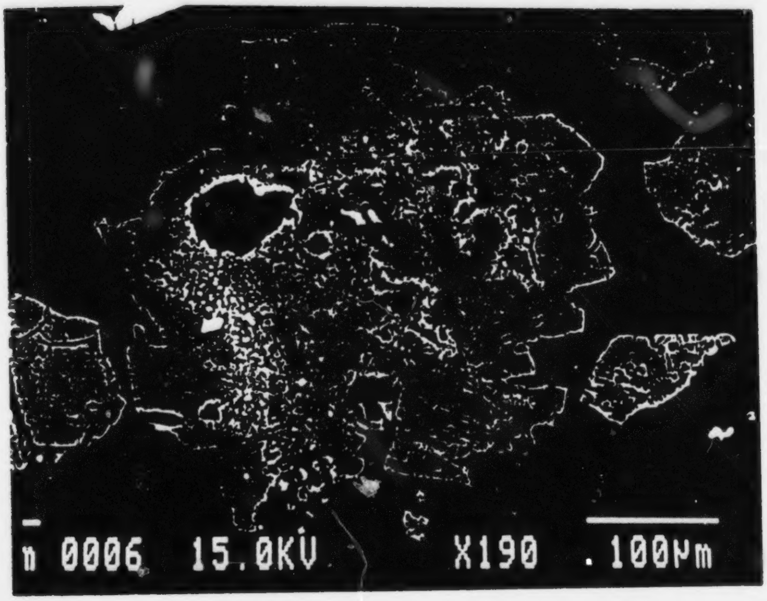
n 0006 15.0KV X190 .100µm

Plate 2 Back-scattered image of a pyrite particle with inhomogeneous distribution of As. Dark areas are As-poor, light areas are As-rich. Note arsenopyrite grains at contact between As-poor and As-rich areas.

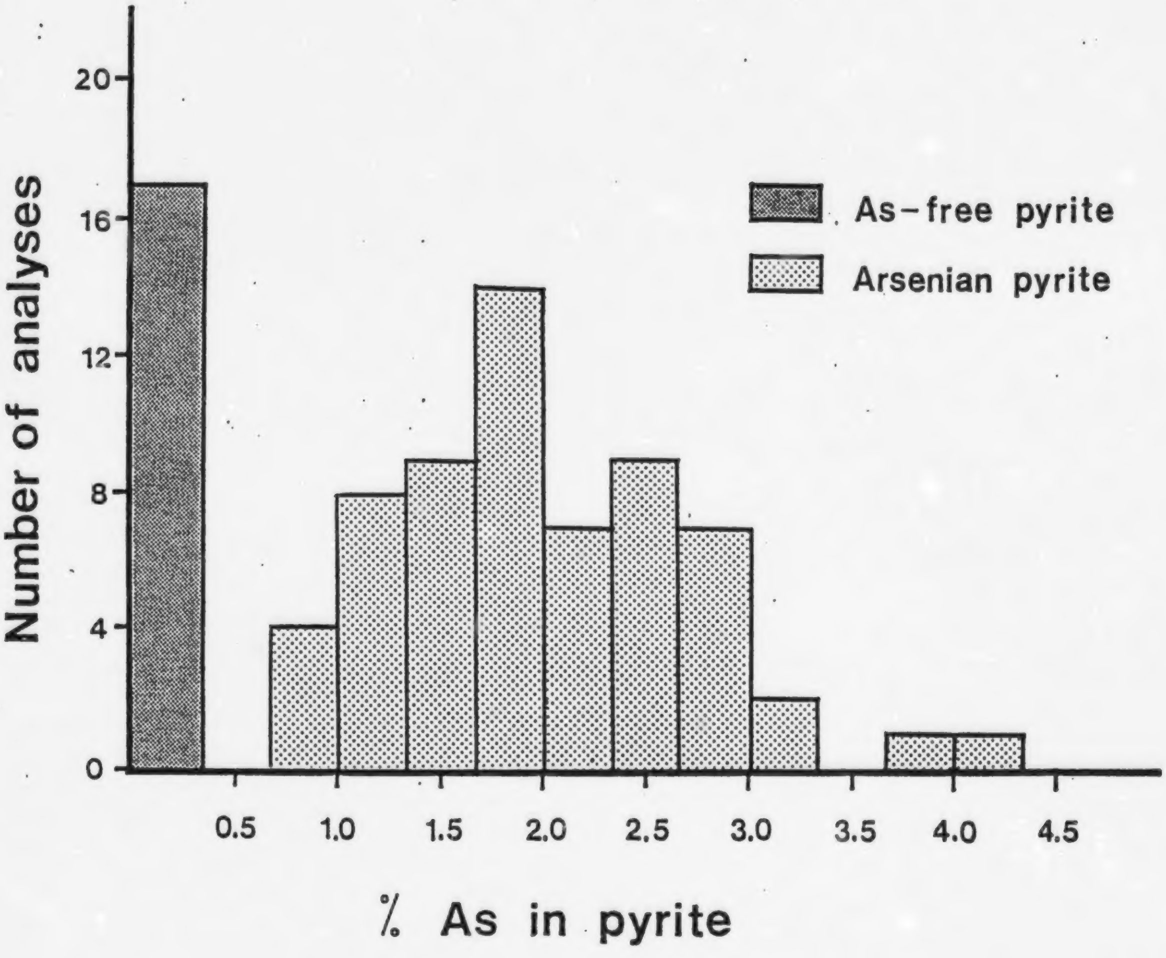

Figure 2
As content of pyrite determined by electron probe microanalysis.

tetrahedrite. Both phases are restricted to intergrowths with chacopyrite and sphalerite.

Gold Minerals

Distinct gold phases, such as native gold, electrum etc. were not recognised in the six polished sections of the sink fraction with a calculated approximate gold content of 34.7 g/t (Table 2).

Invisible Gold

Invisible or sub-microscopic gold is the gold which is not visible under the optical and scanning electron microscopes with a minimum detection limit of 0.1 µm (or 1000 Å). The sub-microscopic gold can be finely dispersed in the crystal lattice of the sulphides in the form of extremely fine inclusions (50-1000 Å), or in solid solution. As Haycock (1937) pointed out "As regards actual milling practice, it may be of little significance whether sub-microscopic gold is merely very finely divided, colloidal or in solid solution, because the lower limit of visible gold falls below the lower limit of the field of cyanidation". Invisible gold in sulphides is not recoverable by direct cyanidation, requiring the prior oxidation of the sulphide in order to become amenable to cyanidation. Both arsenopyrite and pyrite were identified as carriers of invisible gold in the Elmtree ore.

The average concentration of gold in 44 arsenopyrite particles, as determined on the ion microprobe is 123 parts per million (g/t), with a confidence interval of 61 g/t at a 95% significance level. This means that 95 out of 100 arsenopyrite particles should have gold concentrations in the range from 62 to 184 g/t. The distribution of invisible gold in arsenopyrite is shown in Figure 3. Measured gold concentrations ranged from 0.4 to 912. g/t (Table 3).

The average concentration of gold in 82 pyrite particles was 24.1 g/t, with a confidence interval of 5.3 g/t at a 95% significance level. The distribution of invisible gold in pyrite is shown in Figure 4. Measured gold concentrations ranged from 0.9 to 108 g/t (Table 3). Most of the pyrite particles analysed were not homogeneous with respect to their arsenic content, because of the intimate intergrowth of arsenic-poor and arsenic-rich pyrite (Plate 2). In addition, they often contain fine arsenopyrite inclusions. Arsenic was monitored during the ion probe microanalysis and selected pyrite particles were

TABLE 3

INVISIBLE GOLD IN SULPHIDES
(Lacana, Elmtree, N.B.)

Arsenopyrite

Particle #	Au, g/t	Particle #	Au, g/t
4	10.4	63	11.8
5	38.5	64	156.
10	57.5	65	30.
11	7.8	66	542.
17	8.9	67	721.
23	39.2	69	57.7
26	20.	72	450.
30	8.7	73	290.
34	240.	74	32.1
35	49.	77	16.5
38	56.	79	55.6
41	525.	80	8.5
42	7.1	81	110.
46	230.	90	33.
47	17.	93	164.
53	91.	95	31.1
54	50.9	97	912.
57	0.4	99	112.
58	10.5	101	64.8
59	24.5	103	33.3
60	27.7	105	14.8
61	26.5	106	20.

N = 44

$\hat{x} \pm \lambda = 123. \pm 61.$ g/t Au

Pyrite

Particle #	Au, g/t	Particle #	Au, g/t	Particle #	Au, g/t
1	8.7	44	16.8	2'	8.8
2	50.	45	37.1	3'	32.
3	0.91	48	22.7	4'	15.
6	38.7	49	9.7	5'	18.
7	14.	50	4.3	6'	26.
8	14.1	52	1.1	7'	3.2
9	20.1	55s	1.7	8'	1.2
12	1.7	56	102.	9'	47.
13	28.	62	24.	10'	8.2
14	2.3	68	22.	11'	0.9
15	19.4	70	8.1	12'	50.
16	1.4	71	2.7	13'	43.
18	5.2	76	14.	14'	32.
19	2.	78	8.9	15'	11.
20	28.7	82	108.	16'	10.
21	84.9	83	19.	17'	46.
22	2.6	84	78.	18'	4.3
24	20.8	85	37.6	19'	41.
25	51.9	86	7.	20'	5.6
27	27.8	91s	64.	22'	2.2
28a	50.3	92	2.9	23'	17.
29	65.2	94	4.	24'	11.
31	40.1	96	27.1	25'	6.8
32	4.9	98	7.3	26'	2.1
33	42.9	100	55.3	27'	38.
36	22.1	102	7.		
37	18.8	104	11.1		
39	14.3				
40	42.5				
43	67.1				

N = 82

$\hat{x} \pm \lambda = 24.1 \pm 5.3$ g/t Au

FIGURE 3

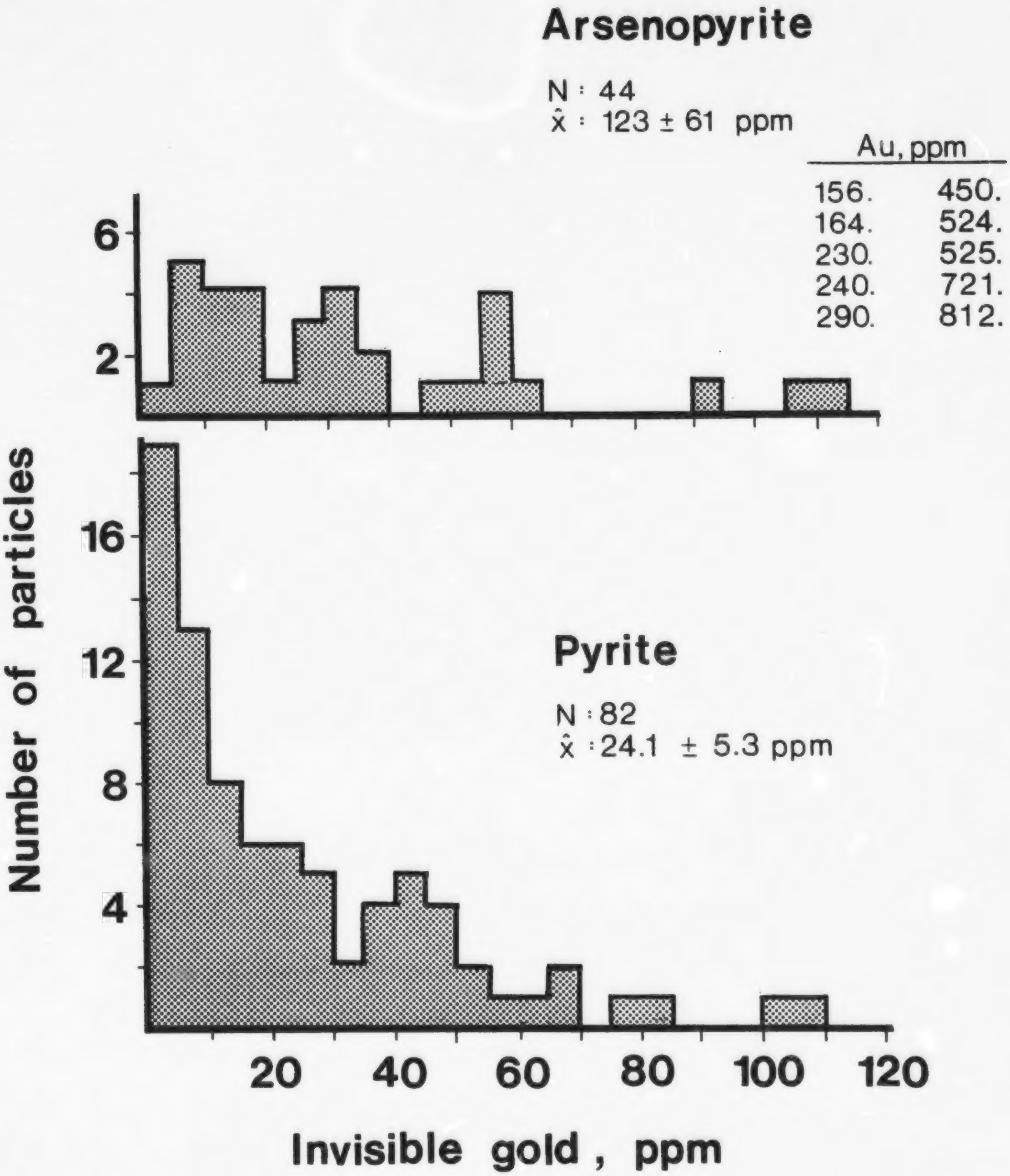

Au, ppm	
156.	450.
164.	524.
230.	525.
240.	721.
290.	812.

analysed with the electron probe. Results are detailed in Appendix A2. From a comparison of the electron and ion probe data for arsenic in pyrite, it is obvious that arsenian pyrites were analysed preferentially for gold, and therefore, the average gold contents of pyrite have been overestimated. A positive correlation was established between the As content and the invisible Au content, shown in Figure 5.

4.4.0 DISCUSSION

Ion probe microanalysis has shown that the Elmtree arsenopyrite carries invisible gold at an average concentration of 123 ± 61 g/t. Image analysis has shown that arsenopyrite represents 3.4 ± 1.0 % of the composite sample #1 by mode. Calculation of the normative proportions of arsenopyrite and pyrite could not be carried out due to the presence of scorodite ($FeAsO_4.2H_2O$). Based on the gold content and abundance of arsenopyrite (Appendix A1), it was determined that 4.24 ± 2.45 g/t Au is in the arsenopyrite. This represents 38.3 ± 22.2 % of the total gold (Table 1). Selective flotation test # 1 of arsenopyrite produced a cleaner concentrate that represented 0.92 Wt. % of the head and assayed 144 g/t Au, which accounted for 12.2% of the gold head sample (Ref: Lakefield Research, 1985). The scorodite and iron oxide coatings of the arsenopyrite particles (Plate 3) will make the flotation of the arsenopyrite more difficult and also adversely effect the separation from the pyrite.

The concentration of invisible gold in the arsenian pyrite was found to be 24.1 ± 5.3 g/t. The proportion of pyrite in the ore is shown to be 6.96 ± 1.1 % by image analysis. This means that 1.68 ± 0.45 g/t Au, which corresponds to 15.2 ± 4.1 % of the total gold is accounted for as invisible gold within the crystal lattice of the pyrite (Table 1). Most of the gold is in the arsenian pyrite which is, however, intimately intergrown with the arsenic-poor pyrite and therefore cannot be liberated by grinding.

Testing has shown that 60. ± 2.7 % of the total gold can be recovered by direct cyanidation and that fine grinds do not significantly improve the recovery (Table 4). Most of the visible gold is reported with the silicates and to a lesser extent with the sulphides (Harris, 1986). However, the amount of visible gold observed in the sink fraction in this study is insignificantly small and cannot account for all the cyanide recoverable gold. Therefore, a large part

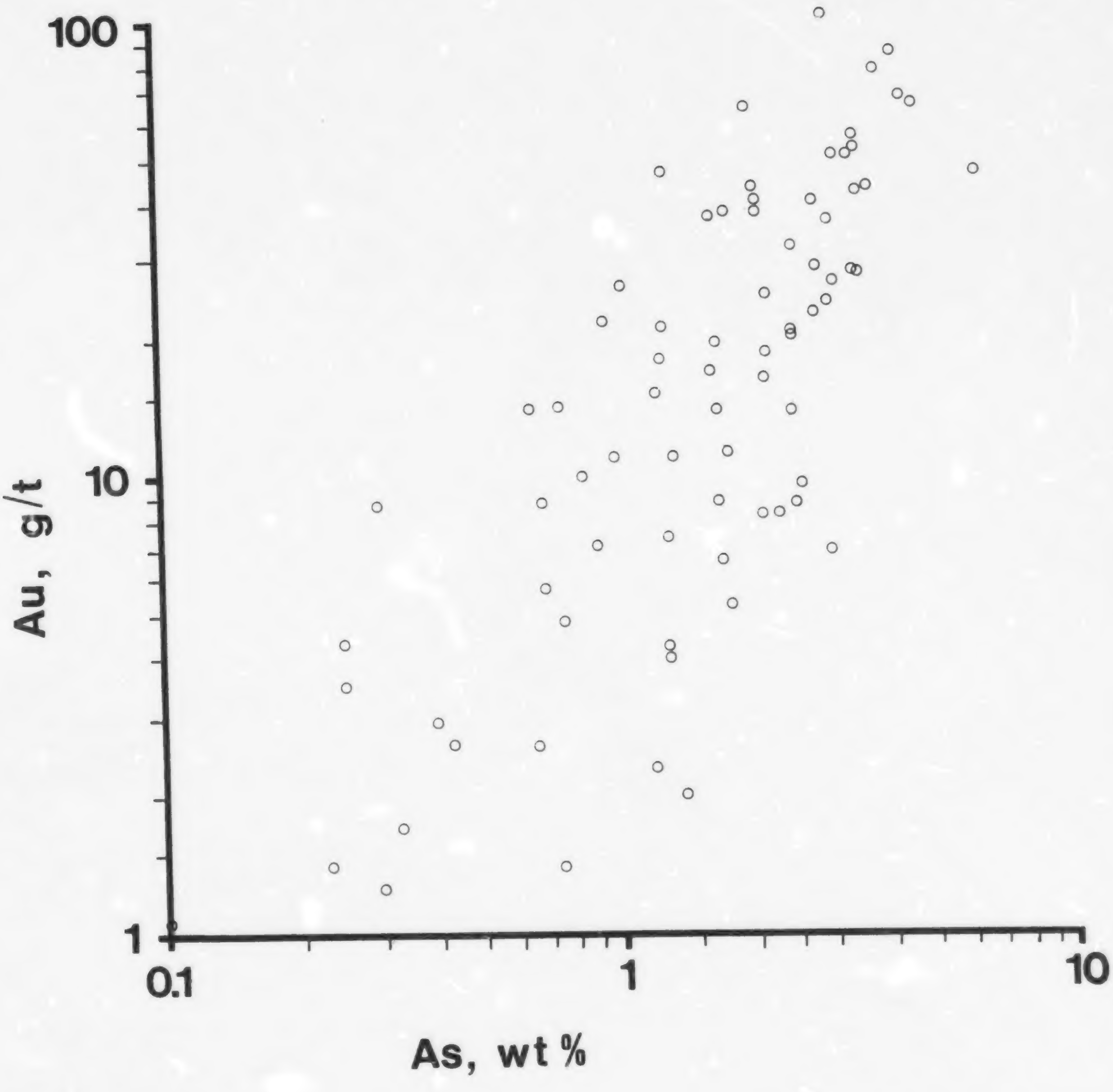

FIGURE 5. Correlation between Au and As in pyrite particles determined by ion probe microanalysis.

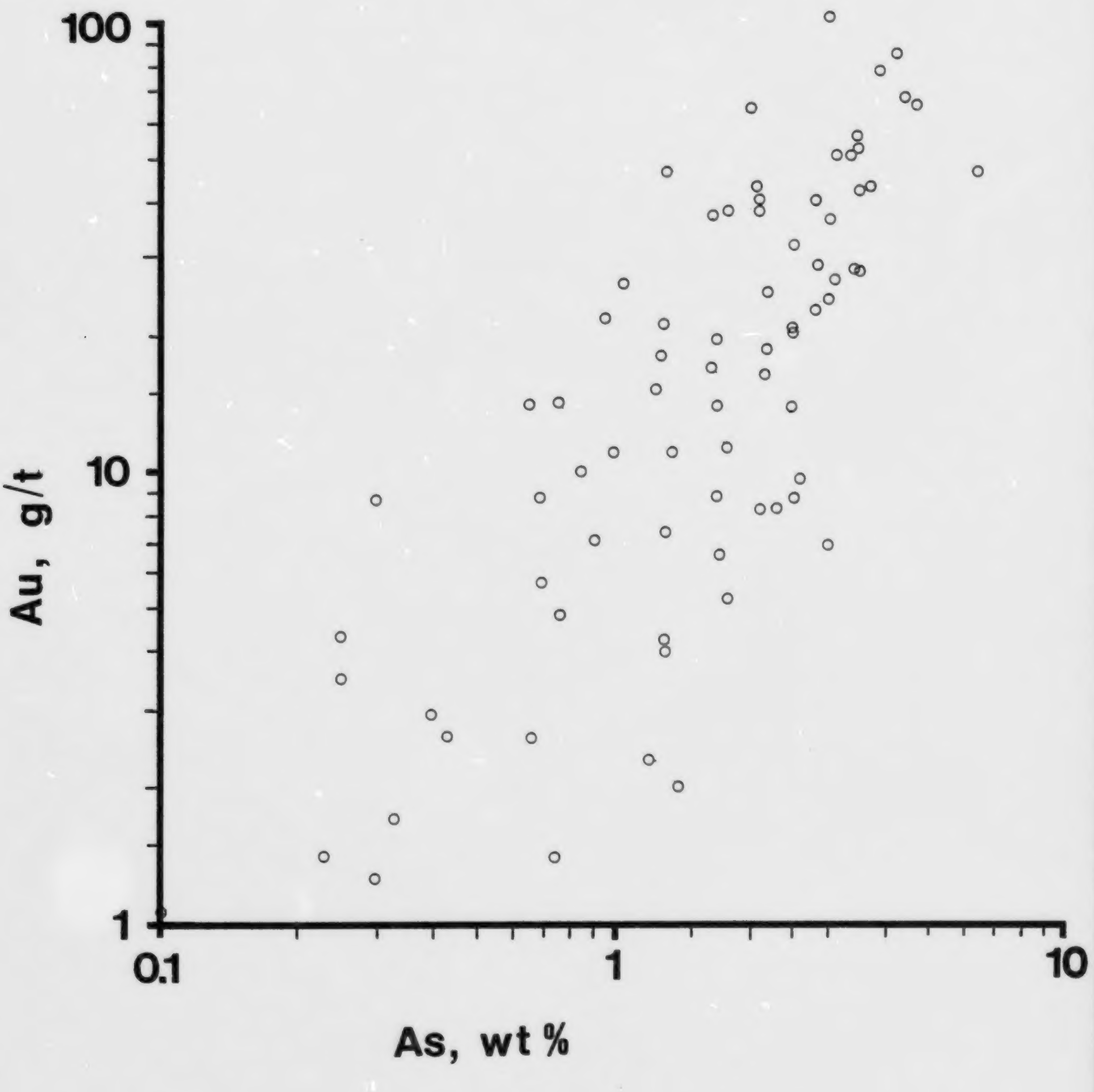

FIGURE 5. Correlation between Au and As in pyrite particles determined by ion probe microanalysis.

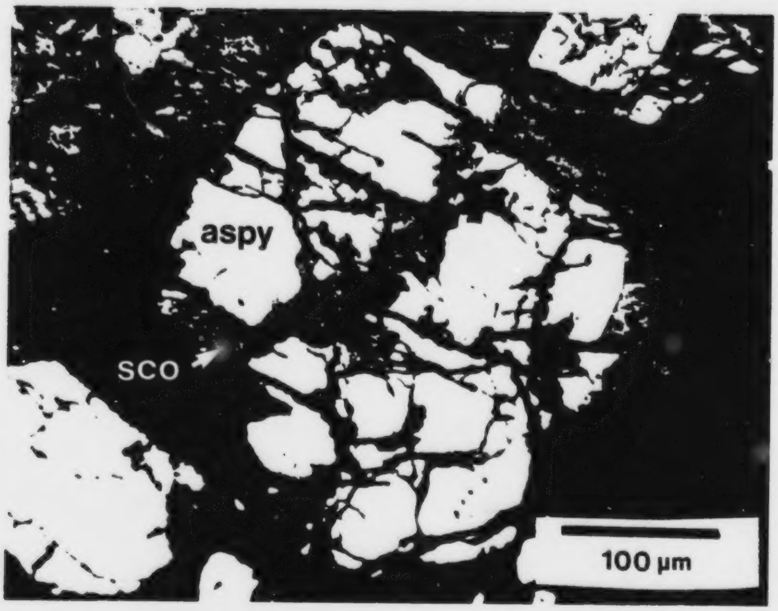
aspy
sco
100 µm

Plate 3 Arsenopyrite grain (aspy) coated with, and containing fracture fillings of scorodite (sco).

of the cyanidable gold must be in a form which is not visible, but is nevertheless amenable to direct cyanidation. Ion probe microanalysis has shown that significant concentrations of gold (Table 5) are associated with the scorodite and the iron oxides and hydroxides, probably as sub-microscopic inclusions. These minerals represented 29.2 ± 7.1 % of the ore by mode. It is therefore concluded that a significant fraction of the cyanidable gold is present within the scorodite and Fe oxides.

The gold-bearing scorodite and part of the iron oxides and hydroxides are oxidation products of the gold bearing asrsenopyrite and pyrite. The balance of the Fe-oxides resulted from the oxidation of the pyrrhotite, the gold content of which was not determined. It is proposed that during the supergene oxidation of the Elmtree deposit, the mobility of gold was extremely low, and the gold did not recrystallize to any significant extent, therefore remaining in the scorodite and oxides as very fine submicroscopic inclusions with a maximum size of less than a few hundeds of Ångstroms (0.0X µm).

The refractory proportions of gold which is refractory to direct cyanidation is 40%. The calculated 'invisible' gold within the arsenopyrite and pyrite, which is not amenable to cyanidation is 53.5 %. This discrepancy is attributed to overestimation in (i) the amount of arsenopyrite present in the composite ore and (ii) of the average 'invisible' gold content of the pyrite present in the composite ore by preferentially analysing arsenian pyrites which have higher gold contents (Appendix A1). The mineralogical distribution for the gold in the composite ore #1 is given in Table 1 and displayed in the form of a pie diagram in Figure 1.

In the disseminated sulphide ore, the cyanide recoverable gold is significantly lower (Lakefield, 1985 and Thibault, 1987)., because there are no gold-bearing scorodite and Fe oxides and hydroxides present. In addition, the presence of pyrrhotite in the disseminated ore will result in a higher consumption of reagant.

4.5.0 CONCLUSIONS

Arsenopyrite and arsenian pyrite contain submicroscopic gold which is refractory to direct cyanidation. The invisible gold content of the arsenopyrite is 123. ± 61. g/t and that of the pyrite is 24.1 ± 5.3 g/t. In the pyrite, the gold content is directly proportional to the

TABLE 4

CYANIDATION TESTS

Test#	K_{80} (µm)	Extrn %	Residue g/t Au	HEAD g/t Calc	HEAD g/t Direct	Yield %
1	50	56.1	4.77	10.9	11.0	56.6
2	24	58.6	4.48	10.8		59.3
3	13	61.6	4.40	11.5		60.0

$$\text{Yield} = \frac{(\text{Direct Head}) - (\text{Residue})}{(\text{Direct Head})}$$

Conditions: 33% solids, 1 g/l NaCN, pH 10.5 - 11.0, 48 hours.

TABLE 5

INVISIBLE GOLD IN SCORODITE AND IRON OXIDES

Scorodite		Iron Oxides	
Particle #	Au, g/t	Particle #	Au, g/t
75	14.5	87	4.1
88	5.8	89	2.0
107	170.	109	3.7
108	15.2	110	8.2
N = 4		N = 4	
$\hat{x} \pm \lambda = 51. \pm 79.$ g/t Au		$\hat{x} \pm \lambda = 4.5 \pm 2.6$ g/t Au	

arsenic content, thus the arsenian pyrite is gold-bearing and the arsenic-poor pyrite is poor in gold. The two types of pyrite are closely intergrown and the arsenian pyrite frequently contains small arsenopyrite inclusions.

In the partially oxidised composite sample #1, it was calculated that 38.3 ± 22.2 % of the gold is in the arsenopyrite and 15.2 ± 4.1 % is accounted for by the pyrite. The calculated sulphide-bound refractory gold is 53.5 % of the total, which is 34 % higher than the non-cyanide recoverable gold (40%). This is attributed to (i) an overestimation of the modal arsenopyrite content (the average gold content of the arsenopyrite 123 61 g/t compares closely with the gold assay of the arsenopyrite concentrate, 144 g/t) and (ii) a bias in the average invisible gold content of the pyrite by analysing more arsenian than non-arsenian pyrites (Appendix A1). The gold recovered by direct cyanidation is 60. ± 2.7 % of the total. Fine grinds have an insignificant effect on the recovery. The cyanide recoverable gold is sub-microscopic in scorodite, Fe oxides and hydroxides, which are the oxidation products of the gold-bearing sulphides, and to a lesser extent, as fine-grained but visible gold in the silicate gangue.

APPENDIX A1.1

ELECTRON PROBE MICROANALYSIS OF HOMOGENOUS PYRITE GRAINS

Grain #	N	x
As-free type:		
76 (part)	2	0.02 ± 0.02
86 (part)	4	0.05 ± 0.06
91	6	0.09 ± 0.07
Arsenian type:		
76 (part)	5	2.13 ± 0.28
86 (part)	6	2.68 ± 0.43
94	6	1.70 ± 0.18
96	10	2.26 ± 0.60
98	11	1.37 ± 0.30
100	11	2.51 ± 0.47
102	6	1.35 ± 0.41
104	6	1.56 ± 0.21

APPENDIX A1.2

ARSENIC CONCENTRATION IN ION PROBED PYRITE

Particle #	As, wt%	Au, g/t
1	2.5	8.7
2	3.4	50.
3	0.23	0.91
6	1.8	38.7
7	1.7	14.
8	2.5	14.1
9	2.5	20.1
12	0.33	1.7
13	3.4	28.
14	1.2	2.3
15	1.7	19.4
16	0.76	1.4
18	1.8	5.2
19	1.4	2.
20	2.8	28.7
21	4.2	84.9
22	0.66	2.6
24	2.5	20.8
25	3.5	51.9
27	3.5	27.8
29	4.7	65.2
31	2.8	40.1
32	0.76	4.9
33	3.5	42.9
36	1.3	22.1
37	2.2	18.8
39	0.76	14.3
40	3.7	42.5
43	4.4	67.1
44	2.2	16.8
45	3.	37.1
48	2.8	22.7
49	2.6	1.3
50	1.3	4.3
52	0.023	1.1
55	0.024	1.7
56	3.	102.
62	3.	24.
68	0.96	22.
70	2.1	8.1
71	0.44	2.7
76	0.64	14.
78	0.69	8.9
82	2.4	108.
83	2.2	19.
84	3.9	78.
86	0.3	7.
85	1.7	37.6
91	2.	64.
92	0.4	2.9
94	1.3	4.
96	3.1	27.
98	1.3	7.3
100	3.4	55.3
102	1.7	7.
104	1.8	11.1
2'	1.7	8.8
3'	2.5	32.
4'	1.25	15.
5'	2.7	18.
6'	1.05	26.
7'	0.25	3.5
8'	0.30	1.2
9'	1.3	47.
10'	2.3	8.2
11'	0.9	7.
12'	3.1	50.
13'	2.1	43.
14'		32.
15'	1.35	11.
16'	0.85	10.
17'	6.4	46.
18'	0.25	4.3
19'	2.6	41.
20'	0.7	5.6
22'	2.2	25.
23'	1.65	17.
24'	1.0	11.
25'	3.0	6.8
26'	2.1	40.
27'	2.1	38.

N = 81

x ± : 1.82 ± 0.53 wt% As

APPENDIX A2

ASSAYS AND IMAGE ANALYSIS

	Mass Split %	Au g/t	Au distribution %
Head	100	11.07	100
Heavy fraction	11.68	34.7 (calc)	30.6
Light fraction	88.32	7.95	63.8

IMAGE ANALYSIS

	Area viewed (mm^2)	# of grains
Heavy fraction	85.0	2798
Light fraction	34.0	2182

PROPORTIONS OF MINERALS

	PROPORTION %				DISTRIBUTION %			
	py	aspy	gangue	sc/ox	py	aspy	gangue	sc/ox
Heavy fraction Vol. %	43.1 ±2.5	13.3 ±2.6	25.5 ±4.8	18.2 ±4.8				
Wt. %	**49.0** **±2.8**	**18.2** **±3.6**	**16.2** **±3.0**	**16.6** **±4.4**	**87.9**	**61.7**	**3.1**	**6.6**
Light fraction Vol. %	0.9 ±0.2	0.8 ±0.3	74.1 ±6.0	24.2 ±5.8				
Wt. %	**1.4** **±0.2**	**1.5** **±0.5**	**66.2** **±5.4**	**30.9** **±7.4**	**12.1**	**38.3**	**96.9**	**93.4**
Head Wt % **(calc)**	**6.9** **±1.1**	**3.4** **±1.0**	**60.4** **±5.6**	**29.2** **±7.1**	**100.0**	**100.0**	**100.0**	**100.0**

* sc/ox = scorodite + Fe oxides and hydroxides.

CHAPTER 5

DETERMINATION OF THE MINERALOGICAL DISTRIBUTION OF GOLD IN A COMPOSITE ORE FROM THE HOWARD ZONE, CONGRESS MINE, B.C.

SSW/PMS/88/15

SUMMARY

The composite ore tested from the Howard 1 and 2 ore zones assayed 12.1 g/t Au, 3.27 Wt. % S, 0.52 Wt. % As and had Te,Bi and organic carbon in insignificant amounts. The gold recoverable by direct cyanidation at K_{80} = 58 µm (250 mesh) is only 10.7%. Fine grinds did not improve the recovery significantly. The refractory gold estimated by cyanidation of a pulverised ore (K_{80} = 12 µm; 1270 mesh) is 76.4 %.

Gold minerals were not recognised during a detailed microscopic study. Ion probe microanalysis identified arsenopyrite as the principal carrier of the submicroscopically refractory gold. The fine-grained arsenopyrite is significantly enriched in gold compared to the coarser variety. The average gold concentration of the fine-grained arsenopyrite is 1630. ppm (g/t) accounting for 75.4% of the total gold. The coarse arsenopyrite has a gold content of 38. ppm (g/t) contributing 1.8% of the head assay. The pyrite, with 1.2 ppm contributes only 0.6%.

Based on the gold mineralogy, size and association, the maximum recoverable gold in a bulk sulphide concentrate is not expected to exceed 60%. Any processing scheme aiming at a recovery exceeding 60% should take into consideration the fine-grained unliberated gold-bearing arsenopyrite associated with the gangue. Selected processing schemes are being tested. The first scheme involves sulphuric acid pretreatment of the ore to dissolve the carbonates, followed by pressure oxidation, neutralization and cyanidation of the autoclave residue. The second test involves the production of a 'dirty' sulphide bulk float to be used as the feed for the autoclave, followed by the neutralization of the autoclave residue with the carbonate-rich flotation tailings, thus saving on lime and exposing the gold in the gangue to cyanidation. Pressure oxidation is the most conservative alternative, and has been adopted in several mines. The gold recovery is expected to exceed 85%, based on the gold mineralogical distribution.

FIGURE 1

MINERALOGICAL DISTRIBUTION OF GOLD

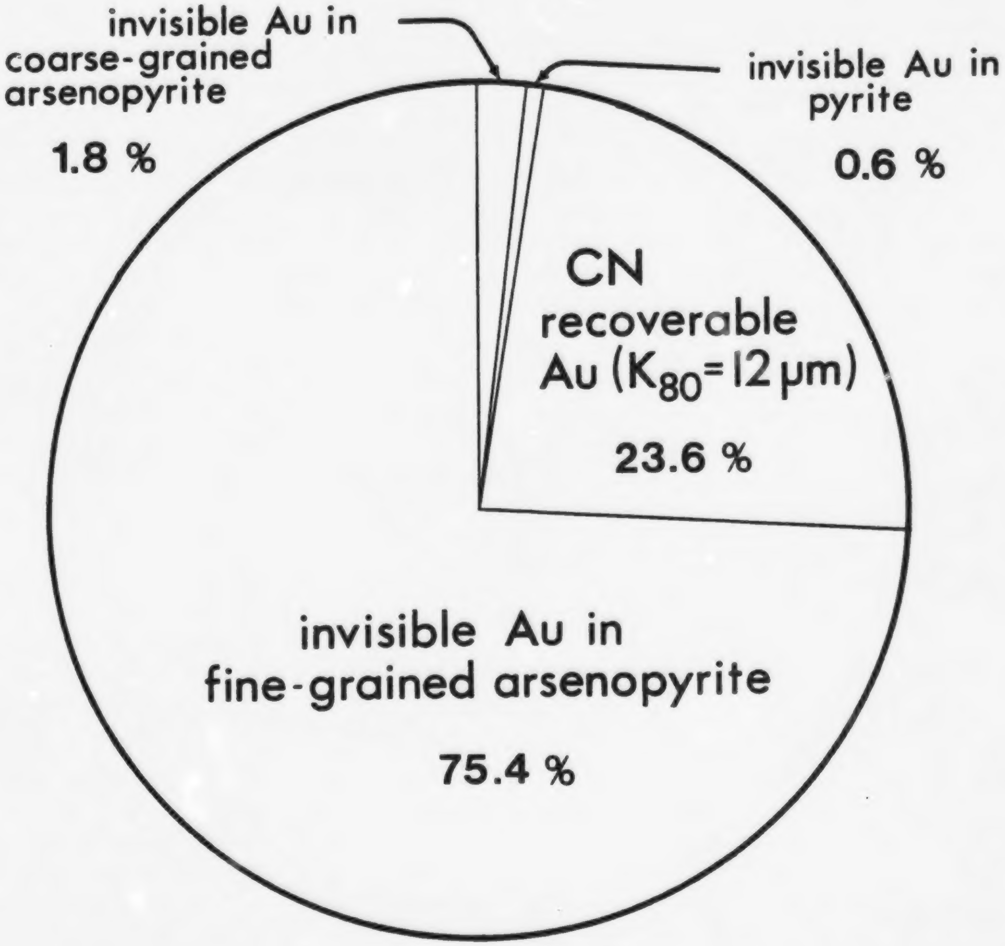

TABLE 1

MINERALOGICAL DISTRIBUTION OF GOLD IN THE COMPOSITE ORE

	Au g/t	Distribution	Precision
Assayed Au	12.1	100.0	
CN recoverable (K_{80} = 12 µm)	2.86	23.6	
Invisible gold in fine-grained arsenopyrite (conc. 1630. ± 1330. ppm) (0.56 Wt. %)	9.13	75.4	± 61.5
Invisible gold in coarse-grained arsenopyrite (conc. 38. ± 17. ppm) (0.57 Wt. %)	0.22	1.8	± 0.8
Invisible gold in pyrite (conc. 1.2 ± 0.61 ppm) (5.73 ± 0.64 Wt. %)	0.07	0.6	± 0.3
Total accounted Au	12.28	101.4	± 62.6

LIST OF TABLES

Table 1 Mineralogical distribution of gold in the composite ore
Table 2 Chemical assays
Table 3 Cyanidation test results
Table 4 Invisible gold in sulphide minerals

LIST OF FIGURES

Figure 1 Mineralogical distribution of gold in the composite ore
Figure 2 Distribution of invisible gold in arsenopyrite
Figure 3 Distribution of invisible gold in pyrite

LIST OF PLATES

Plate 1 Intergrowth of pyrite and marcasite
Plate 2 Fine-grained arsenopyrite in quartz-calcite matrix
Plate 3 Fine-grained arsenopyrite enclosed in quartz - calcite - K-Al-silicate particle
Plate 4 Aggregate of fine-grained arsenopyrite

APPENDICES

A1 Image analysis data and gold assays of density separation.

5.1.0 INTRODUCTION

The president of Levon Resources, Mr. L. Wolfin, requested the determination of the gold mineralogy in the Congress Mine, B.C., as part of the general project on the characterization of Canadian refractory gold ores by ion probe microanalysis. The aim of this project is to provide the basic information that will lead to improved gold recoveries.

Ores from the Howard ore zone of the Congress property feature a complex Au metallurgy, despite a relatively simple sulphide mineralogy of pyrite + arsenopyrite +/- stibnite. Direct cyanidation of the ores has given consistently less than 10 % gold recovery in previous testing. Statistical correlation had suggested that gold was in some way associated with the arsenopyrite and only a single grain of native gold had been identified in the ores prior to the start of the present study. However, doubts remained concerning the association between gold and arsenopyrite, since in some samples, where arsenopyrite contents are negligible, gold contents are significant.

With sulphide contents of the ore less than 10% and only limited success even at fine grinds in producing relatively clean bulk sulphide floats that concentrated most of the gold, Hawthorn (1988) proposed the following challenging flowsheet: Flotation of a bulk sulphide concentrate, followed by biooxidation and conventional cyanidation of the bioleach residue. The gold-bearing carbonate-rich flotation tailings would be used to neutralize the bioleach liquor, thus additionally rendering amenable to cyanidation the gold which is associated with the carbonates. The initial separation of the sulphides from the carbonates is required in order to achieve the low pH required for the bioleach, which has to be neutralized after and increased to a pH of 10.5-11.0 for the cyanidation step. However, the following problems remain: production of a clean bulk sulphide concentrate and the incorporation of a new technology such as bioleaching. Also, the effectiveness in recovering the gold from the carbonate gangue as proposed in the flowsheet is unclear.

The objective of this study is to obtain a complete mineralogical balance for gold that will assist in the development of an effective flowsheet for the recovery of gold.

Two samples were received from Levon Resources. The Chief Geologist with Levon Resources provided a composite ore sample from the Howard 1 and 2 zones, and Mr. Hawthorn, consultant metallurgist, provided a flotation concentrate (#1515) produced from ore from the same zones.

This study was supported by Levon Resources Inc., CANMET, the Geological Survey of Canada and the Department of Supply and Services.

5.2.0 METHODOLOGY

The composite ore was used to obtain the gold mineralogical balance. The procedure followed is that of a process mineralogical study coupled with diagnostic metallurgical testing, and is discussed in the methodology section of the general report (Chryssoulis, 1988). Firstly, the head sample was assayed for Au, and other elements, among which were Te, Sb and Bi, to assess the possibility of gold tellurides, aurostibilte and maldonite being present. These minerals are sparingly soluble in cyanide under normal leaching conditions. The sample was also assayed for preg-robbing organic carbon. Three cyanidation tests were carried out using 500g charges at progressively finer grinds to determine refractoriness to cyanidation and the effect of grinding upon recovery.

A sub-sample of the composite ore was sieved into the following size fractions: +560 µm, 560 - 90 µm and -90 µm. The intermediate fraction, comprizing 29.2 % of the total sample was separated using sodium polytungstate (s.g. 3.0 $g.cm^{-3}$) into light and heavy fractions. Four polished sections were prepared from each of the light and heavy fractions.

The flotation concentrate was treated similarly, and was seived into - 37 µm, 37 - 90 µm and + 90 µm size fractions. The + 90 µm fraction was separated by heavy liquids to remove the majority of gangue minerals, which made up about 25 % of the fraction. Three grain mounts were prepared from the heavy fraction. Further samples of the - 37 µm and 37 - 90 µm size fractions were prepared for examination using the optical microscope.

Optical microscopy was used to determine the mineralogy of the samples. The invisible gold in the sulphide minerals and the arsenic content of pyrite was determined by ion probe microanalysis. The proportions of minerals in the heavy and light fractions were determined by image analysis of the polished blocks.

5.3.0 RESULTS

5.3.1 CHEMICAL ASSAYS

Chemical assays of the composite ore sample is given in Table 2. Also given are the Au, As and S assays of the light fraction and the calculated assays of the heavy fraction.

TABLE 2

CHEMICAL ASSAYS

	mass split %	Au g/t	Au distribution	S %	Te ppm	As ppm	Bi ppm	Sb ppm
Head	100	12.1	100.0	3.27 ±0.34	3	5200	<20	130
Light fraction	94	5.98	53.5	1.79		2700		
Heavy fraction	6	108.1(*)	46.5(*)					

* calculated.

5.3.2 MINERALOGY

Major minerals: Pyrite, arsenopyrite, marcasite.

Minor minerals: Chalcopyrite, sphalerite, galena, stibnite.

Pyrite

Pyrite is the most abundant sulphide mineral. Two texturally distinct types of pyrite are recognised. By mode, they are approximately equal in abundance. The pyrite grains of the first type are more rounded with numerous cavities and contain abundant inclusions of marcasite, chalcopyrite, sphalerite, arsenopyrite and gangue minerals. The pyrites are commonly intergrown with, or enclosed by marcasite and arsenopyrite (Plate 1). The pyrites of the second type are, in general, euhedral or subhedral in form and are free of inclusions. Many of these pyrites are enclosed within gangue minerals.

Arsenopyrite

Two distinct types of arsenopyrite can be recognised, based on grain size. The coarser type are more abundant. These are large grains, of similar size to the first type of pyrites. They contain inclusions of gangue phases and are in appearance, mottled and fractured. They are commonly intergrown with the early pyrite and with marcasite. Marcasite may form a rim surrounding the arsenopyrite grain, or, alternatively, may form a core which is enclosed by arsenopyrite. The fine-grained arsenopyrite is associated exclusively with gangue. Very small needles of arsenopyrite, in the size range from 5 to 25 µm are enclosed within larger grains of gangue. A study of the host gangue phases indicates that it is either quartz (38%), calcite (22%) or an intimate intergrowth of quartz with calcite, frequently also with a K-Al-silicate (42%). Examples of the fine-grained type of arsenopyrite are shown in Plates 2 and 3.

Area measurement was carried out on the heavy and light fractions to determine the proportions of minerals present, and in particular to determine the ratio between the two types of arsenopyrite. Results are given in Appendix A1. For comparative purposes, the proportions of arsenopyrite and pyrite were also calculated on a normative basis from the As and S assays.

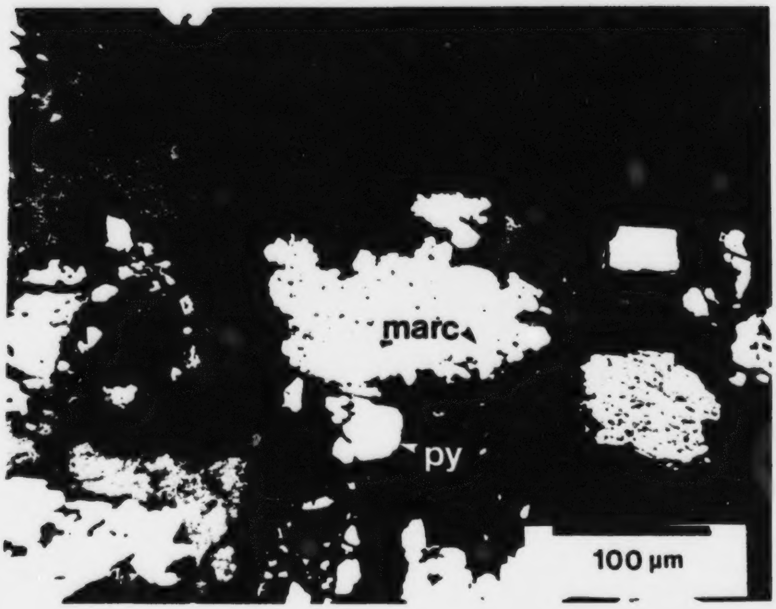
marc
py
100 µm

Plate 1 Intergrowth of pyrite (py) and marcasite (mar). gangue (g).

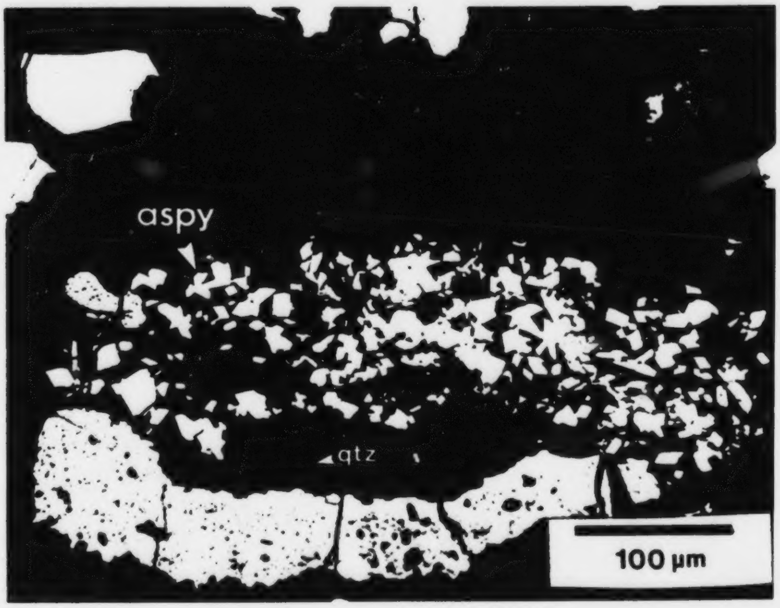
aspy
qtz
100 µm

Plate 2 Fine-grained arsenopyrite (aspy) in matrix of quartz (lighter areas) and calcite (darker areas).

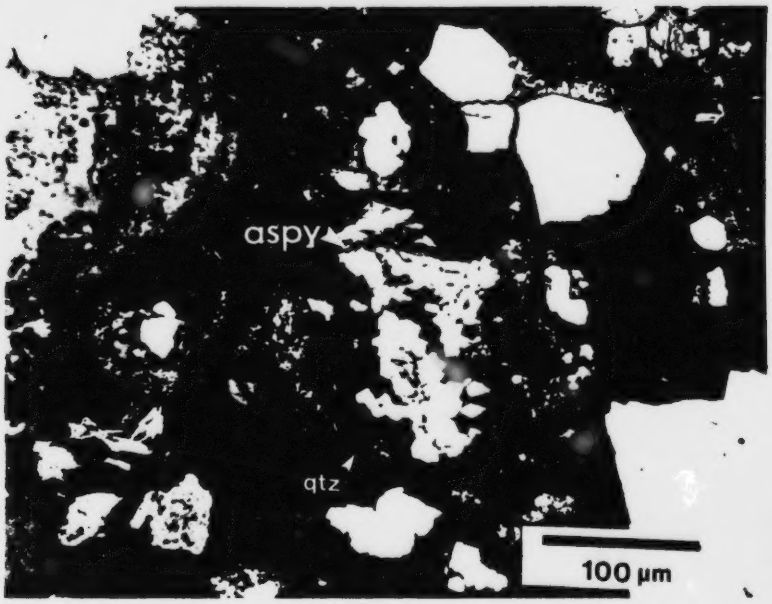
aspy
qtz
100 µm

Plate 3 Fine-grained arsenopyrite (aspy) enclosed in quartz which is itself enclosed in a mica particle.

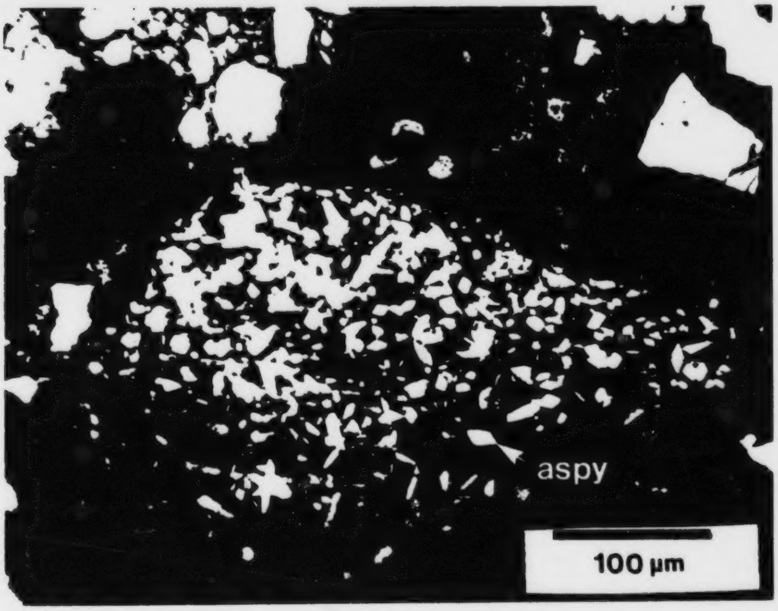

Plate 4 Aggregate particles of fine-grained arsenopyrite (aspy) enclosed in calcite (ca).

Minor Minerals

Liberated grains of **chalcopyrite, sphalerite, galena** and **stibnite** have been noted. Stibnite is more abundant in the concentrate than in the composite ore. These minerals are also present as inclusions within pyrite and arsenopyrite. These minerals together, account for less than 1 % of the sample by volume.

Gold minerals

Cyanidation tests have indicated that only a small fraction of the gold is amenable to direct cyanidation (Table 3). Fine grinds failed to increase the gold recovery significantly. With 80% of the ore finer than 12 µm, only 21.6 % of the gold was recovered. The low head assays for Te (3 ppm), Bi (<20 ppm), Sb (130 ppm; stibnite) and organic carbon preclude the presence of insoluble gold minerals or the presence of preg-robbing to any significant extent. Microscopically, no gold minerals were identified in any of the grain mounts prepared from the composite ore, or the concentrate.

5.3.3 Invisible Gold

Invisible or submicroscopic gold is the gold which is finer than 0.1 µm (=1000 Å) and therefore not visible under the optical and scanning electron microscope. For all purposes, the invisible gold is not recoverable by direct cyanidation. The invisible gold may be in true solid solution in the sulphide minerals, or dispersed in the form of discrete extremely fine inclusions (50-1000 Å) which are only visible by high resolution transmission electron microscopy (HRTEM).

The average concentration of gold in 25 fine-grained arsenopyrite particles, as determined with the ion microprobe was 1630. parts per million (g/t), with a confidence interval of 1330. g/t at a 95 % significance level. This means that in 95 out of 100 cases, the average gold content of the fine-grained arsenopyrite particles will be in the range from 300. to 2960. g/t. Measured concentrations of gold ranged from 25. to 13000. g/t.

The average concentration of gold in the coarse-grained arsenopyrite is lower. The mean concentration in 16 coarse-grained arsenopyrite particles, was 38. g/t, with a confidence interval of 17. g/t at a 95 % significance level. The gold concentrations of individual particles analyzed is given in Table 4, and the distribution of invisible gold in the two types of arsenopyrite particles is shown as a histogram in Figure 2.

TABLE 3

CYANIDATION TEST RESULTS

Test	K_{80} (µm)	Extrn. %	Residue g/t Au	HEAD Calc g/t	HEAD Direct g/t	Yield %
1	58	7.8	10.8	11.7		10.7
2	23	12.9	10.0	11.5	12.1	17.4
3	12	23.6	9.25	12.1		23.6

$$\text{Yield} = \frac{(\text{Direct head}) - (\text{Residue})}{(\text{Direct head})}$$

Conditions: 33% solids, 1 g/l NaCN, pH 10.5 - 11.0, 48 hours.

TABLE 4

INVISIBLE GOLD IN SULPHIDES
(Congress mine, B.C.; Levon Resources)

Pyrite

Particle #	Au, g/t	Particle #	Au, g/t
10	21.	27	1.2
21	0.0 <MDL	28	1.8
22	1.1	30	0.6
23	0.1 <MDL	31	1.1
24	1.0	32	9.0
25	0.3 <MDL	34	1.1
26	1.4	35	0.0 <MDL
27	0.6	36	0.0 <MDL
28	0.2 <MDL	37	0.0 <MDL
32	0.0 <MDL	38	0.0 <MDL
34	0.2 <MDL	44	0.0 <MDL
35	1.5	45	0.9
1	0.1 <MDL	46	0.0 <MDL
3	0.3 <MDL	49	0.4 <MDL
4	0.3, 0.4	50	6.3
5	0.0 <MDL	51	0.5
6	0.0 <MDL	52	0.9
7	0.0 <MDL	54	0.0 <MDL
8	2.5	55	1.7
9	2.3	56	0.5
10	1.0	58	0.8
11	2.6	59	0.0 <MDL
12	1.2	60	0.0 <MDL
13	0.3 <MDL	61	1.2
14	0.4	62	1.4
15	4.2	63	0.0 <MDL
16	1.8	64	0.0 <MDL
17	1.0	65	0.1 <MDL
18	0.8	66	0.1 <MDL
20	0.0 <MDL	68	1.1
21	4.0	70	0.0 <MDL
22	1.5	73	0.0 <MDL
23	1.3	74	1.4
25	0.3 <MDL	75	0.3 <MDL
26	0.0 <MDL	76	0.0 <MDL
		77	5.9
		78	0.0 <MDL
		80	0.0 <MDL
		81	2.0
		82	1.7
		83	0.0 <MDL
		84	0.0 <MDL
		85	0.0 <MDL
		87	0.0 <MDL

N = 79

$\hat{x} \pm \lambda$: 1.2 ± 0.61 g/t Au

Arsenopyrite

coarse grained		fine grained	
Particle #	Au, g/t	Particle #	Au, g/t
11	14.	1	1000.
17	3.8	2	730.
18	76.	3	700.
19	54.	4	660.
30	9.	5	820.
31	12.	6	800.
33	60.	7	370.
39	53.	13	180.
40	72.	20	155.
41	92.	28	780.
42	23.	29	690.
43	100.	57	890.
48	19.	65	800.
66	1.7	67	150.
72	11.6	68	25.
77	9.	69	155.
79	5.4	69A	1200.
		70	95.
		71	880.
		72	105.
		73	13000.
		74	12000.
		75	2500.
		76	1000.
		78	1100.

N = 16

$\hat{x} \pm \lambda$: 38. ± 17. g/t Au

N = 25

$\hat{x} \pm \lambda$: 1630. ± 1330. g/t Au

Marcasite

particle #	Au, g/t
71	0.5
86	0.0 <MDL

N = 2

$\hat{x} \pm \lambda$: 0.25 ± 0.50 g/t Au

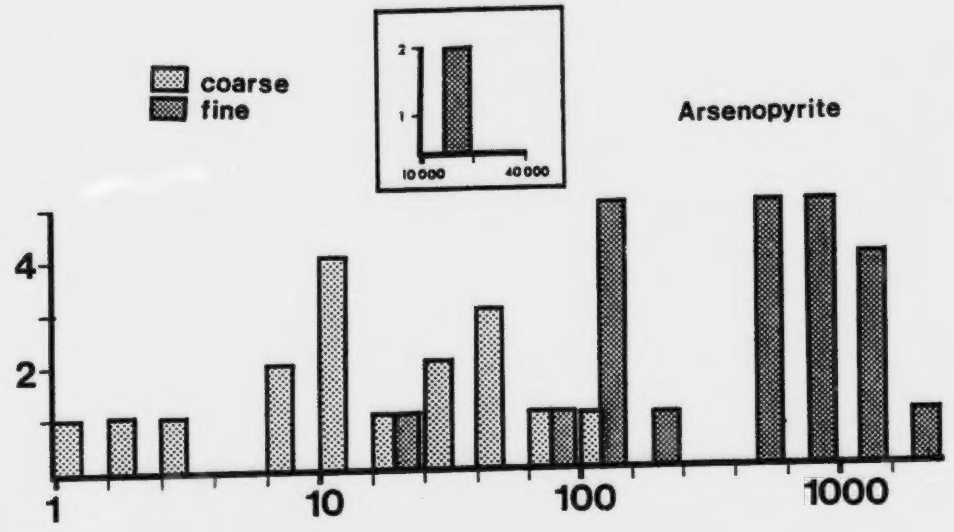

FIGURE 2. Distribution of 'invisible' gold in arsenopyrite. Lighter shading is coarse-graine arsenopyrite, darker shading is fine-grained arsenopyrite.

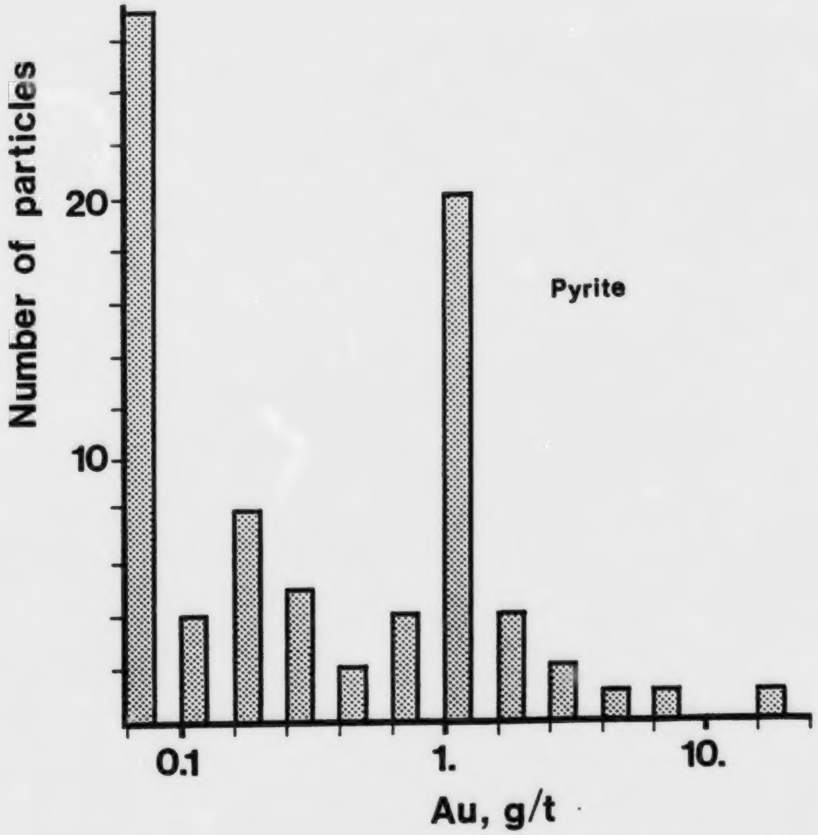

FIGURE 3. Distribution of 'invisible' gold in pyrite.

The average concentration of gold in 79 pyrite particles, was 1.2 g/t, with a confidence interval of 0.61 g/t at a 95 % significance level. There did not appear to be a great difference in gold concentrations between the two types of pyrite. The distribution of invisible gold in pyrite is shown as a histogram in Figure 3. The mean gold concentration of two marcasite particles was 0.25 ± 0.50 g/t.

5.4.0 DISCUSSION

The composite sample from the Howard 1 and 2 ore zones assays 12.1 g/t Au. The maximum recovery obtained by direct cyanidation was only 23.6%. With 80% of the sample finer than 12 µm, the refractoriness cannot be attributed to physical locking. In the absence of gold tellurides or other gold minerals which are insoluble in cyanide, and of preg-robbing carbon, the observed refractoriness is attributed to the presence of invisible or submicroscopic gold. The invisible gold as determined by diagnostic cyanidation testing is 76.4 % of the total.

Arsenopyrite is the principal carrier of the invisible gold in the ore. However, the fine-grained arsenopyrite, with an average gold content of 1630. ppm (g/t) is significantly more enriched than the coarser variety which carries only an average of 38. ppm (g/t) gold (Fig. 2). The fine-grained arsenopyrite, with an abundance of 0.56 Wt. % accounts for 9.13 g/t Au, or 75.4% of the gold assay. The coarse-grained variety, with an abundance of 0.57 Wt. % accounts for 0.58 g/t Au, or 1.8% of the total gold. When combined, both varieties of arsenopyrite account for 77.2 % of the head assay. The pyrite has a minor gold concentration of 1.2 ppm, and contributes insignificantly (0.6%) to the overall gold mineralogical distribution. Bioleach testing with bacilli strains which preferentially attack the arsenopyrite are in agreement with the observed mineralogical distribution for gold (Hawthorn, 1988). The gold mineralogical balance is graphically depicted in Figure 1, with details given in Table 1.

Forty six percent of the total gold reported to the light fraction, which would be a fairly representative example of the final tailings from a successful bulk sulphide float. The principal gold-carrier mineral in the tailings will be gold-rich fine-grained unliberated arsenopyrite. This gold is not amenable to direct cyanidation, nor may it be recovered by flotation because of the size of the arsenopyrite host mineral. Any processing scheme that aims to a gold recovery higher than 60% from the Howard ore must take into consideration the fine-grained gold-bearing arsenopyrite that is associated with the gangue.

5.5.0 CONCLUSIONS

No gold minerals were recognized in the ore. The gold recoverable by direct cyanidation is 10.7 % (K_{80} = 58 µm). The refractory to cyanidation gold is 76.4 % as determined by leaching a pulverized sample (K_{80} = 12 µm). Because of the absence of any gold tellurides, aurostibite, maldonite or preg-robbing organic carbon, the refractory gold should be submicroscopically distributed in the lattice of the sulphide minerals. The gold content of the sulphide particles was determined directly by ion probe microanalysis. Fine-grained arsenopyrite is the principal gold-carrier mineral. With an average gold concentration of 1630. ppm, and an abundance of 0.56 wt. %, it accounts for 75.4% of the total gold. Coarse-grained arsenopyrite has an average gold content of 38. ppm, and an abundance of 0.57 Wt. %, contributing 1.8 % to the gold head assay. The pyrite with 1.2 ppm gold contributes insignificantly to the gold mineralogical balance.

Gold recovery into a bulk sulphide concentrate is not expected to exceed 60% because of the unliberated fine-grained gold-rich arsenopyrite associated with calcite and quartz. In order to obtain higher gold recoveries from the Howard ore, it is neccessary to reach the gold in the fine-grained unliberated arsenopyrite which is refractory to direct cyanidation and is not recoverable by flotation beacause of its size and association. The recommended processing scheme should include a hydrometallurgical step.

APPENDIX A1

IMAGE ANALYSIS AND ASSAYS OF SEPARATION FRACTIONS

Assays:	**Mass Split %**	**Au g/t**	**Au Distribution %**
Head	100	12.1	100.0
Heavy fraction	6	108.0 (calc)	53.55
Light fraction	94	5.98	46.55

Proportions of minerals (Vol. %):

	Py[1]	**aspy (total)**	**fine aspy**	**coarse aspy**	**marcasite**	**gangue**[2]
Heavy fraction	29.5 ±0.4	11.2 ±1.2	2.4 ±0.35	8.9 ±1.6	3.3 ±1.5	55.9 ±6.0
Light fraction	1.5 ±0.4	0.9 ±0.2	0.64 ±0.29	0.25 ±0.08	0.32 ±0.6	97.3 ±0.9
Head (calc.)	3.18 ±0.82	1.52 ±0.4	**0.75** **±0.36**	**0.77** **±0.28**	0.5 ±0.96	94.8 ±1.2
Head (Wt. % from assays)	**5.73**[3] **±0.64**	**1.13**[4]	**(0.56)**[5]	**(0.57)**[5]	-	-

1: including chalcopyrite (<0.1% of head)
2: including stibnite (<0.1% of head)
3: includes marcasite
4: maximum arsenopyrite (assumes no As in pyrite)
5: calculated using ratio from image analysis

Distribution of minerals:

	Py	**aspy (total)**	**fine aspy**	**coarse aspy**	**marcasite**	**gangue**
Heavy fraction	56	44	19	69	40	4
Light fraction	44	56	81	31	60	96
Head	100	100	100	100	100	100

CHAPTER 6

DETERMINATION OF THE DISTRIBUTION OF GOLD IN THE LARA DEPOSIT, VANCOUVER ISLAND, B.C.

SSW/PMS/89/3

SUMMARY

Most of the gold in the Lara ores is cyanide recoverable gold, in the form of fine-grained electrum particles, which have a silver content of 40-50 %. The visible gold preferentially associates with tetrahedrite / tennantite, sphalerite and galena in that order. Fifty percent of the electrum identified in selected concentrate samples were less than 5 µm² in size. The distinct ore types investigated all showed a good response to direct cyanidation with only marginal increase in recovery achieved by finer grinding. Small differences are present in the gold distribution between the different distinct ore types. Cyanidation testing of the composite banded ore gave a recovery of 89.8% at a K_{80} of 18 µm and the composite sample of massive ore gave a significantly lower recovery of only 77.6% at a K80 of 12 µm. The balance is attributed to colloidal gold inclusions (<1 µm²) associated with tetrahedrite / tennantite and possibly sphalerite. However, the possibility of lower recoveries at the fine grind as a result of insufficient active cyanide due to adsorption on sphalerite or pyrite is not ruled out. Optimum recovery of gold in a flotation circuit can be achieved by minimizing losses of tetrahedrite / tennantite, and galena to the zinc concentrate and the final tailings.

The role of the "invisible gold" in the Lara ores is only important in the banded ore. Concentrations of gold within pyrite are 0.16 ± 0.12 g/t. Arsenopyrite, a minor constituent of the pyritic ores contains significant amounts of invisible gold (10. ± 4.7 g/t).

Since the banded ore is enriched in gold relative to the other two ore types and comprises the greatest portion of proven reserves, subsequent testing and mineralogical study should concentrate on this ore, in order to determine the response to flotation and the distribution of the gold-carrier minerals in the final products.

LIST OF TABLES

Table 1 Chemical assays of ores and concentrates
Table 2 Chemical assays of distinct ore types
Table 3 Normative mineralogy of distinct ore types
Table 4 Statistical analysis of electrum grains in ores
Table 5 Statistical analysis of electrum grains in concentrates
Table 6 Electron probe microanalysis
Table 7 Invisible gold in sulphide minerals
Table 8 Cyanidation tests on ore samples
Table 9 Invisible gold in tetrahedrite

LIST OF FIGURES

Figure 1 Size distribution of electrum grains in ores
Figure 2 Size distribution of electrum grains in the concentrates, clustered, based upon association
Figure 3 Correlation between gold and sulphides in the distinct ore types
Figure 4 Cumulative area frequency of electrum grains in concentrate samples and correlation of non-cyanidable gold with grind fineness.
Figure 5 Balance of electrum in concentrates based on area

APPENDICES

A1 Normative sulphide mineralogy of distinct ore types
A2 Image analysis of electrum grains in ore samples
A3 Image analysis of electrum grains in concentrates

6.1.0 INTRODUCTION

Mr. R.J. Bailes, Exploration Manager with Abermin Corporation requested to determine the process mineralogy of gold in the Lara deposit, B.C., as part of the general project on the characterization of Canadian refractory gold ores by ion probe microanalysis. The aim of this major project is to assist in improving the gold recovery by providing detailed information on the gold mineralogical distribution. The approach followed is that of a process mineralogical study coupled with metallurgical testing (Chryssoulis, 1987).

The Lara deposit is a base metal sulphide ore with silver and gold. The major ore minerals are pyrite, sphalerite, chalcopyrite. Tetrahedrite and silver-rich electrum have also been identified as minor minerals. Three distinct ore types exist, the massive, the banded and disseminated ore. The banded ore accounts for most of the proven reserves. The Lara ore will be processed as a base metal ore, and metallurgical testing to that effect has commenced at Lakefield Reserach under the supervision of R.C. Smith Associates, consultants for Abermin Corporation. The gold should account for 60% of the revenue, provided it is recoverable in the right concentrates (Bailes, pers. comm., 1988).

The objective of this particular study was the determination of both the visible and invisible (1) gold in the Lara ore, in order to make predictions regarding the distribution of gold into concentrator products. Because of the distinct sulphide mineralogy and texture, three ore types were examined and tested separately.

Previous metallurgical testing of the Lara ores at Coastech has indicated that the mineralogical distribution of gold should be complex. In flotation tests, Au reported to Cu-concentrate, Zn-concentrate, Pb-concentrate and to flotation tailings. This suggested that the mineralogical distribution of gold particles is poorly defined.

This study was financed by Abermin Corporation, CANMET, the Geological Survey of Canada and the Department of Supply and Services (DSS contract no 23440-7-9037/01 SS).

6.2.0 METHODOLOGY

Three sets of samples were received from Abermin Corporation. Firstly, six different rock chip samples from the

---

(1) 'invisible' gold is a general term including both gold in solid solution in the sulphide crystal lattice and colloidal, less than 0.1 µm, gold inclusions dispersed in the sulphide.

Coronation ore zone were received from the Senior Geologist with Abermin Corporation. These were used for a general microscopic study and corresponded to the following drill-core units: 1) TR43, 2) WH 86-43-1, unit 1-4, 3) DDH 85-15, unit 15-6, 4) DDH 85-34, unit 34-8, 5) DDH 86-139, unit 2-8, and 6) DDH 85-44, unit 21.

Secondly, a suite of samples derived from a series of flotation test products, from testing of head samples 134 and 141 were supplied by Brad Marchant, President of Coastech Research.

Thirdly, a suite of six ore samples, different from the above, and representing six distinct ore types within the deposit were received from Rick Bailes. These were as follows:

(1) low grade material, weakly laminated and **disseminated.**

(2) medium grade **banded ore**, the bulk of mineable grade material,

(3) and (4) high grade **massive** sulphide ore,

(5) **banded ore**

(6) **pyritic ore,** from contact with footwall, locally very chalcopyrite- rich.

A series of 16 one inch in diameter polished blocks were prepared from the first suite of ore samples. These were studied for visible gold using the optical microscope and with the electron microprobe to determine the silver content of electrum grains. The flotation products were sieved and a series of eight polished mounts were prepared from the +90 µm size fraction. These samples were studied under the optical microscope for visible gold, and the invisible gold in sulphide minerals was determined using the ion probe.

The second suite of ore samples were the subject of chemical assaying and cyanidation testing. Ore microscopy was carried out on distinct ore #6. The normative mineralogy of the six distinct ore types was calculated from the chemical assays.

6.3.0 RESULTS

6.3.1 CHEMICAL ASSAYS

Chemical assays of the first suite of ores, and of the flotation test samples were provided by Abermin Corporation and Coastech. Details are given in Table 1. The second set of ore samples were assayed at Lakefield Research. Results of these are given in Table 2.

TABLE 1

CHEMICAL ASSAYS SUPPLIED BY ABERMIN

ORE SAMPLES (SET 1)

SAMPLE	Cu%	Pb%	Zn%	Ag oz/t	Au oz/t
TR-43	3.04	8.30	43.07	14.98	0.717
WH 86-43-1 unit 1-4			N/A		
DDH 85-15 unit 15-6	1.94	1.01	11.1	3.12	0.255
DDH 85-34 unit 34-8	1.16	0.39	5.32	1.73	0.057
DDH 86-139 unit 2-8	2.08	7.75	32.29	15.71	0.419
DDH 85-44 unit 21	0.36	8.37	33.0	14.40	0.073

B FLOTATION PRODUCTS AND HEAD SAMPLES

	S^* %	As^* %	Cu^x %	Pb^x %	Zn^x %	Fe^x %	Ag^x g/t	Au^x g/t
Head #134	9.91	0.043	1.11	0.67	5.69	5.99	103	4.22
Head #141	8.29	0.035	0.36	0.89	5.00	5.30	67	3.80
Test 3-1 Pb Ro-conc	-	-	2.67	10.90	8.05	24.80	500	10.80
Test 3-2 Cu-Pb Ro-conc 3	-	-	1.15	2.25	9.70	25.30	235	19.00
Test 3-4 Pb conc 1	-	-	3.25	12.60	7.25	32.10	505	12.40

---

* Determined July 1988 SSW/ Lakefield Research.

x From Coastech.

TABLE 2

CHEMICAL ASSAYS OF ORE SAMPLES (SET 2)

Sample	Cu %	Zn %	Pb %	As %	S %	Sb %	Au g/t		Ag g/t
								x	
1:Disseminated	0.30	2.61	0.30	0.043	4.87	0.009	0.95 1.18	1.07 ±0.23	57.9
2:Banded	2.41	11.4	1.12	0.18	14.1	0.060	4.10 4.73	4.42 ±0.62	123.
3:Massive	1.15	15.9	6.56	0.013	12.8	0.055	2.22 2.17	2.20 ±0.06	250.
4:Massive	1.30	12.0	5.44	0.064	7.56	0.080	1.04 1.08	1.06 ±0.04	362.
5:Banded	0.56	3.49	0.54	0.045	9.93	0.004	2.33 2.22	2.27 ±0.11	59.6
6:Pyritic	0.25	1.33	0.53	0.087	10.7	0.030	2.50 5.24 7.47 3.93 4.20	4.12 ±2.35	33.8

: confidence interval of mean at a 95% significance level.

6.3.2 MINERALOGY OF ORE SAMPLES (First set)

Major minerals:	Sphalerite, galena, pyrite, chalcopyrite, tetrahedrite.
Minor minerals:	Arsenopyrite, pyrrhotite, cubanite, molybdenite, electrum.

The six samples evidenced the range of different types of ore in the deposit, from massive polymetallic ores to banded and laminated ores with a large gangue component.

Pyrite

Pyrite is present as euhedral and subhedral blastic grains. Inclusions of chalcopyrite, sphalerite, and less commonly galena and tetrahedrite are widespread, as are inclusions of silicate gangue phases. Fracturing is common in the pyrite, with galena the most common infilling mineral. Sphalerite and chalcopyrite are also abundant as fracture fillings in pyrite.

Sphalerite

Sphalerite is a major component of the ores, forming the bulk of the matrix cementing the pyrite blasts. Inclusions of chalcopyrite (chalcopyrite disease) and of galena are ubiquitous, and the minerals sphalerite, chalcopyrite, galena and tetrahedrite are commonly intergrown with one another.

Chalcopyrite

Fine-grained matrix chalcopyrite, intergrown with sphalerite and galena, contains abundant inclusions of galena and tetrahedrite, but never of sphalerite.

Galena

Galena is abundant in the matrix and is normally intergrown with sphalerite, tetrahedrite and chalcopyrite. Galena is also widely enclosed within pyrite.

Tetrahedrite-Tennantite

Matrix tetrahedrite grains are generally small and are intergrown with sphalerite and chalcopyrite. Inclusions of these minerals are widespread, especially of galena. Silicate inclusions within tetrahedrite are also common, and inclusions of electrum are also moderately abundant. Tetrahedrite appears strongly associated with galena in all of the ores studied. Electron probe microanalysis of the tetrahedrite-tennantite has shown that the average silver and arsenic contents are 1.06 % and

16.0 wt. % respectively (CANMET, 1986). Grains of tetrahedrite-tennantite from the Extension zone were lower in As and contained > 10 Wt. % Ag.

Minor Minerals

Fine-grained arsenopyrite was noted as inclusions within pyrite and within the matrix. Pyrrhotite, cubanite and molybdenite were noted as inclusions within chalcopyrite.

Normative Mineralogy

The normative mineralogy of the distinct ore types has been calculated from the chemical assays (Appendix A1). Details are given in Table 3. The ores have total normative sulphide contents ranging from 11.2 wt. % (disseminated ore) to 33.9 wt. % (massive ore). Sphalerite and pyrite are the most abundant sulphide minerals. The massive ore contains the highest amounts of galena and sphalerite, while the banded ore contains the highest content of chalcopyrite and tetrahedrite-tennantite. The pyritic ore from the footwall contains the highest content of pyrite. Contents of the other sulphide minerals are low in this ore type.

6.3.2.1 VISIBLE GOLD

The visible gold minerals reported in a CANMET (1986) study of drill core samples is a silver-rich electrum (52.3 to 58.0 % Au). In total, 33 electrum grains were identified, of which 20 were associated with sphalerite. In this study, a total of **eighty seven** electrum grains were identified in samples from the ore (1st set), the concentrates and the pyritic ore (#6).

Ores

Twenty four grains of electrum were identified in the ore chip samples investigated (Appendix A2). Three different paragenetic associations were recognized: (a) associated with galena in fractures in pyrite, (b) as inclusions within matrix sphalerite and (c), associated with tetrahedrite as inclusions or epitaxial growth phases.

Two grains were observed in fracture fillings within pyrite. Each was entirely surrounded by galena. The grains were 2 μm² and 20 μm² in size. A single grain was noted enclosed in sphalerite, of 30 μm² in size. **The remaining 21 grains were in a paragenetic association with matrix tetrahedrite, either included within, or combined with that mineral.** Some of these

TABLE 3

NORMATIVE SULPHIDE MINERALOGY OF ORE TYPES (wt.%)

	Banded	Massive	Disseminated	Pyritic
Galena	1.0	6.9	0.4	0.6
Chalcopyrite	3.3	3.0	0.5	0.7
Sphalerite*	11.3	21.2	4.0	2.0
Tetrahedrite-Tennantite**	0.7	0.4	0.2	0.0
Pyrite	12.7	2.4	6.1	18.1
Total sulphide	29.0	33.9	11.2	21.4
Gangue (by difference)	71.0	66.1	88.8	78.6

* assuming 3% Fe in sphalerite (standardless quantification using Tracor Northern EDX program).

** all As and Sb calculated as end member tennantite ($Cu_3AsS_{3.25}$).

grains also appeared to be filling fractures in the tetrahedrite. The size of these grains was generally small. Of the 21 grains, 17 were 10 µm² or less, 3 were between 10 and 40 µm² and a single grain was 350 µm² in size. The total electrum area observed was 552 µm². Table 4 shows a statistical analysis of the population. The grain size distribution in the ores is shown as a histogram in Figure 1. Although there seems to be a strong correlation between electrum and tetrahedrite, it should be stressed that the sample suite was biased towards samples which contained tetrahedrite.

Concentrates

Fifty six grains of electrum were identified (Appendix A3). The total area was 904 µm² and the average particle size was 16 µm². **Twenty two grains were enclosed in tetrahedrite (38% of the total area)** and 14 were in association with galena (25% of total area). The remainder were observed liberated and enclosed in chalcopyrite, pyrite, sphalerite and gangue. Details are given in Table 5. Grain size was coarsest for the particles associated with galena and liberated grains (Figure 2). A number of the particles associated with galena were enclosed or combined with larger grains of sphalerite or pyrite.

Distinct ore type #6

Seven grains of electrum were observed, with a total area of 360 µm² (Appendix A2). One single grain, combined with pyrite accounted for 86% of the area. Four grains were enclosed in sphalerite, one grain was enclosed in gangue and one grain was enclosed in tetrahedrite. The presence of large grains may help explain the poor reproducibility of the gold assay on this sample (Table 2).

The electrum grains in the ore samples are **silver rich.** The average gold content of ten grains, as determined with the electron probe is **49.24 ± 2.51 %.** This compares closely with the composition of the electrum reported by CANMET (1986). The electrum grains in the concentrates are also silver-rich, as determined by optical microscopy. Details are given in Table 6.

Diagnostic **cyanidation tests** were performed on the second suite of ores. Three 500 g charges using progressively finer grinds were used to determine the cyanide recoverable gold and the effect of grinding upon recovery. Results and conditions are given in Table 7. Three samples were chosen, representing the distinct ore types; (i) banded ore, samples #2 and #5 combined; (ii) massive ore, samples #3 and #4 combined and (iii) pyritic ore sample #6.

TABLE 4

STATISTICAL ANALYSIS OF ELECTRUM IN ORES

(A) Total population

Number of grains = 24

Total electrum area = 552 μm^2

Mean grain size (x) = 23 μm^2

Standard deviation on mean (σ) = 70.5 μm^2

Confidence interval of mean (λ) = 29 μm^2
at 95% significance level

(B) Grains enclosed in tetrahedrite only

Number of grains = 21

Total electrum area = 500 μm^2

Mean grain size (x) = 24 μm^2

% of grains < 10 μm^2 = 76 %

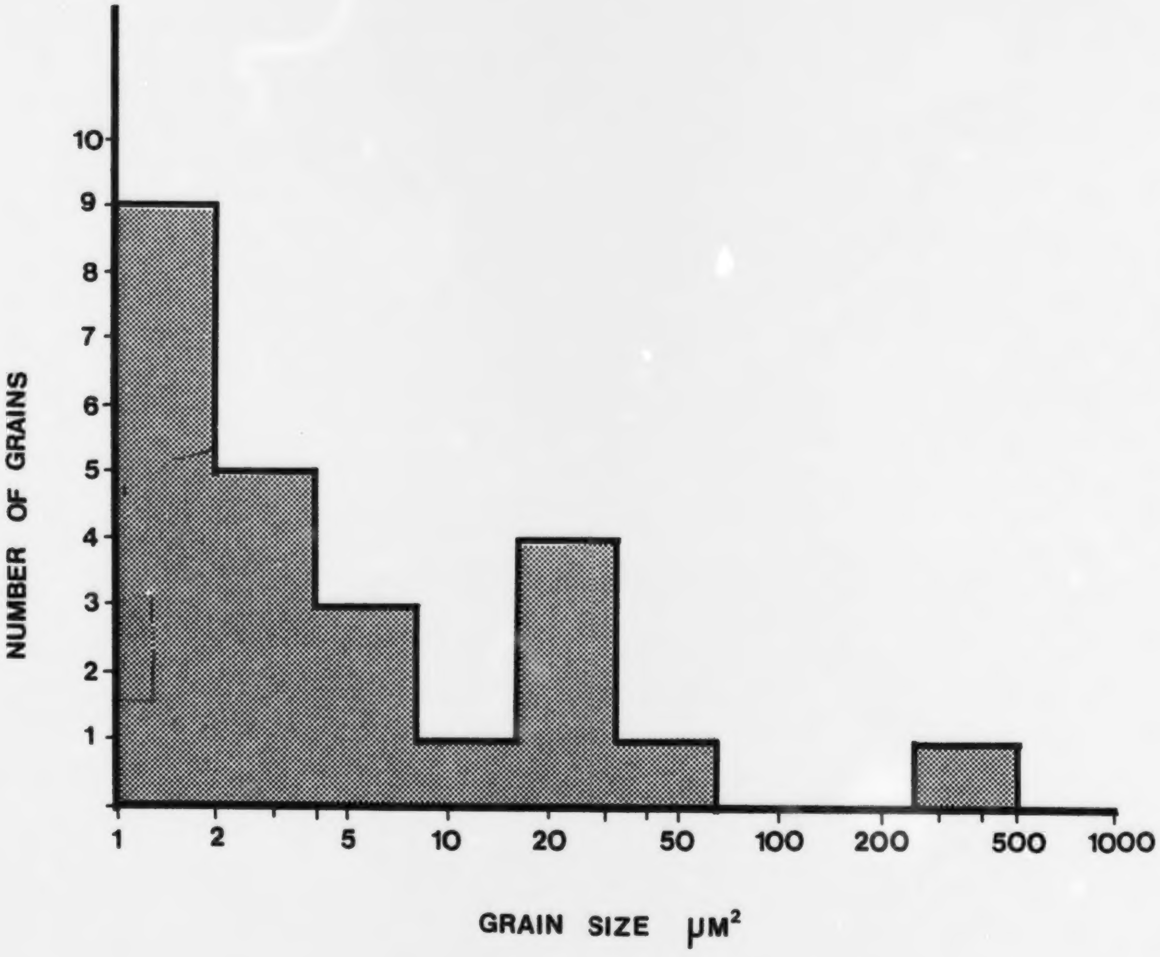

FIGURE 1. Histogram of electrum grain size in the ore samples.

TABLE 5

STATISTICAL ANALYSIS OF ELECTRUM GRAINS IN Cu-Pb CONCENTRATES

Number of sections studied = 4
Total number of electrum grains = 56

Association	N	total area	x grain size	% of total area
1) Liberated	3	95	32	11
2) Enclosed in chalcopyrite	2	14	7	2
3) Enclosed in galena	4	57	14	9
Combined with galena	1	25	25	
4) Enclosed in tetrahedrite	22	340	15	37
5) Enclosed in sphalerite[1]	14	170	12	19
Combined with sphalerite	1	1	1	
6) Enclosed in pyrite	2	5	2	22
Combined with pyrite[2]	5	192	38	
7) Enclosed in gangue	2	5	2	0
TOTAL	56	904	16	(100)

---

[1] of those grains, some are enclosed in galena (within sphalerite)	6	59	10	7
[2] of those grains, some are combined with galena on edge of pyrite	3	80	27	9

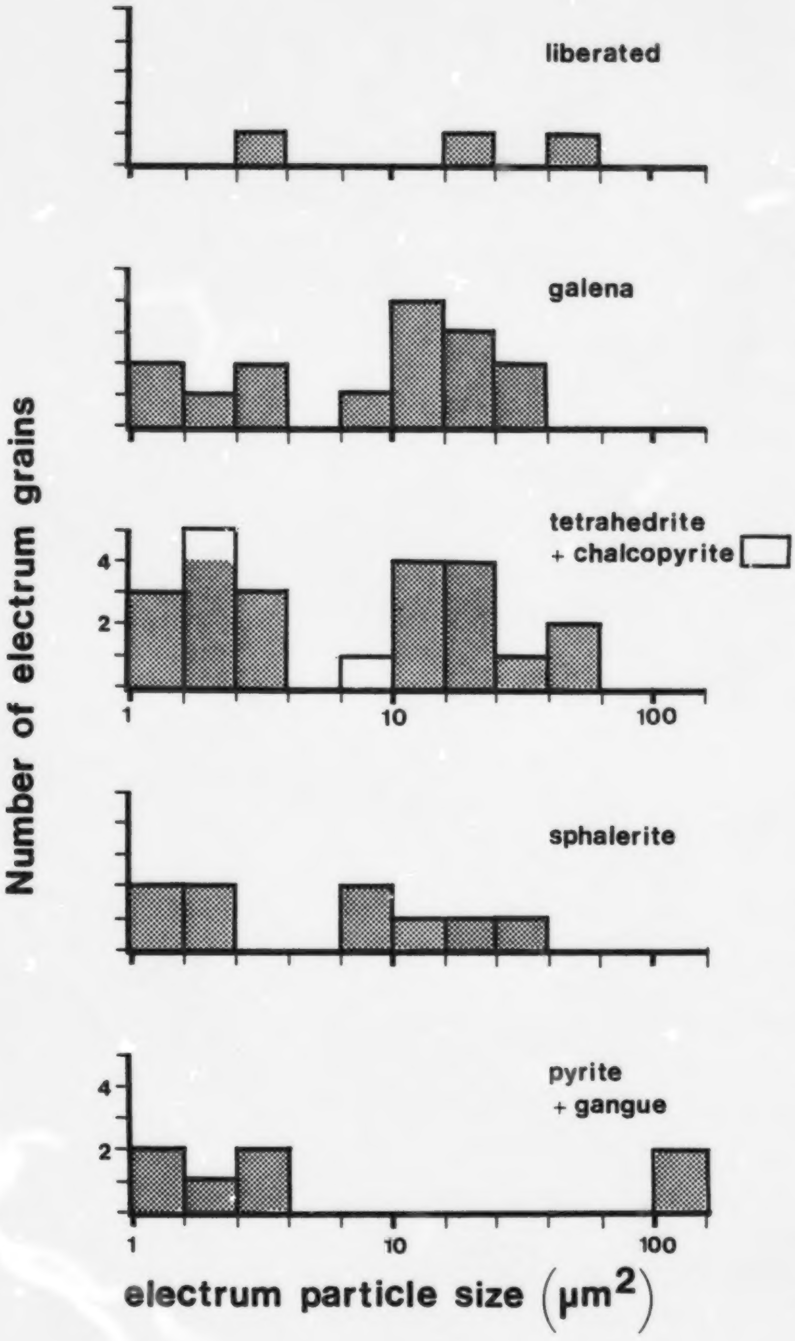

FIGURE 2. Histogram of electrum grain size in the concentrates, subdivided by mineralogical association.

TABLE 6

ELECTRON PROBE MICROANALYSIS OF ELECTRUM GRAINS

		WEIGHT %		
Grain #	Association	Au	Ag	Total*
1	Liberated	52.17	41.86	93.03
3	"	45.61	49.99	95.60
5	Enclosed in cpy	44.46	48.74	93.20
6	Enclosed in gal	45.81	47.69	93.50
7	"	56.02	36.23	92.24
9	"	45.21	46.78	91.99
14	Enclosed in tet	50.26	45.97	96.23
15	"	48.43	45.22	93.65
17	"	50.78	44.03	94.81
24	"	53.67	40.27	93.94
mean (n = 10)		49.24 ± 2.51	44.68 ± 2.66	93.82 ± 0.87

STANDARDS:

	Au	Ag	Total
Ag (100 % Ag) x (N=10	0.00	100.03	100.03
Au (100 % Au) x (N=10)	100.43	0.06	100.49

---

* Due to small grain size, totals were in the 93 - 96 % range.

TABLE 7

CYANIDATION TEST RESULTS OF DISTINCT ORE TYPES

Ore type (sample #)	K_{80} (µm)	Extraction Au %	Residue g/t Au	Head calc	Head direct
Banded	45	84.3	0.73	4.64	
(#2 and #5)	28	91.2	0.39	4.45	2.93
	18	91.9	0.30	3.70	(3.34)*
Massive	35	77.7	0.43	1.93	
(#3 and #4)	20	74.8	0.47	1.86	1.70
	12	77.6	0.38	1.70	(1.60)*
Pyritic	17	93.8	0.15	2.40	2.50
(#6)					(4.12)*

Ore Type (Sample #)	K_{80} (µm)	Au recovery %	Au recovered g/t
Banded	45	75.1	2.20
(#2 and #5)	28	86.7	2.54
	18	89.8	2.63
Massive	35	74.7	1.27
(#3 and #4)	20	72.4	1.23
	12	77.6	1.32
Pyritic (#6)	17	94.0	2.35

$$\text{Au recovery} = \frac{\text{(mean direct head)} - \text{(residue)}}{\text{(mean direct head)}}$$

Conditions: 33% solids, 1 g/l NaCN, 48 hours, pH 10.5 - 11.0

* calculated from the assays of the component samples.

Correlation between gold and sulphide in the distinct ore types

A strong correlation is noted between the gold content and total sulphide in all ore types (Figure 3). In the massive ore type (#3 and #4), there is a good correlation between the gold content and the proportions of the main sulphides present, galena and sphalerite. In the case of the disseminated ore (#1) and the banded ore (#2, and #5), a correlation is noted between gold content and the proportions of galena, sphalerite, and chalcopyrite. A correlation between gold and tetrahedrite-tennantite is noted only in ore #2. A strong correlation exists for the pyritic ore #6 between Au content and the proportion of normative pyrite.

6.3.2.2 INVISIBLE GOLD

The invisible gold concentration in pyrite, galena, chalcopyrite, arsenopyrite and tetrahedrite was investigated. Invisible gold is minor in the Lara samples. Only one minor mineral, arsenopyrite, contains significant levels of gold in solid solution. The invisible gold is not recoverable by direct cyanidation.

The average gold concentration in 88 pyrite particles is 0.16 parts per million (g/t), with a confidence interval of 0.12 g/t at a 95% significance level. This means that in 95 out of 100 cases, the average gold content of the pyrite particles would be in the range from 0.04 to 0.28 g/t. Measured concentrations ranged from zero to 4.0 g/t. The minimum detection limit (5σ) for gold in pyrite was 0.25 g/t.

The average gold concentration in 17 galena particles is 0.10 parts per million (g/t), with a confidence interval of 0.04 g/t at a 95% significance level, and the average gold concentration in 9 chalcopyrite particles was 0.01 ± 0.03 g/t. Ten arsenopyrite grains were analyzed. The average concentration of invisible gold was 10. ± 4.7 g/t. The concentrations of invisible gold in individual grains analyzed is given in Table 8.

The ion probe has shown that the tetrahedrite / tennantite is a good host for colloidal gold. This was somewhat expected since tetrahedrite carries most of the fine-grained electrum (Table 5). The invisible gold content of 19 tetrahedrite particles was 54. ± 70. ppm (Table 9). The large confidence interval is attributed to the non-uniform distribution of the colloidal gold. There is some evidence that the tetrahedrite / tennantite from the massive ore has more colloidal gold. However, more grains of tetrahedrite would have to be analysed to confirm this. In one grain, there is evidence of solid solution gold or very fine colloidal gold (Table 9).

FIGURE 3

Correlation between gold and normative sulphide mineralogy

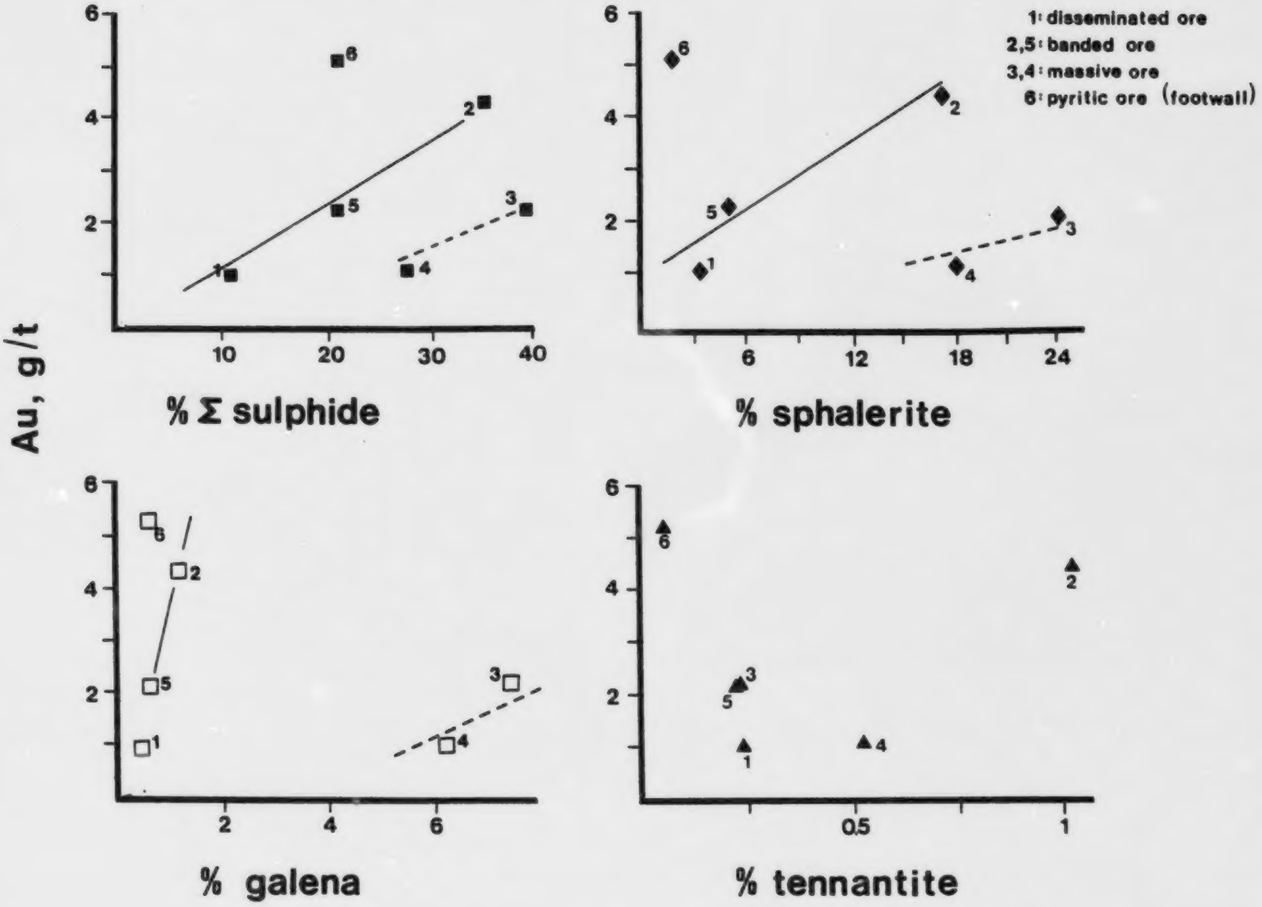

TABLE 8

INVISIBLE GOLD CONCENTRATION IN SULPHIDES
(Lara, Vancouver Island B.C.; Abermin)

Pyrite

particle #	Au, g/t	particle #	Au, g/t	particle #	Au, g/t	particle #	Au, g/t
1	0.0 <MDL	30	0.0 <MDL	$69^{\#}$	0.0 <MDL	$99^{@}$	0.0 <MDL
2	0.0 <MDL	31	0.0 <MDL	71^{*}	0.0 <MDL	$100^{@}$	0.0 <MDL
3	0.0 <MDL	37	0.0 <MDL	72^{*}	0.0 <MDL	$101^{@}$	0.0 <MDL
4	0.0 <MDL	38	0.0 <MDL	73^{*}	1.3	$102^{@}$	0.04 <MDL
5	0.0 <MDL	41	0.0 <MDL	76^{*}	0.0 <MDL	$103^{@}$	0.09 <MDL
6	0.0 <MDL	47	0.12 <MDL	77^{*}	0.0 <MDL	$104^{@}$	0.0 <MDL
7	0.0 <MDL	48	0.03 <MDL	78	0.0 <MDL	$105^{@}$	0.0 <MDL
8	0.06 <MDL	49	0.01 <MDL	$79^{\#}$	0.0 <MDL	$106^{@}$	0.0 <MDL
9	0.18 <MDL	$52^{@}$	0.0 <MDL	$80^{\#}$	0.14 <MDL	$108^{@}$	0.0 <MDL
10	0.0 <MDL	$54^{@}$	0.0 <MDL	$82^{\#}$	0.0 <MDL	$120^{@}$	0.8
16	3.4	$55^{@}$	0.0 <MDL	$83^{\#}$	0.55	$122^{@}$	0.0 <MDL
17	4.0	$56^{@}$	0.25	$84^{\#}$	0.07 <MDL	$123^{@}$	0.0 <MDL
19	0.0 <MDL	$57^{@}$	0.04 <MDL	$85^{\#}$	0.0 <MDL	$124^{@}$	0.0 <MDL
20	0.0 <MDL	$58^{@}$	0.1 <MDL	$86^{\#}$	0.0 <MDL	$128^{@}$	0.02 <MDL
21	0.0 <MDL	$59^{@}$	0.0 <MDL	$90^{\#}$	0.0 <MDL	$129^{@}$	0.0 <MDL
22	0.0 <MDL	$60^{@}$	0.17 <MDL	$91^{\#}$	0.09 <MDL	132^{+}	0.08 <MDL
23	0.0 <MDL	$61^{@}$	0.0 <MDL	$92^{\#}$	0.0 <MDL	133^{+}	0.0 <MDL
24	0.17 <MDL	$62^{@}$	0.0 <MDL	$93^{\#}$	0.12 <MDL	137^{+}	0.0 <MDL
25	0.0 <MDL	$63^{@}$	0.0 <MDL	$94^{\#}$	0.24	138^{+}	0.03 <MDL
26	0.0 <MDL	$66^{\#}$	0.0 <MDL	$95^{\#}$	0.1 <MDL	139^{+}	0.34
27	0.0 <MDL	$67^{\#}$	0.7	$96^{\#}$	0.3	140^{+}	0.28
28	0.0 <MDL			$97^{\#}$	0.05 <MDL	141^{+}	0.0 <MDL
29	0.0 <MDL						

N =88

$\hat{x} \pm \lambda$: 0.16 ± 0.12

Galena

particle #	Au, g/t	particle #	Au, g/t
11	0.02 <MDL	50	0.28
15	0.21 <MDL	$51^{@}$	0.14 <MDL
18	0.09 <MDL	$53^{@}$	0.04 <MDL
35	0.06 <MDL	$89^{@}$	0.02 <MDL
36	0.07 <MDL	$107^{@}$	0.02 <MDL
39	0.12 <MDL	$109^{@}$	0.02 <MDL
42	0.09 <MDL	$117^{@}$	0.27
43	0.06 <MDL	$120^{@}$	0.03 <MDL
45	0.05 <MDL		

N = 17

$\hat{x} \pm \lambda$: 0.10 ± 0.04

Chalcopyrite

particle #	Au, g/t
32	0.0 <MDL
44	0.12 <MDL
$74^{@}$	0.0 <MDL
$111^{\$}$	0.01 <MDL
$112^{\$}$	0.0 <MDL
$116^{\$}$	0.0 <MDL
$125^{\$}$	0.0 <MDL
$126^{\$}$	0.0 <MDL
$127^{\$}$	0.0 <MDL

N = 9

$\hat{x} \pm \lambda$: 0.01 ± 0.03

Arsenopyrite

particle #	Au, g/t
$68^{\#}$	16.5
$70^{\#}$	17.5
1	5.6
2	5.6
3	1.9
4	17.0
6	2.0
7	4.2
8	7.8
10	22.

N = 10

$\hat{x} \pm \lambda$: 10. ± 4.7

@: core sample WH 86-43-1 unit 1-4
#: core sample DDH 85-15 unit 15-6
+: core sample DDH 85-34 unit 34-8
$: core somple DDH 85-44 unit 21

TABLE 9 INVISIBLE GOLD IN TETRAHEDRITE

	Particle No.	Au, ppm
Concentrates:	12	0.2
	13	1.6
	33	0.7
	34	0.3
	40	0.3
	46	0.8
Sample DDH-85-44:	81	22.6
	88	0.2
Sample DDH-85-44:	113	0.4
	114	0.2
	115	0.3
	118	0.3
	119	0.5
Sample DDH 85-15:	98	520.0 *
	121	0.2
	130	450.0 *
	131	0.2
	134	0.3
	135	22.0

N = 19, x ± = 54. ± 70.

* Gold micro-inclusions.

To date, sphalerite could not be analysed for invisible gold. However, based on the CANMET findings of electrum inclusions in sphalerite (1986), it is strongly suspected that sphalerite contains colloidal gold, accounting for part of the mineralogically unaccounted gold.

6.4.0 DISCUSSION

The results of the cyanidation tests indicate that most of the gold in the Lara ore is recoverable by direct cyanidation. At moderately fine grinds ($K_{80} \sim 40$ µm), 74.7 % of the gold was extracted from the massive ore and 75.1% from the banded ore. Increased fineness improved the gold recovery only marginally for the banded ore, and not at all for the massive ore. The interpretation of the cyanidation results, depicted in Figure 4, is that the greater recovery by progressively finer grinding of the massive ore can be explained by the microscopically determined presence of numerous small inclusions in the 1-20 μm^2 size range (Figure 5). However, this is not the case for the banded ore.

The refractory to cyanidation gold cannot be balanced by the invisible gold in pyrite, galena, chalcopyrite and tetrahedrite-tennantite. Ion probe microanalysis of 127 grains of these minerals determined gold concentrations of 0.16 ± 0.12 g/t in pyrite with a MDL of 0.25 g/t, 0.10 ± 0.04 g/t in galena with a MDL of 0.25 g/t, and 0.01 ± 0.03 g/t in chalcopyrite with a MDL of 0.3 g/t. The tetrahedrite / tennantite has more invisible gold, and in particular, some grains contain numerous inclusions of a gold mineral, possibly electrum. The invisible gold contributed by tetrahedrite / tennantite in the banded ore, where it is most abundant accounts for approximately 12 % of the head assay. The sulphide which concentrates most of the invisible gold is arsenopyrite, with a gold content of 10. ± 4.7 g/t. However, it contributes insignificantly to the overall gold mineralogical balance because it is extremely scarce. Arsenopyrite is most abundant in the pyritic ore from the footwall.

Sphalerite particles could not be analysed with the ion probe because they were strongly charging under the primary ion beam. It is possible that sphalerite has colloidal electrum, that is mostly not amenable to cyanidation. This possibility is supported by the identification of numerous fine visible electrum inclusions (2-10 µm) in sphalerite from an early drill core (CANMET, 1986) and the observed increase in refractoriness to direct cyanidation with higher contents of sphalerite (Tables 3 and 7). However, this could result because the active cyanide concentration decreased by absorption on the sphalerite surface.

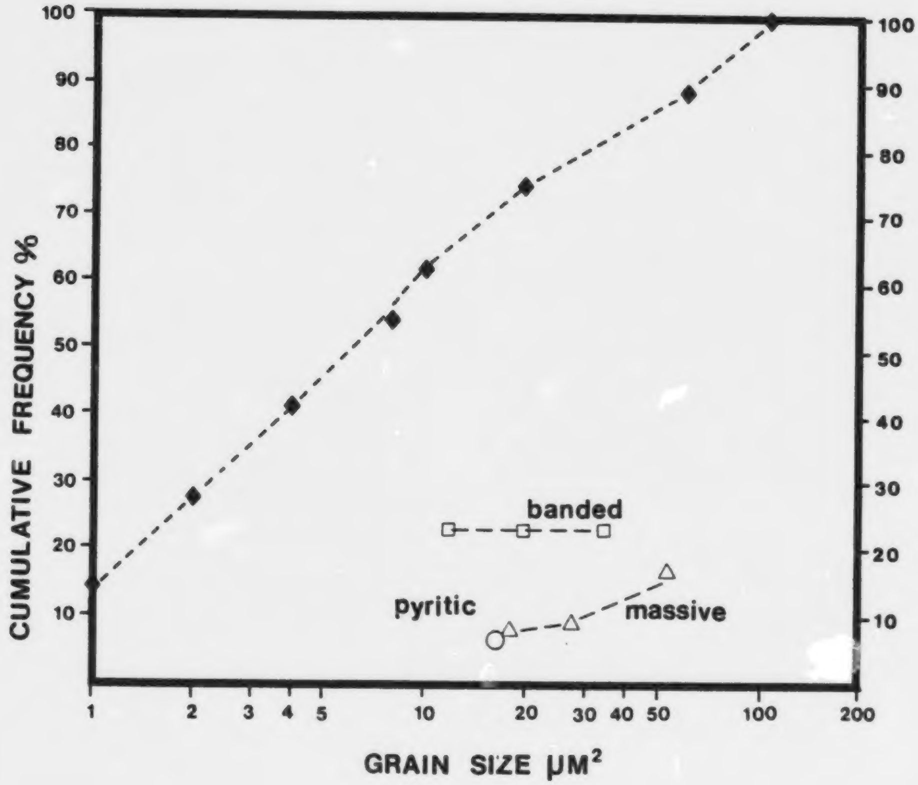

FIGURE 4. Cumulative frquency of electrum grains in samples and correlation of non-cyanidable gold with grind fineness (K_{80}).

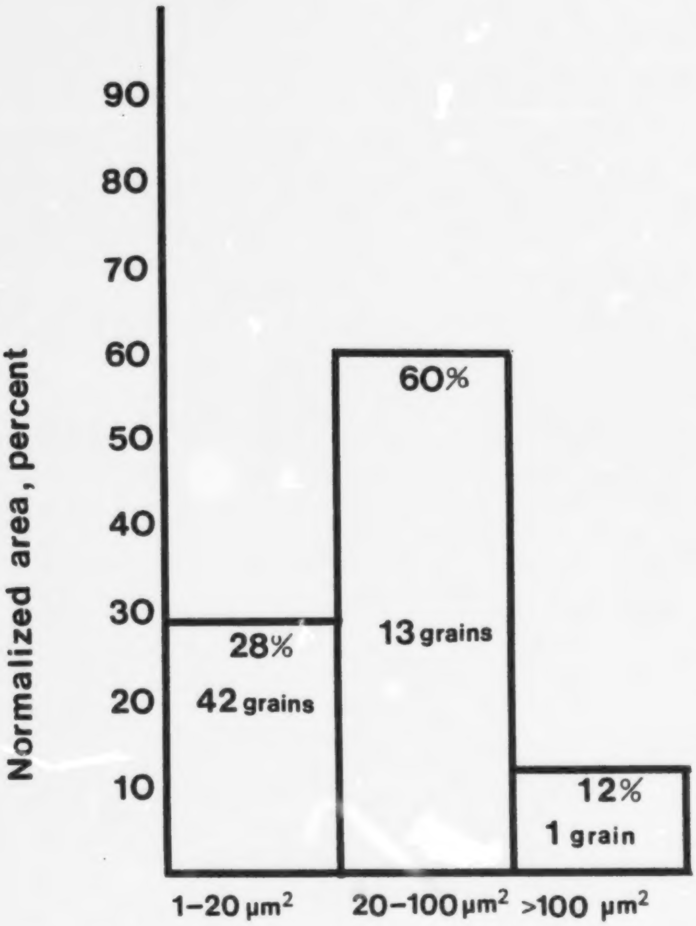

FIGURE 5. Balance of electrum in concentrates based upon area of grains.

6.5.0 CONCLUSIONS

The conclusions of the present study on the gold process mineralogy are as follows:

(i) the principal gold carrier mineral is silver-rich electrum;

(ii) the electrum is fine grained down to sub-microscopic size particles, i.e. less than 1 μm,

(iii) electrum is associated mostly with tetrahedrite, sphalerite and galena in that order,

(iv) the host of the electrum varies with ore type,

(v) visible electrum accounts for 70-95% of the gold head assay depending on ore type, while colloidal electrum or native gold accounts for the balance,

(vi) the invisible gold content in pyrite, the dominant sulphide in the Lara ores is insignificant; 0.16 ± 0.12 g/t Au,

(vii) arsenopyrite, a minor constituent of the pyritic ore contains 10. ± 4.7 g/t Au,

(viii) the colloidal gold content of tennantite / tetrahedrite is 54. ± 70. g/t Au,

Gold losses by flotation are expected to be in the following forms:

(i) electrum in the slimes because of its fineness and composition,

(ii) electrum in the zinc concentrate because of its association,

(iii) colloidal gold or electrum in sphalerite, and tetrahedrite/ tennantite in the zinc concentrate and the final tailings.

APPENDIX A2

NORMATIVE SULPHIDE MINERALOGY OF ORE SAMPLES (wt. %)

	Dissem (1)	**Banded (2)**	**Massive (3)**	**Massive (4)**	**Banded (5)**	**Pyritic (6)**
Galena	0.35	1.29	7.57	6.28	0.62	0.61
Chalcopyrite	0.52	5.38	2.98	2.92	1.27	0.66
Sphalerite	3.97	17.33	24.17	18.24	5.30	2.02
Tennantite*	0.24	1.06	0.23	0.55	0.23	0.04
Pyrite	6.11	11.24	4.78	0	14.20	18.13
(Σ sulphide	**11.19**	**36.30**	**39.73**	**27.99**	**21.62**	**21.50)**
Gangue (by difference)	88.81	63.70	60.27	72.01	78.38	78.50

* all As and Sb calculated as tennantite.

APPENDIX A3

ELECTRUM GRAINS IN THE ORES

A) Ore Suite (1st Set)

Grain	Association	Size (μm^2)
1	Enclosed in sphalerite	30
2	Enclosed in pyrite	2
3	"	20
4	Enclosed in tetrahedrite	350
5	"	30
6	"	10
7	"	8
8	"	4
9	"	3
10	"	4
11	"	4
12	"	2
13	"	1
14	"	7
15	"	5
16	"	1
17	"	35
18	"	2
19	"	1
20	"	1
21	"	3
22	"	2
23	"	2
24	"	25

B) Distinct Ore #6

Grain	Association	Size (μm^2)
1	Enclosed in sphalerite	28
2	"	6
3	"	4
4	"	3
5	Combined with pyrite	310
6	Enclosed on tetrahedrite	2
7	Enclosed in gangue	7

APPENDIX A3

ELECTRUM GRAINS IN CU-PB CONCENTRATES

Grain	Association	Size (μm^2)	Grain	Association	Size (μm^2)
1	Liberated	5	29	Encl. in tet.	8
2	"	60	30	"	1
3	"	30	31	"	10
			32	"	40
4	Encl. in cpy	10			
5	"	4	33	Encl. in sph.	15
			34	"	2
6	Encl. in gal.	50	35	"	8
7	"	5	36	"	45
8	"	1	37	"	2
9	"	1	38	"	30
10	Comb. with gal	25	39	"	8
			40	" (1)	8
11	Encl. in tet.	20	41	" (1)	15
12	"	4	42	" (1)	20
13	"	5	43	" (1)	4
14	"	10	44	" (1)	2
15	"	20	45	" (1)	10
16	"	60	46	"	1
17	"	40	47	Comb. with sph	1
18	"	15			
19	"	12	48	Encl. in py	4
20	"	60	49	"	1
21	"	2	50	Comb. with py	2
22	"	3	51	" (2)	25
23	"	3	52	" (2)	45
24	"	3	53	" (2)	10
25	"	30	54	"	110
26	"	2			
27	"	1	55	Encl. in gangue	1
28	"	1	56	"	4

TOTAL = 56 grains Σ area = 904 μm^2 $\bar{x}$ area = 16 μm^2

---

(1) Enclosed in galena within sphalerite particle
(2) Combined with galena on edge of pyrite particle

CHAPTER 7

GOLD MINERALOGICAL DISTRIBUTION IN COMPOSITES CBE-QP-1 AND CBW-87-1 FROM THE GOLDEN POND PROPERTY, QUEBEC

SSW/PMS/89/04

SUMMARY

Native gold or electrum is the principal gold-carrier mineral in composite samples CBE-QP-1 (11.0 g/t Au) and CBW-87-1 (6.6 g/t Au) from Golden Pond, Quebec. Ninety three and seventy nine percent of the gold is respectively recoverable by direct cyanidation.

Arsenopyrite is the second in importance gold carrier mineral in the two composite samples. Invisible gold in arsenopyrite accounts for 3.4 % (CBE-QP-1) and 11.9 % (CBW-87-1) of the gold head assays. The arsenopyrite content of the two samples is comparable. However, the invisible gold concentration is significantly higher in the CBW-87-1 arsenopyrite, 41.4 ppm, compared to 18.3 ppm for sample CBE-QP-1. A positive correlation was documented between fineness of arsenopyrite crystals and their invisible gold concentration. In sample CBW-87-1, fine arsenopyrites assayed 98.9 ppm, compared to the coarser arsenopyrites which assayed 23.2 ppm. Pyrite is an insignificant carrier of invisible gold.

The gold not recovered by direct cyanidation from composites ground to 95% minus 200 mesh is mostly invisible gold in arsenopyrite, taking into account the bias towards analyzing larger grains, and to a lesser extent as fine inclusions of gold locked in sulphides, primarily pyrite. The theoretical maximum gold recovery based on the data availiable is 96.4% for sample CBE-QP-1 and 88.0% for sample CBW-87-1, on the assumption that all visible gold is recoverable.

FIGURE 1

GOLD MINERALOGICAL BALANCES
(Golden Pond, Quebec)

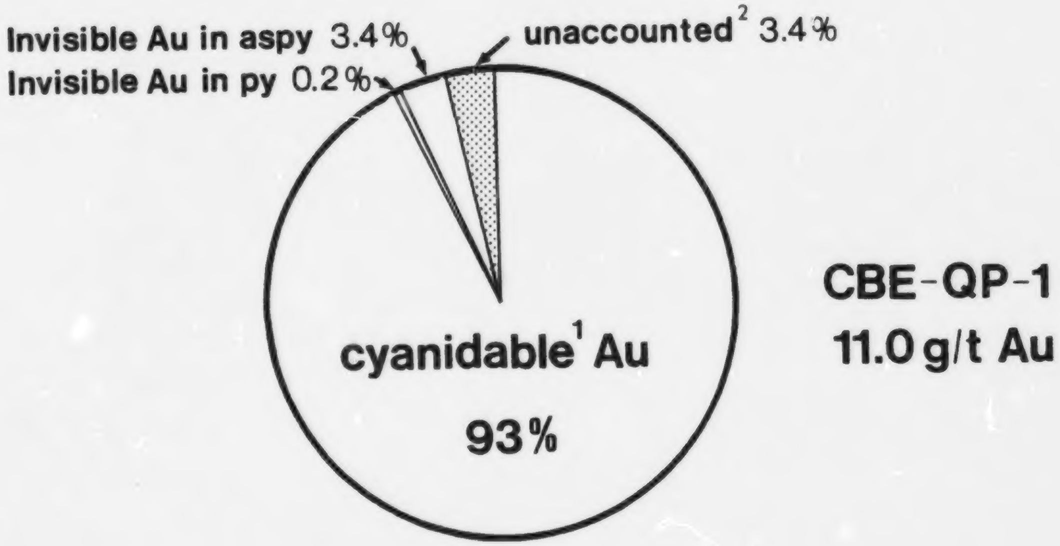

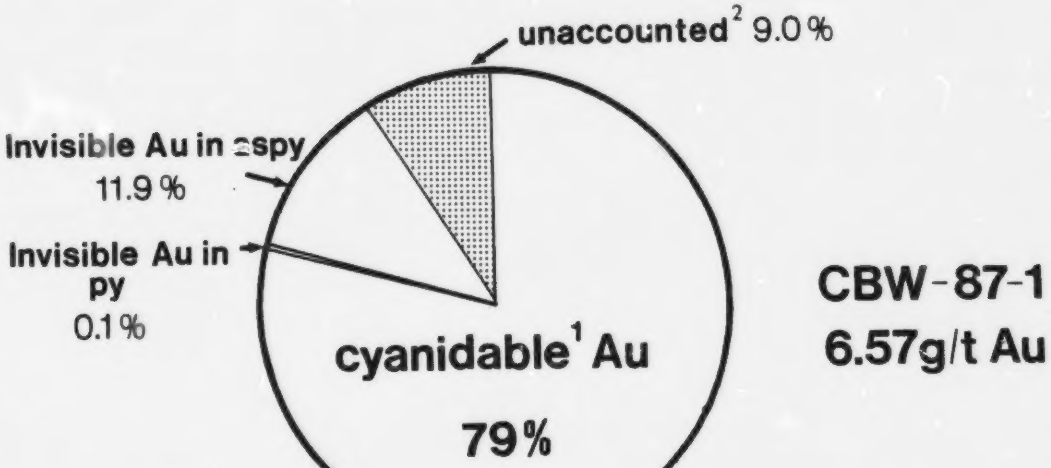

---

[1] 95% - 200 mesh

[2] primarily as invisible Au in aspy and very fine-grained gold inclusions.

TABLE 1

GOLD MINERALOGICAL DISTRIBUTION IN COMPOSITE CPE-QP-1

	Au g/t	Au %
HEAD	**11.0**	**100.0**
CYANIDABLE Au[1]		**93.0**

Visible gold association determined in the +100 mesh sink fraction:

Pyrite	64.9
Arsenopyrite	1.4
Liberated	33.7
	100.0

	Au g/t	Au %
UNRECOVERED Au		**7.0**
Invisible gold		
In arsenopyrite (1.87 wt. %)[2]	**18.3 ± 5.7**	**3.4 ± 1.1**
In pyrite (2.06 wt. %)[2]	**1.1 ± 0.7**	**0.2 ± 0.1**

Unaccounted gold (3.4%) is in the form of fine gold inclusions and as invisible gold in fine-grained arsenopyrite.

---

[1] 95% -200 mesh.

[2] normative, from As head assay.

TABLE 2

GOLD MINERALOGICAL DISTRIBUTION IN COMPOSITE CBW-87-1

	Au g/t	Au %
HEAD	6.57	100.0
CYANIDABLE Au[1]		79.0

Visible gold association determined in the +100 mesh sink fraction:

Pyrite	5.6
Arsenopyrite	0.1
Liberated	94.3
	100.0

	Au g/t	Au %
UNRECOVERED Au		21.0
Invisible gold		
In arsenopyrite (1.87 wt. %)[2]	41.4 ± 19.0	11.9 ± 5.4
In pyrite (1.80 wt. %)[2]	0.23 ± 0.24	0.1 ± 0.1

Unaccounted gold (9.0%) is in the form of fine gold inclusions and as invisible gold in fine-grained arsenopyrite.

---

[1] 95% -200 mesh.

[2] normative, from As head assay.

LIST OF TABLES

TABLE 1 Gold mineralogical distribution (CBE-QP-1)
TABLE 2 Gold mineralogical distribution (CBW-87-1)
TABLE 3 Chemical assays of composite ores
TABLE 4 Invisible gold in arsenopyrite
TABLE 5 Invisible gold in pyrite

LIST OF FIGURES

FIGURE 1 Mineralogical distribution of gold
FIGURE 2 Size distribution of gold
FIGURE 3 Cumulative frequency diagram of visible gold size distribution
FIGURE 4 Distribution of invisible gold in arsenopyrite

LIST OF PLATES

PLATE 1 Two textural types of pyrite in the composites
PLATE 2 Back-scattered image of pyrite grain showing As zonation
PLATE 3 Fine and coarse grained arsenopyrite
PLATE 4 Aggregate of fine-grained arsenopyrite

APPENDICES

A1 Calculation of proportions of major mineral components
A3 Image analysis of gold

7.1.0 INTRODUCTION

The Director of INCO Gold, Mr. R.A. Alcock provided two samples from the Golden Pond deposit, Quebec, in order to determine the invisible gold concentration in the two major sulphides: pyrite and arsenopyrite. This study is part of the general project on the direct determination of the invisible gold concentration in refractory gold ores. The objective of this project is to assist in the planning and optimization of metallurgical testing of refractory gold ores by providing detailed gold mineralogical distributions. The approach is that of a process mineralogical study coupled with diagnostic metallurgical testing.

The samples provided were sized, sink fractions from composites CBE-QP-1 and CBW-87-1. The head samples assayed 11.0 and 6.6 g/t respectively. Recoveries by direct cyanidation were 93 and 79% by grinding to 95% minus 200 mesh. Assays and cyanidation test data were provided by INCO and are given in Table 3.

The objectives of this study were: (i) to determine the invisible gold concentration in the arsenopyrite and pyrite, (ii) obtain the mineralogical balances for gold and (iii) identify mineralogical factors responsible for the observed difference in gold recovery.

The study was financed by INCO Limited, CANMET, the Geological Survey of Canada and the Department of Supply and Services (DSS contract # 5055.23440-7-9037).

7.2.0 METHODOLOGY

The sink fractions received were produced using methylene iodide (s.g. 3.3 $g.cm^{-3}$) and were coarser than 150 µm (100 mesh). From each sample, six 1" polished sections were prepared for examination with the reflected light microscope, for gold area measurement and ion probe microanalysis. Two sections were made from the unsieved sample, three from the 150-560 µm size fraction and one from the +560 µm fraction.

Reflected light microscopy was used to determine the size and association of the gold minerals. The arsenic content of the pyrites was determined by electron probe microanalysis. The balance of pyrite and arsenopyrite required for the determination of the gold contributed by these two minerals was determined by area measurement. Details on the methods used are given in the experimental section of the general report.

Invisible gold is the gold which cannot be detected by optical or electron microscopy. It includes both colloidal and solid solution gold.

TABLE 3

CHEMICAL ASSAYS

	CBE-QP-1	CBW-87-1
Au (ppm)	**11.0**	**6.57**
Cu (%)	< 0.02	< 0.02
Ni (%)	< 0.02	< 0.02
Fe (%)	4.62	3.23
S (%)	1.47	1.33
As (%)	0.86	0.86
C, organic (%)	0.32	0.18

CALCULATED ASSAY OF HEAVY FRACTION (+100 mesh)

	Mass Split %	Assay, Wt. % S	Assay, Wt. % As	Calculated Distribution S	Calculated Distribution As
CBE-QP-1	3.0	24.8	13.0	50.6	45.1
CBW-87-1	2.3	21.0	11.3	36.3	30.2

AREA MEASUREMENT OF SINK FRACTION

	Wt. % pyrite	Wt. % arsenopyrite	Wt. % gangue
CBE -QP-1	45.5	33.4	21.1
CBW-87-1	49.4	36.4	14.2

CYANIDATION TESTS

	Au extraction (%)
CBE-QP-1	93
CBW-87-1	79

conditions: grind 95% -200 mesh, 48 hour CN leach, 50% solids, 1 g/l NaCN, pH 11.0-11.6.

7.3.0 RESULTS

7.3.1 CHEMICAL ASSAYS

Chemical assays of the composite ore samples, which were supplied by INCO Ltd. are given in Table 3, and correspond to the whole, unseparated sample. Also shown are the calculated S and As assays and distributions of these elements in the heavy separates supplied.

7.3.2 MINERALOGY

Major Minerals:	Pyrite, arsenopyrite.
Minor Minerals:	Chalcopyrite, sphalerite, galena, tetrahedrite, pyrrhotite, native gold.

Both composite ores were very similar in mineralogy, and differed from one another only in the relative proportions of phases.

7.3.2.1 Sulphides

Euhedral to subhedral grains of **arsenopyrite** are present in all the samples, accounting for about 25% of the composite ore by mode. These are characterized by widespread inclusions of silicates, but only rarely of other sulphide minerals. Two generations of arsenopyrite are present. One is coarse-grained and generally fresh in appearance. A second type of arsenopyrite is much smaller in grain size and is found as aggregates enclosed within gangue minerals. Aggregated masses of these smaller grains are common in the samples studied.

Two generations of **pyrite** are recognized. The "early" pyrite is typically well-rounded and mottled in appearance. It contains ubiquitous inclusions of silicate minerals and of other sulphide species (primarily chalcopyrite and sphalerite), which are frequently large. The grains are commonly fractured. The "late" pyrite is subhedral and much fresher in appearance. Inclusions are much more rare in this type, although inclusions of silicates and of other sulphide minerals (chalcopyrite, galena and pyrrhotite) are present. Plate 1 illustrates the two distinct types of pyrite present in the concentrates.

The "early" pyrites appeared to be of greater average grain size than the "late" pyrites and were especially concentrated in the +560 µm size fraction. In general, however, the two types appeared to be of approximately equal abundance in the sections investigated. Neither type of pyrite was observed to be closely intergrown with arsenopyrite grains.

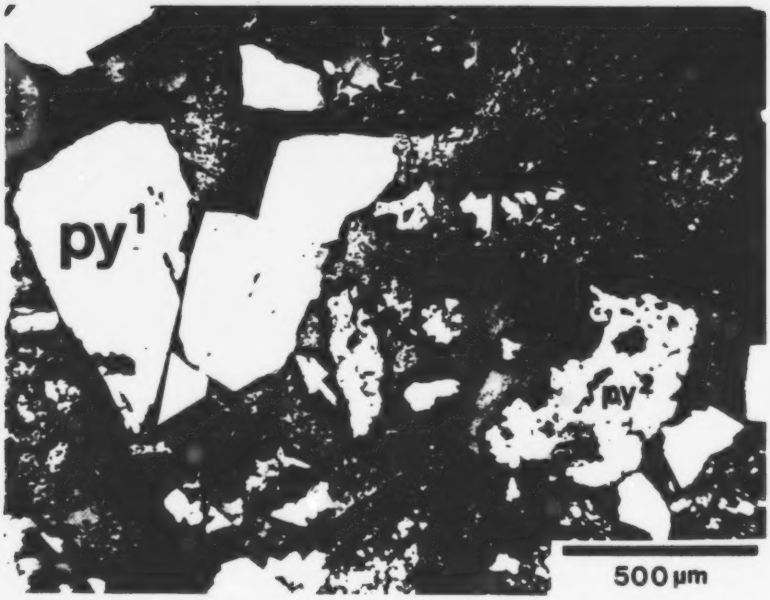
py^1
py^2
500 µm

Plate 1 Two types of pyrite in the Golden Pond ores. On the left, "late" pyrite as large blasts (py^1), to the right "early" pyrite intergrown with quartz (py^2).

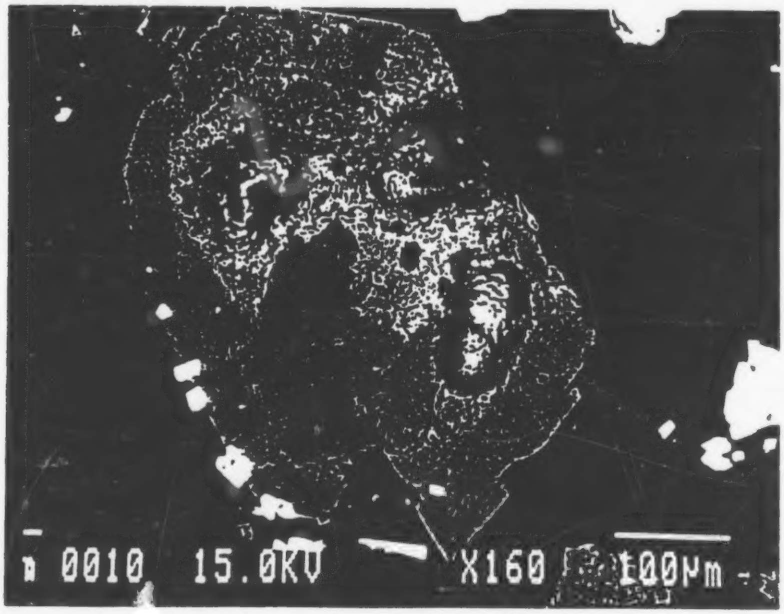
0010 15.0KV X160 100µm

Plate 2 Zonation of As in pyrite. back scattered image shows dark areas of As-poor pyrite, and lighter areas of arsenian pyrite.

Grains of chalcopyrite and **sphalerite** contain inclusions of the other sulphide minerals. Notably, sphalerite contains abundant chalcopyrite inclusions as 'chalcopyrite disease'. **Pyrrhotite** and **galena** are very minor constituents and are generally only present as inclusions within pyrite and arsenopyrite. A single grain of **tetrahedrite** was noted, intergrown with galena and sphalerite. Minerals other than pyrite and arsenopyrite together account for considerably less than 1% of the concentrates.

Area measurements were performed to determine the relative proportions of arsenopyrite, pyrite and gangue. The arsenic content of the pyrite was determined with the electron and ion microprobes (Table 5). Arsenian pyrites contained up to 4 Wt. % As. However, most of the pyrites had arsenic concentrations below the minimum detection limit (0.3 Wt. %). This enabled the proportions of arsenopyrite and pyrite to be calculated on a normative basis (Appendix A1). Unfortunately, during the ion probe microanalysis, As was not monitored simultaneously. The arsenian pyrite appears in the form of zones within arsenic poor pyrite particles (Plate 2).

7.3.2.2 Visible gold

Native gold or electrum is the only visible gold mineral in the Golden Pond composite samples. Ninety nine grains of gold were found in the twelve blocks examined (Appendix A2). The grains ranged in size from less than 1 µm², to 23,400 µm². The gold grains were noted as inclusions within pyrite (80) and a smaller population (16) as inclusions within arsenopyrite. Additionally, 3 of the larger grains were liberated. The size distribution of gold grouped by mineralogical association is given in Figure 2. The cumulative area diagram in Figure 3, indicates that the gold size distribution is similar for the two samples studied. In composite CBE-QP-1, 65% of the visible gold is associated with pyrite, 34% is liberated and 1% is enclosed in arsenopyrite. In composite CBW-87-1, one large grain weights the population significantly. Ninety four percent is liberated, almost 6% is associated with pyrite and only 0.1% is enclosed in arsenopyrite. Pyrite is therefore the main host mineral for native gold. The gold grains are equally distributed between the two morphological types of pyrite identified. Gold inclusions are rounded to elongate in shape. Since they concentrate along fractures, they should be more readily amenable to cyanidation. Calculations on the visible gold content are given in Appendix A2.

7.3.2.3 Invisible gold

Arsenopyrite is the principal carrier of invisible gold in the Golden Pond deposit. The average gold concentration of 44 arsenopyrite particles from composite CBE-QP-1 is 18.3 ppm, with a confidence interval of 5.7 ppm at a 95% significance level. This means that in 95 out of 100 cases, the average arsenopyrite gold concentration is in the range from 12.6 to 24.0 g/t. The

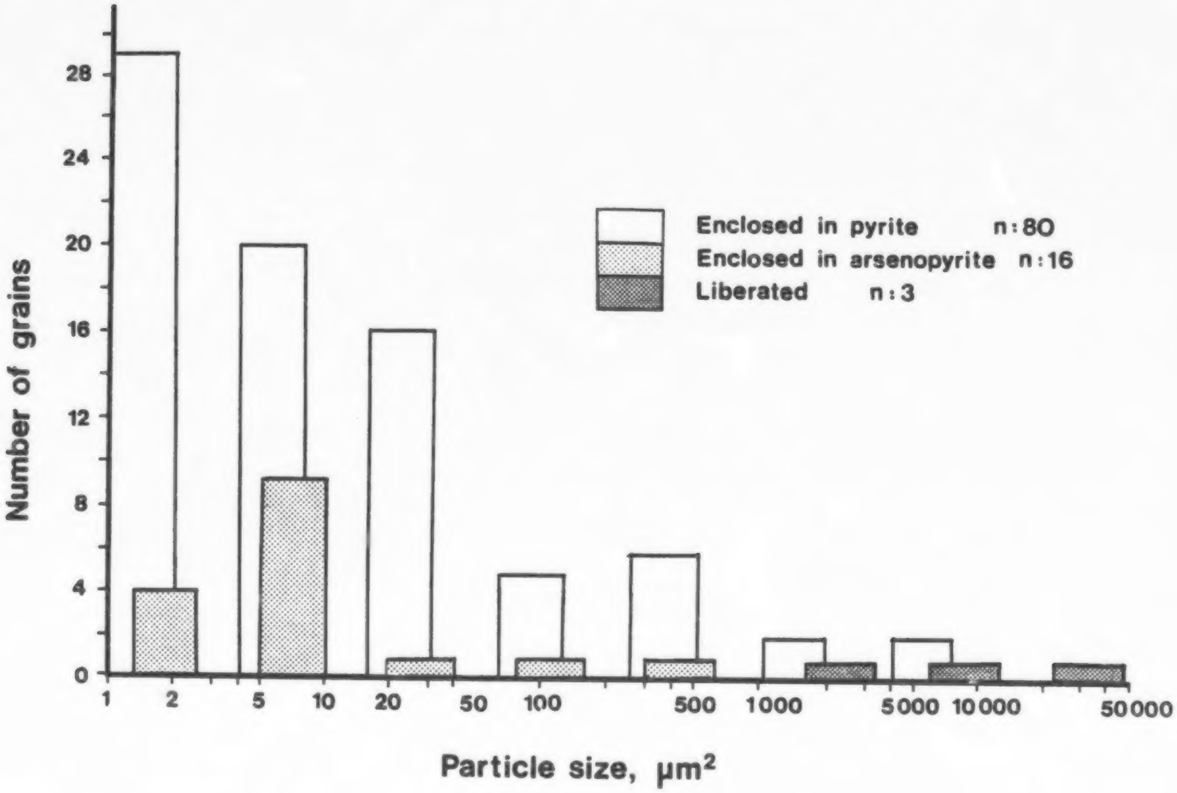

FIGURE 2. Size distribution of gold particles in the composites, divided by association.

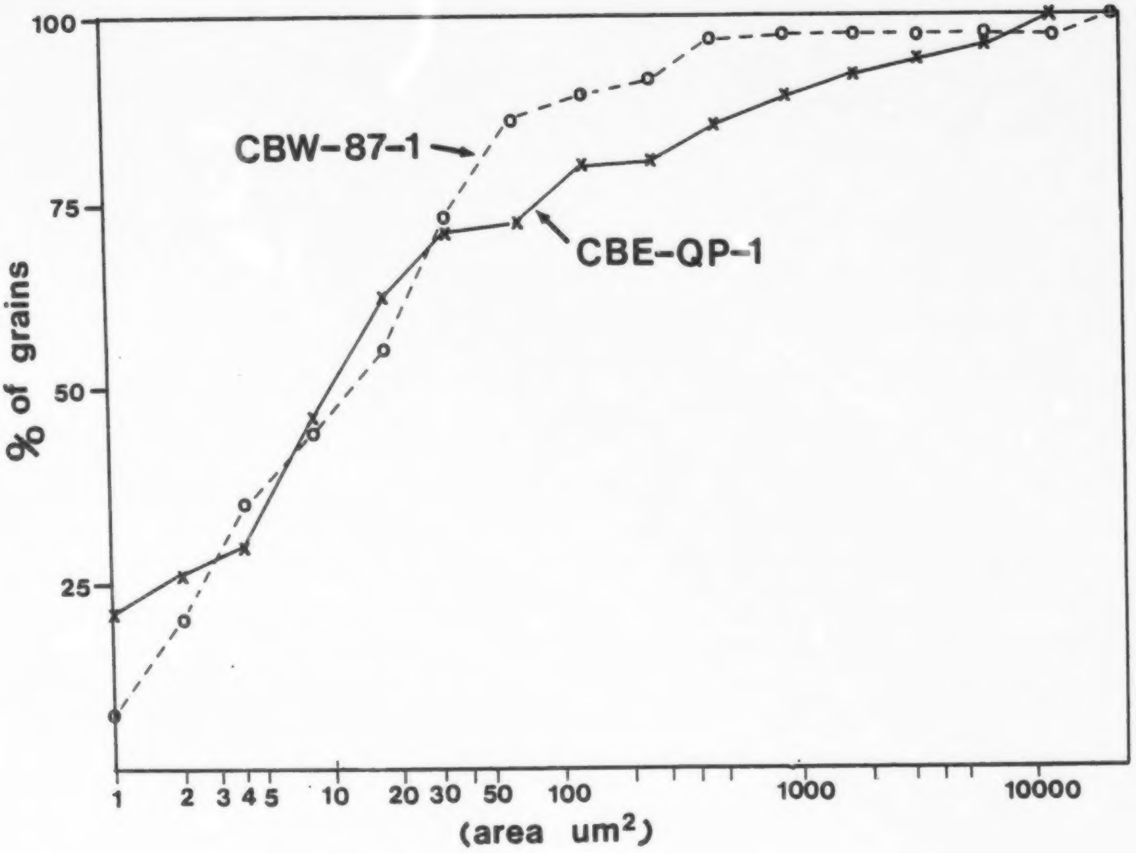

FIGURE 3. Cumulative frequency diagram of gold particle size in the two composites, by number of grains.

invisible gold distribution is depicted in Figure 4. As in several other, but not all the ores studied, a negative correlation exists between arsenopyrite grain size and the invisible gold content. Thus, nine fine grained arsenopyrites had an average gold content of 39.1 ± 13.2 ppm and thirty five coarse grained arsenopyrites assayed only 13.3 ± 5.0 ppm Au. More important to note is that the two invisible gold distributions are statistically different. To determine the gold concentration in the fine grained arsenopyrite, aggregate particles composed of fine grained arsenopyrite were analyzed.

The average invisible gold concentration of 10 pyrite particles as determined with the ion probe was 1.1 g/t, with a confidence interval of 0.9 g/t. Two of these were arsenian and contained 4.1 g/t and 1.7 g/t.

In the composite CBW-87-1, the average invisible gold concentration of 50 arsenopyrite particles is 41.4 ppm with a confidence interval of 18.6 ppm at 95% significance level. This means that in 95 out of 100 cases, the average invisible gold concentration in the CBW-87-1 arsenopyrite is within the range from 22.8 to 60.0 g/t. Therefore the arsenopyrite in the CBW-87-1 composite is significantly more enriched in visible gold compared to the CBE-QP-1 arsenopyrite. The finer arsenopyrite particles (n=12) have a higher invisible gold contentration, 98.9 ± 61.5 ppm compared to the coarser arsenopyrite particles (n=38) which assayed 23.2 ± 10.2 ppm.

The invisible gold content of the pyrite is significantly lower. The average gold content of 14 pyrite particles as determined with the ion probe was 0.23 g/t, with a confidence interval of 0.24 g/t. Ion probe microanalysis results are given in Tables 4 (arsenopyrite) and 5 (pyrite).

7.4.0 DISCUSSION

In the case of composite CBE-QP-1, 93% of the gold was recovered by direct cyanidation from a sample ground 95% minus 200 mesh. The invisible gold in arsenopyrite accounts for 3.4% of the head assay, as determined from the invisible gold concentration (18.3 ppm) and the modal arsenopyrite (1.87 Wt. %). The invisible gold in pyrite is only 0.2% of the head assay. Therefore the total accounted gold is 96.4 %. The unaccounted gold (3.4%) is expected to be: (i) very fine native gold, 1-2 µm in size encapsulated in pyrite and arsenopyrite and (ii) invisible gold in fine-grained arsenopyrite. Invisible gold and encapsulated fine-grained gold is not recoverable by direct cyanidation.

The gold recovery by direct cyanidation from composite CBW-87-1 was 79%, considerably less than for CBE-QP-1. Ion probe microanalysis has shown that the invisible gold

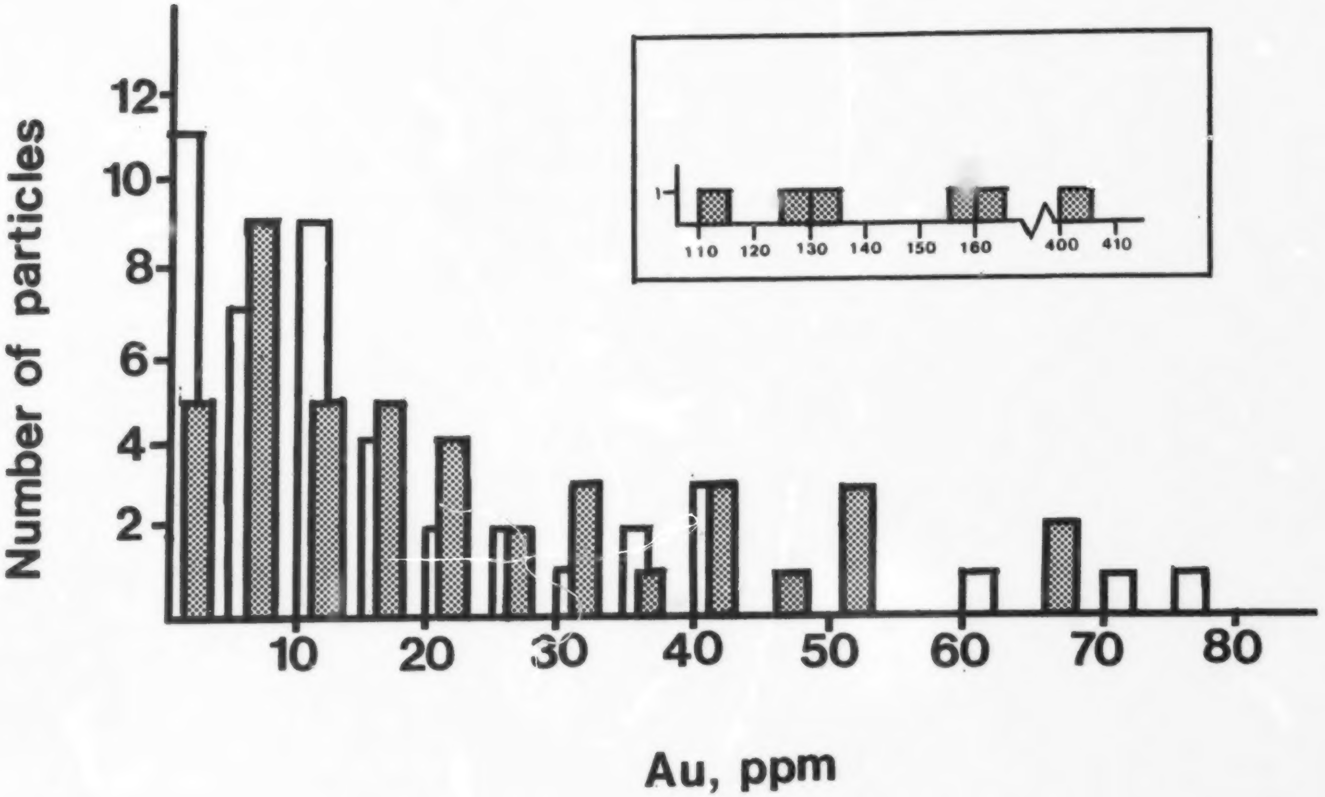

Histogram of invisible gold concentrations in arsenopyrite.

CBE - QP - 1 (white columns) N = 44, $\hat{x} \pm \lambda = 18.3 \pm 5.7$ ppm
CBW - 87 - 1 (shaded columns) N = 49, $\hat{x} \pm \lambda = 41.7 \pm 19.0$ ppm

TABLE 4

INVISIBLE GOLD IN ARSENOPYRITE
(Golden Pond, Quebec)

CBE-QP-1

No	Au, ppm	No	Au, ppm
17	5.0	101	17.3
18	3.4	102	64.2
19	19.3	103	11.2
21	10.0	104	12.3
22	72.8	106	30.0
23	1.7	107	13.0
24	25.4	108	11.9
25	4.6	109	14.0
27	8.0	110	1.1
28	2.2	111	36.4
30	0.3	112	5.9
31	8.6	113	41.7
55	45.2	116	27.1
56	1.2	119	17.5
57	14.7	120	42.4
59	10.7	121	23.0
61	3.4	123	19.7
62	4.4	124	24.6
63	4.2	125	36.6
64	0.5	126	77.4
66	10.5	127	9.4
70	17.3	128	6.1

N = 44

$\hat{x} = 18.3 \pm 5.7$ ppm

CBW-87-1

No	Au, ppm	No	Au, ppm
3	1.5	51	114.
4	3.4	52	18.8
5	34.0	53	8.6
6	13.1	78	67.6
7	13.9	80	1.3
8	12.8	81	48.7
10	6.1	82	6.0
11	5.7	83	37.4
13	45.0	84	10.6
14	2.0	85	19.3
33	2.2	86	23.7
34	5.2	87	52.1
36	5.5	89	53.3
37	16.2	90	28.2
39	16.8	91	134.8
40	52.3	92	402.
41	23.6	93	70.6
42	1.9	94	12.1
43	8.9	95	15.3
44	31.6	96	65.7
45	22.7	97	28.5
46	9.6	98	128.8
47	33.1	99	3.8
48	6.7	100	161.0
50	158.0		

N = 50

$\hat{x} = 41.4 \pm 18.6$ ppm

TABLE 5

INVISIBLE GOLD IN PYRITE (Golden Pond, Quebec)

CBE-QP-1

No	Au (ppm)	As (%)
1	3.3	0.036
2	0.5	0.090
9	0.7	0.063
12	4.1	1.400
15	0.1	0.110
38	0.0	0.044
49	0.0	0.130
54	1.7	0.110
79	0.1	0,160
88	0.5	0.078

N : 10

$\hat{x} \pm \lambda$: 1.1 ± 0.9

CBW-87-1

No	Au (ppm)	As (%)
16	0.2	0.280
20	0.1	0.210
25	0.1	0.160
29	0.0	0.300
32	0.0	0.100
58	0.0	0.130
60	0.0	0.150
65	0.0	0.062
67	0.0	0.032
69	0.0	0.047
105	0.0	0.140
114	1.2	0.740
115	0.2	0.100
117	1.4	0.740

N : 14

$\hat{x} \pm \lambda$: 0.2 ± 0.25

concentration in arsenopyrite is more than double in CBW-87-1 and, additionally, the abundance of arsenopyrite is slightly greater. Arsenopyrite accounts for 11.9% of the gold head assay determined from the invisible gold concentration in arsenopyrite, 41.4 ppm and the modal arsenopyrite, 1.87 %. The invisible gold in pyrite is insignificant (0.1%). Therefore the accounted gold total is only 91%. The unaccounted gold, as in the other composite sample is expected to be as invisible gold in fine-grained arsenopyrite (Plates 3 and 4), since ion probe microanalysis was biased towards larger arsenopyrites and as very fine grained 1-2 µm in size encapsulated native gold.

7.5.0 CONCLUSIONS

Native gold or electrum is the principal gold-carrier mineral in the two composite samples from the Golden Pond deposit. The silver content of the gold mineral was not determined. Gold recovery by direct cyanidation was 93% (CBE-QP-1) and 79% (CBW-87-1).

Ninety percent of the gold grains observed in the +100 mesh sink fraction of composite CBW-87-1 were in the size range from 2 to 150 μm^2, and in the range 1 to 1600 μm^2 in composite CBE-QP-1. The median gold particle size is 9 and 10 μm^2 respectively. Unliberated gold is primarily associated with pyrite and to a lesser extent with arsenopyrite.

Arsenopyrite is the other gold-carrier mineral in the Golden Pond deposit. Gold concentration in arsenopyrite ranges from 1.1 to 77.4 ppm in composite CBE-QP-1 and from 15. to 402. ppm in composite CBW-87-1. The average invisible gold content is 18.3 ppm in the CBE-QP-1 arsenopyrite, and more than twice as much, 41.4 ppm in sample CBW-87-1. The finer grained arsenopyrite has a significantly higher gold content compared to the coarser one. Invisible gold in arsenopyrite accounts for 3.4% (CBE-QP-1) and 11.9% (CBW-87-1) of the gold head assays. Therefore it is concluded that the experienced lower gold recovery by direct cyanidation of the composite CBW-87-1, 79%, is attributed primarily to invisible gold in arsenopyrite and to a lesser extent to encapsulation of the principal gold carrier mineral in pyrite.

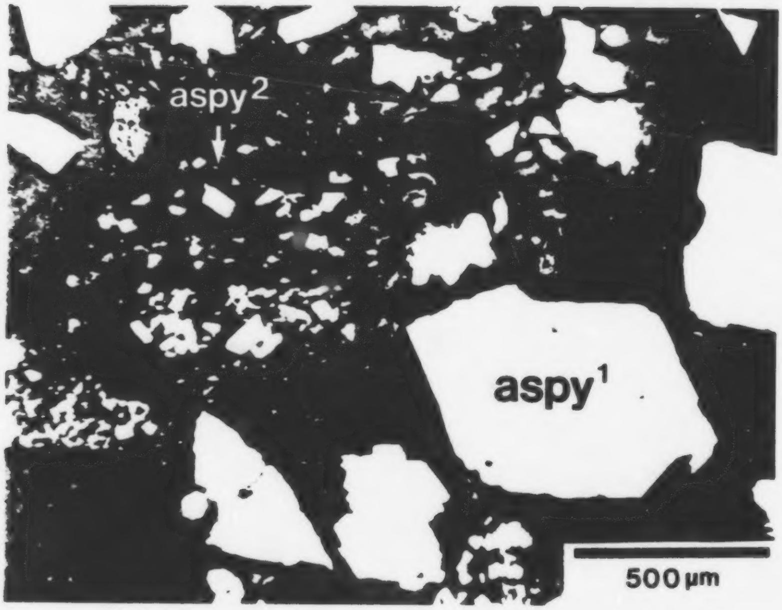
aspy^2
aspy^1
500 µm

Plate 3 Coarse-grained (aspy^1) and fine-grained (aspy^2) arsenopyrite.

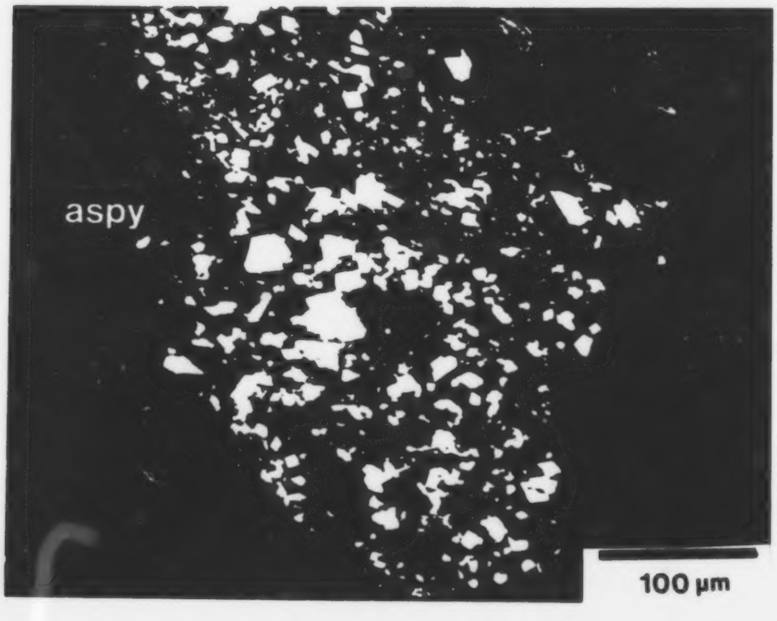

Plate 4 Aggregate of fine-grained arsenopyrite enclosed within a particle of silicate gangue.

APPENDIX A1

Calculation of proportions of arsenopyrite and pyrite in the composite samples

(1) CBE-QP-1

% aspy = Wt. % As head assay / % As in aspy

= 0.86 / 0.46

= **1.87 %**

% py = (Wt. % S head assay - Wt. % S in aspy) / % S in py

(Wt. % S in aspy = 0.2 x % aspy)

= (1.47 - 0.37) / 0.52

= **2.06 %**

2) CBW-87-1

% aspy = Wt. % As head assay / % As in aspy

= 0.86 / 0.46

= **1.87 %**

% py = (Wt. % S head assay - Wt. % S in aspy) / % S in py

(Wt. % S in aspy = 0.2 x % aspy)

= (1.33 - 0.37) / 0.52

= **1.80 %**

assumption: As in pyrite is insignificant (<5% of total aspy).

APPENDIX A2

GOLD GRAINS IN COMPOSITE CBE-QP-1

Grain	Association	Size (μm^2)
1	Enclosed in py	450
2	"	7
3	"	1
4	"	30
5	"	2
6	"	3
7	"	65
8	"	35
9	"	10
10	"	900
11	"	6000
12	"	10000
13	"	800
14	"	30
15	"	2875
16	"	1600
17	"	125
18	"	5
19	"	4
20	"	2
21	"	1
22	"	2
23	"	1
24	"	1
25	"	1
26	"	16
27	"	3
28	"	6
29	"	5
30	"	7
31	"	120
32	"	5
33	"	12
34	"	1
35	"	1
36	"	350
37	Enclosed in py	10
38	"	32
39	"	10
40	"	1
41	Enclosed in aspy	10
42	"	300
43	"	15
44	"	2
45	"	1
46	"	1
47	"	5
48	"	15
49	"	30
50	"	1
51	"	14
52	"	100
53	"	5
54	"	8
55	Liberated	11000
56	"	1200

N : 56

$\hat{X} \pm \lambda$: 647 ± 567 μm^2

median : 10 μm^2

Σ area : 36226 μm^2

APPENDIX A2

GOLD GRAINS IN COMPOSITE CBW-87-1

Grain	Association	Size (μm^2)
1	Enclosed in py	35
2	"	35
3	"	280
4	"	50
5	"	3
6	"	14
7	"	5
8	"	2
9	"	2
10	"	1
11	"	30
12	"	22
13	"	6
14	"	8
15	"	30
16	"	4
17	"	15
18	"	350
19	"	30
20	"	25
21	"	10
22	"	8
23	"	5
24	"	20
25	"	2
26	"	20
27	"	2
28	"	4
29	"	3
30	"	60
31	"	150
32	"	5
33	"	2
34	"	110
35	"	3
36	"	2
37	Enclosed in py	4
38	"	1
39	"	1
40	"	35
41	Enclosed in aspy	11
42	"	9
43	Liberated	23400

N : 43

$\hat{X} \pm \lambda$: 577 ± 1087 μm^2

median : 9 μm^2

Σ area : 24814 μm^2

APPENDIX A2

VISIBLE GOLD IN COMPOSITE CBE-QP-1

Total area studied: 5 x 4.91 cm^2 = 24.96 cm^2

Coverage of sample (determined by point counting) = 35 %

Total sample area covered = 8.74 cm^2

Total sample weight (unit depth: 10^{-4}, av. sp. grav: 4.9 $g.cm^{-3}$) = 42.83 x 10^{-4} g

- -

Total gold area = 36226 μm^2

= 0.0003622 cm^2

Average gold content (estimated) = 95 %

Total gold weight (unit depth: 10^{-4} av. spec. grav: 19.3 $g.cm^{-3}$). = 66.42 x 10^{-8} g

Total visible gold concentration relative to sulphide = 155 ppm

---

APPENDIX A2

VISIBLE GOLD IN COMPOSITE CBW-87-1

Total area studied: 5 x 4.91 cm^2 = 24.96 cm^2

Coverage of sample (determined by point counting) = 35 %

Total sample area covered = 8.74 cm^2

Total sample weight (unit depth: 10^{-4}, av. sp. grav: 5.05 $g.cm^{-3}$) = 44.14 x 10^{-4} g

Total gold area = 24814 μm^2

= 0.0002481 cm^2

Average gold content (estimated) = 95 %

Total gold weight (unit depth: 10^{-4} av. spec. grav: 19.3 $g.cm^{-3}$). = 45.55 x 10^{-8} g

Total visible gold concentration relative to sulphide = 103 ppm

CHAPTER 8

DETERMINATION OF INVISIBLE GOLD IN FLOTATION PRODUCTS AND FOUR ORE TYPES FROM THE HW MINE, B.C.

SSW/PMS/89/05

SUMMARY

The gold mineralogy in the HW base metal ore was determined by optical and scanning electron microscopy, electron and ion probe microanalysis, coupled with diagnostic cyanidation testing and image analysis of the gold minerals. The gold mineralogy has been shown to be complex, in terms of size distribution and association of visible gold, and the presence of colloidal as well as solid solution gold; probably the result of several distinct episodes of gold mineralization.

The principal gold carrier mineral is electrum with 22 to 30 Wt. % silver. Electrum is either very coarse grained (average size 2000 μm^2) or very fine grained (less than 4 μm^2), with medium size grains notably missing. Electrum is more gold-rich in the bornite rich ores where it is found in myrmekitic intergrowths of galena with chalcocite. The association of coarse grained electrum with galena is important. The fine grained electrum is associated primarily with sphalerite and pyrite. The extremely fine grained electrum is enclosed in tetrahedrite- tennantite. The average solid solution gold concentration in arsenian tetrahedrite-tennantite is 6.3 ppm. Galena and bornite carry trace amounts of solid solution gold, 1.78 and 0.67 ppm respectively. Gold concentration in pyrite, tetrahedrite and coarse chalcopyrite is insignificant (< MDL). Fine grained chalcopyrite is a significant carrier of colloidal gold and in the copper concentrate there is an indication that it is the principal gold carrier accounting for the bulk of the gold assay (7.5 - 11.5 g/t Au).

The multiple nature of gold in the HW ore has been a formidable challenge in the determination of the gold distribution in the various ore types and products. The mineral processor faces the same challenge when attempting to concentrate the gold in the copper concentrate. Coarse grained electrum is recovered to the copper concentrate, however, any losses to the zinc concentrate or tailings may account for a significant fraction of the lost gold. The relatively high silver content of the electrum is detrimental to flotation, as a result of possible coatings. Determination of coarse grained electrum in the tailings and the zinc concentrate and comparative examination of their surface chemistry could assist recovery to the copper concentrate.

TABLE 1

MINERALOGICAL DISTRIBUTION OF GOLD IN THE FOUR MAIN ORE TYPES

	Polymetallic	Bedded	Cu-pyrite	Bornite-rich
Visible gold	(***)	(***)	(***)	***
Micro-inclusions in tetrahedrite	*	(*)	(*)	*
Invisible gold				
in chalcopyrite	*	*	**	
in tetrahedrite-tennantite	**			
in bornite				*
in galena				*

*** very important (>40% of total)
** important (10-40% of total)
* insignificant (<10% of total)
brackets indicate speculative interpretation

TABLE 2

MINERALOGICAL DISTRIBUTION OF GOLD IN MILL FEED AND ZINC CONCENTRATE

MILL FEED	**g/t**	**distribution**
Assay	2.68	100
CN- recoverable gold	1.69	63
Visible gold	1.21	45
Non-cyanidable gold	0.99	37

ZN CONCENTRATE	**g/t**	**distribution**
Assay	4.17 ± 0.10	100 ± 2.4
CN- recoverable gold	2.00[1]	72
Visible gold	2.30	55
Non-cyanidable gold	1.17[2]	28

---

[1] Minimum value (see text)
[2] Maximum value

LIST OF TABLES

Table 1 Mineralogical distribution of gold in four ore types
Table 2 Mineralogical distribution of gold in the products
Table 3 Chemical assays
Table 4 Electron probe analysis of electrum particles
Table 5 Summary of invisible gold analysis
Table 6 Cyanidation tests

LIST OF FIGURES

Figure 1 EDX spectra of tetrahedrite - tennantite minerals
Figure 2 Histogram of electrum particle size in Cu-concentrate
Figure 3 Distribution of invisible gold in pyrite
Figure 4 Invisible gold in tetrahedrite-tennantite
Figure 5 Depth profile and inclusion of electrum in tetrahedrite
Figure 6 Distribution of colloidal gold in fine-grained chalcopyrite

LIST OF PLATES

Plate 1 Electrum in sphalerite - galena - tetrahedrite
Plate 2 Electrum combined with pyrite
Plate 3 Fine-grained inclusions of electrum in pyrite
Plate 4 Myrmekitic intergrowths of galena and chalcocite with electrum in the bornite-rich ore
Plate 5 Electrum in the bornite-rich ore
Plate 6 Electrum associated with sphalerite, chalcopyrite and gangue
Plate 7 Electrum enclosed in gangue
Plate 8 Liberated electrum in the copper concentrate
Plate 9 Liberated electrum in the copper concentrate
Plate 10 Etched fine-grained chalcopyrite

APPENDICES

A1 Image analysis of electrum particles
A2 Calculation of visible gold
A3 Ion probe microanalysis data
A4 Normative mineralogy of ore types
A5 Modal analysis of products

8.1.0 INTRODUCTION

Westmin Resources Ltd. requested the determination of the gold mineralogical distribution in samples from the concentrator and the four distinct ore types of the HW deposit on Vancouver Island. This study is part of the general project on the characterization of Canadian refractory gold ores by ion probe microanalysis. The aim of the project is to assist in the optimization of the gold recovery by providing detailed information on the gold mineralogical distribution. The approach followed is that of a process mineralogical study coupled with diagnostic metallurgical testing (Chryssoulis, 1987).

The objective of the HW study is to provide detailed information on the nature, size distribution and association of the gold-carrier minerals in samples from the concentrator. The main thrust of the study is directed to the determination of the invisible gold concentration in pyrite, chalcopyrite, bornite, galena, sphalerite and tetrahedrite-tennantite, as previous studies have indicated the presence of visible gold in only minor amounts.

Typically the HW concentrator produces two concentrates: a Cu and a Zn concentrate. Occasionally, it also produces a Pb concentrate. Gold is recovered into the Cu concentrate , which assays 11.5 g/t Au, and to a lesser extent in the zinc concentrate which assays 5.3 g/t. At present, about 25 % of the gold reports to the flotation tailings.

Four distinct ore facies have been recognized in the HW mine. These differ from each other in the relative proportions of the sulphide minerals and from a textural point of view. The Au assays of the four ore types are similar in magnitude, ranging from 2.3 to 3.2 g/t, but the mineralogical distribution of gold within each ore type is believed to be different.

The study was financed by Westmin Resources Ltd., CANMET, the Geological Survey of Canada, and the Department of Supply and Services (DSS contract no 23440-7-9037/01 SS). The study of the four ore types is not part of the DSS contract, and was not financed by Westmin Resources Ltd..

8.2.0 METHODOLOGY

Samples of the millfeed, the copper and zinc concentrates and the final tailings were received from Mr. Chuck Leggett, mill

---

1. **Invisible gold** is the gold which is not visible under the optical and scanning electron microscopes; therefore it includes solid solution and colloidal gold distributed in the crystal lattice of sulphide and sulpharsenide minerals.

metallurgist at the HW mine. Mr. Cliff Pearson, chief geologist, provided chip samples of the four distinct ore types.

Ores (chip samples)

The following four ore types were studied: 21173L **(Polymetallic ore)**, 21174L **(Bedded Cu-Zn ore)**, 21175L **(Cupriferous pyrite ore)** and a **Bornite - rich ore**. Eleven polished blocks were prepared and examined: 2 from the bedded Cu-Zn ore, 2 from the polymetallic ore, 2 from the cupriferous pyrite ore, and 5 from the bornite-rich ores.

Mill feed

A mill feed sample from HW was used for diagnostic metallurgical testing and a detailed process mineralogical study. The procedure followed is described in the section on methodology in Chapter 1. A sub-sample was sieved into the following size fractions: -53 µm, 53-560 µm, and +560 µm. The 90-560 µm fraction, representing 37% of the weight of the total sample was separated using sodium polytungstate (S.G. = 3.0 $g.cm^{-3}$). The sink fraction represented 75 % by weight of the total size fraction. Six polished sections were prepared from the sink fraction for further study.

Cu concentrate

The Cu concentrate sample was sieved into the following three size fractions: -53 µm, 53-90 µm, and +90 µm. The +90 µm fraction represented 6% by weight of the total sample. Eight polished blocks were prepared from this fraction. In addition, 4 blocks were prepared from each of the other size fractions. All size fractions were studied microscopically for gold minerals and selected chalcopyrite particles were analyzed with the ion microprobe. A gravity separation test was performed on a 1 kg charge of the copper concentrate in order to preconcentrate coarse-grained gold.

Zn concentrate

The Zn-concentrate sample was treated similarly to the mill feed (see above). Cyanidation tests were performed on progressively finer charges and the sample was studied optically for gold minerals. The subsample was sieved into three size fractions: -53 µm, 53-90 µm and +90 µm. The +90 µm fraction represented 4.3 wt% . Five polished sections were prepared from the coarser fraction and three from each of the finer fractions.

The invisible gold concentration in pyrite, chalcopyrite, bornite, tetrahedrite and galena were determined by ion probe microanalysis (Chryssoulis et al., 1986). Mineral particles from the mill feed, the copper concentrate and the four ore types were analyzed. Sphalerite could not be analyzed because it was charging under the primary ion beam. The ion microprobe is the most sensitive micro analytical tool for the analysis of precious metals including Ga and Ge. The Minimum Detection Limit, MDL, (3σ) for gold in pyrite is 300 ppb, which is three orders of magnitude more sensitive than that of the new generation of electron microprobes. Therefore it is ideal for the quantification of trace amounts of gold in common sulphides.

The visible gold content was determined by direct cyanidation. Diagnostic cyanidation tests were performed on three 500g charges of the mill feed and the zinc concentrate. Conditions are given in Table 6. Progressively finer grinds were used to determine the cyanide recoverable gold and the effects of grinding upon recovery. The gold recoverable at the finest grind (K_{80} < 20 µm) is the most accurate measure of the visible gold concentration, provided that all necessary precautions were taken with respect to the solubility of gold tellurides if present, and the presence of cyanides or preg-robbing carbon. The association and composition of the visible gold minerals were determined by optical microscopy and electron probe microanalysis respectively. The size of the gold particles was determined by image analysis. As in the case of the other ores tested the modal gold is less than the cyanidable gold.

8.3.0 RESULTS

8.3.1 Chemical Assays

Westmin Resources supplied the chemical assays for Au, Ag, Cu, Pb, Zn, Fe, and S carried out on the four ore types. A further series of analyses for Fe, As, Sb, Ba, S^{2-} and SO_4^{2-} on the ore samples was carried out. The mill feed and zinc concentrate samples were analyzed for Au, S, Te, Bi, Sb and As while the copper concentrate was analyzed for Au and As only. Details of all analyses are given in Table 3.

8.3.2 Mineralogy of ores and mill feed
(except bornite-rich ores)

The bedded Cu-Zn ores, cupriferrous pyrite ore and the polymetallic ores differ from one another in texture in the proportions and grain size of ore minerals.

TABLE 3

CHEMICAL ASSAYS

Ore types (Westmin data, average analyses)

	Au (g/t)	Ag (g/t)	Cu (%)	Pb (%)	Zn (%)	Fe (%)	S (%)
Polymetallic ore	2.6	80	2.2	2.2	12.5	16.0	29.51
Bedded Cu-Zn ore	2.4	22	2.8	0.15	6.5	29.9	42.22
Cu-pyrite ore	2.3	17	3.3	0.05	1.0	37.5	63.34
Bornite - ore	3.2	120	2.5	1.4	11.2	9.5	21.47

ORE TYPES (SSW data)

	Fe (%)	S^{2-} (%)	SO_4^{2-} (%)	As (ppm)	Sb (ppm)	Ba (ppm)
Polymetallic ore	13.2	36.6	0.030	0.047	0.002	0.012
Bedded Cu-Zn ore	29.2	35.2	0.080	0.059	0.19	0.011
Cu-pyrite ore	37.5	41.6	0.140	0.025	0.005	0.035
Bornite - ore	9.5	13.6	0.240	0.30	0.27	1.15

PRODUCTS (SSW data)

	Au (g/t)	S (%)	Te (ppm)	Bi (ppm)	Sb (ppm)	As (ppm)
Millfeed	2.68	30.4	12	20	30	560
Zn-concentrate	4.17 ± 0.10	33.9	23	30	80	630
Cu-concentrate	11.50	-	-	-	-	3800

Major minerals:	Pyrite, chalcopyrite, sphalerite
Minor minerals:	Tetrahedrite, tennantite, galena, bornite, covellite, chalcocite, electrum, wehrlite, arsenopyrite, bismuthinite, altaite, hessite.

Pyrite

Pyrite is the most ubiquitous sulphide mineral, present as euhedral and subhedral grains belonging to a single genetic type. Inclusions of other sulphide minerals (chalcopyrite, sphalerite and galena, in order of importance) are widespread.

Chalcopyrite and Sphalerite

Chalcopyrite and sphalerite form the matrix which cements the pyrite grains together. Inclusions of other sulphide minerals are widespread in the pyrite, sphalerite, chalcopyrite and galena are the most important.

Arsenopyrite

Tiny needles of arsenopyrite are a minor constituent of the ores, intergrown with both pyrite and matrix minerals.

Tetrahedrite-tennantite

Tetrahedrite and tennantite are present in all ore types, but are concentrated in the **polymetallic ore**. They are normally intergrown with chalcopyrite, sphalerite and galena. Inclusions of galena within tetrahedrite are common. A range of compositions within the tetrahedrite-tennantite solid solution series were noted. Representative EDX spectra are shown in Figure 1. Only small amounts of silver were present. There is a strong correlation between Ag and Fe contents.

Galena

Isolated small grains of galena occur, often intergrown with chalcopyrite and sphalerite. Epitaxial bismuthinite was noted.

Telluride minerals

Altaite (PbTe), Wehrlite (BiTe) and Hessite (Ag_2Te) are important trace constituent minerals of the ores. Altaite and hessite occur closely associated with the galena, often as small inclusions, where the galena itself is present as an inclusion within chalcopyrite. Grain size of the telluride minerals is generally less than 2 μm^2. The grains of wehrlite were present as inclusions within chalcopyrite, each less than 1 μm^2 in size. A total of 13 grains of altaite, 5 grains of hessite and 3 grains of wehrlite were seen. **No gold tellurides were identified.**

Figure 1

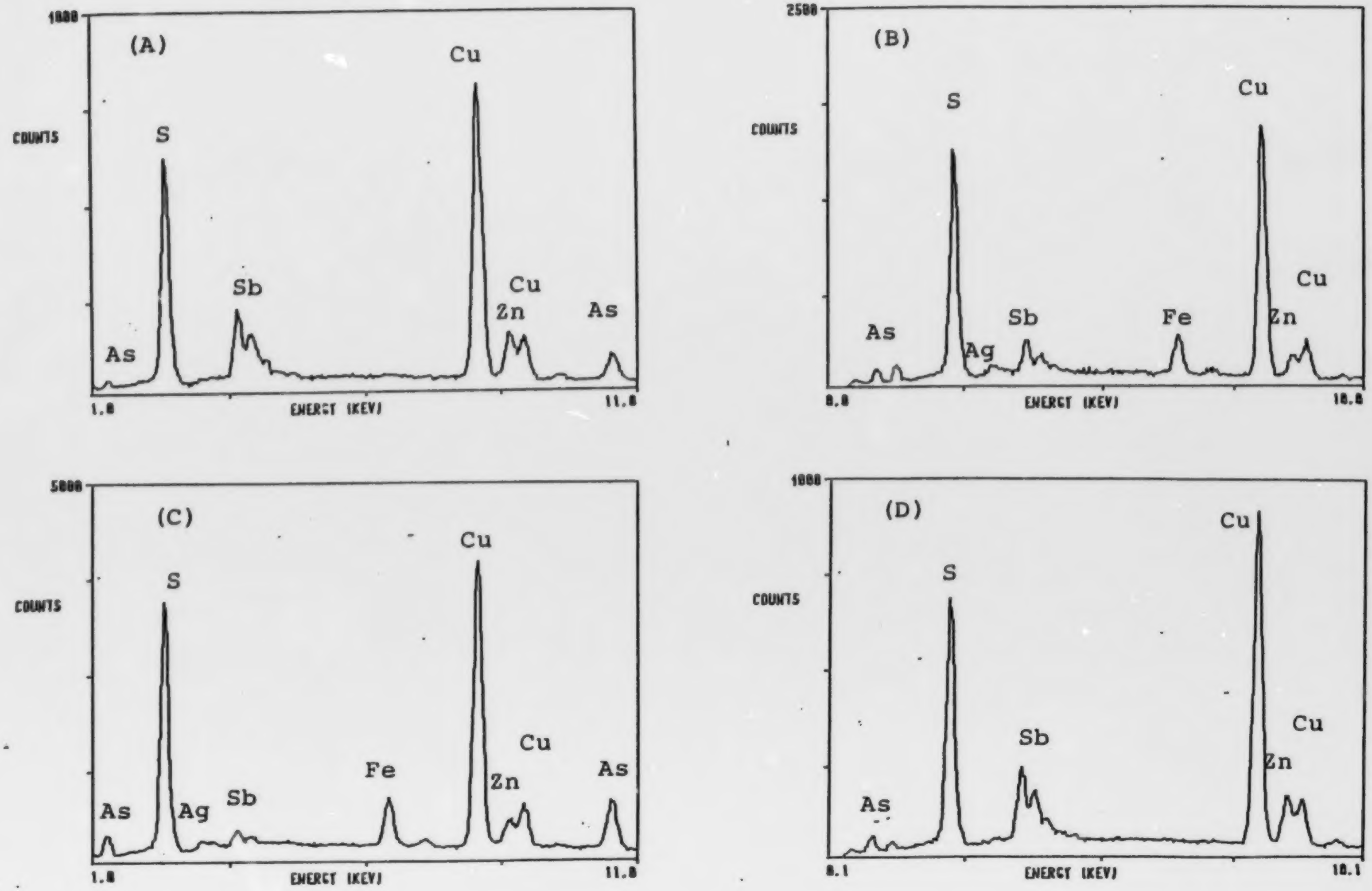

(A)	Tetrahedrite	Bedded Cu-Zn ore
(B)	Tetrahedrite-tennantite	Polymetallic ore
(C)	Tennantite	Polymetallic ore
(D)	Tetrahedrite	Bornite-rich ore

Gold Minerals

Four grains of electrum have been identified in mill feed. Two paragenetic associations appear to be present. Gold occurs either in association with matrix galena, or as inclusions within pyrite (Plates 1, 2 and 3). The two larger grains (50 and 340 μm^2 in area) were in the former paragenetic asociation (Appendix A1). The mean gold content of the electrum in the mill feed is 70.5 wt%. Results are given in Table 4. The mineralogical balance of visible gold is given in Appendix A2. The visible gold, 1.21 g/t, accounts for 45% of the gold head assay and 72% of the directly cyanidable gold.

8.3.2.1 Bornite-rich ores

Major minerals:	Bornite, pyrite, chalcopyrite, tetrahedrite, galena, sphalerite.
Minor minerals:	Covellite, chalcocite, stromeyerite, bournonite, electrum.

A very different mineralogy is shown by the bornite-rich ores. Electrum is present within myrmekitic intergrowths of chalcocite with galena (Plates 4 and 5). These intergrowths are also closely associated with tetrahedrite. The tetrahedrite and bornite occur as large single grains and contain inclusions of the other minerals. The matrix of the ore is made up of galena and sphalerite. Bournonite is commonly included within galena.

Tetrahedrite

EDX analysis of tetrahedrite in the bornite rich ores has shown only nearly end member tetrahedrite to be present. Silver and Fe are present in minor amounts.

Covellite and chalcocite

EDX analysis showed that these minerals conformed to the expected stoichiometry and that the silver concentration is less than 0.5 wt%.

Gold minerals

Electrum is exclusively associated with the myrmekitic intergrowths of galena with chalcocite. Five electrum grains were noted (Appendix A1) and all formed an epitaxial pattern around small tetrahedrite grains (Plate 4). The composition of the the electrum was determined by EDX microprobe analysis. The mean gold concentration of four electrum grains is 77.9 wt% which is statistically different from the gold content of the

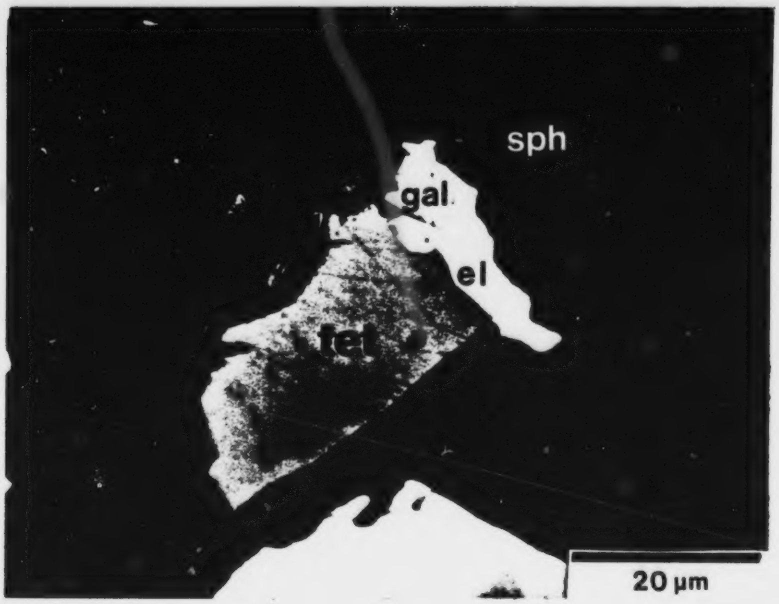
sph
gal
el
tet
20 µm

Plate 1 Electrum (el) associated with sphalerite (sph), galena (gal) and tetrahedrite (tet).

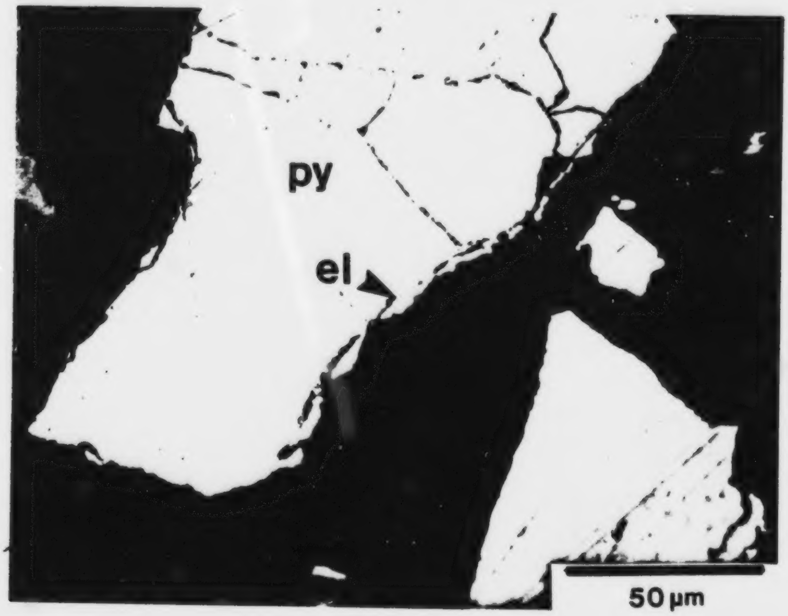

Plate 2 Electrum (el) combined with pyrite (py). Chalcopyrite, originally from a fracture in pyrite forms the margin of the pyrite grain.

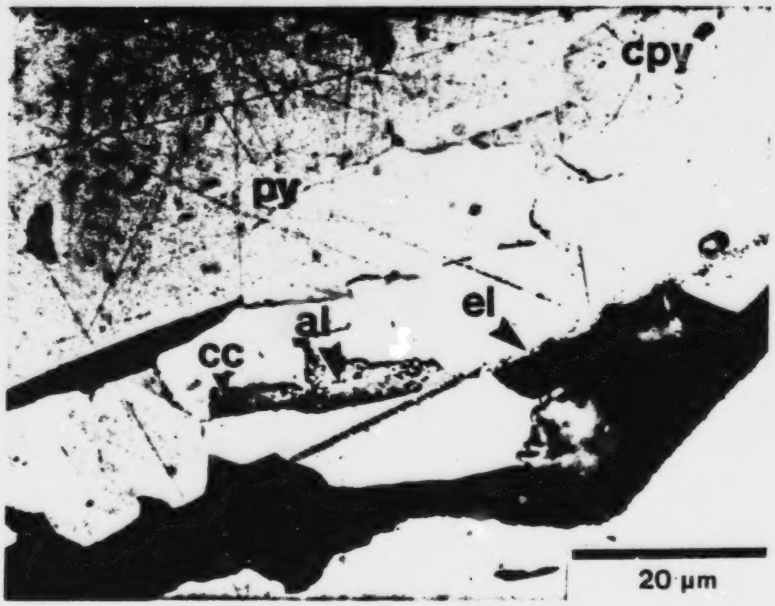

Plate 3 Fine-grained electrum (el) inclusions in pyrite. Chalcopyrite (cpy), chalcocite (cc) and altaite (al) are also enclosed in the pyrite.

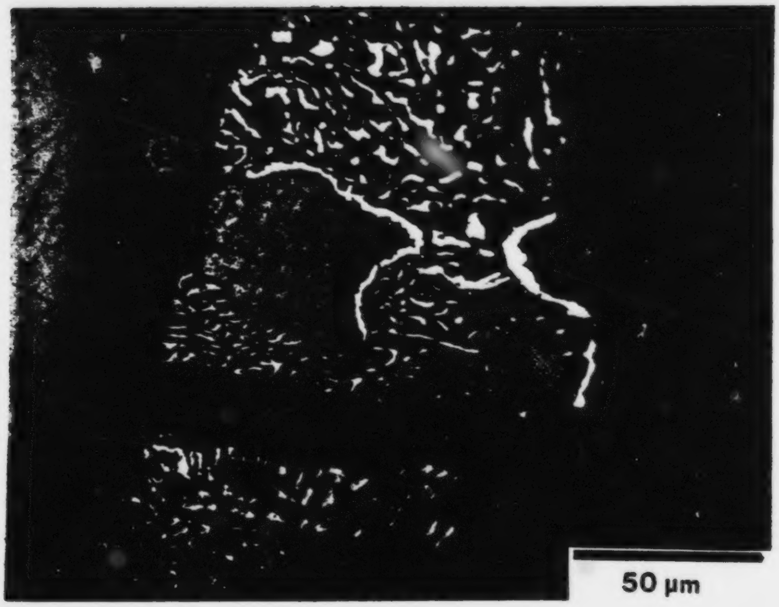

Plate 4 Electrum (el) in myrmekitic intergrowths of galena with chalcocite.

TABLE 4

ELECTRON PROBE MICROANALYSIS OF ELECTRUM GRAINS

Grain	Number of points	Ag	Au	Total
		weight % (x)(1)		
Mill feed				
1	1	30.55	69.08	99.63
2	6	30.70	70.48	101.18
3	5	29.94	71.27	101.21
4	2	30.34	71.05	101.39
mean (x)		**30.38**	**70.47**	**100.85**
λ		**± 0.33**	**± 0.98**	**± 0.82**
Bornite-rich ores				
1	9	21.40	79.56	100.96
2	5	25.46	73.24	98.70
3	1	21.67	79.78	101.45
4	5	21.66	79.07	100.73
mean (x)		**22.55**	**77.92**	**100.46**
(2)		**± 1.95**	**± 3.13**	**± 1.21**

(1) average of six spot determinations
(2) confidence interval at 95% significance level

$\lambda = \frac{2\sigma}{\sqrt{N}}$

electrum in the mill feed and 10% higher (Table 4). The area of the grains ranged from 24 µm² to 676 µm². The total area of electrum was 1500 µm². The observed electrum accounts for 90 % of the head assay.

8.3.3 Mineralogy of Products

8.3.3.1 Zinc concentrate

Major minerals: Sphalerite, pyrite, chalcopyrite

Minor minerals; Galena, tetrahedrite, electrum, altaite, bornite, wehrlite, covellite, native-Cu, and arsenopyrite.

Tetrahedrite and telluride minerals are common minor minerals in the zinc concentrate samples.

Gold Minerals

Nine particles of electrum were noted in a sample of zinc concentrate (Appendix A1). Six grains, representing 15% of the total area were enclosed in sphalerite (Plate 6). One grain (55% of the total area) was liberated, one grain (6% of the total area) was combined with chalcopyrite, and one grain (25% of the total area) was enclosed in gangue (Plate 7). The total area of electrum was 73 µm². The visible gold, 2.3 g/t, accounts for 55% of the gold head assay and 89% of the directly cyanidable gold (Appendix A2).

8.3.3.2 Copper concentrate

Major minerals: Chalcopyrite, pyrite, sphalerite, tetrahedrite

Minor minerals: Bornite, covellite, galena.

The concentrate contains grains of chalcopyrite with lesser amounts of pyrite and sphalerite. Tetrahedrite is the fourth commonest mineral present. The tetrahedrite grains contain inclusions of sphalerite and galena.

Gold minerals

Native gold or electrum were not observed during detailed examination of ten polished grain mounts prepared from the copper concentrate. This was unexpected, considering the assay of the sample (11.5 g/t) and the fact that the invisible gold concentration in chalcopyrite is very low (Table 5). It was reasoned that if the average electrum particle size was 50 µm²,

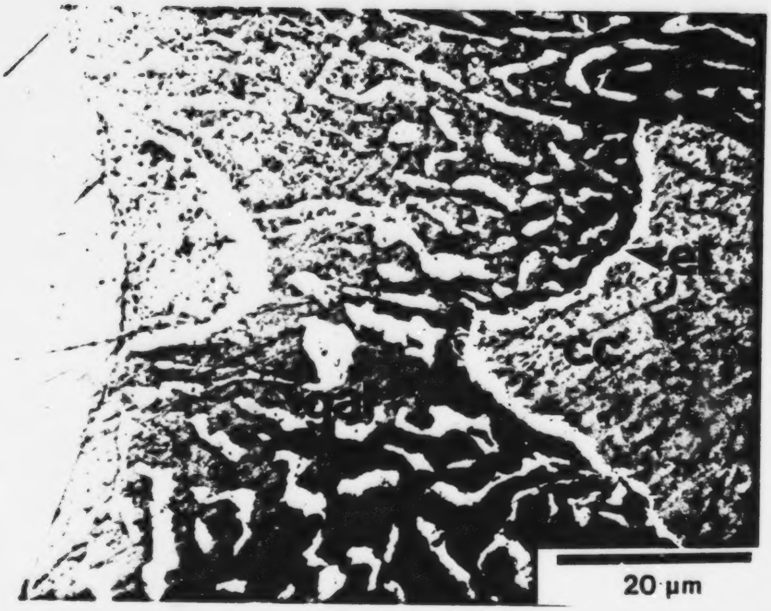
el
cc
gal
20 µm

Plate 5 Electrum (el) at margin between galena (gal) and chalcocite (cc).

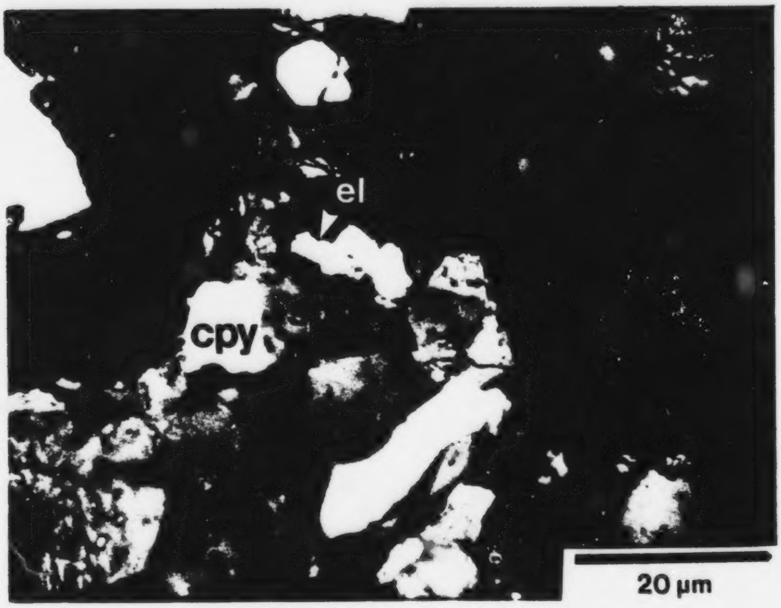

Plate 6 Electrum (el) associated with sphalerite (sph), chalcopyrite (cpy) and gangue (g).

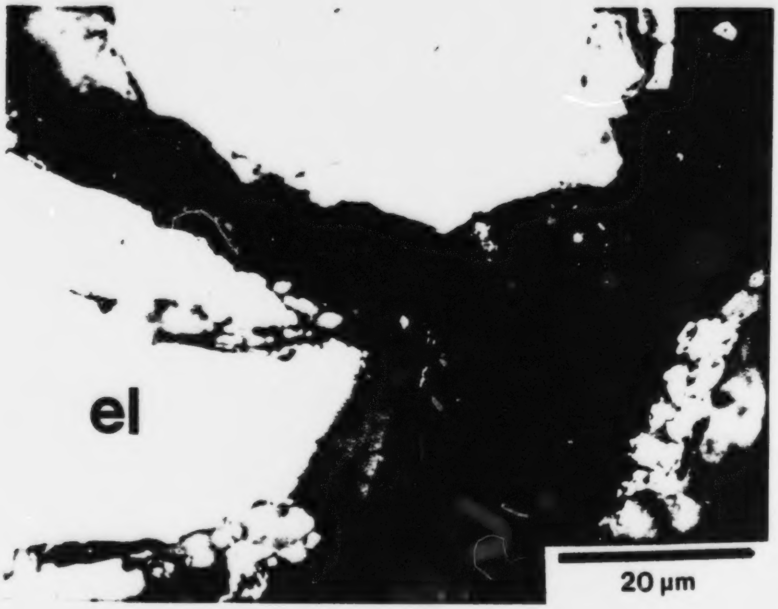

Plate 7 Electrum (el) enclosed in gangue (g).

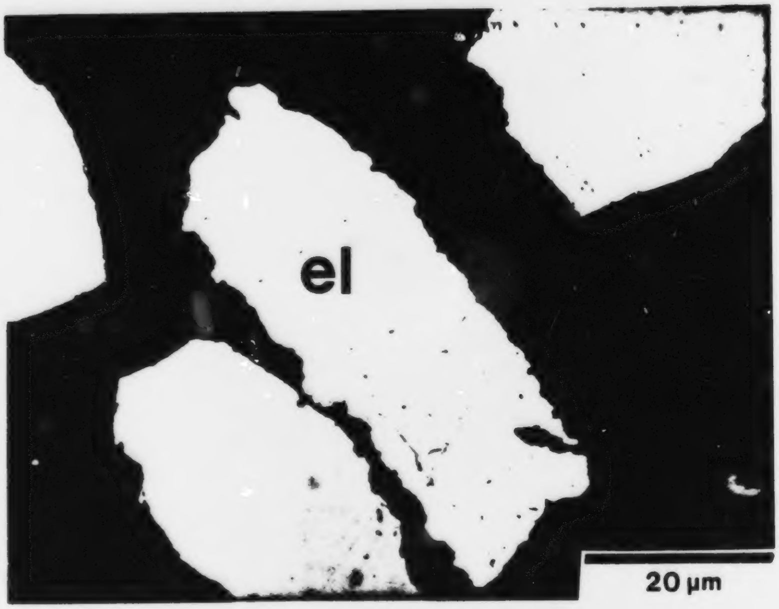

Plate 8 Liberated electrum (el) in the copper concentrate.

TABLE 5

INVISIBLE GOLD IN SULPHIDE MINERALS; ppm

		polymetallic ore	Bedded ore	Cu-pyrite ore	Bornite-rich ore	Mill Feed
Pyrite	N	26	11	12	10	33
	x ±	0.18 ± 0.08	0.27 ± 0.21	0.33 ± 0.16	0.18 ± 0.21	0.27 ± 0.21
Tetrahedrite	N	32	3	7	23	
	x ±	5.1 ± 3.7	0.23 ± 0.06	0.24 ± 0.1	0.34 ± 0.22	
Bornite	N				16	2
	x ±				0.67 ± 0.20	0.40 ± 0.60
Chalcopyrite	N	5	4			12
	x ±	0.18 ± 0.16	0.20 ± 0.08			3.0 ± 1.3*
Galena	N				4	
	x ±				1.78 ± 1.11	

---

* fine-grained chalcopyrite

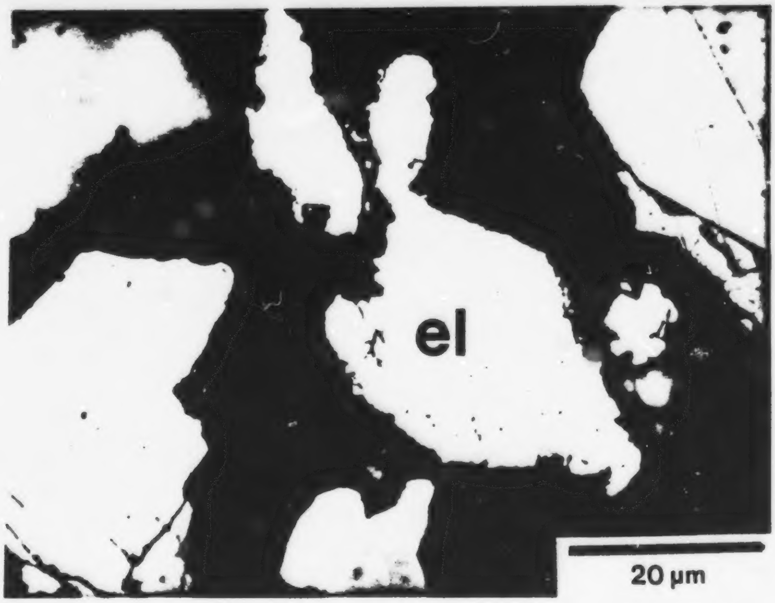

Plate 9 Liberated electrum (el) in the copper concentrate.

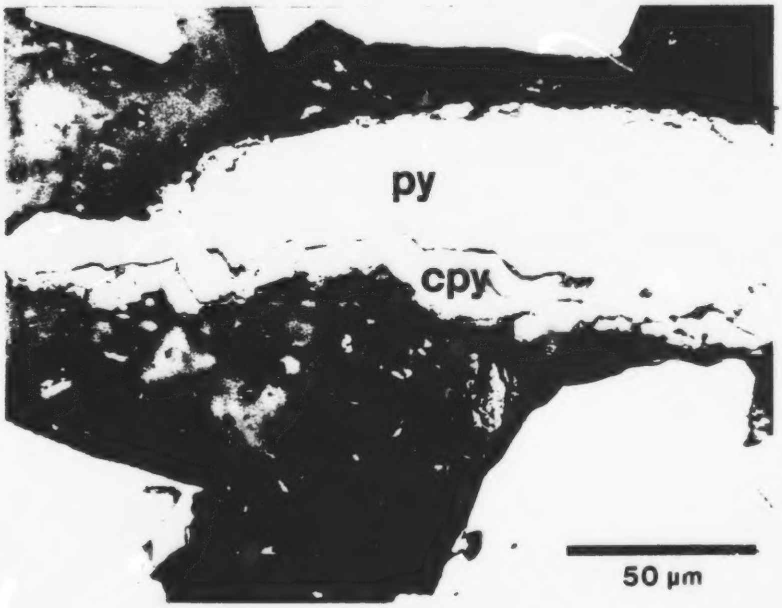

Plate 10 Etching of chalcopyrite (cpy) reveals some of that mineral to be composed of fine-grained aggregates.

the probability of not having seen one of the 45 grains that would be expected is 10^{-20}. If the average grain size was 500 µm², the probability of not having seen one of the 4.5 grains expected is 0.01. However, if the grains are sufficiently large, say 3000 µm², then the chances of not having seen such a grain exceed the chances of having seen such a grain. This suggested that the visible gold in the copper concentrate could be made up of large grains which were not seen in the sample examined due to the nugget effect.

In order to confirm this, a gravity separation was carried out on a 1 kg subsample of copper concentrate. One polished block was prepared from the gravity concentrate (representing 0.1 wt.% of the head sample). It contained 35 grains of electrum, with a mean area of 2091 µm² (Appendix A1, Plates 8 and 9). The size distribution of the grains is shown in Figure 2. The calculated Au assay of this gravity concentrate is 1600 g/t, based on a 70.5 wt% gold content of the electrum (Table 4). In this way, it was shown that large liberated electrum grains account for only 14% of the gold in the copper concentrate.

The gravity table tailings assayed 8.37 g/t, indicating that most of the gold in the copper concentrate has to be very fine-grained or colloidal.

8.3.4 Invisible gold

Invisible gold is the gold which is either in solid solution in the crystal lattice of the sulphides or is in colloidal form, that is sub-micron inclusions of gold minerals, and is thus invisible under the optical and scanning electron microscopes. The invisible gold is mostly not recoverable by direct cyanidation and requires prior oxidation of the host sulphides in order for the gold to be recovered. The invisible gold concentration in sulphide minerals from HW was found to be low, with the exception of the tetraherdrite-tennantite and fine-grained chalcopyrite.

Pyrite particles from the mill feed, bedded Cu-Zn ore, cupriferous pyrite ore, polymetallic ore and the bornite-rich ore were analysed using the ion microprobe. The mean Au concentration of 92 particles was 0.25 parts per million (g/t), with a confidence interval of 0.09 ppm at a 95 % confidence interval (Figure 3). This means that 95 out of 100 pyrite particles would have a gold concentration in the range from 0.16 to 0.34 ppm. The minimum detection limit (MDL) (3σ) for gold in pyrite is 0.3 ppm. Statistically, there is no difference between the gold concentration of pyrites from the four ore types.

Figure 2 Histogram showing the size distribution of electrum particles in the gravity concentrate produced from the Cu-concentrate. n = 35

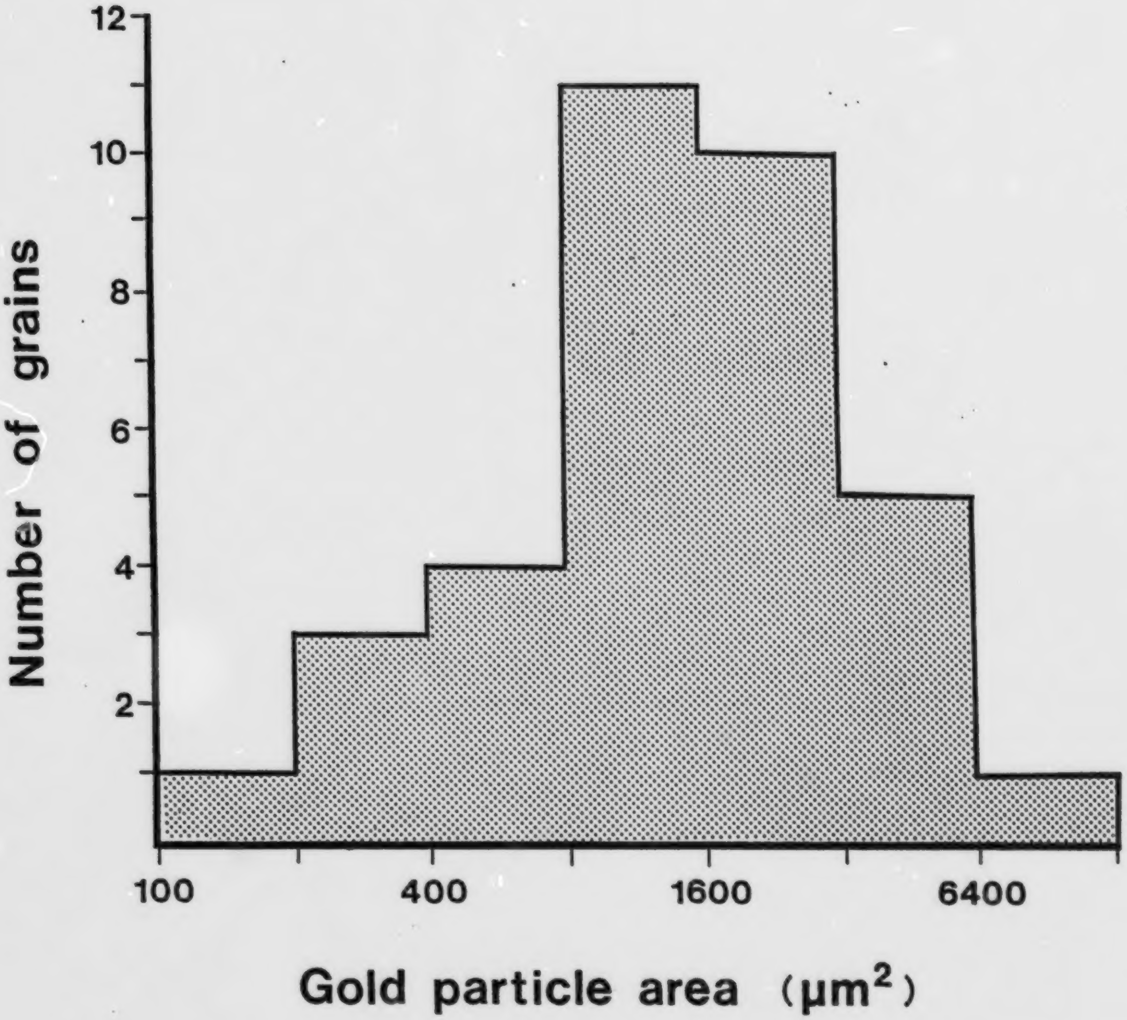

FIGURE 3

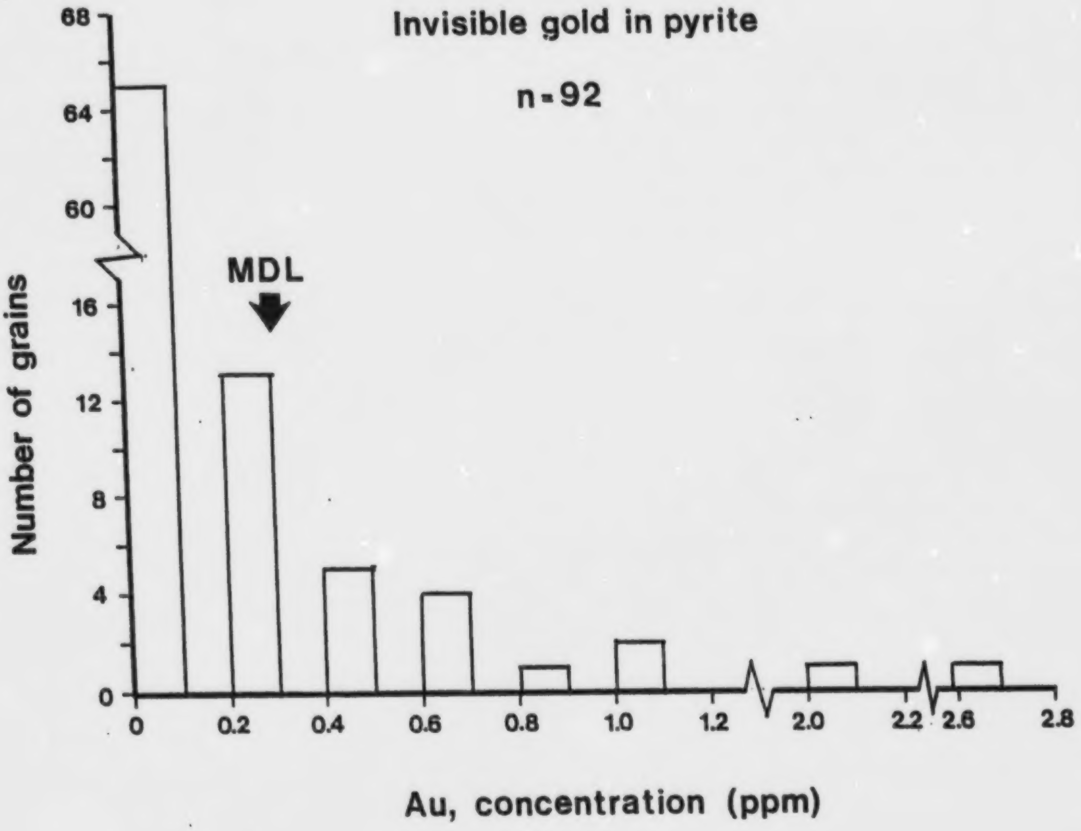

Distribution of invisible gold in pyrite.

Tetrahedrite-tennantite particles were analysed for gold in all four ore types and the copper concentrate. The mean concentration of tetrahedrite particles from the cupriferrous pyritic ore, the bedded Cu-Zn, and the bornite-rich ore was comparable (0.31 ppm) with a confidence interval of 0.15 ppm. In the polymetallic ore, the gold concentration of tetrahedrite was higher. The mean concentration of 32 particles was 5.1 ppm with a confidence interval of 3.7 ppm. The mean gold concentration of the 16 tetrahedrite-tennantite particles from the copper concentrate is 1.4 ± 1.5 ppm. The large confidence intervals in the last two samples are due to the presence of gold-rich tetrahedrites with gold concentrations higher than 10 ppm (Figure 4). Inclusions of a gold mineral, probably electrum were noted on 4 out of the 81 depth profiles. Such electrum grains were all smaller than 1 μm^2. Some tetrahedrites contain 2 or more such grains. A representative depth profile is shown in Figure 5.

The mean concentration of gold in 9 large chalcopyrite grains was 0.19 ± 0.10 ppm. The mean concentration in 4 galena particles was determined to be 1.78 ± 1.11 ppm and in the bornite 0.63 ± 0.19 ppm. The data is summarized in Table 5. The ion probe microanalysis data is given in full in Appendix A3.

The persuit for the principal gold carrier mineral in the copper concentrate (part 3.3.2) eventually led to the analysis of the fine-grained chalcopyrite. It was determined that the **fine-grained chalcopyrite is gold bearing.** The mean concentration of 12 particles was 3.0 ± 1.3 ppm (Figure 6). The fine-grained chalcopyrite was identified by etching a polished mount of the mill feed (Plate 10).

8.3.5 Diagnostic cyanidation tests

The gold recovery by direct cyanidation of the mill feed was 51 % at K_{80} = 60 µm. By pulverising the sample (K_{80} = 15 µm) the recovery increased only 12% to 63%, indicating significant amounts of very fine grained, colloidal and solid solution gold. A similar increase in recovery with finer grinding as anticipated (part 3.3.1) is shown by the zinc concentrate. The recovery was increased from 52% at K_{80} = 47 µm to 63% at K_{80} = 14 µm. The cyanidation results and conditions are given in Table 6.

FIGURE 4

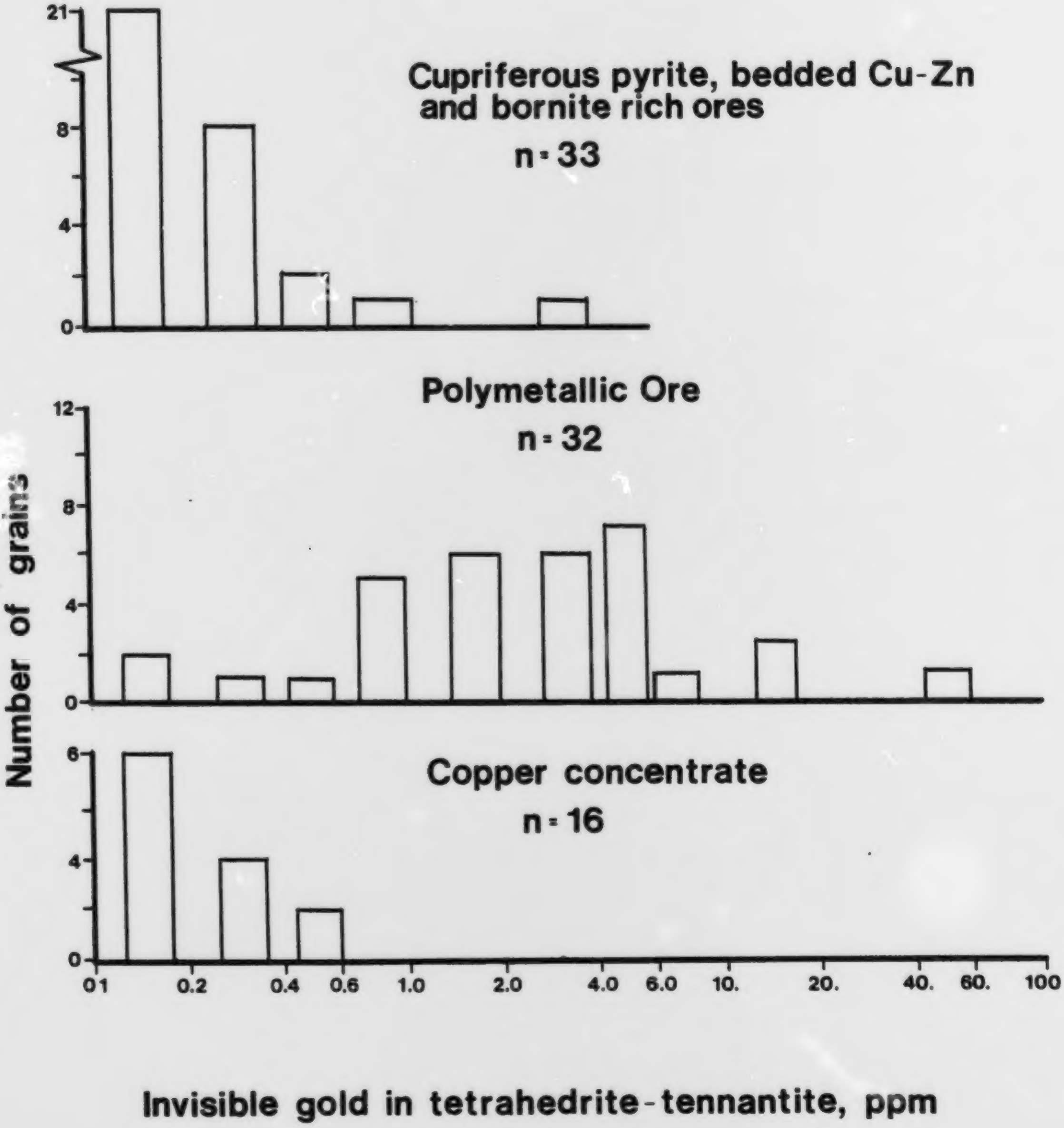
21
8
4
0
Cupriferous pyrite, bedded Cu-Zn and bornite rich ores
n = 33
12
8
4
0
Polymetallic Ore
n = 32
Number of grains
6
4
0
Copper concentrate
n = 16
01
0.2
0.4
0.6
1.0
2.0
4.0
6.0
10.
20.
40.
60.
100
Invisible gold in tetrahedrite-tennantite, ppm

FIGURE 5

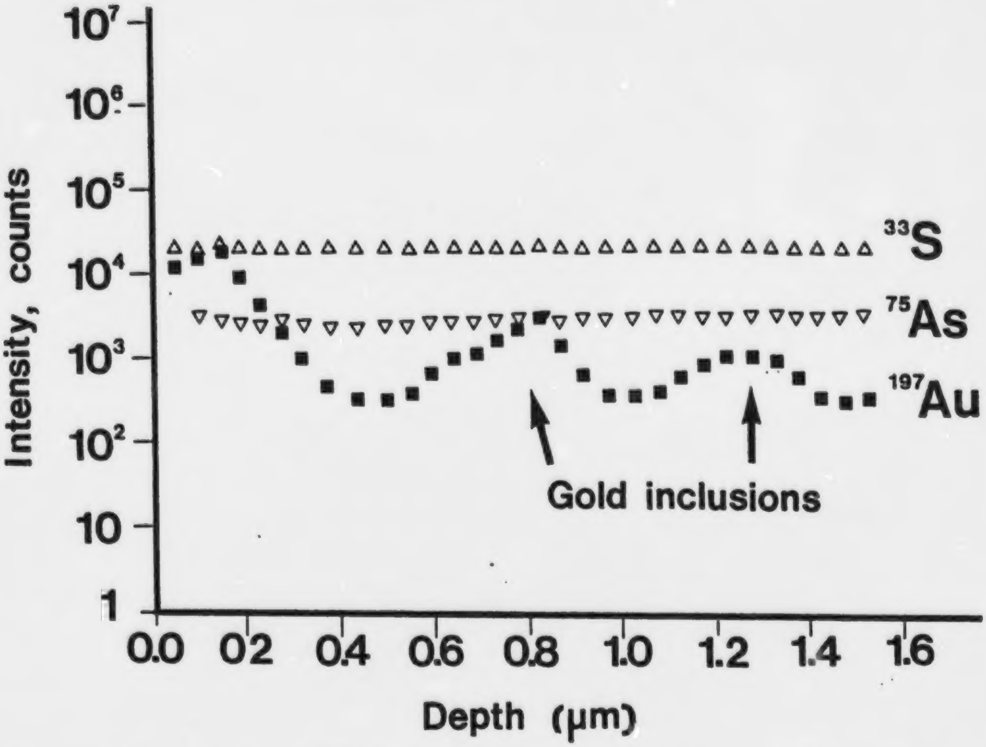

Ion probe depth profile of a tetrahedrite grain indicating the presence of inclusions of a gold mineral, probably electrum.

FIGURE 6

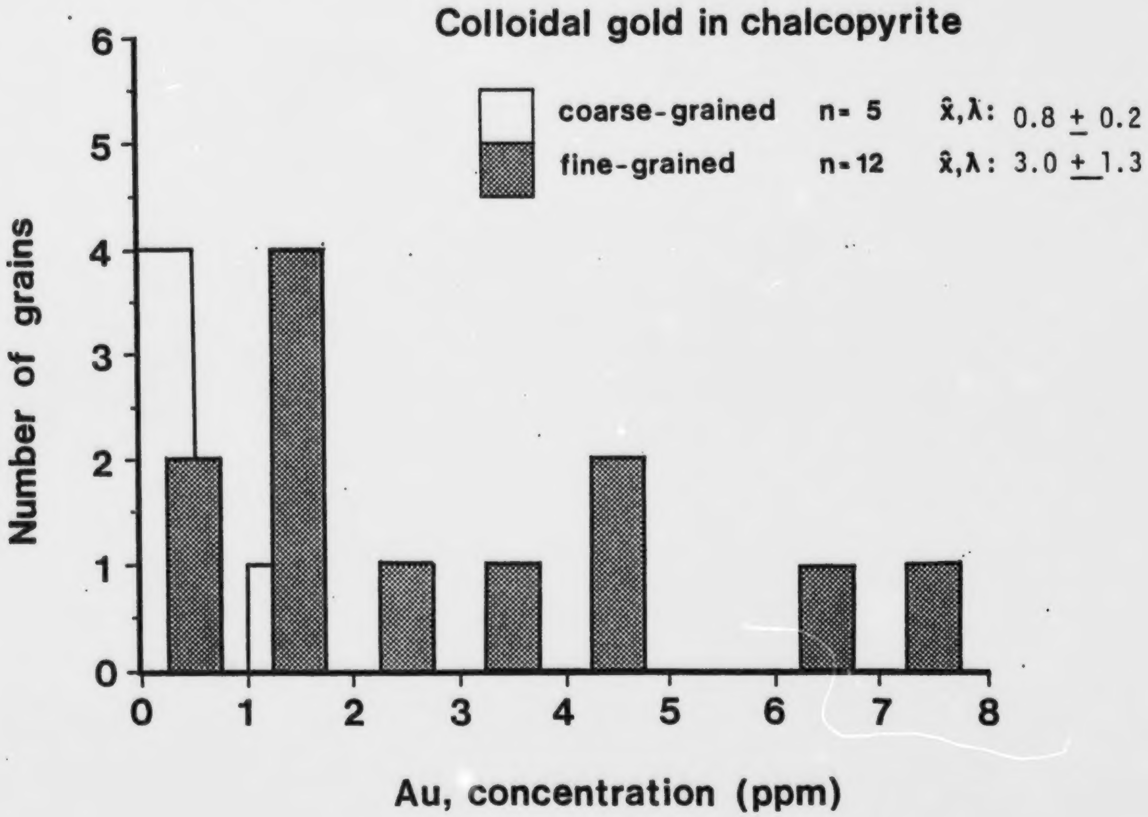

Distribution of colloidal gold in fine and coarse grained chalcopyrite.

TABLE 6

CYANIDATION TEST RESULTS

MILL FEED

		Au g/t, %				
			HEAD			
Test #	K_{80}(µm)	Residue	Calc	Direct	% Extn.	Yield
1	60	1.31	2.94	2.68	55.0	51
2	27	1.24	2.47		49.7	54
3	15	0.99	2.39		58.7	63

ZN CONCENTRATE

		Au g/t, %				
			HEAD			
Test #	K_{80}(µm)	Residue	Calc	Direct	% Extn.	Yield
1	47	1.96	4.59	4.17 ± 0.10	57.3	53
2	22	1.16	4.10		71.7	72
3	14	1.57	4.00		60.8	62

$$\text{Yield} = \frac{(\text{Direct head}) - (\text{Residue})}{(\text{Direct head})}$$

8.3.6 Normative mineralogy and image analysis

The normative mineralogy of the four distinct ore types was calculated on a normative weight percent basis from the chemical assays. Details and the calculations used are presented in Appendix A4. Image analysis of the mill feed, copper concentrate, zinc concentrate and flotation tailings (Appendix A5) was carried out to determine the proportions of minerals present in those samples.

8.4.0 DISCUSSION

The ore samples

The HW ore is mineralogically complex, and the distribution of gold within the ore is likewise so. Visible and invisible gold are present in varying amounts in the ores studied. Size and association of the visible gold vary significantly between ore types. The presence of colloidal gold and solid solution gold in some sulphides complicate the recovery of gold in a base metal ore flotation circuit.

Diagnostic cyanidation testing of the mill feed indicated that at least 63% of the gold is in a recoverable form, i.e. native gold or electrum. Fine grained gold is important, as demonstrated by the 10% increase in recovery when the sample was pulverised. The fine grained gold extends to colloidal gold in chalcopyrite and to a lesser extent in tetrahedrite where it is also encountered also as solid solution gold. Four grains of electrum were identified in the mill feed. The coarser grains were associated with sphalerite / galena, while the finer grains were enclosed in pyrite.

In the bornite-rich ore, electrum, exclusively associated with chalcocite-galena myrmekitic intergrowths is the principal gold carrier mineral, accounting for at least 90% of the gold. This ore has the highest assay (3.2 g/t). Both galena and bornite carry solid solution gold in minor amounts (0.67 and 1.78 ppm respectively). The gold content of the sphalerite is not known, while pyrite and tetrahedrite have insignificant gold concentrations, less than the MDL's of the ion probe (0.3 and 0.2 ppm respectively).

In the polymetallic ore, both pyrite and coarse-grained chalcopyrite have gold concentrations less than the respective minimum detection limits, 0.3 and 0.2 ppm. Arsenian tetrahedrite and tennantite carry both solid solution gold (6.3 ppm) and gold micro-inclusions, while end-member tetrahedrite has no gold. It is not surprizing that visible gold was not identified in the two sections examined, considering that the polymetallic ore assays 2.6 g/t gold of which some is colloidal and solid solution gold.

In the bedded Cu-Zn ore, the ion probe data show that the invisible gold concentration in pyrite, coarse chalcopyrite and tetrahedrite is within the minimum detection limit of the instrument,- 0.2-0.3 ppm. Therefore, the bulk of the gold is expected to be visible. At least 6 polished sections would have to be studied in order to verify the presence of visible gold.

In the cupriferrous pyrite ore, both tetrahedrite and pyrite do not contribute to the gold mineralogical balance. It is anticipated that the gold is distributed between two carriers: electrum or native gold and colloidal gold in chalcopyrite.

The Products:

In the zinc concentrate, 72% of the gold was recoverable by direct cyanidation. This is a minimum value since cyanide is adsorbed onto sphalerite and complexes with soluble zinc. Nine grains of visible gold were seen in sections of the zinc concentrate sample. The visible gold observed accounts for 55% of the head assay. Of the two largest grains, one was liberated and the other was enclosed in gangue minerals. The non-leachable gold is in the form of micro-inclusions in tetrahedrite-tennantite and possibly in sphalerite. The importance of sphalerite as a gold carrier is not known. Charging problems inhibited the ion probe microanalysis of sphalerite.

The most challenging of all the HW samples studied, proved to be the copper concentrate sample. The reported head assay from the mine is 7.5 g/t, compared to 11.5% from Lakefield Research. Both visible and invisible gold are present in the copper concentrate. Most interesting is the extreme size distribution of electrum in the concentrate, with 14% (or 21%) of the assayed gold present as very coarse particles (Plates 8 and 9, Figure 2). The average size of the coarse electrum is 2091 μm^2, with 90% of the grains within the range from 425 to 5415 μm^2. Chalcopyrite is believed to be the principal gold carrier mineral in the copper concentrate. Ion probe microanalysis demonstrated the presence of colloidal gold in the fine-grained chalcopyrite, however in amounts insufficient to account for the balance of gold. Tetrahedrite-tennantite and galena are both trace gold carriers, accounting for 1% combined.

8.5.0 CONCLUSIONS

Invisible gold has been identified in the HW ores. Chalcopyrite is the principal carrier of colloidal gold, while arsenian tetrahedrite and tennantite have the highest solid solution gold concentration, 6.3 ppm. Of the other sulphides, not including sphalerite, only galena and bornite carry invisible gold in trace amounts, 1.78 and 0.67 ppm respectively.

Visible gold in the form of electrum is the principal gold carrier in the four ore types and the concentrator products. In the bornite-rich ore, electrum in chalcocite-galena myrmekitic intergrowths accounts for 90% of the gold assay. The electrum shows an extremely discontinuous size distribution: very coarse and very fine with relatively little in between. The association of electrum is complex. The coarse electrum is associated with galena, chalcocite and sphalerite, while the fine-grained electrum is enclosed in pyrite and tetrahedrite-tennantite.

The large size variation of electrum, its complex associations and the presence of colloidal gold in chalcopyrite make optimization of the gold recovery in the HW base metal flotation circuit a formidable challenge. The coarseness of electrum grains as well as relatively high silver content can adversely affect their recovery into the copper concentrate. The colloidal gold, unlike the solid solution gold is not hosted in specific minerals and can be distributed in several cogenetic sulphides and gangue minerals.

APPENDIX A1

IMAGE ANALYSIS OF ELECTRUM PARTICLES

Grain #	Association	Size (sq µm)
MILL FEED		
1	Combined sphalerite/ galena	340
2	"	50
3	Enclosed in pyrite	1
4	"	1
BORNITE RICH ORES		
1	Combined galena/ chalcocite	259
2	"	504
3	"	676
4	"	37
5	"	24
Zn-CONCENTRATE		
1	Enclosed in sphalerite	1
2	"	4
3	"	1
4	"	2
5	"	1
6	"	2
7	Liberated	40
8	Combined with chalcopyrite	4
9	Enclosed in gangue	18

Cu-CONCENTRATE (gravity separation, all grains liberated)

	size		size		size		size
1	2850	11	350	21	560	31	5080
2	425	12	1830	22	1170	32	360
3	870	13	2350	23	1000	33	770
4	2350	14	930	24	5720	34	3090
5	1150	15	1020	25	2430	35	1610
6	1600	16	1510	26	1625		
7	3440	17	2810	27	155		
8	1420	18	3720	28	1225		
9	670	19	5415	29	860		
10	1250	20	9370	30	2215		

x ± : 2091
+ 643 µm²

APPENDIX A2

CALCULATION OF VISIBLE GOLD CONCENTRATION

CALCULATION OF VISIBLE GOLD IN MILL FEED

Total area covered: 6 x 4.91 cm^2 = 29.46 cm^2

Coverage of sample (from point counting) = 30 %

Area covered = 8.84 cm^2

Total sample weight (unit depth; 10^{-4} cm, av. spec. grav; 5.0 $g.cm^{-3}$) = 44.19 x 10^{-4} g

- -

Total gold area = 392 μm^2
= 39.2 x 10^{-8} cm^2

Gold content (EPMA) = 70.47 ± 0.98 %

Total gold weight (unit depth; 10^{-4}, av. spec. grav; 19.3 $g.cm^{-3}$) = 53.31 x 10^{-10}g

Gold concentration relative to sulphide = 1.21 ppm

- -

Visible gold content = 1.21 ppm

CALCULATION OF VISIBLE GOLD IN THE ZINC CONCENTRATE

Total area covered: = 4.91 cm^2

Coverage of sample (from point counting) = 22 %

Area covered = 1.08 cm^2

Total sample weight (unit depth; 10^{-4} cm, av. spec. grav; 4.0 g.cm^{-3}) = 4.32×10^{-4} g

* * *

Total gold area = 73 µm^2
= 7.3×10^{-8} cm^2

Gold content = 70.47 ± 1.0 %

Total gold weight (unit depth; 10^{-4}, av. spec. grav; 19.3 g.cm^{-3}) = 9.93×10^{-10} g

Gold concentration relative to sulphide = 2.30 ppm

* * *

Visible gold content = 2.30 ppm
± 0.41

APPENDIX A3

ION MICROPROBE DATA

INVISIBLE GOLD CONCENTRATION

INVISIBLE GOLD CONCENTRATION IN SULPHIDES
(Cupriferous pyritic ore)

Pyrite

particle #	Au, ppm
1	0.1
2	0.3
3	0.4
4	0.4
7	1.0
8	0.7
9	0.4
10	0.0
11	0.1
12	0.3
13	0.1
14	0.2

N : 12

$\hat{x} \pm \lambda$: 0.33 ± 0.16

MDL : 0.2 ppm

Tetrahedrite

particle #	Au, ppm
5	0.2
6	0.5
145	0.1
146	0.3
147	0.2
148	0.2
149	0.2

N : 7

$\hat{x} \pm \lambda$: 0.24 ± 0.10 ppm

MDL : 0.2 ppm

INVISIBLE GOLD CONCENTRATION IN SULPHIDES

(Bedded Cu-Zn ore)

Pyrite

particle #	Au, ppm
132	0.0
133	0.1
135	0.2
136	0.1
137	0.6
138	1.2
139	0.1
141	0.2
142	0.4
143	0.1
144	0.2

N : 11

$\hat{x} \pm \lambda$: 0.27 ± 0.21 ppm

MDL : 0.3 ppm

Chalcopyrite

particle #	Au, ppm
57	0.3
58	0.2
59	0.2
60	0.1

N : 4

$\hat{x} \pm \lambda$: 0.2 ± 0.08

MDL : 0.2 ppm

Tetrahedrite

particle #	Au, ppm
129	0.2
130	0.2
140	0.3

N : 3

$\hat{x} \pm \lambda$: 0.23 ± 0.06 ppm

MDL : 0.2 ppm

INIVISIBLE GOLD CONCENTRATION IN SULPHIDES
(Polymetallic ore)

Pyrite

particle #	Au, ppm
98	0.2
99	0.1
100	0.5
101	0.2
102	0.0
103	0.0
105	0.2
106	0.2
108	0.0
110	0.1
111	0.2
112	0.0
113	0.3
114	0.4
115	0.7
116	0.1
117	0.0
120	0.2
121	0.1
122	0.0
123	0.0
126	0.1
166	0.5
167	0.0
168	0.0
183	0.7

N : 26

$\hat{x} \pm \lambda$: 0.18 ± 0.08 ppm

MDL : 0.3 ppm

Chalcopyrite

particle #	Au, ppm
104	0.2
107	0.2
109	0.5
118	0.0
119	0.0

N : 5

$\hat{x} \pm \lambda$: 0.18 ± 0.16

MDL : 0.2 ppm

Tetrahedrite-Tennantite

particle #	Au, ppm
124	17.
125	4.7
127	2.5
150	5.8
151	59.
152	2.6
153	1.1
154	1.8
155	2.0
156	0.3
157	0.6
158	7.2
159	1.2
160	0.8
161	0.9
162	0.2
163	5.6
164	5.5
165	2.6
169	2.0
170	0.9
171	3.1
172	5.2
173	0.8
174	0.2
175	11.
176	1.3
177	3.3
178	5.0
179	3.5
180	6.0
181	0.7

N : 32

$\hat{x} \pm \lambda$: 5.1 ± 3.7 ppm

MDL: 0.2 ppm

INVISIBLE GOLD CONCENTRATION IN SULPHIDES
(Bornite-rich ore)

Pyrite

particle #	Au, ppm
1	0.2
10	0.2
62	0.0
78	1.1
85	0.0
86	0.0
87	0.1
88	0.0
89	0.1
99	0.1

N : 10

$\hat{x} \pm \lambda$: 0.2 ± 0.2 ppm

MDL : 0.3 ppm

Bornite

particle #	Au, ppm
2	0.6
8	0.3
9	1.5
14	0.8
15	0.4
16	0.7
21	0.3
63	1.6
64	1.0
65	0.8
67	0.5
68	0.6
69	0.2
79	0.3
80	0.4
82	0.6

N : 16

$\hat{x} \pm \lambda$: 0.67 ± 0.20 ppm

MDL : 0.2 ppm

Tetrahedrite

particle #	Au, ppm
3	0.2
4	0.3
5	0.2
6	0.8
7	0.3
11	0.6
12	0.3
13	0.3
61	0.2
66	0.3
70	0.1
71	0.2
72	0.2
73	0.3
74	0.1*
75	2.6
76	0.1
77	0.2
81	0.1
83	0.2
84	0.1
91	0.2
92	0.1

N : 23

$\hat{x} \pm \lambda$: 0.34 ± 0.22 ppm

* : + Au inclusion

Galena

particle #	Au, ppm
17	0.9
18	3.4
19	2.2
20	0.6

N : 4

$\hat{x} \pm \lambda$: 1.78 ± 1.11

MDL : 0.2 ppm

INVISIBLE GOLD CONCENTRATION IN SULPHIDES

(HW, Vancouver Island, B.C.)

(Mill feed, Sept. 1987)

Pyrite

Particle #	Au, ppm
21	0.0
22	0.0
23	0.0
24	0.3
25	0.3
26	2.8
30	0.0
31	0.2
32	0.0
33	0.0
34	0.0
35	0.8
36	0.0
37	0.1
38	0.0
39	0.0
40	0.0
41	0.1
42	2.2
43	0.0
44	0.3
45	0.6
46	0.3
47	0.0
48	0.0
49	0.0
50	0.0
51	0.4
52	0.5
53	0.1
54	0.2
55	0.0
56	0.0

N : 33

x ±λ: 0.27 ± 0.21 ppm

MDL : 0.3 ppm

Chalcopyrite

Particle #	Au, ppm
1f	0.7
2f	7.7
3f	2.7
4f	6.5
5c	0.5
6c	1.0
7f	4.3
8c	1.2
9f	1.4
10f	1.5
11f	1.3
12f	4.2
14c	0.8
15f	3.3
16f	1.0
17f	1.3
27c	0.7

N : 17

x ±λ: 2.4 ± 1.0 ppm

MDL : 0.2 ppm

c : coarse
f : fine

fine chalcopyrite
x ±λ: 3.0 ± 1.3

Bornite

Particle #	Au, ppm
28	0.7
29	0.1

N : 2

x ±λ: 0.4 ± 0.6 ppm

INVISIBLE GOLD CONCENTRATION IN SULPHIDES

(Copper concentrate)

Tetrahedrite - Tennantite

Particle #	Au, ppm
15	0.6
16	0.5
17	0.4
18	0.1
19	0.1
20	0.2
21	0.1
22	8.5 (+Au inc.)
23	0.4
24	0.1 (+Au inc.)
25	0.1
26	0.3
27	0.3
28	0.2
29	10.
30	0.2

N : 16

$\hat{x} \pm \lambda$: 1.4 ± 1.5 ppm

MDL : 0.2 ppm

APPENDIX A4

NORMATIVE MINERALOGY OF ORE TYPES

	Polymetallic ore	Bedded Cu-Zn ore	Cu-Pyrite	Bornite rich ore
Galena	2.54	0.17	0.03	1.62
Chalcopyrite	6.01	6.80	9.42	-
Bornite	-	-	-	2.09
Sphalerite	19.00	9.88	1.61	17.02
Pyrite	53.33	56.37	72.63	13.32
Tetrahedrite-Tennanite	0.23	0.86	0.14	2.27
Barite	0.02	0.02	0.06	1.96
Other gangue*	18.87	25.90	16.26	61.72
Total	100.00	100.00	100.00	100.00

* by difference

CALCULATION OF NORMATIVE MINERALOGY (wt. %)

x_{Pb} = Pb assay
x_{Cu} = Cu assay
x_{Zn} = Zn assay
x_{Ba} = Ba assay
x_{S} = S assay
x_{As} = As assay
x_{Sb} = Sb assay

1) G (wt% galena) = x_{Pb}. 1.154

2) Cpy (wt% chalcopyrite) = (x_{Cu} - 0.52T).2.89
T is wt% tennantite (point 5)

Or, alternatively bornite may be calculated;
Bo (wt% bornite) = (x_{Cu} - 0.52T).1.58

3) Sp (wt% sphalerite) = x_{Zn}.1.52
* assuming 2% Fe in sphalerite

4) B (wt% barite) = x_{Ba}.1.70
* assuming no other sulphates are present

5) Te (wt% tetrahedrite-tennantite)
(expressed as tennantite)
= (x_{As} - (As_{py}.Pm) + (Sb x 74.92/121.75)).4.87

As_{py} is the concentration of arsenic in pyrite if any
Pm is the normative mode% proportion of pyrite (point 6)
* assuming no other As or Sb minerals are present
* assuming no Zn, Fe or Ag in the tetrahedrite-tennantite

6) Py (wt% pyrite)
= (x_S - (G.0.154 + S.0.33 + Cpy.0.349* + B.0.23
+ Te.0.28)).1.873

* If bornite has been calculated then Bo.0.256 should be used in place of Cpy.0.349.

7) R (wt% gangue, other than barite)
= 100 - (G + Cpy + Sp + B + Py + Te)

APPENDIX A5

AREA MEASUREMENT

PRODUCTS

SAMPLE	# OF AREAS MEASURED	TOTAL AREA MEASURED (mm^2)	TOTAL # OF GRAINS	AREA COVERED BY GRAINS (%)	# OF GRAINS						PROPORTIONS OF MINERALS					
					Py	Cpy	Sph	Tet	Bn	G	Py	Cpy	Sph	Tet	Bn	G
Mill Feed	4	33.9	1253	40.8 ±7.0	912	192	79	3	0	87	77.5 ±1.1	8.4 ±1.7	6.9 ±2.2	0.1 ±0.1	-- --	7.2 ±1.5
Zn-conc.	2	17.0	1576	27.9 ±5.3	182	42	1300	3	0	49	11.9 ±1.8	3.7 ±0.2	79.2 ±8.6	0.2 ±0.1	-- --	5.0 ±1.5
Cu-conc.	4	33.9	3112	23.1 ±4.1	265	2604	120	29	4	90	12.2 ±2.2	76.8 ±5.2	3.8 ±0.9	1.1 ±0.9	0.1 ±0.3	6.0 ±4.3
Tailings	2	17.0	1559	33.4 ±2.6	1426	12	68	0	0	85	87.5 ±1.7	0.6 ±0.2	2.5 ±0.4	--	--	9.4 ±1.5

G = Gangue

CHAPTER 9

DETERMINATION OF INVISIBLE GOLD IN SULPHIDE MINERALS FROM THE ESTRADES DEPOSIT, QUEBEC.

SSW/PMS/89/7

SUMMARY

In the composite 4-C from the Estrades deposit (Quebec), eighty one percent of the gold head assay is visible gold recoverable by direct cyanidation. Finer grinding did not improve the recovery. Based on the mineralogical study of three flotation concentrates, it was determined that 95% of the visible gold is liberated and coarse grained. The remaining 5% of the visible gold is fine-grained, associated with galena, pyrite and gangue.

The invisible gold within sulphide minerals accounted for 15.1% of the head assay. Pyrite carries 8.9% and arsenopyrite accounts for 5.6%. Arsenopyrite is only a minor component of the ore, 0.36%. It is fine-grained and associated with the pyrite. A total of 96.5% of the gold head assay has been accounted in the composite 4-C .

TABLE 1

MINERALOGICAL DISTRIBUTION OF GOLD IN COMPOSITE ORES

	g/t	Distribution %
Assay	3.38	100.0
CN^- recoverable gold		81.4
Invisible gold in pyrite (0.67 ± 0.53 ppm) (44.9 wt.%, calc. from image analysis of heavy fraction	0.30	8.9
Invisible gold in arsenopyrite (54. ± 36. ppm) (0.36 wt. %, calc. from As assay	0.19	5.6
Invisible gold in marcasite (0.91 ± 0.55 ppm) (1.5 wt. %, calc. from image analysis	0.014	0.4
Invisible gold in chalcopyrite (0.13 ± 0.09 ppm) (4.3 wt.%, calc. from image analysis	0.006	0.2
Total accounted gold	3.26	96.5

FIGURE 1

MINERALOGICAL DISTRIBUTION OF GOLD

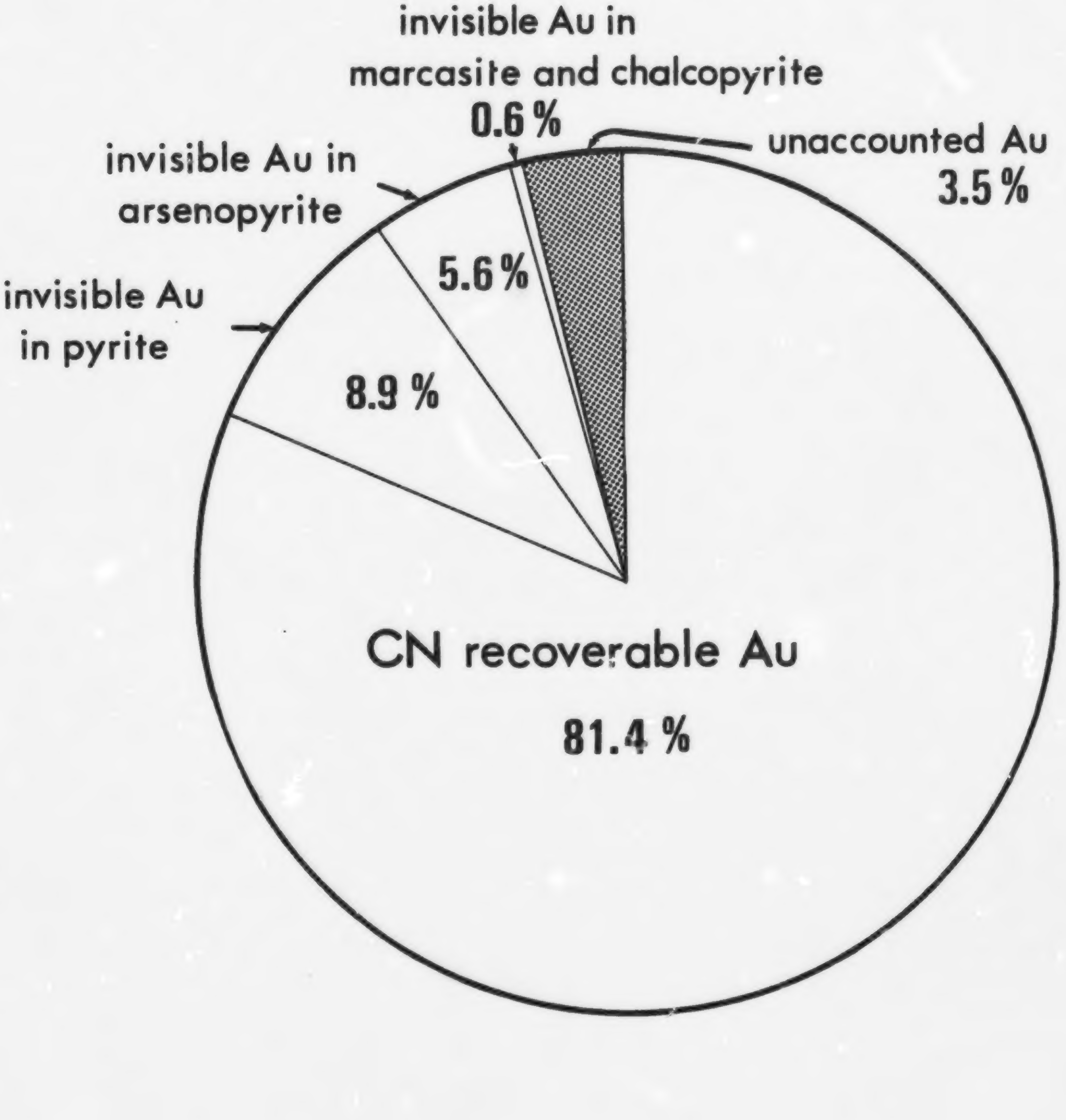

LIST OF TABLES

TABLE 1 Mineralogical distribution of gold
TABLE 2 Cyanidation test results
TABLE 3 Chemical assays
TABLE 4 Invisible gold in sulphide minerals

LIST OF FIGURES

FIGURE 1 Mineralogical distribution of gold
FIGURE 2 Size distribution of electrum grains
FIGURE 3 Distribution of invisible gold

LIST OF PLATES

PLATE 1 Fine-grained pyrite
PLATE 2 Intergrowth of sphalerite and marcasite
PLATE 3 Arsenopyrite associated with pyrite
PLATE 4 Arsenopyrite enclosed in pyrite
PLATE 5 Chalcopyrite coated by covellite
PLATE 6 Association of galena, altaite and tetrahedrite
PLATE 7 Liberated grain of electrum
PLATE 8 Liberated grain of electrum

APPENDICES

A1 Size analysis
A2 Electrum grains identified in flotation products
A3 Image analysis of heavy fraction

9.1.0 INTRODUCTION

Mr. Art Winckers, Metallurgist with Teck Corporation requested the determination of the invisible gold concentration in the sulphides from the Estrades deposit, Quebec, as part of the general project on the characterization of Canadian refractory gold ores by ion probe microanalysis. The aim of this major project is to assist in improving the gold recovery by providing detailed information on the gold mineralogical distribution. The approach followed is that of a process mineralogical study coupled with metallurgical testing (Chryssoulis, 1987).

The objective of this particular study was to provide data on the mineralogical distribution and specifically determine the invisible gold content of the major sulphides in order to evaluate possibilities for improving the gold recovery to the copper concentrate.

Previous mineralogical investigation of ore from the Estrades property has indicated a complex mineralogy and a measure of uncertainty concerning the mineralogical distribution of gold. Although gold alloy phases (mainly very Ag-rich electrum) had been noted, a significant proportion of the gold was believed to be invisible, present in solid solution or in colloidal distribution within the common sulphide minerals.

The study was financed by Teck Corporation, CANMET, the Geological Survey of Canada and the Department of Supply and Services (DSS contract # 50SS.23440-7-9037).

9.2.0 METHODOLOGY

A composite ore sample (# 4-C) was received from Lakefield Research, at the instruction of Teck Corporation, and was used for the mineralogical and metallurgical investigation. The procedure followed is described in the section on methodology of the general report (Chryssoulis, 1989). Cyanidation tests were performed on three 500g charges using progressively finer grinds to determine the cyanide recoverable gold and the effect of grinding upon recovery. Conditions are given in Table 2.

A sub-sample was sieved into the following size fractions; -53 µm (corresponding to 6% by weight of the total sample), 53-90 µm (6%), 90-300 µm (14%), 300-560 µm (10%) and +560µm (64%). Heavy liquid separation using sodium polytungstate (S.G. 3.0 $g.cm^{-3}$) was performed on the 90 - 300 µm and 300 - 560 µm fractions. The 90-300 µm fraction separated into 70% heavy and 30% light fractions and the 300-560 µm fraction separated into 62% heavy and 38% light fractions. The results of sieve testing are given in Appendix A1. A series of twelve polished blocks were prepared.

TABLE 2

CYANIDATION RESULTS (LAKEFIELD RESEARCH)

Test No.	K_{80} (µm)	%Extrn. Au	Residue g/t Au	HEAD Calc.	HEAD Direct
1	48	84.0	0.47	2.93	3.38
2	22	74.9	0.63	2.72	
3	14	78.8	0.63	2.97	

Test No.	Au recovery %	Au recovered g/t
1	86.1	2.91
2	81.4	2.75
3	81.4	2.75

$$\text{Au recovery} = \frac{\text{(mean direct head) - (residue)}}{\text{(mean direct head)}}$$

Conditions: 1 g/l NaCN, pH 10-10.5, 33% solids, 48 hours.

Additional samples, for examination of the visible gold were taken from a series of flotation tests carried out by Lakefield Research. These were 1) a Cu Ro-concentrate, 2) a Cu-Pb separation and 3) a Cu 1st cleaner scavenger concentrate.

Optical microscopy was used to determine the gold minerals, their size and distribution. The invisible gold in the sulphide minerals was determined by ion probe microanalysis. The mineral quantities required for the gold mineralogical distribution were determined by image analysis of the polished blocks, with the exception of arsenopyrite which was calculated from the head As assay, attributing all As to arsenopyrite.

9.3.0 RESULTS

9.3.1 CHEMICAL ASSAYS

Chemical assays of the composite # 4-C are given in Table 3. Also given is the Au assay of the light fraction and the calculated assay of the heavy fraction.

9.3.2 MINERALOGY

9.3.2.1 SULPHIDE MINERALOGY

Major minerals:	Pyrite, sphalerite, chalcopyrite, marcasite.
Minor minerals:	Galena, pyrrhotite, arsenopyrite, cubanite, covellite, tetrahedrite, electrum, altaite.

Two types of **pyrite** are recognized in the samples. The larger pyrite grains are generally fresh in appearance, although fracturing is common. This type contains abundant inclusions of silicate gangue minerals and of other sulphide phases, notably of arsenopyrite, chalcopyrite and galena. The second type is aggregates of small pyrite euhedra (Plate 1). The pyrite content, 44.9 wt. % of the head sample was determined from the sink fraction, assuming that the float fraction had no pyrite.

Small **marcasite** grains occur as intimately grown aggregates, associated primarily with sphalerite (Plate 2), but also associated with chalcopyrite, pyrite, galena and arsenopyrite. **Arsenopyrite** is present in minor amounts, as small blasts associated with pyrite and marcasite (Plates 3 and 4). The normative arsenopyrite content of the head sample is 0.36 wt %.

Sphalerite contains abundant inclusions of **chalcopyrite**, as chalcopyrite disease. Small inclusions of galena are also present in the sphalerite. **Pyrrhotite** occurs as small inclusions within both pyrite and chalcopyrite. **Cubanite** is enclosed included in chalcopyrite, which also contains inclusions of

TABLE 3

CHEMICAL ASSAYS

	mass split %	Au (g/t)	Au distribution	S %	Te ppm	As ppm	Bi ppm	Sb ppm	Cu %	Ag g/t
Head	100	3.38	100.0	24.4 ±8.5	<3	1650 ±100	30	50	1.05	123
Light frac.	30	0.19	1.5							
Heavy frac.	70	4.75(calc)	98.5							

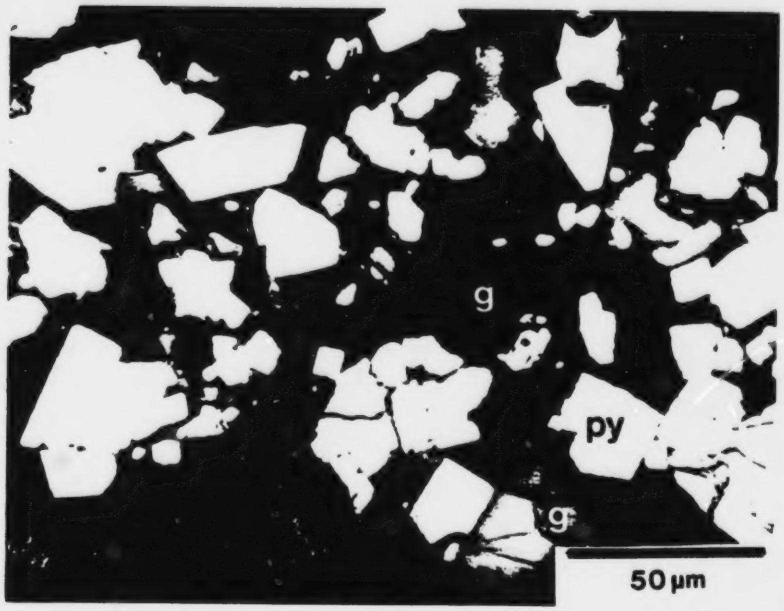

Plate 1 Aggregates of fine-grained pyrite (py) enclosed in gangue (g).

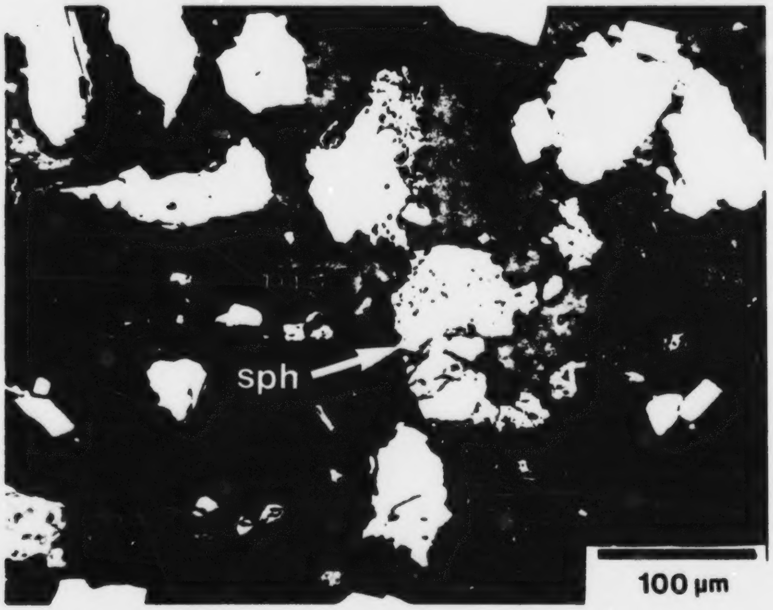

Plate 2 Intergrowth of marcasite (mar) with sphalerite (sph).

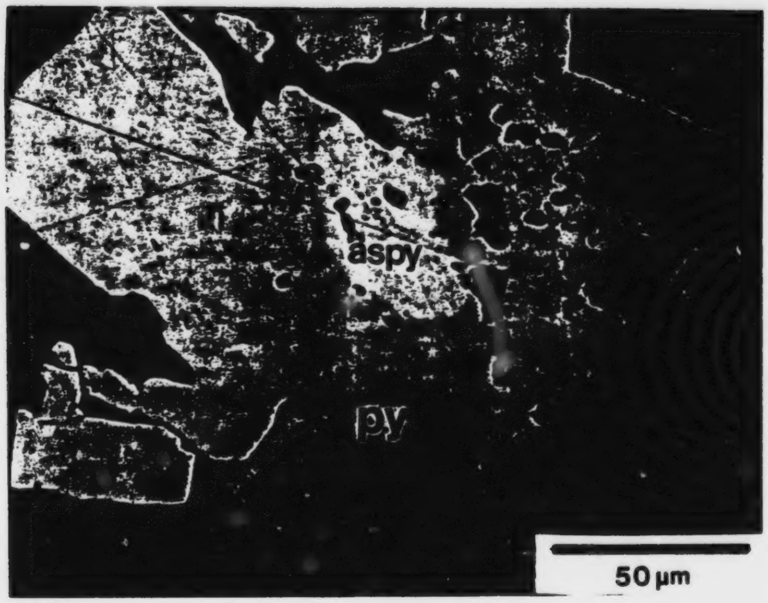
aspy
py
50 µm

Plate 3 Arsenopyrite (aspy) intergrown with pyrite (py).

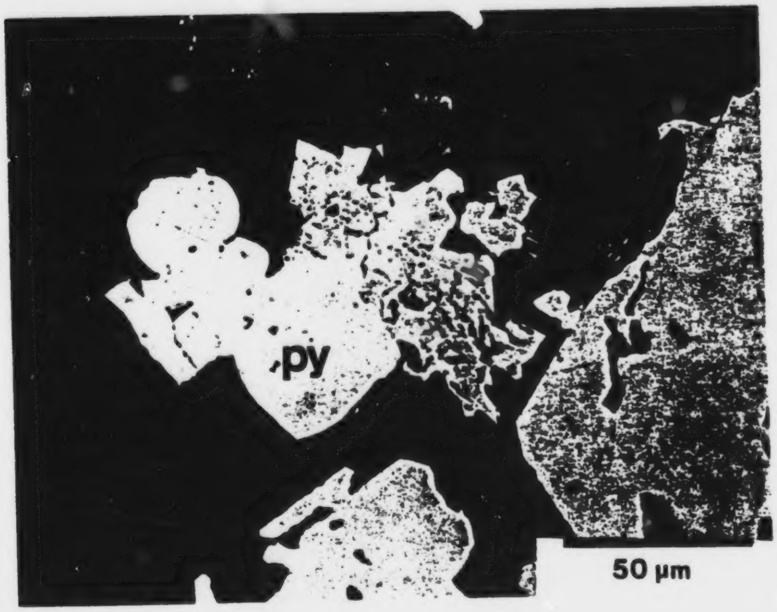

Plate 4 Arsenopyrite (aspy) enclosed within pyrite (py).

sphalerite and galena. Small grains of **tetrahedrite** are associated with both sphalerite and chalcopyrite. **Covellite is found on the surface of chalcopyrite** (Plate 5). **Ataite** (PbTe) inclusions are present within galena (Plate 6).

9.3.2.2 GOLD MINERALOGY

Gold Minerals

Only two small grains of electrum were identified in the composite ore investigated. One grain (size 8 μm²) occurred as an inclusion in pyrite, the other (6 μm²) was present as an inclusion within galena.

In the flotation products, a total of **53** particles of electrum were seen (Appendix A2). In the Cu-Rougher concentrate, 18 of the 21 particles observed, accounting for 99.7 % of the total area were **large liberated particles**, (Plates 7 and 8) with an average size of 225 sq μm². The remaining 3 particles were **enclosed in galena.** In the Cu-Pb separation concentrate, 12 of the 16 grains were liberated, accounting for 97.9 % of the total area. In the Cu 1st cleaner scavenger concentrate, 2 of the 16 grains were liberated, accounting for 85.1 % of the area. The remaining particles were enclosed in galena (1.1 % of area), enclosed in sphalerite (2.5 %), enclosed in pyrite (2 %), enclosed in gangue (9.2 %) and enclosed in tetrahedrite (0.1 %).

The presence of large liberated grains explains the low amount of visible gold observed in the composite ore. A statistical analysis of the population is given in Appendix A2, and the size distribution of the particles is shown as a histogram in Figure 2.

Invisible gold

'Invisible' or sub-microscopic gold is the gold which is below the minimum detection limit of the scanning electron microscope, of 0.1 μm (=1000 Å). The invisible gold is dispersed in the crystal lattice of the host mineral as extremely fine but dicrete inclusions in the size range 50 to 1000 Å, only visible by high resolution transmission electron microscopy, or is in solid solution in the sulphide. Whichever of these two forms the gold is in, it is below the lower size limit of the field of conventional cyanidation.

In the Estrades ore, pyrite, chalcopyrite, marcasite and arsenopyrite were analyzed with the ion microprobe. Due to charging, it was not possible to analyze sphalerite grains. Sphalerite is a major component of the Estrades ores.

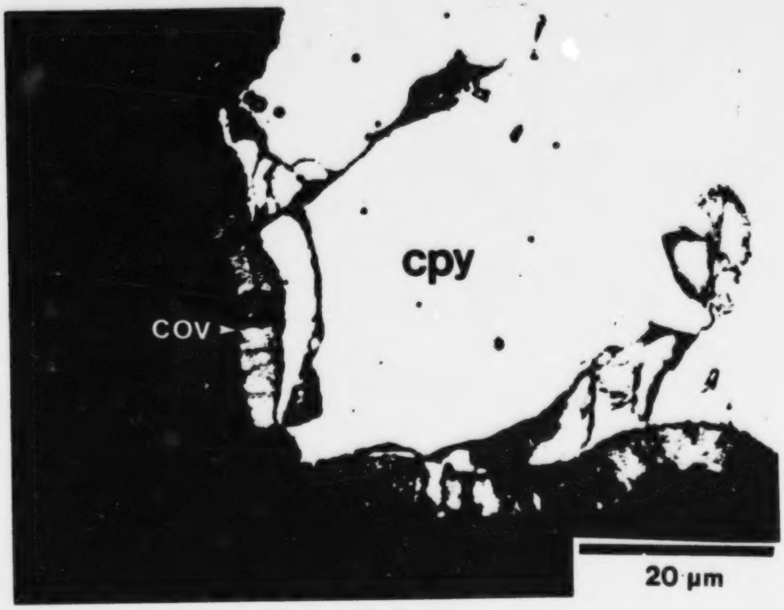
cpy
cov
20 µm

Plate 5 Chalcopyrite (cpy) coated by covellite (cov).

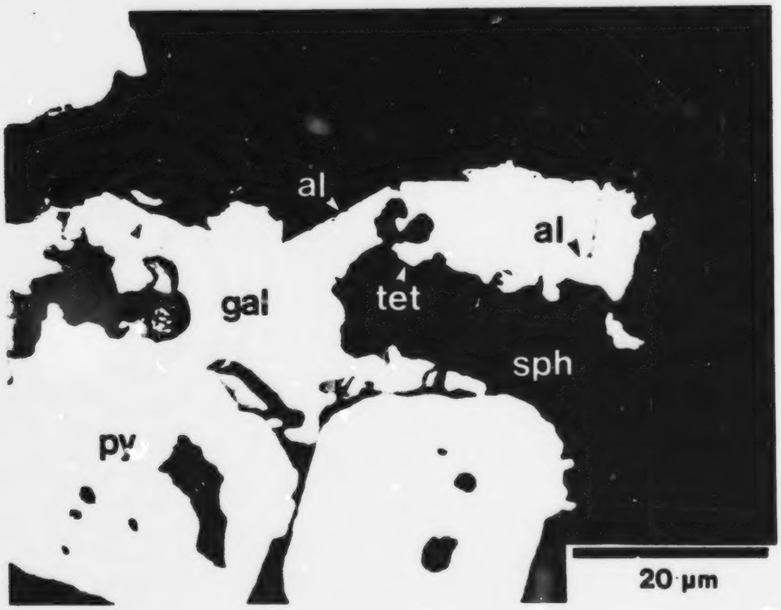
al
al
gal
tet
sph
py
20 µm

Plate 6 Association of galena (gal) and sphalerite (sph). The galena has inclusions of altaite (al). Tetrahedrite (tet) is enclosed in the sphalerite.

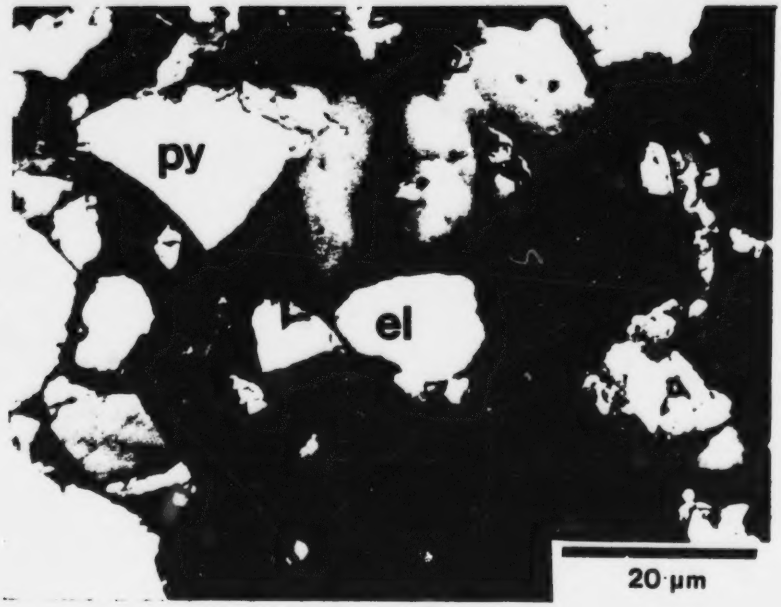

Plate 7 Liberated grain of electrum (el).

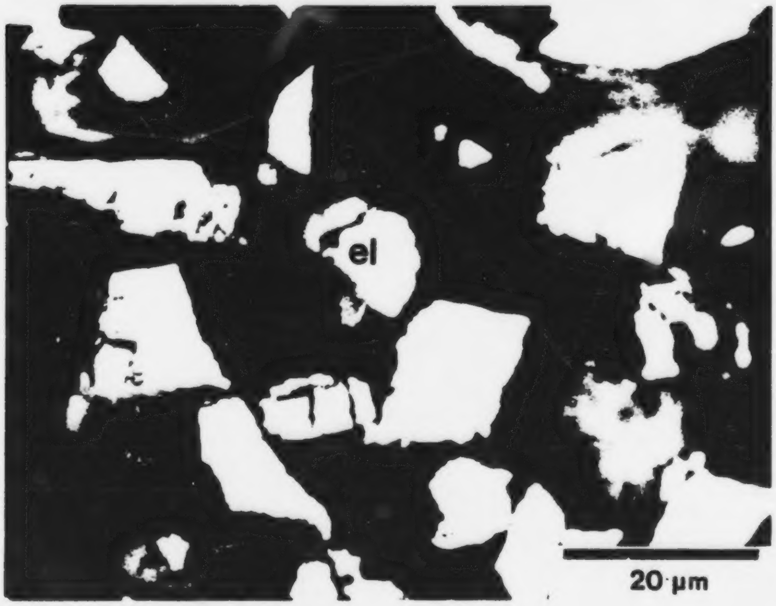

Plate 8 Liberated grain of electrum (el).

FIGURE 2

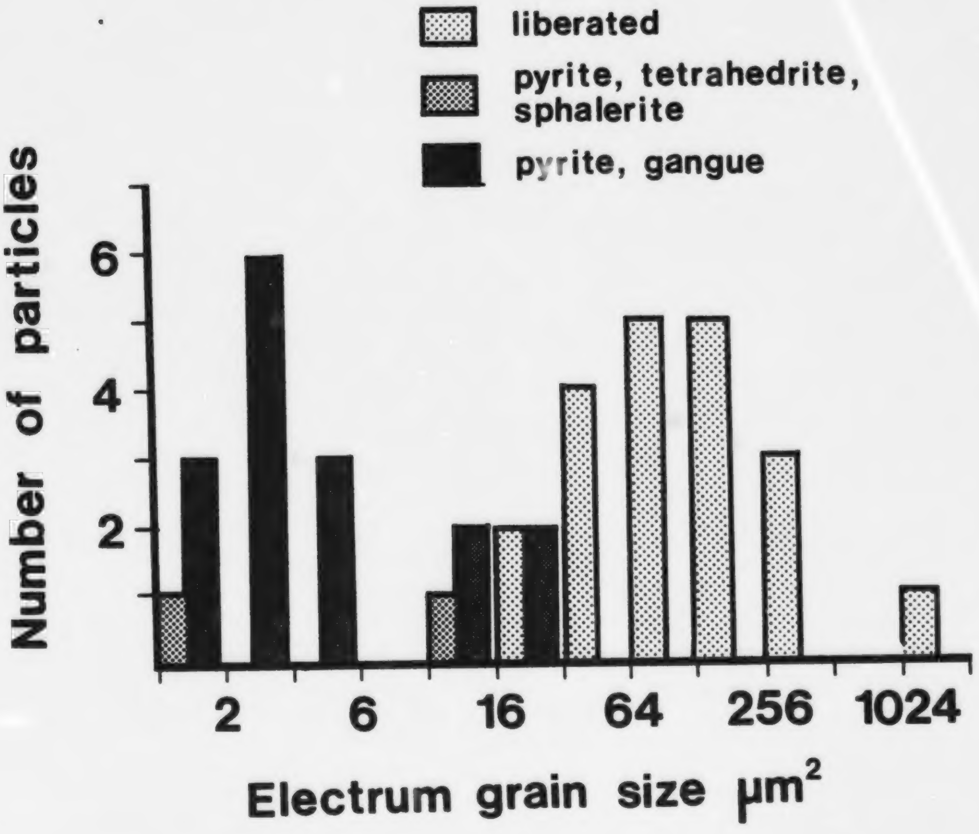
liberated
pyrite, tetrahedrite, sphalerite
pyrite, gangue
Number of particles
6
4
2
2
6
16
64
256
1024
Electrum grain size μm²

The average concentration of gold in 59 **pyrite** particles, as determined by ion probe microanalysis was 0.67 parts per million (g/t), with a confidence interval of 0.53 g/t at a 95% significance level. This means that in 95 out of 100 cases, the average gold content of pyrite would be in the range from 0.14 to 1.20 g/t. Measured gold concentrations were in the range from less than the minimum detection limit (0.3 ppm) to 12.0 g/t. Only two pyrite particles with gold concentrations in excess of 5 g/t were determined. These particles are included in the average above. The mean concentration of gold in pyrite, if these two particles are ignored is 0.33 ± 0.20 g/t. The small aggregated pyrite contained higher concentrations of gold.

The average concentration of gold in 10 **arsenopyrite** particles was **54.** ± 36. ppm. Measured concentrations ranged from less than the minimum detection limit (0.2 ppm) up to 170 ppm.

The average concentration of gold in 12 **chalcopyrite** particles was 0.13 ± 0.09 ppm. The average gold concentration in 18 **marcasite** grains was 0.91 ± 0.55 ppm. Concentrations ranged from 0.1 up to 4.1 ppm. Two galena particles contained 0.2 and 0.4 ppm, and a tetrahedrite particle had gold below the minimum detection limit (0.2 ppm). The distribution of gold in solid solution within pyrite, arsenopyrite, marcasite, and chalcopyrite (Table 4) and is shown as a series of histograms in Figure 3.

9.4.0 DISCUSSION

Cyanidation testing has shown that approximately 81-86% of the total gold in the head sample of Estrades ore is recoverable by direct cyanidation, and that finer grinding will not increase the recovery. The cyanidation data indicated that most of the gold is coarse-grained. Although the amount of visible gold seen in the ore samples was low, presumably due to the nugget effect, the amount of visible gold seen in the flotation products is in accordance with the conclusion that 80% of the total gold is as visible grains, and that some 95% of the visible gold is as large grains of greater than 100 μm^2 in size.

The remainder of the gold is invisible within the sulphide minerals. The concentrations of invisible gold in pyrite and arsenopyrite have been determined to be 0.67 g/t and 54. g/t respectively. The invisible gold in pyrite accounts for **8.9%** of the head assay and the invisible gold in arsenopyrite accounts for **5.6%**. The contribution of chalcopyrite and marcasite is negligible (totalling 0.6%). Invisible gold in pyrite, arsenopyrite, chalcopyrite and marcasite accounts for 15.1% of the head assay. With 81.4% of the gold recoverable by direct cyanidation after pulverisation, the unaccounted gold is 3.5% (Figure 1).

FIGURE 3

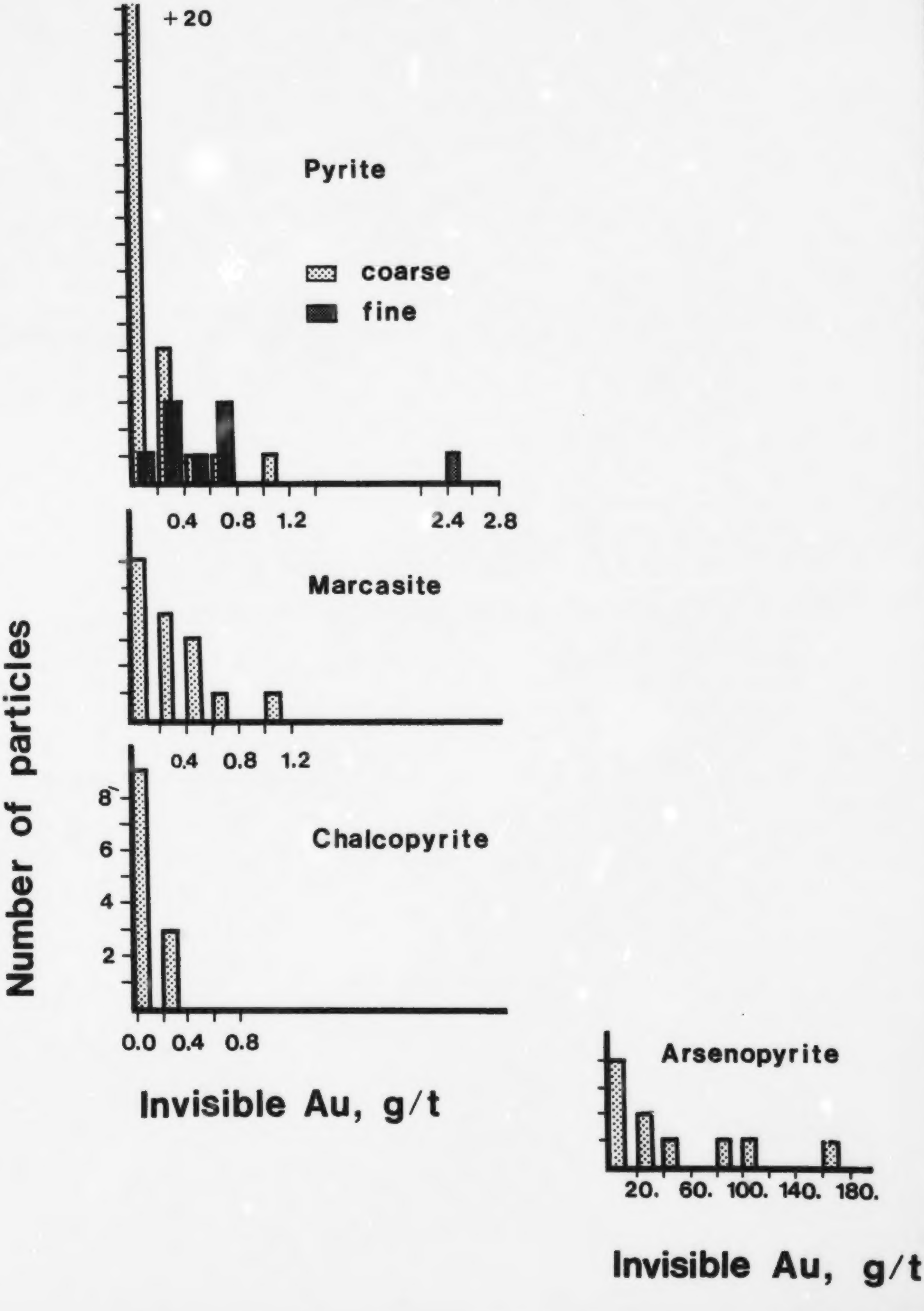
+20
Pyrite
coarse
fine
0.4
0.8
1.2
2.4
2.8
Marcasite
0.4
0.8
1.2
Chalcopyrite
8
6
4
2
0.0
0.4
0.8
Number of particles
Invisible Au, g/t
Arsenopyrite
20.
60.
100.
140.
180.
Invisible Au, g/t

Table 4

INVISIBLE GOLD CONCENTRATION IN SULPHIDES
(Estrades deposit, Teck)

Pyrite

particle #	Au, g/t	particle #	Au, g/t
1	1.1	48	0.0 <MDL
2	0.0 <MDL	49	0.0 <MDL
3	0.6	50	0.0 <MDL
4	0.1 <MDL	51	0.0 <MDL
5	0.6	54	0.2 <MDL
6	0.0 <MDL	55	0.0 <MDL
7	0.0 <MDL	58	0.0 <MDL
11	0.0 <MDL	59	0.0 <MDL
13	0.0 <MDL	60	0.0 <MDL
16	0.0 <MDL	61	0.3
18	0.0 <MDL	62	0.2 <MDL
19	0.0 <MDL	63	0.2 <MDL
20	0.0 <MDL	64	0.0 <MDL
21	0.1 <MDL	68s	0.3
28	0.0 <MDL	69s	0.7
29	0.0 <MDL	76s	0.4
30s	2.5	77s	0.3
32	0.2 <MDL	78s	0.5
33	0.0 <MDL	80	0.4
36	0.0 <MDL	82	0.2 <MDL
37	0.2 <MDL	83s	9.1
38s	0.8	84	0.0 <MDL
39	0.0 <MDL	85	0.3
41s	4.2	92	0.0 <MDL
42	0.0 <MDL	97s	0.8
42	0.0 <MDL	96s	0.2 <MDL
43	0.0 <MDL	97	0.0 <MDL
44	0.0 <MDL	103s	2.9
46	0.0 <MDL	104s	12.0
47	0.0 <MDL		

N: 59

x ± λ: 0.67 ± 0.53

Arsenopyrite

particle #	Au, g/t
17	120.
34	40.
35	170.
45	96.
52	0.0 <MDL
70m	17.
79m	6.0
86	0.9
89m	57.
91m	29.

N : 10

x ± λ: 54. ± 36.

Chalcopyrite

particle #	Au, g/t
8	0.0 <MDL
9	0.0 <MDL
10	0.1 <MDL
14	0.0 <MDL
15	0.0 <MDL
22	0.1 <MDL
25	0.3
26	0.4
27	0.4
56	0.0 <MDL
57	0.0 <MDL
65	0.2 <MDL

N: 12

x ± λ : 0.13 ± 0.09

Marcasite

particle #	Au, g/t	particle #	Au, g/t
12	0.1 <MDL	88	2.9
66	0.6	90	0.4
67	0.6	93	0.9
71	0.4	94	0.8
72	0.1 <MDL	99	4.1
74	0.1 <MDL	98	0.2
75	0.2 <MDL	100	1.1
81	0.3	101	3.1
87	0.4	102	0.1 <MDL

N: 18

x ± λ: 0.91 ± 0.55

Galena

particle #	Au, g/t
40	0.4
73	0.2

Tetrahedrite

particle #	Au, g/t
53	0.0 <MDL

---

s: aggregate of small pyrite crystals, Plate 3.
m: associated with marcasite, Plate 4.

9.5.0 CONCLUSIONS

On average, 81.4% of the gold in the composite 4-C is recoverable by direct cyanidation. Optical examination of a Cu-Pb concentrate has shown that 95% of the visible gold is liberated and coarse-grained, greater than 100 μm^2 in size. The remaining 5% of the visible gold is fine-grained, associated with galena, pyrite and gangue.

The remaining gold in the composite is accounted for by the invisible gold, within the crystal lattice of pyrite and arsenopyrite. Concentrations of invisible gold in these minerals are 0.67 g/t and 54. g/t respectively. Invisible gold in pyrite accounts for 8.9% of the gold head assay in the composite and invisible gold in the arsenopyrite accounts for 5.6 ± 3.9 % of the total gold. A total of 96.5 ± 11.5 % of the gold in the composite 4-C was accounted.

APPENDIX A1

RESULTS OF SIEVE TESTING AND HEAVY LIQUID SEPARATION

FRACTION	MASS SPLIT %	SINK	FLOAT
-53 µm	5.8	4.4 (75.0%)	1.4 (25.0%)
53 - 90 µm	5.2	3.7 (72.0%)	1.5 (28.0%)
90 - 300 µm	14.1	10.2 (72.0%)	3.9 (28.0%)
300 - 560 µm	9.4	6.5 (69.2%)	2.9 (30.8%)
+ 560 µm	65.5		
Total	100.0		

APPENDIX A2

ELECTRUM GRAINS IDENTIFIED IN FLOTATION PRODUCTS

APPENDIX A2

ELECTRUM GRAINS IDENTIFIED

A) Copper Rougher Concentrate, 105 g/t Au

Grain	Association	Size (μm^2)
1	Liberated	500
2	"	130
3	"	50
4	"	20
5	"	100
6	"	30
7	"	160
8	"	60
9	"	60
10	"	110
11	"	60
12	"	100
13	"	120
14	"	350
15	"	115
16	"	250
17	"	200
18	"	1700
19	Enclosed in galena	1
20	"	3
21	"	10

B) Cu-Pb Separation, 48 g/t Au

Grain	Association	Size (µm^2
1	Liberated	295
2	"	265
3	"	190
4	"	40
5	"	25
6	"	30
7	"	360
8	"	140
9	"	60
10	"	160
11	"	240
12	"	85
13	Combined with oxides	280
14	Enclosed in pyrite	18
15	Combined with pyrite	25
16	Enclosed in gangue	4

C) 1st Copper Cleaner Scavenger concentrate, 17 g/t Au

Grain	Association	Size (μm^2)
1	Liberated	280
2	"	240
3	Enclosed in galena	1
4	"	5
5	"	1
6	Enclosed in tetrahedrite	1
7	Enclosed in sphalerite	15
8	Enclosed in pyrite	2
9	"	8
10	Combined with pyrite	2
11	Enclosed in gangue	25
12	"	5
13	"	3
14	"	3
15	"	2
16	Combined with gangue	18

APPENDIX A2

MINERALOGICAL DISTRIBUTION OF ELECTRUM GRAINS

	Cu-Ro conc	Cu-Pb sepn	Cu 1st ClScCo
Number of grains	21	16	16
Total area (μm^2)	4069	2217	611
Au assay (g/t)	105	48	17
Liberated			
# of grains	18	13[1]	2
% of total area	99.7	97.9	85.1
Galena association			
# of grains	3	0	3
% of total area	0.3	-	1.1
Tetrahedrite association			
# of grains	0	0	1
% of total area	-	-	0.1
Sphalerite association			
# of grains	0	0	1
% of total area	_	_	2.5
Pyrite association			
# of grians	0	2	3
% of total area	-	1.9	2.0
Gangue association			
# of grains	0	1	6
% of total area	_	0.2	9.2

(1) one grain, composite with oxides

Liberated grains, average size

$x = 206\ \mu m^2 \pm 102$
$N = 33$

Galena, tetrahedrite, sphalerite association
average size

$x = 5\ \mu m^2 \pm 4$
$N = 8$

Pyrite, gangue association, average size

$x = 10\ \mu m^2 \pm 5$
$N = 12$

APPENDIX A3

IMAGE ANALYSIS OF HEAVY FRACTION

Number of areas measured: 8

Total area measured: 173.2 mm^2

Total number of grains: 2140

Area covered by grains: 577.8 mm^2 (27%)

Proportions of minerals:

Mineral	# of grains	area	Proportion		Relative
		mm^2	volume %	wt. %	Error (%)
Pyrite	1281	339.5	57.0 ± 1.7	64.2 ± 1.9	3
Sphalerite	434	115.6	20.0 ± 2.4	18.5 ± 2.2	12
Chalcopyrite	83	26.0	4.5 ± 0.5	4.3 ± 0.5	10
Galena	30	3.9	0.7 ± 0.6	1.2 ± 1.0	90
Marcasite	36	7.8	1.4 ± 0.7	1.5 ± 0.8	48
Tetrahedrite	1	1.2	0.2 ± 0.4	0.3 ± 0.5	195
Total Sulphide	1865	494.0	83.3 -	-	-
Gangue	275	83.8	16.2 -	-	-
Total	2140	577.8	100. -	-	-

CHAPTER 10

DIRECT DETERMINATION OF THE INVISIBLE GOLD AND COMPLETE MINERALOGICAL DISTRIBUTION IN THE MASSIVE SULPHIDE ORE FROM KETZA RIVER (Y.T.)

SSW/PMS/88/09

SUMMARY

Native gold, with 7.5% silver, is the only gold mineral in the Ketza River massive sulphide ore. The average gold grain size is 32 µm². 97.6% of the gold grains fall into the size range of less than 1 µm² to 256 µm². Native gold associated with arsenopyrite tends to be finer grained and enclosed, while the gold associated with pyrrhotite is coarser and to a great extent is combined. Native gold accounts for 75% of the gold head assay (Figure 1).

Arsenopyrite is the principal gold-bearing mineral in the sulphide ore, concentrating most of the invisible gold. The concentration of the solid solution gold in the arsenopyrite is 11.9 ± 2.2 g/t. The gold enrichment ratio relative to pyrrhotite is 24. The invisible gold in the arsenopyrite accounts for 19.2% of the gold head assay (Figure 1, Table 1).

Sixty eight percent of the gold in the Ketza River massive sulphide ore is recoverable by direct cyanidation at a relatively coarse grind (K_{80} = 150 mesh). From the thirty two percent of the gold that reported to the cyanide leach residue, nineteen percent is in solid solution in the arsenopyrite, and six percent is in the form of very fine inclusions of gold (< 20 µm²) in the arsenopyrite. Concentration of the arsenopyrite from the cyanide leach residue will enhance the gold recovery by an additional twenty to twenty five percent, leading to overall gold recoveries in the range from 88 to 93 percent in the massive sulphide ore.

TABLE 1

GOLD MINERALOGICAL DISTRIBUTION

	Au (g/t)	Au (%)	precision
Head (calculated)	13.0	100.0	
Visible Au			
In arsenopyrite[1]	4.5 ± 2.1	34.6	± 16.1
In pyrrhotite[2]	4.1 ± 5.0	31.5	± 38.4
Invisible gold			
In arsenopyrite (21 wt %)[3]	11.9 ± 2.2	19.2	± 4.5
In pyrrhotite (71 wt %)[3]	0.48 ± 0.18	2.6	± 1.0
In pyrite (2 wt %)[3]	2.3 ± 0.96	0.4	± 0.17
Unaccounted gold		11.7	

---

[1] Including chalcopyrite, pyrite, marcasite and liberated gold.

[2] Including gangue minerals, bismuthinite.

[3] Normalised to 100%.

Cyanide test results

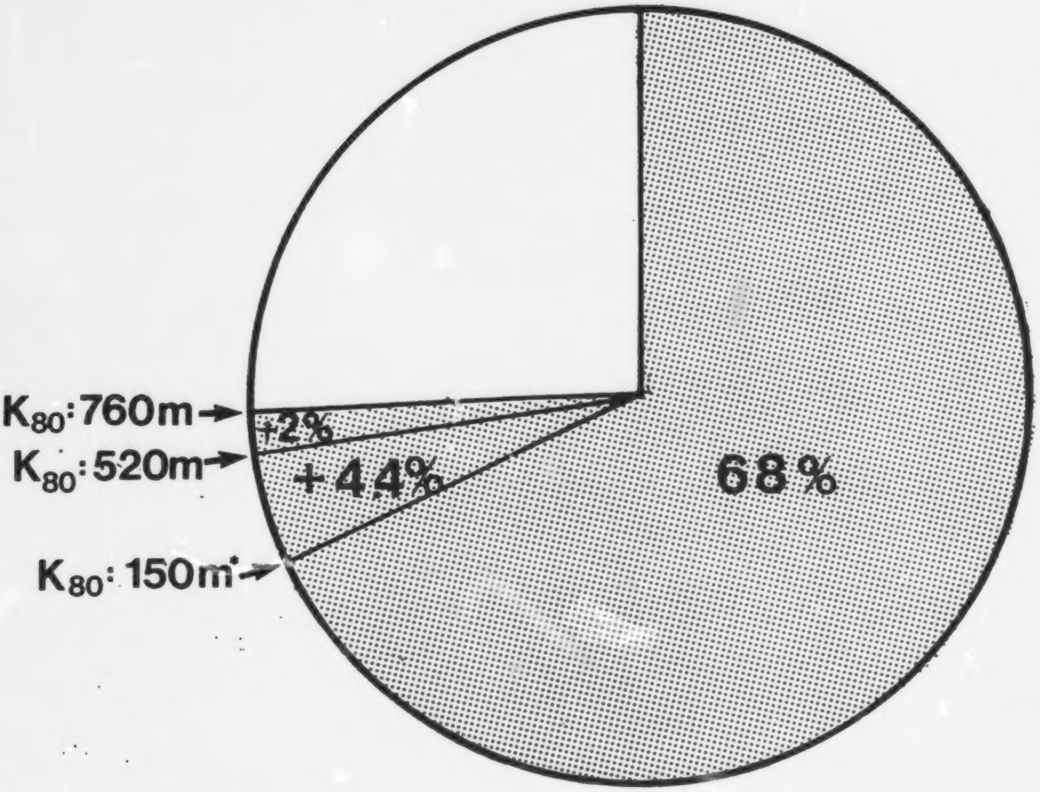

*Tyler Mesh

33% solids

1g/t NaCN

pH 10.5-11

48 hours

FIGURE 1

MINERALOGICAL DISTRIBUTION OF GOLD

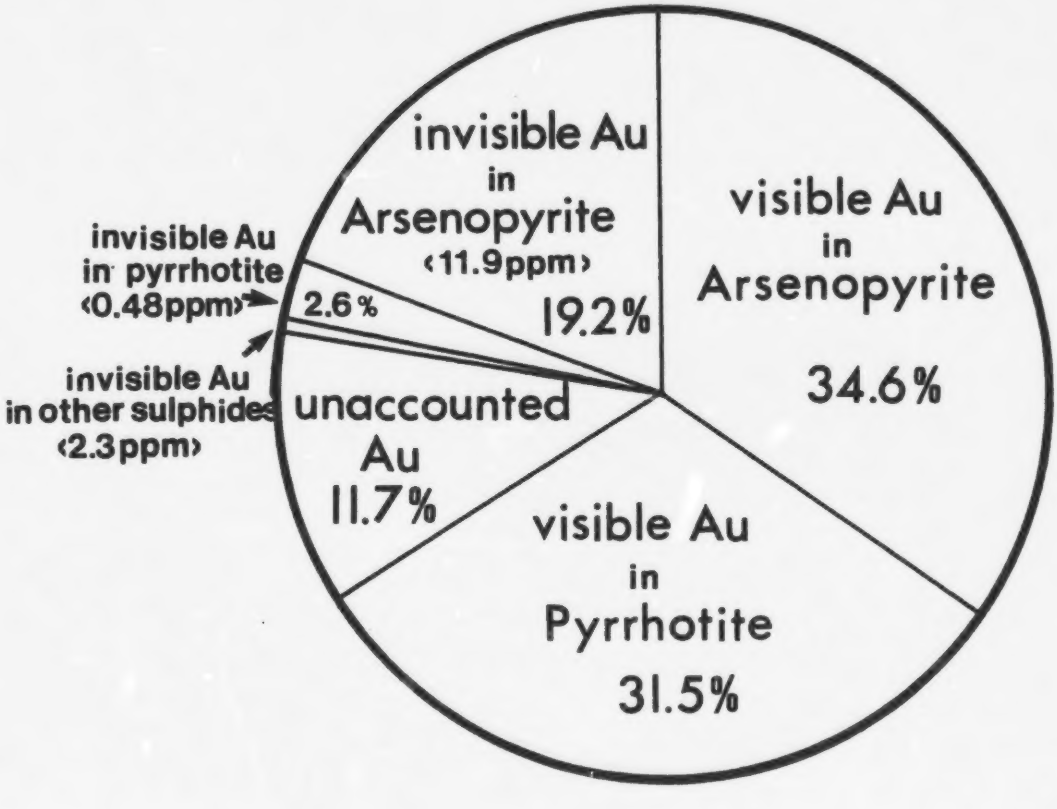

LIST OF TABLES

Table 1 Gold mineralogical distribution

Table 2 Composite massive sulphide ore assays

Table 3 Direct cyanidation results

Table 4 Statistical analysis of gold grains (by mode)

Table 5 Statistical analysis of gold grains (by area)

Table 6 Silver concentration in native gold

Table 7 Pyrrhotite compositions

Table 8 Magnetic separation results

LIST OF FIGURES

Figure 1 Gold mineralogical distribution

Figure 2 Size distribution of native gold

Figure 3 Distribution of invisible gold in arsenopyrite

Figure 4 Distribution of invisible gold in pyrrhotite

Figure 5 Mineral association and particle size of native gold

Figure 6 Relative proportions of native gold grouped by size and mineralogical distribution

Figure 7 Size distribution of enclosed and combined gold

APPENDICES

A1 Image analysis of native gold

A2 Calculation of invisible gold

A3 Ion microprobe data for gold in sulphides

A4 Flotation test results

A5 Magnetic separation results

A6 Assays of magnetic separation fractions

10.1.0 INTRODUCTION

A five kilogram composite sample of the massive sulphide ore from Ketza River Y.T. was sent by J. Toohey, project geologist of CANAMAX Resources Inc. in order to determine quantitatively the gold dissolved in the crystal lattice of the major sulphides, pyrrhotite and arsenopyrite. The objective of this study is to provide a complete mineralogical balance for gold that can be used to establish strategies for the most efficient recovery of the gold from the sulphide ore.

The auriferous sulphide ore in the Ketza River ore field is stratabound within a limestone horizon. Numerous sulphide ore bodies have been identified in the horizon and all have similar characteristics. The sulphides typically account for 50 to 60% of the ore by mode and are coarse-grained. The major sulphides are pyrrhotite and arsenopyrite, in the ratio 4:1. Minor sulphides include pyrite, marcasite and chalcopyrite. Native gold with minor silver (Chryssoulis, 1986) is the only gold mineral that was identified in the sulphide ore. The main sulphide ore body has a grade of 11.9 ± 2.2 g/t gold. Exploitation of the sulphide ore is crucial to the long term viability of the mine because of the large tonnages involved.

Extensive cyanidation testing of the sulphide ore, performed by Lakefield Research in 1986, yielded residues assaying from 0.60 to 7.67 g/t gold (Jackman, 1986, 1987). The gold recoveries were in the range from 38 to 77.3 percent. Because of the moderate gold recovery and the high reagent consumption, (Jackman, 1986, 1987) cyanidation alone is not considered as a viable option for the sulphide ore. At present, only the oxide is leached in a 350 tonnes per day plant. A detailed mineralogical study (Chryssoulis, 1987) of a cyanide leach residue, assaying 4.9 g/t gold revealed only trace amounts of native gold, accounting for only 5% of the lost gold. It was concluded that the remainder had to be in the crystal lattice of the sulphides. The gold is invisible under the optical and electron microscopes. The invisible gold is not recoverable by direct cyanidation. However, if the invisible gold is concentrated in the arsenopyrite it will be possible to enhance the gold recovery.

The final task of this study is to identify the strategies to improve the gold recovery based on the gold mineralogical distribution, the size and association of the native gold. As part of this task, preliminary metallurgical tests were carried out.

This study was financed 50% by CANMET, through an ammendment to the DSS contract #50SS.23440-7-9037, and 50% by CANAMAX Resources Inc.

10.2.0 METHODOLOGY

The composite sample was analyzed for Au, Ag, S, As, Sb, Bi, Te and organic carbon (Table 2).

The crushed composite was sieved into four size fractions: +500 µm, 500-90 µm, and -37 µm. A total of 32 polished blocks from the two intermediate size fractions were prepared for examination under the microscope, image analysis and ion probe microanalysis.

Optical microscopy was used to determine the gold mineral's size and association. The silver content of the native gold was determined by electron probe microanalysis. The invivsible gold in the sulphide minerals was determined by ion probe microanalysis (Chryssoulis, 1987). Pyrrhotite and arsenopyrite, required for the gold mineralogical distribution, were determined from the arsenic assay and the mass split of the sink fraction of a heavy liquid separation test (2.9 $g \cdot cm^{-3}$). This was possible because the pyrrhotite is free of arsenic, and arsenopyrite is the only arsenian mineral in the ore. The other sulphides account for only a few percent of the ore. In the massive sulphide ore the light fraction is mainly quartz and accounts for 6 wt.% of the composite sample.

Cyanide leaching was used to verify the visible gold content of the sulphide ore as measured from optical microscope images, and to determine the effect which grinding has on gold recovery. The K_{80} values in micrometers were 106, 58, 28 and 19 µm, corresponding approximately to the following Tyler mesh sizes: 150, 260, 520, and 760. The tests were done with 30% solids, using 1 g NaCN per tonne of ore. The pH was controlled with lime at 10.5 to 11. The tests lasted 48 hours.

10.3.0 RESULTS

10.3.1 VISIBLE GOLD

Results given in Table 3 indicate that 68% of the gold is recoverable by direct cyanidation at K_{80}: 150 mesh.

TABLE 2

HEAD ASSAYS AND ANALYSES

Au	x_{Au} (direct):	13.73	g/t
		+/- 1.6	g/t
	x_{Au} (calculated):	13.00	g/t
		+/- 0.4	g/t

Ag:	3.7	ppm
S:	32.6	%
As:	10.2	%
Bi:	300	ppm
Sb:	30	ppm
C (organic):	< 0.05	%
Te:	< 3	ppm

TABLE 3

CYANIDE TEST RESULTS

Test No.	K_{80} µm	% Extraction Au	Residue g/t Au	Head g/t Au calc.	Head g/t Au direct
1	105	68.0	4.19	13.2	12.1
2	58	72.9	3.52	13.0	12.6
3	28	72.4	3.68	13.3	15.1
4	19	74.4	3.18	12.4	15.1

Conditions:
33% solids
1 g/t NaCN
pH 10.5 - 11.0
48 hours.

Finer grinding improved recovery only marginally. Seventy four percent of the gold was recovered by pulverizing the sample (K_{80}: 760 mesh).

Native gold is the only gold mineral in the Ketza River sulphide ore, identified during a detailed study of fourteen polished sections. In total, 123 gold grains were identified (Appendix A2). Ninety one gold grains are associated with arsenopyrite (74%), and twenty one are associated with pyrrhotite (17%). Of the remaining 9%, two are liberated, two are enclosed in gangue, five are enclosed in chalcopyrite, one is in pyrite and one gold grain is combined with bismuthinite. Results are summarized in Table 4.

The gold grains associated with arsenopyrite are mostly enclosed and are significantly finer than the gold which is associated with pyrrhotite (Figure 2). In terms of area, the 92 gold grains associated with arsenopyrite account for only a marginally larger fraction of the visible gold (49.6%) when compared to the 21 gold grains associated with the pyrrhotite. The implications of this on the effective gold recovery are discussed in the next section. The results are detailed in Table 5. The area measurement calculations are summarized in Appendix A3.

The average silver content of sixteen gold grains was determined to be 7.5 ± 1.7 weight percent. This compares closely with the average silver content of 7.0 wt.% determined in an earlier study (Chryssoulis, 1986). The minimum and maximum silver content is 3.1 and 13.0 wt.% respectively. Results are presented in Table 6. The light fraction assayed 5.56 g/t gold.

10.3.2 INVISIBLE GOLD

Invisible gold is the gold which is in solid solution in the crystal lattice of the sulphides and is therefore invisible under the optical or electron microscopes. The invisible gold is not recoverable by direct cyanidation and requires prior oxidation of the host sulphide in order to be recovered.

The average gold concentration of 88 arsenopyrite particles as determined with the ion probe, is 11.9 parts per million (g/t) with a confidence interval of 2.2 g/t at a 95% significance level. This means that in 95 out of 100 arsenopyrite particles, the gold concentration will be in the range from 9.7 to 14.1 g/t. The arsenopyrite particles can be clustered into four destinct populations, on the basis of their gold content (Figure 3). The average gold content of the four populations are 5.3 ± 0.8, 13.5 ± 0.8, 23.4 ± 1.7, and 44.3 ± 5.5 g/t respectively.

TABLE 4

STATISTICAL ANALYSIS OF GOLD GRAINS (BY MODE)

Total area of gold observed = 3947 sq µm
+/- 2484 sq µm

Number of gold grains = 123

Number of polished sections studied = 14

Observed visible gold per sample = 282 sq µm
+/- 177 sq µm

= 8.6 ppm
+/- 5.4 ppm

Association	# of grains	% of total
Enclosed in arsenopyrite	72	59
Combined with arsenopyrite	19	15
ASSOCIATED WITH ARSENOPYRITE	91	74
Enclosed in pyrrhotite	14	11
Combined with pyrrhotite	7	6
ASSOCIATED WITH PYRRHOTITE	21	17
Enclosed in chalcopyrite	5	4
Enclosed in pyrite	1	1
Enclosed in gangue	2	2
Liberated	2	2
Combined with bismuthinite	1	1
TOTAL	123	100

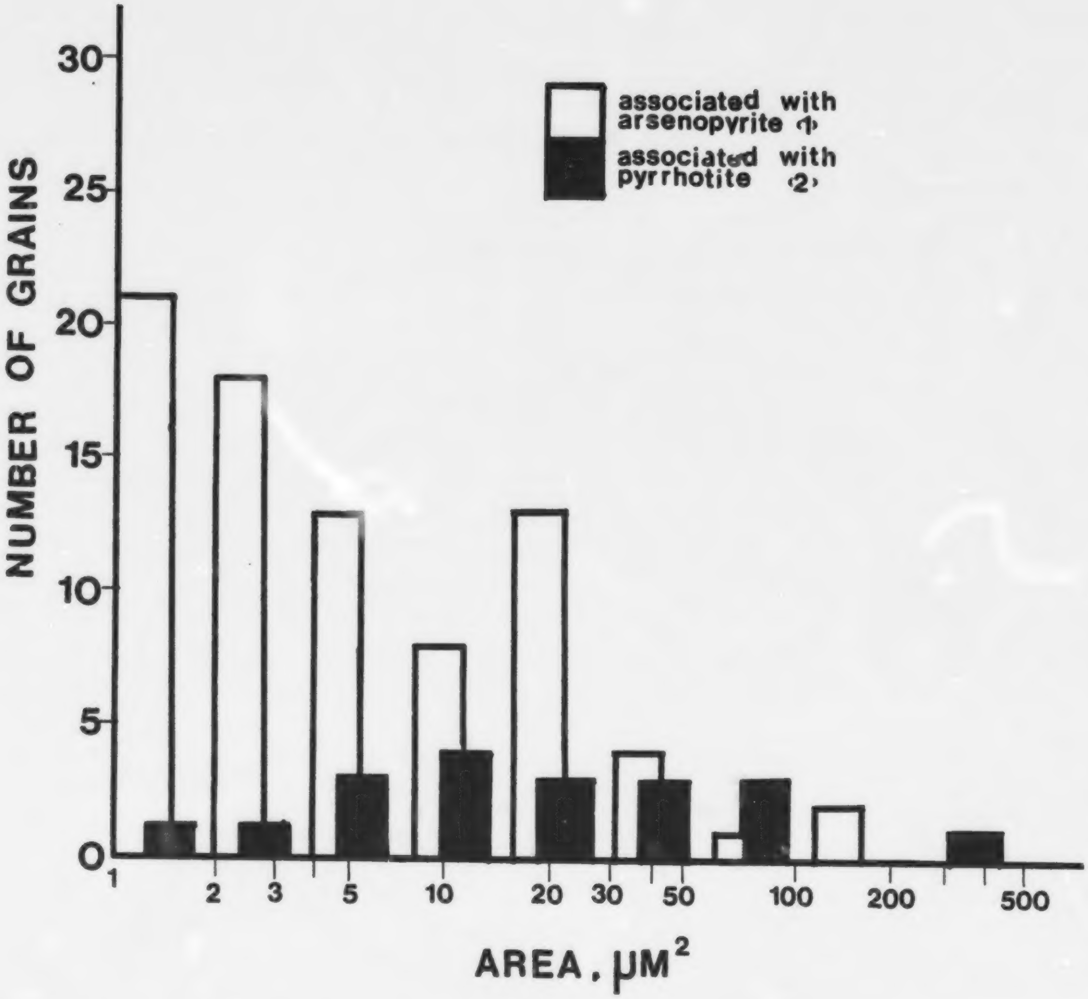

FIGURE 2. Histogram of grain size for gold in the studied samples, divided by mineralogical association.

(1) Also grains enclosed in chalcopyrite, pyrite and liberated grains

(2) Also grains enclosed in gangue and combined with bismuthinite

TABLE 5

STATISTICAL ANALYSIS OF GOLD GRAINS (BY AREA)

		Σ AREA	x	%
1a	Grains enclosed in arsenopyrite	1051	15	26.6
1b	Grains combined with arsenopyrite	905	48	23.0
1	**Grains associated with arsenopyrite**	**1956**	**21**	**49.6**
2	Grains enclosed in chalcopyrite	46	9	1.1
3	Grains enclosed in pyrite	10	10	0.3
4	Liberated	26	13	0.6
A	**Total flotable fraction**	**2038**		**51.6**
5a	Grains enclosed in pyrrhotite	142	10	3.6
5b	Grains combined with pyrrhotite	1722	246	43.6
5	**Grains associated with pyrrhotite**	**1864**	**89**	**47.2**
6	Grains enclosed in gangue	39	19	1.0
7	Combined with bismuthinite	6	6	0.2
B	**Total non-flotable fraction**	**1909**		**48.4**
	GRAND TOTAL	**3947**	**32**	**100.0**
		(σ=	112)	
		(λ=	20)	

$$\lambda = \frac{2\sigma}{\sqrt{N}}$$

TABLE 6

ELECTRON PROBE MICROANALYSIS OF ELECTRUM PARTICLES

		WEIGHT %		
Grain no.		Au	Ag	Total
1		94.41	5.59	100*
2		96.16	3.84	100*
3		91.89	8.11	100*
4		93.01	6.99	100*
5		94.98	3.11	98.69
6		93.09	6.91	100*
7		96.33	3.59	99.92
12		94.05	10.12	104.17
18		83.68	11.81	95.94
75	x (n=3)	95.32	4.49	99.81
92		94.07	3.39	97.47
93		91.66	8.34	100*
94		87.04	12.96	100*
95		92.49	7.51	100*
111	x (n=10)	87.48	11.78	99.26
112	x (n= 9)	87.95	11.82	99.77
Mean		92.1 ± 1.8	7.5 ± 1.7	99.6
STANDARDS:				
Au (100% Au)		100.43	0.06	100.49
Ag (100% Ag)		0.00	100.06	100.06

* = Normalized to 100%. Totals less than 95% due to small size of particle analysed.

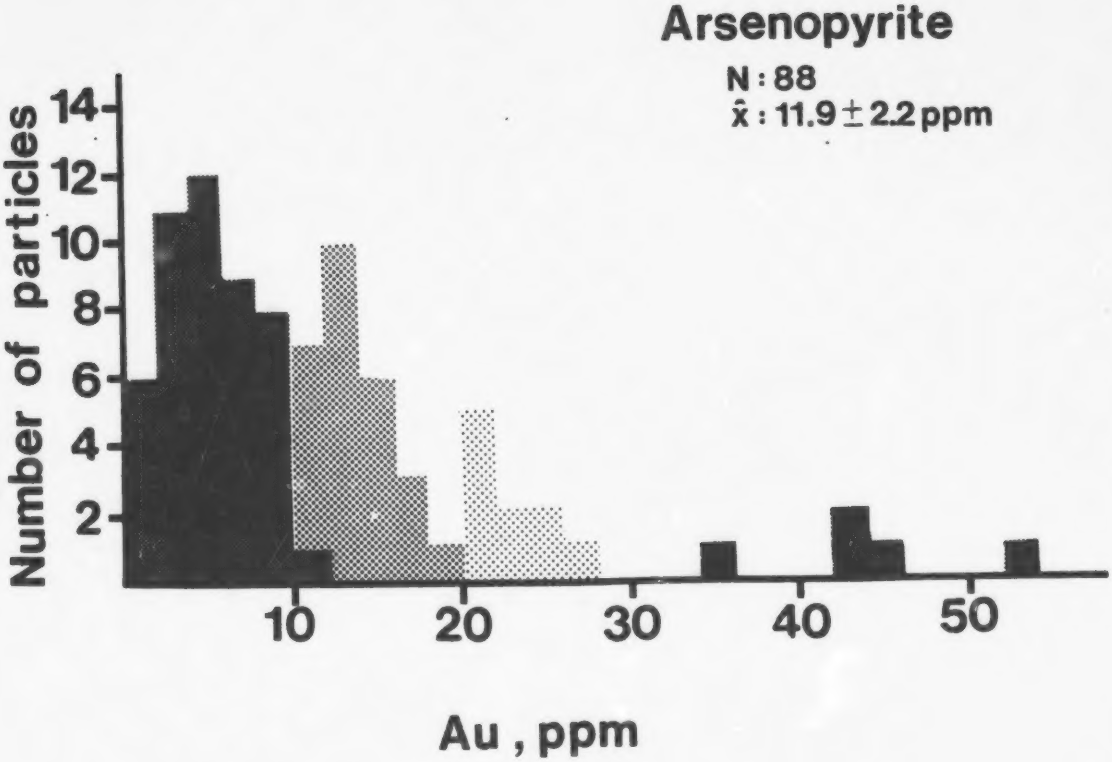

FIGURE 3. Histogram showing the gold in solid solution in arsenopyrite particles, as determined by ion probe microanalysis.

The gold content of the pyrrhotite is significantly lower (Figure 4). The average gold content of 25 pyrrhotite particle analyzed with the ion probe is 0.48 parts per million (g/t) with a confidence interval of 0.18 g/t gold. This indicates that 95 out of 100 pyrrhotite particles will have gold contents within the range from 0.30 to 0.60 g/t. Only three of the pyrrhotite particles had gold concentrations exceeding 1 g/t.

The average gold concentration of three chalcopyrite particles was 2.4 ± 0.9 g/t gold. The average gold concentration of five pyrite and marcasite particles was 2.1 ± 1.6 g/t. The ion probe data, together with representative in-depth gold concentration profiles are included in Appendix A4.

10.4.0 DISCUSSION

Any metallurgical scheme used to optimize the recovery of the gold from the Ketza River sulphide must take into consideration: (i) the gold mineralogical distribution; (ii) the size and; (iii) the association of the gold minerals and gold-bearing minerals. Consideration of these factors will enable effective bench-scale metallurgical test programs to be outlined. This will reduce the cost of the metallurgical testing by eliminating schemes which will not give good gold recoveries.

Both pyrrhotite and arsenopyrite, the major sulphide minerals in the Ketza River sulphide ore, are coarse-grianed. Thus, they can be liberated from each other at a relatively coarse grind, K_{80} = 100 - 150 mesh. A series of cyanidation tests indicated that 68% of the gold recoverable at a coarse grind (K_{80} = 150 mesh) and that further grinding has a limited effect on increasing gold recovery. Pulverization of the sample (K_{80} = 760 mesh) gave a gold recovery of 74.4% which is only 6.4% higher than that of the coarse grind. The amount of native gold determined by image analysis, 66%, when precision is taken into consideration, compares closely with the cyanidation results (Table 1 and Figure 1). Native gold is recoverable by direct cyanidation.

A size analysis of the native gold grains indicated that most of the fine-grianed gold (less than 20 square micrometers in area) is enclosed (60%) or combined (15%) with arsenopyrite (Figure 5). On the contrary, 70% of the coarse-grained gold (more than 100 square micrometers in area) is combined with pyrrhotite (Figure 5). Pyrrhotite comminutes easier than arsenopyrite, thus exposing the

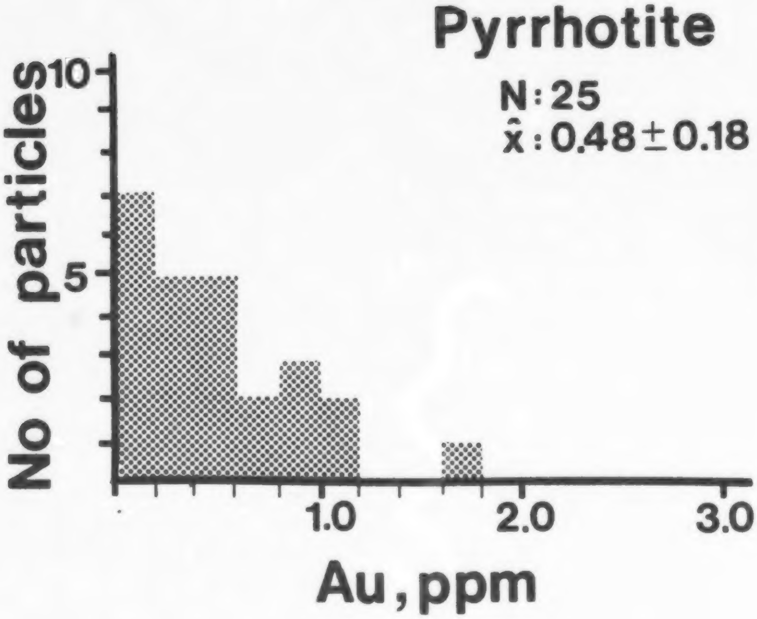

FIGURE 4. Histogram showing the gold in solid solution in pyrrhotite particles, as determined by ion probe microanalysis.

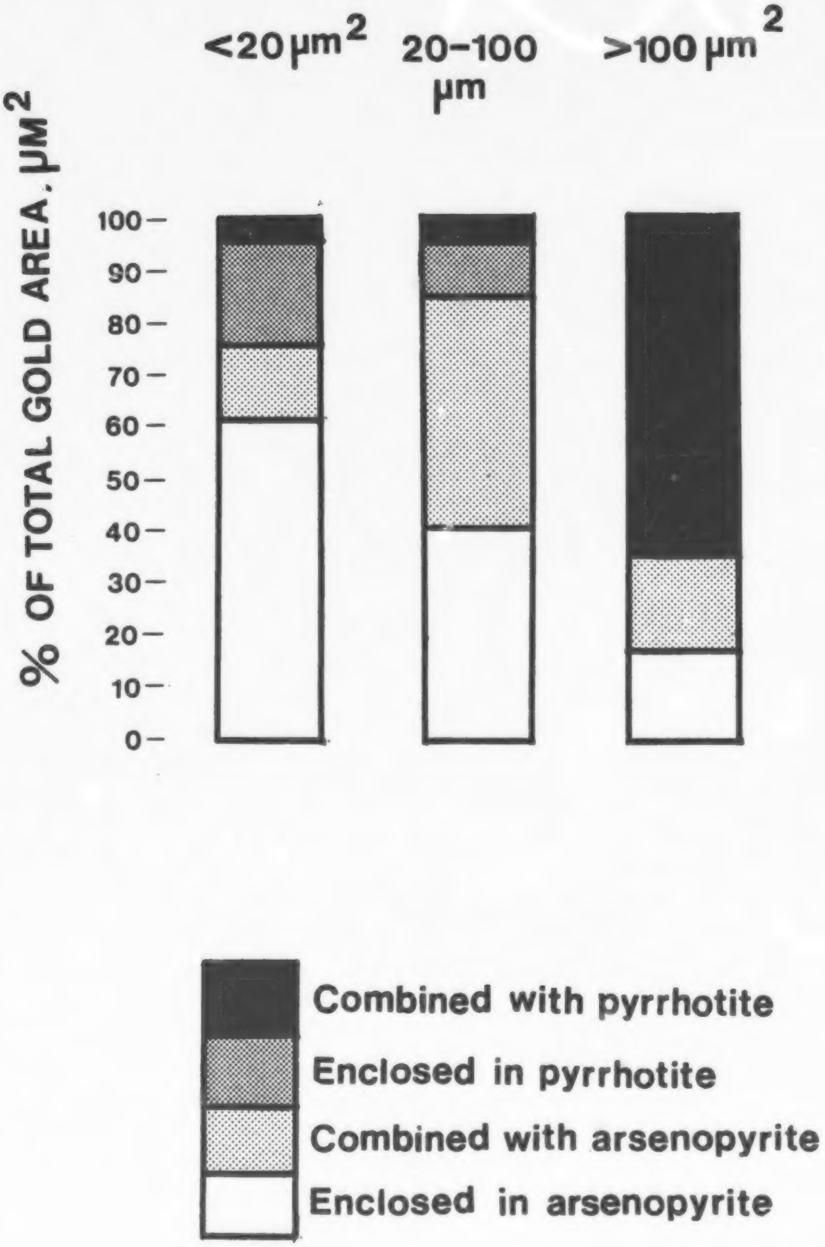

FIGURE 5. Diagram showing proportions of visible gold grains in different mineralogical associations at three size fractions, as a percentage of the total area of visible gold in that size fraction.

associated, mostly intercrystalline(1), coarser grained gold. On the contrary, the relatively harder to grind arsenopyrite retains its enclosed finer gold grains. Therefore, with a coarse grind the coarser gold which is mostly associated with pyrrhotite, becomes exposed or liberated while much of the finer grained gold remains enclosed in the arsenopyrite (Figure 6).

Image analysis of the visible gold in the head sample and the cyanide leach residue (Chryssoulis, 1987) demonstrated that the gold reported to the leach residue is not native gold. The cyanidation of a pulverized sample confirmed this conclusion. Therefore, part of the gold had to be in the form which is not recoverable by direct cyanidation. The lack of organic carbon precluded the possibility of preg-robbing.

The invisible gold, i.e. the gold in solid solution in the crystal lattice of the sulphide minerals in the Ketza River ore, is concentrated preferentially in the arsenopyrite. The average gold concentration of the arsenopyrte is 11.9 g/t and that of the pyrrhotite is 0.48 g/t. Therefore, gold has been enriched in the arsenopyrite by a factor of 24. The arsenopyrite is four times less abundant than the pyrrhotite. The pyrrhotite accounts for approximately 80% of the sulphide minerals in the ore.

The complete gold mineralogical balance for the Ketza River sulphide ore is depicted in the form of a pie diagram in Figure 1. Superimposed (transparent overlay) are the results of direct cyanidation tests conducted on the composite ore sample, at progressively finer grinds. Direct measurements with the ion microprobe, of the gold locked in the crystal lattice of the sulphides, determined that 22.1% of the gold head assay is actually in the form of invisible gold. This figure compares closely with the gold content of the cyanide leach residue, 25.4%, as the invisible gold is not amenable to direct cyanidation. This information, if it had been available at an earlier stage, could have saved considerable time and money spent in trying to improve the gold recovery by direct cyanidation. The unaccounted gold in the mineralogical distribution is 11.7%, part of which is native gold and the rest is believed to be in finer grained gold-rich arsenopyrite (Table 5).

The light fraction in the massive sulphide ore is composed mostly of quartz, and assays 5.56 g/t Au. However, it contributes only 2.6% towards the gold mineralogical distribution because it accounts for 6 wt.% of

---

(1) Intercrystalline gold: gold between pyrrhotite particles

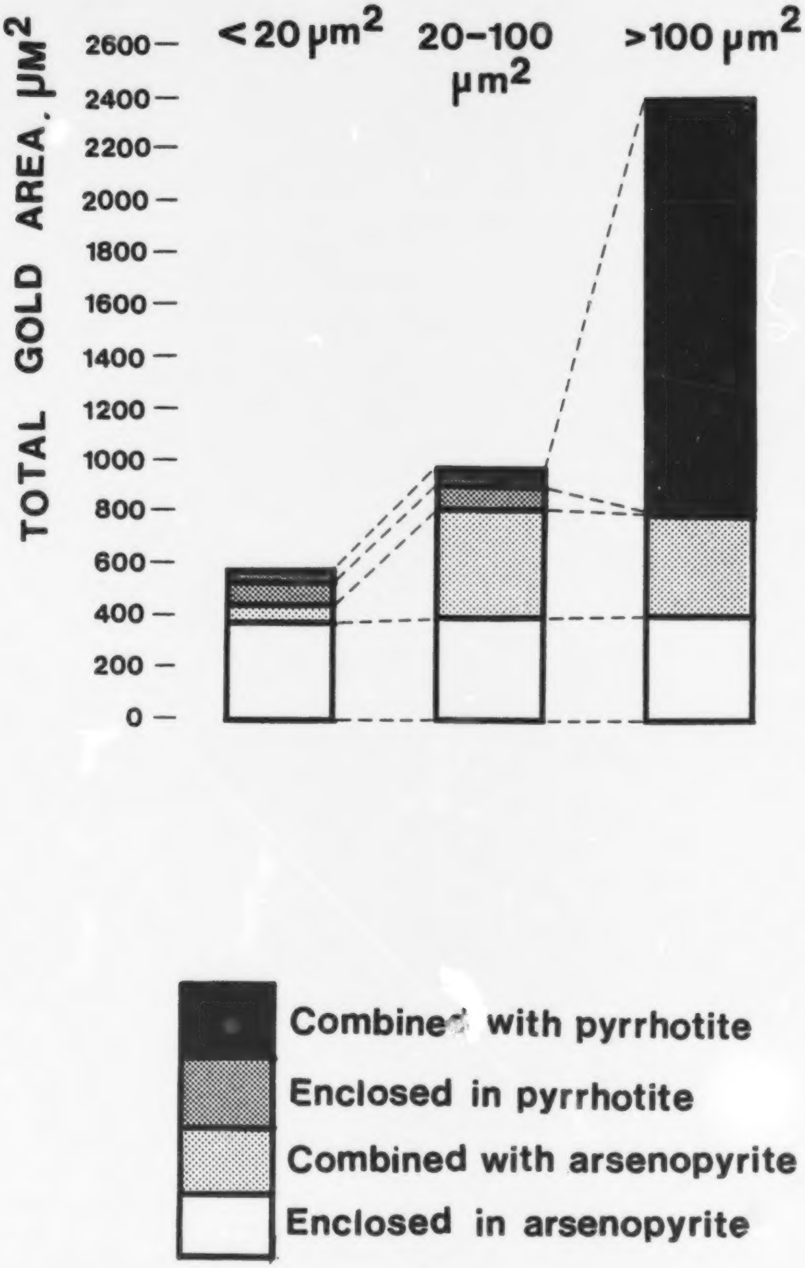

FIGURE 6. Diagram showing proportions of visible gold grains in different mineralogical associations at three size fractions, as a proportion of the total area of visible gold observed in the sample.

the ore. This 2.6% is part of the 11.7% of the unaccounted gold.

Almost fifty four percent of the gold in the Ketza River ore is associated with the arsenopyrite, 19.2% is in the form of invisible gold and 6.6% is as in fine inclusions of native gold (Figure 6). Both forms are not recoverable by direct cyanidation. On the other hand, most of the visible coarser gold is with the pyrrhotite which contains only trace amounts of invisible gold.

Based on this distribution of the gold in the Ketza River ore, preliminary metallurgical tests were carried out with the objective of producing arsenopyrite concentrates by froth flotation and magnetic separation. The tests ideally should be done on the cyanide leach residue, but because of anticipated problems it was decided to undertake the preliminary tests on the head sample.

The separation of the arsenopyrite from the pyrrhotite by flotation is achieved by selectively depressing the pyrrhotite. This was done by briefly preaerating the pulp using soda ash to control the pH at 10. The arsenopyrite was activated with copper and floated in a rougher concentrate, which was cleaned once to produce a cleaner concentrate. Conditions and flotation results are given in Appendix A5. The concentrate of the best test assayed 31.4 g/t gold, and contained 96.6% of the arsenic and 83.7% of the total gold. The rougher tails assayed 2.60 g/t gold. The concentrate represented 34.8% of the total weight, which indicates that a significant fraction of the pyrrhotite had also floated. Ideally, the arsenopyrite concentrate should represent 20 wt.% of the head. The flotation of the pyrrhotite is not attributed to poor liberation (K_{80} = 150 mesh), but to the presence of a pyrrhotite which is not readily depressed. The Ketza River pyrrhotite is sulphur-rich, which probably less readily oxidized. There is also an indication that the pyrrhotite associated with gold has an even higher sulphur content (Table 7), and therefore could be reporting to the rougher concentrate.

The separation of the pyrrhotite from the arsenopyrite by magnetic separation was tested using the Frantz Isomagnetic separator. Conditions and results are given in Appendix A6. To determine the effect which particle liberation may have on the magnetic separation, three size fractions were tested. Results summarized in Table 8 indicate a small improvement on the gold grade of the non-magnetic fraction with finer size, while keeping the mass split of the non-magnetic fraction at less than 20% of the head. The non-magnetic portion of the 70- 170 mesh size fraction assayed 35.8 g/t gold and 30.09 wt.% arsenic. The calculated gold assay, after correcting for the mostly

TABLE 7

ELECTRON PROBE MICROANALYSIS OF PYRRHOTITE GRAINS

BARREN Po

		Wt. % S	N
Grain	#1	39.39 ± 0.13	10
	#2	39.09 ± 0.12	10
	#3	39.29 ± 0.13	10
	#4	39.35 ± 0.08	10
	#5	39.25 ± 0.15	10
	#6	39.10 ± 0.16	10
	#7	39.72 ± 0.23	9
	#8	39.27 ± 0.13	10
	#9	39.65 ± 0.11	10
	#10	39.44 ± 0.19	9
	#11	39.64 ± 0.13	10
	#12	39.48 ± 0.17	10
	#13	39.52 ± 0.13	9
	#14	39.56 ± 0.11	10
	#15	39.43 ± 0.10	10
	$\Sigma\ \bar{x}$	39.41 ± 0.10	(147)

GOLD-BEARING Po

		Wt. % S	N
Grain	#101	40.01 ± 0.19	10
	#102	39.58 ± 0.15	9
	#103	39.61 ± 0.16	10
	#104	39.59 ± 0.18	10
	$\Sigma\ \bar{x}$	39.70 ± 0.21	(39)

SUMMARY

Type	Wt % S	N
Barren (No Gold)	39.41 ±0.10	147
With Gold Inclusions	39.70 ±0.21	39
FeS Standard (36.5 % S)	36.50 ±0.13	15

quartz gangue (6 wt.%, 5.56 g/t Au) which reports to the non-magnetic fraction, is 55.5 g/t gold. Magnetic separation of the finest size fraction (170 -270 mesh) was not successful because of the small sample tested.

The arsenopyrite concentrate produced by flotation is comparable to the non-magnetic fraction in terms of gold grade, but, the proportion of total gold recovered in the flotation concentrate is twice as high. However, the mass split of the concentrate produced by froth flotation is double that of the non-magnetic fraction. By removing the gangue from the non-magnetic fraction, an arsenopyrite concentrate can be produced, with a calculated gold assay of 55.5 g/t.

Preliminary electron probe data on the composition of the pyrhotite associated with gold indicate that this pyrrhotite is more sulphur-rich. The sulphur-rich pyrrhotite is more magnetic (Palache, 1944) and less readily oxidizable. This would explain why the magnetic portion of the 70 to 170 mesh size fraction has a higher gold assay (8.8 g/t) compared to the rougher tails of the sample ground to K_{80} = 150 mesh (2.6 g/t).

10.5.0 CONCLUSIONS

On the process mineralogy of gold:

Native gold is the only gold mineral in the Ketza River sulphide ore. It is relatively poor in silver, containing 7.5 ± 1.7 wt.% Ag. The average size of the gold grains is 32 μm^2, with 97.6% of the grains falling in the size range from < 1 μm^2 to 256 μm^2. Most of the finer grained gold tends to be enclosed in the arsenopyrite, while the coarser grained gold is combined with chalcopyrite, which is present in only minor amounts. Native gold accounts for almost 75% of the gold head assay. Native gold can be recovered by direct cyanidation when it is exposed.

Arsenopyrite is the principal gold-bearing sulphide mineral in the ore, containing most of the invisible gold. The gold concentration in the arsenopyrite is 11.9 ± 2.0 g/t. The gold enrichment ratio relative to pyrrhotite is 24. The invisible gold gold in the arsenopyrite accounts for 19.2% of the gold head assay. Therefore, arsenopyrite is the second gold-carrier mineral, after native gold. Native gold and arsenopyrite together account for approximately 95% of the gold in the Ketza River ore. The invisible gold is not recoverable by direct cyanidation.

Pyrrhotite is the most abundant mineral in the massive sulphide ore. The relative ratio of pyrrhotite to arsenopyrite is 4/1. The invisible gold in the pyrrhotite lattice is only 2.6% of the head assay. Chalcopyrite concentrates invisible gold to some extent (2.6 g/t). but since it is present only in trace amounts its contribution to the gold mineralogical balance is insignificant.

On the gold recovery:

Sixty eight percent of the gold in the massive sulphide ore is recoverable by direct cyanidation at a coarse grind, K_{80} = 150 mesh. Further grinding increased the gold recovery only marginally. A pulverized sample, K_{80} = 760 mesh, gave a gold recovery of 74.4%. The gold which is recoverable from a coarser grind is the coarser grained native gold which is associated preferentially with the pyrrhotite. Since pyrrhotite communites easier than arsenopyrite during grinding, the native gold associated with pyrrhotite is prefferentially leached during cyanidation.

The gold reporting to the cyanide leach residue (32%) includes the invisible gold in the arsenopyrite (19.2%), pyrrhotite (2.6%) and the fine-grained native gold enclosed in the arsenopyrite (6.6%). Therefore, the enhancement of the gold recovery from the massive sulphide ore is the challenge of producing an arsenopyrite concentrate to which approximately 25% of the gold head assay will report. Thus, gold recoveries in the range from 88 to 85% could be achieved.

The arsenopyrite concentrate produced from the concentrate ore by froth flotation assayed 31.4 g/t gold with 96.6% of the arsenic and 83.7% of the gold reporting to the concentrate. The mass split of the concentrate was rather high (34.8%) because of the flotation of a pyrrhotite fraction which is, presumably, not readily depressed.

The arsenopyrite concentrate produced by magnetic separation assayed 36.8 g/t gold with 69% of the arsenic and only 45% of the gold reporting to the concentrate. The mass split of the non-magnetic fraction was 15.9% of which approximately 38% is gangue, mainly quartz. The calculated gold assay of the arsenopyrite concentrate corrected for the gangue is 55.5 g/t gold.

TABLE 8 MAGNETIC SEPARATION TESTS

	Mass Split	Au Assay (g/t)	% Distribution Au
200-500 µm			
Head (Calc)	100	12.57	100
Magnetic fraction	75.3	9.46	54
Intermediate frac.	6.3	9.95	5
Non-magnetic frac.	18.4	28.10	41
200-90 µm			
Head (calc.)	100	12.96	100
Magnetic fraction	74.9	8.08	42
Intermediate frac.	12.2	13.40	13
Non-magnetic frac. (aspy and gangue)	15.9	36.80	45
Non-magnetic frac. (aspy conc, calc.)	9.9	55.50	45
90-53 µm			
Head (calc.)	100		
Magnetic fraction	57.7	6.31	29
Intermediate frac.	9.3	-	(29)
Non-magnetic frac.	33.0	16.2	42

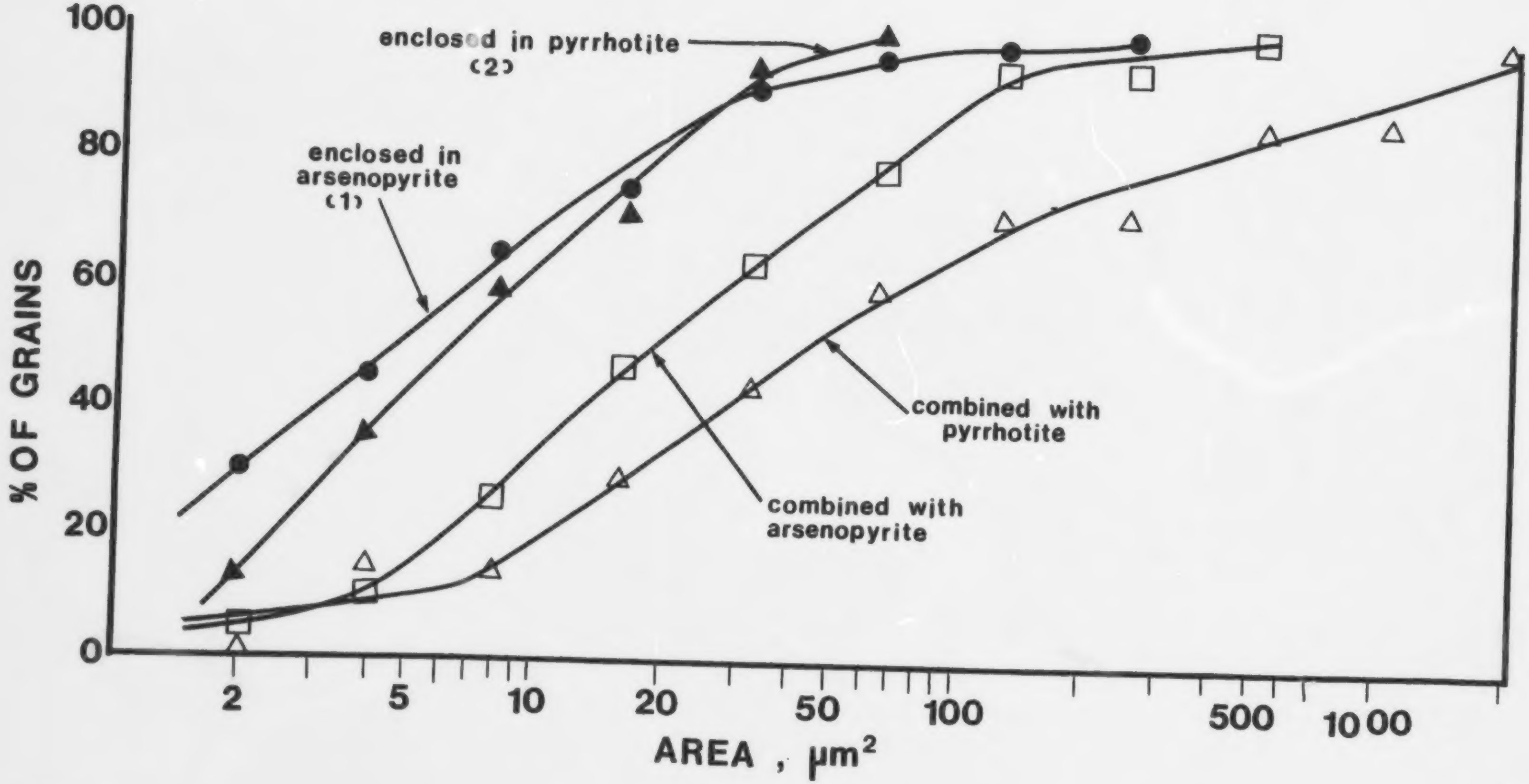

FIGURE 7. Cumulative frquency diagram for grains of visible gold, grouped by mineralogical association.

(1) Also grains enclosed in pyrite, chalcopyrite and liberated grains.

(2) Also grains enclosed in gangue and combined with bismuthinite.

APPENDIX A2

CALCULATION OF INVISIBLE GOLD

APPENDIX

GOLD GRAINS OBSERVED IN THE POLISHED SECTIONS STUDIED

Enclosed in arsenopyrite:

Grain	Size (μm^2)
1	29
2	5
3	6
4	33
5	12
6	11
7	11
8	1
9	22
10	2
11	1
12	1
13	10
14	5
15	1
16	1
17	2
18	34
19	4
20	1
21	2
22	1
23	32
24	6
25	2
26	1
27	1
28	18
29	16
30	26
31	7
32	2
33	1
34	3
35	2
36	2
37	20
38	19
39	2
40	5
41	41
42	1
43	24
44	5
45	3
46	10
47	2
48	110
49	1
50	8
51	5
52	25
53	4
54	30
55	7
56	5
57	5
58	1
59	3
60	1
61	15
62	4
63	5
64	4
65	2
66	40
67	2
68	18
69	5
70	1
71	140
72	160

APPENDIX (continued)

GOLD GRAINS OBSERVED IN THE POLISHED SECTIONS STUDIED

Grain	Size (μm^2)
Combined with arsenopyrite:	
73	76
74	36
75	86
76	45
77	6
78	69
79	31
80	17
81	10
82	9
83	3
84	5
85	400
86	45
87	10
88	2
89	10
90	35
91	10
Enclosed in pyrrhotite:	
92	47
93	17
94	4
95	1
96	13
97	1
98	11
99	7
100	6
101	3
102	4
103	3
104	5
105	20

Grain	Size (μm^2)
Combined with pyrrhotite:	
106	9
107	3
108	18
109	38
110	102
111	446
112	1106
Enclosed in gangue:	
113	20
114	19
Enclosed in pyrite:	
115	10
Enclosed in chalcopyrite:	
116	6
117	5
118	2
119	28
120	5
Liberated:	
121	18
122	8
Combined with BiS_2:	
123	5

APPENDIX

CALCULATION OF VISIBLE GOLD IN THE STUDIED SAMPLES

Total area studied: (14 x 4.91 cm^{2}) = 68.74 cm^{2}

Coverage of sample = 24.5 %
(determined by point counting) +/- 2.1 %

Total sample area covered = 16.84 cm^{2}

Total sample weight (unit depth; 10^{-4}
cm, av. spec. grav., 4.90 g.cm^{-3}) = 82.52 x 10^{-4} g
(est. 80% Po, 20% Aspy)

Total gold area = 3947 µm^{2}

+/- 2484 µm^{2}

= 394.4 x 10^{-8} cm^{2}

Average gold content of grains (1) = 93 %

Total gold weight (unit depth; 10^{-4}
cm, av. spec. grav.; 19.3 g.cm^{-3}) = 7.1 x 10^{-8} g

Total gold concentration relative to
sulphide = 8.6 ppm

+/- 5.4 ppm

'Visible' gold = 8.6 ppm

+/- 5.4 ppm

(1) From previous report

APPENDIX A3

ION MICROPROBE DATA FOR GOLD IN SULPHIDES

Invisible gold in arsenopyrite

Particle #	Au (ppm)	Particle #	Au (ppm)	Particle #	Au (ppm)
3	13.	48	20.5	102	11.2
4	46.	49	4.8	103	9.2
5	13.	50	6.8	104	10.1
6	5.9	51	14.6	105	1.3
7	21.	52	2.1	106	1.8
8	17.	53	12.9	110	11.4
9	18.	54	5.7	111	7.9
12	5.	55	22.3	112	7.1
13	14.5	56	10.1	113	21.7
14	2.3	57	42.7	114	36.0
15	12.5	58	5.0	115	4.6
16	1.8	59	11.7	116	1.3
17	14.5	60	25.3	117	20.0
18	13.	61	4.2	118	13.0
19	16.	63	13.6	120	8.2
21	5.8	64	10.5		
22	3.5	65	7.9		
24	2.1	66	4.9		
27	18.	67	4.2		
28	2.9	68	3.4		
29	4.8	69	14.5		
30	2.2	70	21.9		
31	8.5	75	6.0		
32	10.	76	26.7		
33	25.3	85	28.8		
34	6.7	90	44.0		
37	7.0	92	3.3		
38	6.7	93	8.5		
39	9.6	94	24.2		
40	11.8	95	12.6		
42	6.9	96	4.1		
43	11.3	97	13.3		
44	13.6	98	9.0		
45	25.3	99	3.8		
46	2.	100	2.4		
47	12.2	101	0.8		

x ± λ : 11.93 ± 2.05 ppm

Invisible gold in pyrrhotite, chalcopyrite, pyrite and marcasite

Particle #	Au (ppm)	Particle #	Au (ppm)
Pyrrhotite		Chalcopyrite	
1	0.33	2	3.3
10	0.50	107	1.9
11	0.00	108	2.0
23	0.00	x ± λ :	2.4 ± 0.9
25	0.00		
26	0.23		
35	1.10		
36	0.62	Pyrite	
41	0.22		
62	0.19		
71	0.63	20	1.2
74	0.25	72	2.7
77	0.52	73	5.0
78	1.01		
80	0.84		
81	0.98		
82	0.30	Marcasite	
83	0.13		
84	0.59		
86	0.89	108	1.0
87	1.7	x ± λ :	2.5 ± 1.8
88	0.48		
89	0.45		
119	0.00		
120	0.00		
x ± λ :	0.48 ± 0.18 ppm		

APPENDIX A4

FLOTATION TEST RESULTS

#	K_{80} (µm)	Product	Wt %	Assays			% Distribution		
				Au g/t	As %	S %	Au	As	S
6	70	Cl. conc	6.7	26.8	3.88	35.6	14.8	3.1	8.2
		Ro conc	23.1	16.6	7.27	34.3	31.6	20.0	27.1
		Scav conc	22.6	11.4	3.67	32.5	21.3	9.8	25.1
		Scav Tail	54.3	10.5	10.90	25.7	47.1	70.2	47.8
		Head (calc)		12.1	8.43	29.2			
7	147	Cl. conc (non-mag)	4.8	26.8	19.9	27.1	9.9	9.8	4.5
		Cl. conc (mag)	0.8	44.0	22.7	27.0	2.7	1.9	0.7
		Cl conc	5.6	29.3	20.3	27.1	12.6	11.7	5.2
		Ro conc	33.9	33.6	27.0	26.2	87.3	93.7	30.4
		Scav conc	11.7	10.3	3.99	32.4	4.2	4.8	13.0
		Scav tail	54.4	0.82	0.28	30.4	3.5	1.5	56.6
		Head (calc)		13.0	9.77	29.2			
8	100?	Cl conc (non-mag)	34.2	31.4	31.7	27.7	82.1	95.2	32.0
		Cl conc (mag)	0.6	33.7	26.6	27.0	1.6	1.4	0.5
		Cl conc	34.8	31.4	31.6	27.7	83.7	96.6	32.5
		Ro conc	46.0	25.4	24.1	29.7	89.3	47.5	46.2
		Scav conc	9.5	5.97	1.58	34.6	4.3	1.3	11.1
		Scav Tail	44.5	1.89	0.30	28.4	6.4	1.2	42.7
		Head (calc)		13.1	11.4	29.6			

APPENDIX A5

MAGNETIC SEPARATION TESTS

#	Size fraction	Weight	Distribution	Assays		% Distribution	
		(g)	%	Au (g/t)	As (%)	Au	As
	200-500 µm						
1	head			9.10			
	(calc. head)			12.57		100	100
2	Magnetic	126.4	75.3	9.46	5.34	54	39
3	Intermediate	10.5	6.3	9.95	9.30	5	5
4	Non-magnetic	30.9	18.4	28.10	31.50	41	56
5	magnetic (dupl.)			8.53			
	200-90 µm						
6	head			12.4			
	(calc. head)			12.96		100	100
7	Magnetic	133.6	74.9	8.08	3.55	42	32
8	Intermediate	22.6	12.2	13.4	5.01	13	8
9	Non-magnetic (aspy & quartz)	29.5	15.9	36.80	30.09	45	60
	aspy conc (calc)		9.9	55.50	48.33	45	60
10	Magnetic (dupl.)			7.15			
	90-53 µm						
	(calc. head)			12.77			
11	Magnetic	21.7	57.7	6.31	1.99	29	
12	Intermediate	3.5	9.3	-		29	
13	Non-magnetic	12.4	33.0	16.2	11.40 (double checked)	42	
14	Light fraction (float at SG:3)	13.7		5.56			

APPENDIX A6

ASSAYS OF MAGNETIC SEPARATION FRACTIONS

(37 - 500 µm Size fraction)

	Mass Split (wt. %)	Au (g/t)	As (wt.%)	Fe (wt.%)	apy (wt%)	po (wt%)	recovery (%)	Au in apy (g/t)	Au in apy (%)	Au in po* (g/t)	Au in po* (%)	visible Au** (g/t)	visible Au** (%)	visible Au Measured g/t	CN- recoverable Au (g/t)	CN- recoverable Au (%)
Head (Sink Fraction)	100	12.3	8.20		17.8	80.8		2.1	17	0.4	3	9.3	80			
Head		13.0	10.20		22.2			2.6	20					8.6 (66%)	10.2	74.4
Magnetic fraction (Hand Magnet)	76	6.6, 6.7	3.03, 3.07		6.6		43	0.8	11	0.5	8	5.4	81			
Intermediate Fraction (Frantz Isomagnetic Separator, 0.8 A)	10	13.1	7.50		16.3		11	2.0	15	0.4	3	10.7	82			
Non-magnetic fraction	14	38.6	37.60	34.3	81.7	13.5	46	9.8	25	0.0	0	28.8	75			
Calculated head		(11.77)						(2.18)	18	(0.42)	4	(9.17)	78			
Difference		-0.53						+0.08		+0.02		-0.63				

---

* assuming po = 100 - aspy

** visible Au = $Au_{total} - (Au_{aspy} + Au_{po})$

CHAPTER 11

POROCESS MINERALOGICAL STUDY OF THE PEEL ZONE HIGH GRADE AND AB COMPOSITES AND THE LAB ZONE COMPOSITE FROM THE KETZA RIVER MINE, YUKON TERRITORIES.

SSW/PMS/89/06

SUMMARY

Three composite samples, representative of potential sulphide mill feed from the Ketza River property were examined in order to determine the mineralogical distribution of gold. In particular, the invisible gold concentration in the arsenopyrite was measured in a high grade composite from the Peel zone (25 g/t Au), a moderate grade composite from the Peel zone (11.0 g/t Au) and a representative composite from the LAB zone (11.8 g/t Au).

The principal gold mineral is native gold with 7.5 wt. % Ag. The size distribution and association of native gold varies considerably. In the high grade composite, the mean size (50% ordinate on cumulative frequency diagram) is 5000 μm^2, with 90% of the total gold area as grains in the size range from 1000 to 12000 μm^2. The fine grained gold (< 20 μm^2) represents only 1.0% of the head assay and is mostly associated with arsenopyrite. In the Peel zone composite AB, the gold grains are smaller with a mean size of 60 μm^2. Ninety percent of the total gold area is as grains which are in the size range from 5 μm^2 to 200 μm^2. Of the fine grained gold, 25% is enclosed in pyrrhotite, that is 4.5% of the head assay. Gold in the LAB zone is similarly fine grained with a mean size of 70 μm^2, with ninety percent of the total gold area as grains in the range between 5 and 250 μm^2. Of the fine grained gold, 15% is enclosed in pyrrhotite, that is 2.2% of the head assay.

Gold recovery by direct cyanidation at a coarse grind, K_{80} = 100 µm was 70.0% from the Peel zone AB composite and 81.2% for the LAB composite. Finer grinding improved the recovery to 73.3% and 87.5% respectively. In the case of the high grade composite, the recovery, as anticipated, was higher compared to the other ores (91.9%) and finer grinding did not further improve the recovery.

The invisible gold concentrates in the arsenopyrite. Average solid solution gold in arsenopyrite ranged from 12.2 ppm in composite AB to 17.5 ppm in the high grade composite. Statistically there is no difference in the gold content of the arsenopyrite from the three samples tested. However, there are several populations of arsenopyrite based on their gold content. These populations are equally represented in all three ores. The other sulphides have no detectable invisible gold. **Arsenopyrite is the carrier of both the invisible gold and the bulk of the fine grained gold.**

Based on the gold mineralogical distribution (Figure 1) and previous metallurgical testing, the flowsheet in Figure 2 is proposed for optimum recovery, keeping in mind reagent consumption, retention time and tailings stability. The main feature of this flowsheet is the separation of the pyrrhotite from the arsenopyrite in order to avoid the uneccessary overgrinding of the pyrrhotite, which results in high reagent consumption and retention time.

Expected recoveries using the proposed flowsheet are given in Table 1. Gold losses will be in the form of invisible gold in arsenopyrite (Table 2) and fine grained gold enclosed in pyrrhotite (Table 3).

FIGURE 1

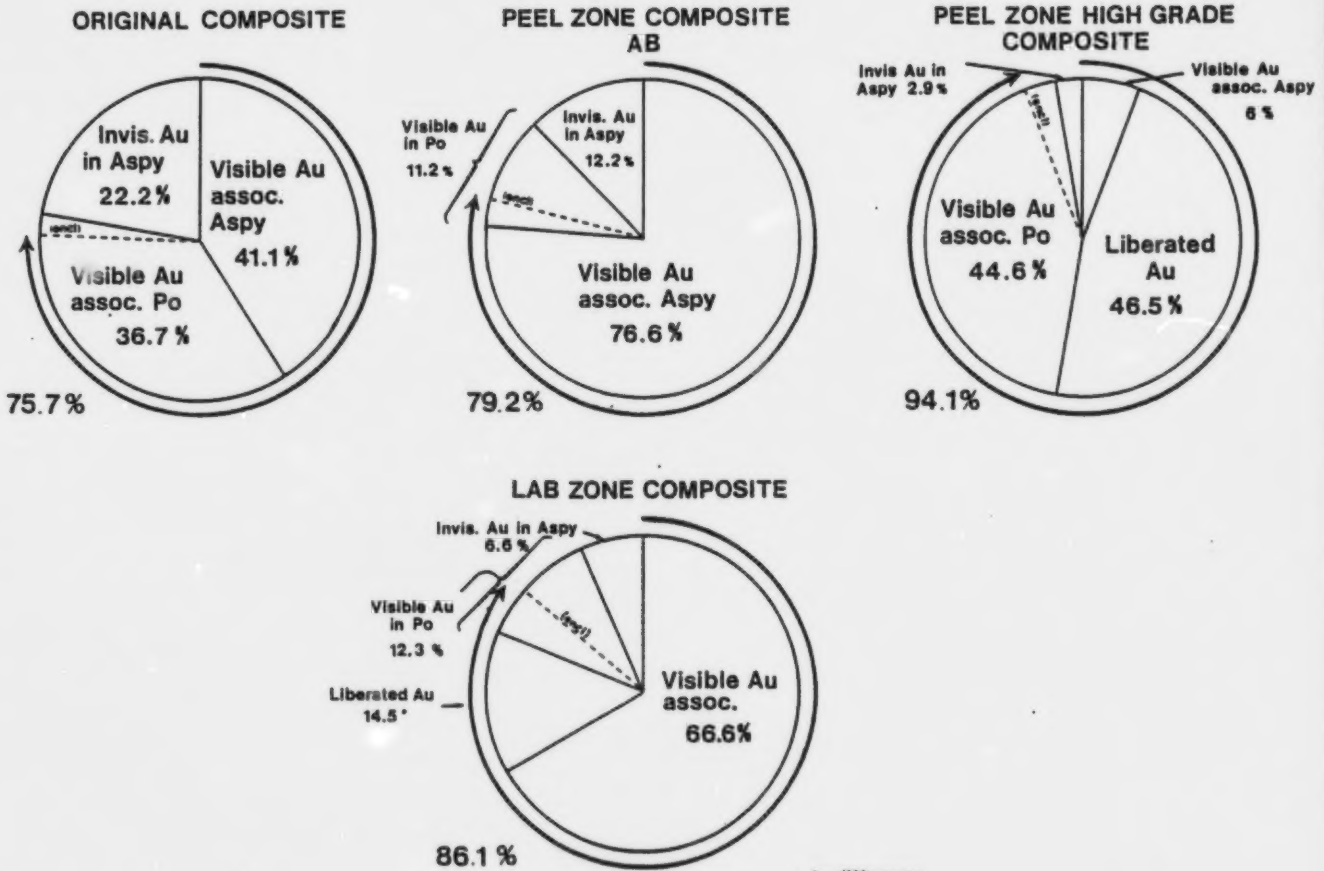

* by difference

Mineralogical balances for gold in four Ketza River composites.

Clockwise arrow denotes maximum recoverable Au using flowsheet #1.

[1] includes visible gold associated with py, cpy and other non-magnetic phases.

Figure 2. Proposed flowsheet for treatment of the Ketza River sulphide ore.

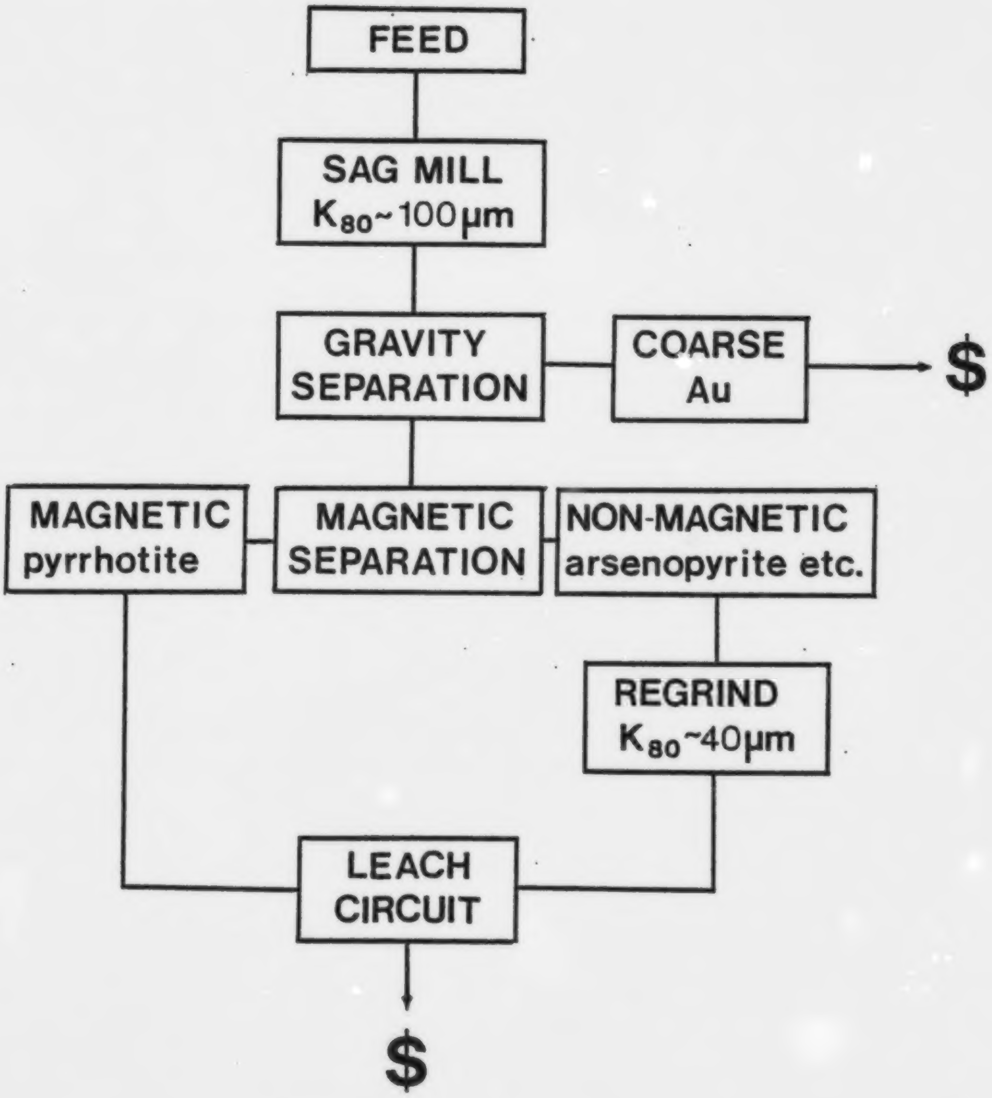
FEED
SAG MILL
K80~100μm
GRAVITY SEPARATION
COARSE Au
$
MAGNETIC pyrrhotite
MAGNETIC SEPARATION
NON-MAGNETIC arsenopyrite etc.
REGRIND
K80~40μm
LEACH CIRCUIT
$

TABLE 1

ESTIMATED MAXIMUM RECOVERABLE Au USING FLOWSHEET #1

	%
Peel zone high grade composite	94.1
Peel zone composite AB	79.2
LAB zone composite	86.1

TABLE 2

INVISIBLE GOLD IN ARSENOPYRITE

	% of head assay
Peel zone high grade composite	2.9 ± 0.8
Peel zone composite AB	12.2 ± 3.6
LAB zone composite	6.6 ± 0.8 [1]

[1] includes 0.7% in pyrite

TABLE 3

ENCLOSED GOLD
as a percentage of head assay

	In aspy[1]	In Po
Peel zone high grade composite	4.6	3.0[2]
Peel zone composite A+B	26.0	8.6
LAB zone composite	19.4	7.3

---

[1] including cpy, py, gangue

[2] excluding ore 85-90/68364

LIST OF TABLES

Table 1 Estimated maximum recoverable gold

Table 2 Invisible gold in arsenopyrite

Table 3 Summary of distribution of enclosed gold in the three composites.

Table 4 Chemical assays of the ores

Table 5 Results of cyanide leach testing

LIST OF FIGURES

Figure 1 Mineralogical balances for gold in the Peel zone high grade composite, the Peel zone composite AB, the LAB zone composite and the original composite.

Figure 2 Proposed flowsheet #1

Figure 3 Distribution of visible gold in the high grade composite, by association at four size ranges as a proportion of the total area of gold.

Figure 4 Distribution of visible gold in the composite high grade composite, by mineralogical association at four size ranges as a proportion of the total area of each size fraction.

Figure 5 Cumulative frequency diagram of visible gold sizes in the three composites.

Figure 6 Distribution of gold by mineralogical association at three size fractions in Peel zone composite AB.

Figure 7 Distribution of gold by mineralogical association at three size fractions in the LAB zone composite.

LIST OF PLATES

Plate 1 Blastic arsenopyrite in the high grade composite.

Plate 2 Gold particle in high grade composite associated with arsenopyrite.

Plate 3 Gold particle associated with pyrrhotite and native bismuth in the high grade composite.

Plate 4 Large gold particles enclosed in a pyrrhotite-gangue middling particle.

Plate 5 Fine grained gold associated with arsenopyrite in the high grade composite.

Plate 6 Fine grained gold associated with fractures in arsenopyrite in the high grade composite.

Plate 7 Large grain of gold combined with pyrrhotite from the high grade composite.

Plate 8 Large grain of gold associated with pyrrhotite and native bismuth in the high grade composite.

Plate 9 Large grain of gold combined with arsenopyrite from composite AB.

Plate 10 Large gold grain combined with native bismuth from composite AB.

Plate 11 Gold grain associated with arsenopyrite from the LAB composite.

Plate 12 Association of gold with chalcopyrite in the LAB composite.

Plate 13 Intercrystalline coarse grained gold.

Plate 14 Intercrystalline coarse grained gold.

APPENDICES

A1 Image analysis of gold particles in the three composites.

A2 Statistical analysis of results of image analysis of gold particles.

A3 Calculation of visible gold in the composites.

A4 Size distribution of gold particles in the three composites.

A5 Ion probe microanalysis results.

A6 Histograms showing the distribution of invisible gold in each of the three composites.

A7 Results of modal mineralogy and separation tests.

11.1.0 INTRODUCTION

In 1988, a composite sample of massive sulphide from Ketza River, Y.T. was studied in order to determine the concentrations of gold in the sulphide minerals (invisible gold) and to determine the complete mineralogical balance for gold in the composite (Chapter 10). The objective of the present study is to provide a **complete mineralogical balance in a further three composites**, in order to test variations in the distribution of both visible and invisible gold between the distinct parts of the main orebody and a satellite orebody in the Ketza River ore field.

The three ores tested are: 1) **High grade composite from the Peel zone,** composed from four samples associated with cross-cutting veins, each of which assayed more than 0.7 oz/t. These were sent by J. Toohey, Project geologist with CANAMAX Resources Inc., 2) **Composite from the Peel zone AB**, and 3) **A composite from the LAB zone.** A five kilogram sample of each of the latter two ores were supplied by Bacon, Donaldson and Associates Ltd., Vancouver, who carried out the metallurgical testing on these samples.

The previous investigation of the Ketza River sulphides (1) determined that, in that composite ore, 75% of the gold head assay is accounted for as native gold. The grains of native gold were associated with both arsenopyrite and pyrrhotite, the two major sulphide minerals. Coarser-grained gold is associated with pyrrhotite, while the finer grained gold is mostly enclosed in arsenopyrite. Invisible gold was present within the arsenopyrite at a concentration of 11.9 ± 2.2 g/t, and accounted for 19.2% of the gold head assay. Based upon subsequent testwork (2), gold recovery from the original composite was found to be 95.8 % if the proposed flowsheet of direct cyanidation followed by selective flotation of arsenopyrite from the leach residue was followed. An alternative process was recommended involving direct cyanidation followed by magnetic separation of arsenopyrite. A combined gold recovery of 87.6% was achieved using this method.

This study was financed 50% by CANMET, through an amendment to the DSS contract # 50SS.23440-7-9037, and 50% by CANAMAX Resources Inc.

11.2.0 METHODOLOGY

Each composite head sample was analyzed for Au and As (Table 4). The crushed composite was sieved into three size fractions: -53 µm, 53-300 µm and +300 µm. Au assays were made on the -53µm fraction in each case. Heavy liquid

TABLE 4

CHEMICAL ASSAYS

	HEAD	-53 µm FRACTION	53-300 µm SINK FRACTION	53-300 µm LIGHT FRACTION
PEEL ZONE HIGH GRADE COMPOSITE				
Au (direct), g/t	14.5	24.4	21.7	8.24
Au (calc), g/t	25.0	-	28.0	-
As, Wt. %	1.93	-	-	-
Arsenopyrite, Wt. %	4.2	-	-	-
PEEL ZONE COMPOSITE AB				
Au (direct), g/t	11.0	9.33	11.4	1.61
Au (calc), g/t	-	-	12.7	-
As, Wt. %	5.27	-	-	-
Arsenopyrite, Wt. %	11.0	-	-	-
LAB ZONE COMPOSITE				
Au (direct), g/t	11.8	11.5	13.1	1.18
Au (calc), g/t	-	-	14.1	-
As, Wt. %	2.15	-	-	-
Arsenopyrite, Wt. %	4.7	-	-	-

media separation was carried out on the 53-300 µm fraction of each, using sodium polytungstate solution with a working density of 3.0 g.cm^{-1} (Appendix A7). The proportion of the float to sink fractions was calculated, and both fractions were assayed for Au. Polished blocks were prepared from the sink fraction of the 53-300 µm fraction; 20 for the high grade composite, 12 for composite AB, and 10 for the LAB zone composite.

Optical microscopy was used to determine the size and association of the gold minerals. The invisible gold in the sulphide minerals was determined by ion probe microanalysis.

Cyanide leaching was used to verify the visible gold content of the composites as measured by optical microscopy, and to determine the effect which grinding has upon gold recovery. For each, one cyanidation test was carried out at a relatively coarse grind (K_{80} = 90-104 µm; 140-170 mesh). A second test was made on a different sub-sample which had undergone much finer grinding to K_{80} = 25 µm; 540 mesh). Test conditions were as follows: 30% solids, 1 g/l NaCN, pH 10.5 - 11.0, 48 hours. Results are shown in Table 5.

11.3.0 RESULTS

11.3.1 Mineralogy

All three composites contained pyrrhotite and arsenopyrite, with minor pyrite and chalcopyrite. Trace amounts of marcasite, native bismuth and bismuthinite were also recognized.

The proportions of pyrrhotite, arsenopyrite, pyrite and chalcopyrite, which are required for the gold mineralogical distribution were calculated. The proportion of arsenopyrite in each composite was calculated from the As assay. This is possible since the As content of the pyrite is low, and pyrite is a minor phase (with the exception of the LAB composite). The Peel zone high grade composite contains 4.2 Wt. % arsenopyrite, the Peel zone composite AB contains 11.0 Wt. % arsenopyrite and the LAB zone composite contains 4.7 Wt. % arsenopyrite. The proportions of pyrrhotite, pyrite and chalcopyrite were measured by image analysis (Appendix A7). The proportion of gangue is calculated from the weight proportion of the light fraction and accounts for 9.7 % of the high grade composite, 15.2 % of the composite AB and 17.6% of the LAB composite.

TABLE 5

RESULTS OF CYANIDATION TESTS

ORE	K_{80}	REAGENT CONS.		Residue	Calc.	Recovery	Direct	Recovery
	(µm)	NaCN	CaO	Au, ppm	head	% Au[1]	head	% Au[2]
PEEL ZONE COMPOSITE AB	104.0	10.61*	2.51	3.30	10.8	69.4	11.0	66.3
	24.9	11.21*	2.29	2.94	12.0	75.5		80.2
LAB ZONE COMPOSITE	104.0	4.17*	1.75	2.22	12.6	82.4	11.8	82.4
	24.9	7.31*	1.89	1.48	13.4	88.9		94.5
PEEL HIGH GRADE COMPOSITE	90.1	4.19*	1.89	1.91	23.6	91.9		
	25.4	7.63*	1.82	1.83	19.2	90.5		

* no preaeration

[1] using calculated head

[2] using direct head

Only in one of the high grade samples (KR 84-29/67213) were distinct morphological types of arsenopyrite recognized, including a distinct type with blastic inclusions of silicate gangue.

11.3.2 Visible Gold

11.3.2.1 High Grade Composite

Results of the cyanide leach testing on the high grade composite indicate that 91.9 % of the gold can be recovered at K_{80} = 90 µm; 170 mesh. Finer grinding to K_{80} = 25 µm; 540 mesh) did not improve recovery, which was 90.5 %.

Native gold is the only gold mineral identified in the high grade composite. **Twenty** polished sections were investigated with the optical microscope and a total of **111** grains of gold were identified (Appendix A1). Fifty six gold grains were associated with pyrrhotite (50%). An example is shown in Plate 2. Forty one grains were associated with arsenopyrite (37%). Of the fourteen remaining grains, seven were liberated, three are associated with chalcopyrite, three are associated with pyrite and one was combined with native bismuth. Many of the gold grains associated with pyrrhotite were also intimately associated with bismuth and bismuthinite (Plate 3). Although no grains were observed completely enclosed within gangue, a number of very large gold grains were observed in a pyrrhotite-gangue middling particle (Plate 4). Statistical results are given for the composited high grade ore in Appendix A2.

From the data set, it would appear that the proportions of gold grains in different associations differ between the four samples. However, it is believed that this is largely due to the relatively small number of polished sections examined from each sample (five).

In terms of area, the 41 grains associated with arsenopyrite account for only 2.2% of the total gold, since most gold grains associated with arsenopyrite were small and filled fractures and cracks within the arsenopyrite (Plates 5 and 6). The average size of the gold grains associated with arsenopyrite was 28 µm². In contrast, the grains associated with pyrrhotite were generally large (Plates 7 and 8), and they accounted for 45.9% of the total gold area. The average size of the grains associated with pyrrhotite was 431 µm². The size distribution of gold particles is shown in Appendix A4.

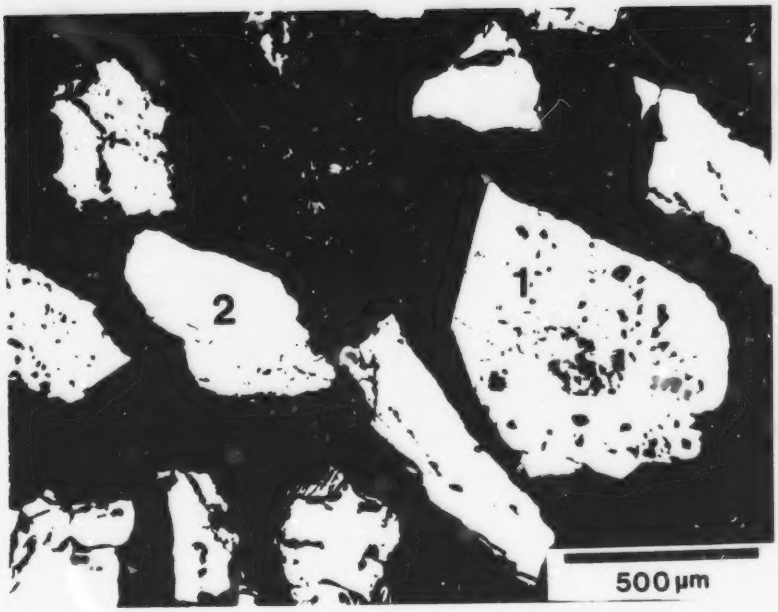

Plate 1 Two types of arsenopyrite are present in high grade sample KR-84-29/67213. The first (1) contains large rounded inclusions of quartz. The second (2) is free of inclusions. The two are often intergrown.

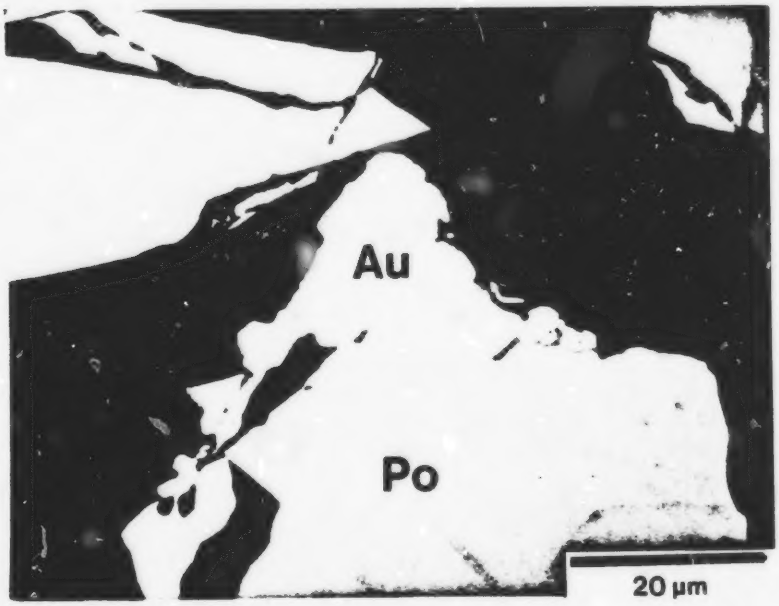

Plate 2 A large grain of native gold (Au) combined with pyrrhotite (po); the most important association of native gold in the Peel zone high grade composite.

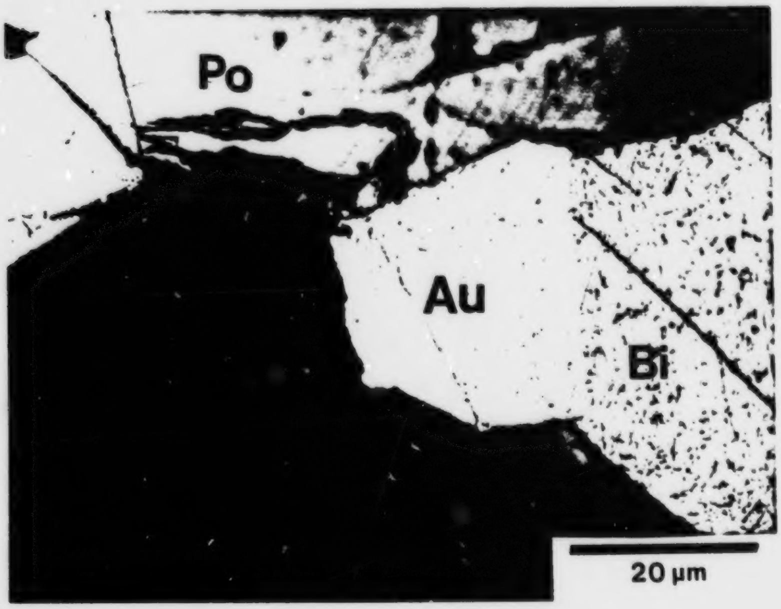
Po
Au
Bi
20 µm

Plate 3 A grain of native gold (Au) combined with pyrrhotite (po) in association with native bismuth (Bi).

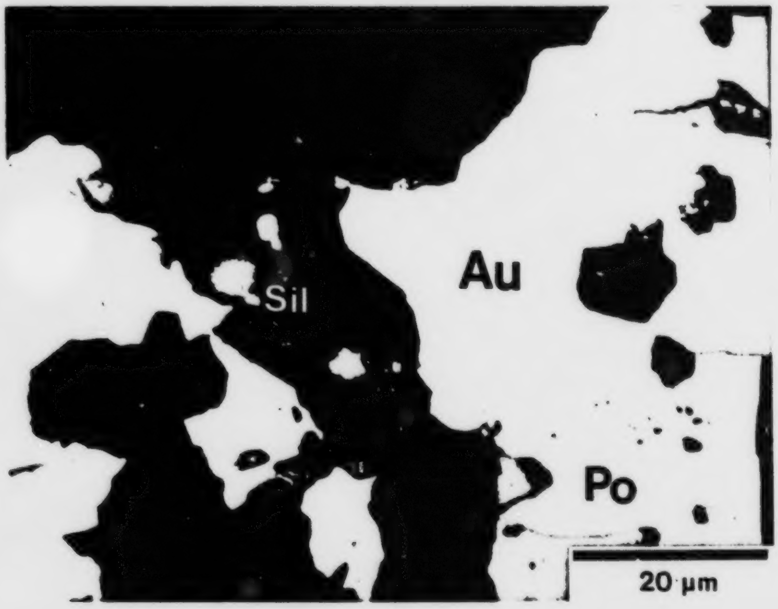
Au
Sil
Po
20 µm

Plate 4 Large grains of native gold (Au) enclosed within a large pyrrhotite (po) - silicate gangue (sil) particle.

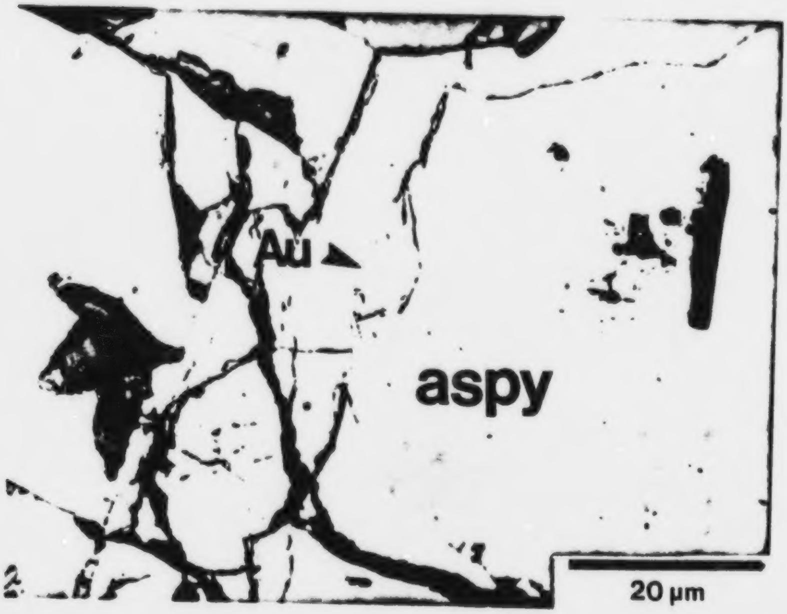
Au
aspy
20 µm

Plate 5 Numerous fine grains of native gold (Au) within a fracture in an arsenopyrite particle (aspy).

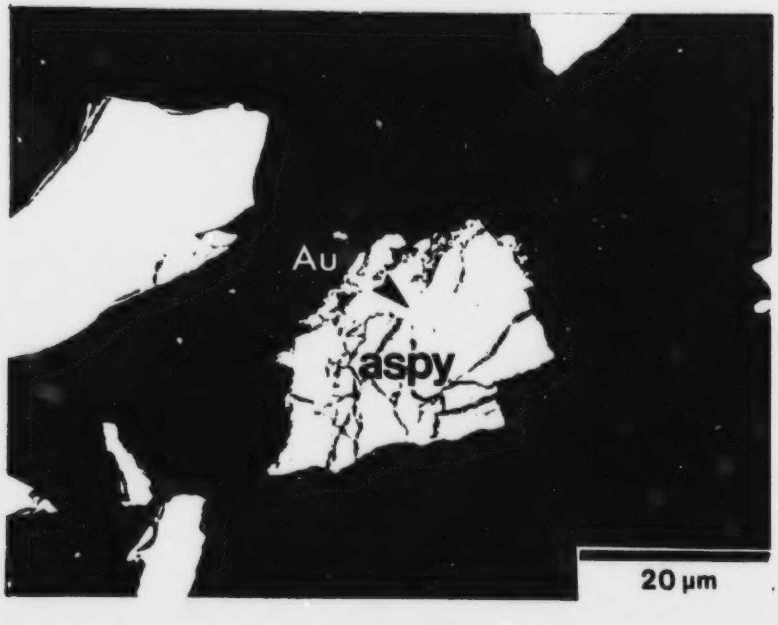
Au
aspy
20 µm

Plate 6 Larger grain of native gold (Au) combined in a highly fractured arsenopyrite particle (aspy).

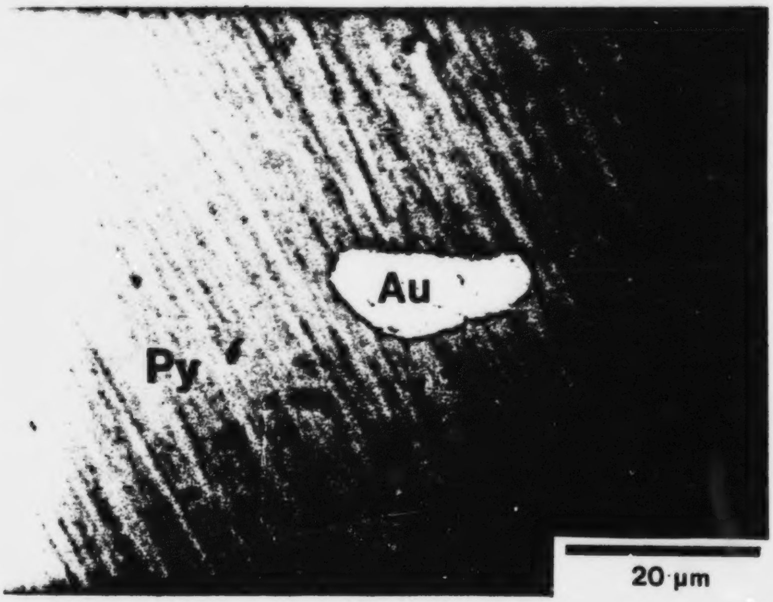

Plate 7 Large rounded inclusion of native gold (Au) in a pyrite particle (py).

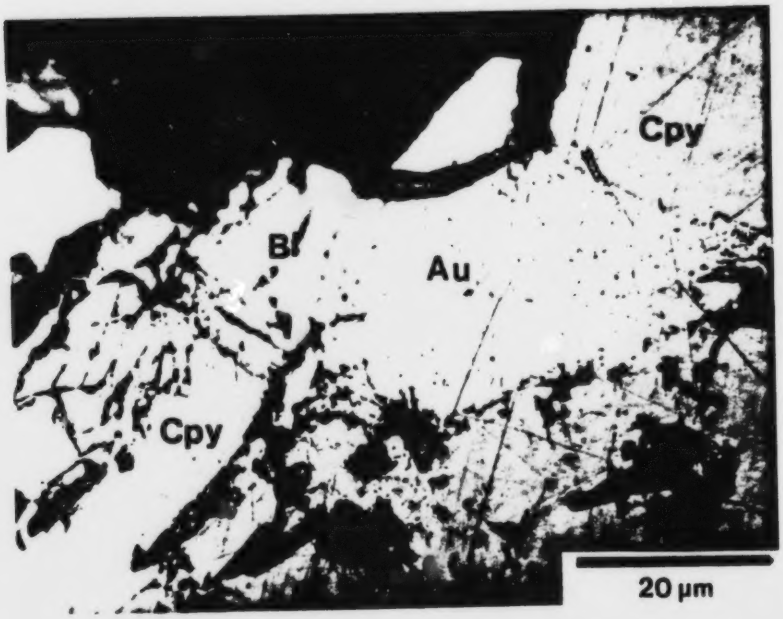
Cpy
Bi
Au
Cpy
20 µm

Plate 8 Grain of native gold (Au) combined with chalcopyrite (cpy) and associated with native bismuth (Bi).

However, the largest contribution to total area comes from the seven liberated grains which have a very great average size (3607 µm²) and contribute 47.9% to the total gold area.

The contribution to total area by large grains (exceeding 1000 µm²) is very high; 93%. Thus, the presence of a relatively small number of such larger grains (11 grains, or 10% of the total) controls the distribution of visible gold in this composite, and increases the average grain size to 474 µm². The implications for the recovery of gold from the high grade composite are discussed later. The calculations from the area measurement of visible gold are summarized in Appendix A3. The nugget effect induced by the presence of a small number of large grains places limitations upon the precision by which the balance of visible gold can be estimated in the high grade composite.

11.3.2.2 Peel zone composite AB

Results of the cyanide leach testing on the composite A+B indicate that 70.0 % of the gold can be recovered at K_{80} = 104 µm; 140 mesh. Finer grinding to K_{80} = 25 µm; 540 mesh) improved recovery by a significant amount to 73.3%.

Native gold is the only gold mineral identified in the AB composite. **Twelve** polished sections were investigated with the optical microscope and a total of **eighty five** grains of gold were identified (Appendix A1). Fifty five gold grains were associated with arsenopyrite (65%). Many of the larger of these were combined with arsenopyrite, as in the example shown in Plate 9. Sixteen grains were associated with pyrrhotite (19%). Of the fourteen remaining grains, eleven are associated with chalcopyrite, one is enclosed in pyrite and two larger grains are combined with native bismuth and bismuthinite. One of these is shown in Plate 10. Results of the mineralogical investigation of the AB composite are analyzed in Appendix A2.

In terms of area, the 55 gold grains associated with arsenopyrite account for 64 % of the total gold. The average size of the gold grains associated with arsenopyrite was 20 µm². The grains associated with pyrrhotite accounted for 12.7% of the total gold area. The grains associated with chalcopyrite accounted for 5.7% of the total and the two large grains combined with native bismuth accounted for 23.3% of the total area. The size distributions of gold are shown in Appendix A4.

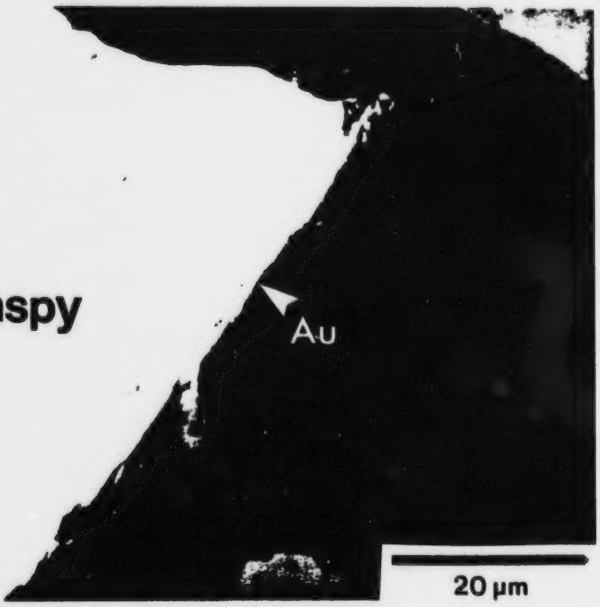
aspy
Au
20 µm

Plate 9 Typical occurence of gold in the Peel zone composite AB. A grain of native gold (Au) combined with arsenopyrite (aspy).

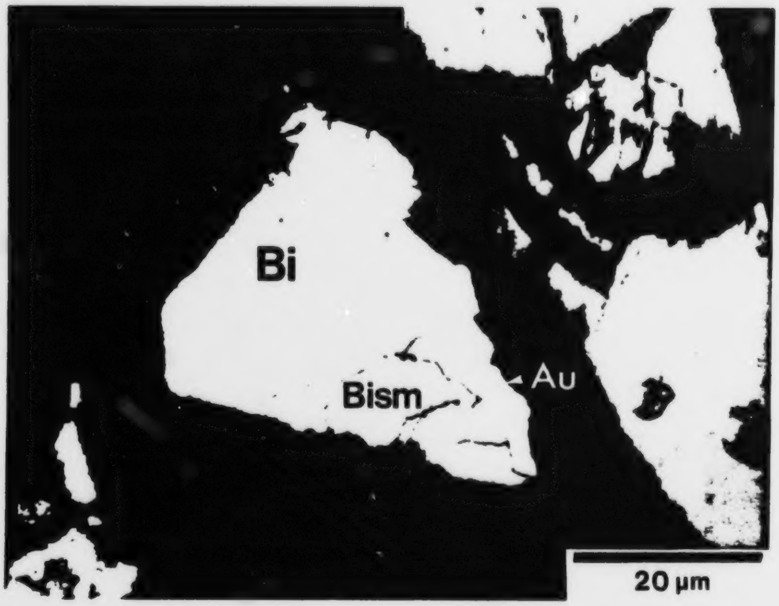
Bi
Bism
Au
20 µm

Plate 10 Larger native gold grain (Au); the grain is combined with native bismuth (Bi) and bismuthinite (Bism).

The average size of gold grains in the composite AB is much less compared to that of the high grade ores (23 µm²). The contribution to total area by grains greater than 100µm² in size is 43.6%, from grains 20-100 µm², 36.0% and the smallest grains, less than 20 µm² in size contribute 20.4%.

The calculations from the area measurement of visible gold in the Peel zone composite AB are summarised in Appendix A3.

11.3.2.3 LAB zone composite

Results of cyanide leach testing on the LAB zone composite indicate that 81.2 % of the gold can be recovered at K_{80} = 94 µm; 160 mesh. Finer grinding to K_{80} = 27µm; 540 mesh) improved recovery by a significant amount to 87.5%.

Native gold is the only gold mineral identified in the LAB composite. **Twenty** polished sections were investigated with the optical microscope and a total of **one hundred and sixty nine** grains of gold were identified (Appendix A2). One hundred and five gold grains were associated with arsenopyrite (62%). An example is shown in Plate 11. Many of the grains associated with arsenopyrite also showed a strong association with chalcopyrite (Plate 12). Forty grains were associated with pyrrhotite (24%). Of the twenty four remaining grains, twelve are associated with chalcopyrite, seven are enclosed in gangue, three are liberated and two were combined with native bismuth. Results of the mineralogical investigation of the LAB ore are analyzed in Appendix A2. One very large liberated grain was observed (4420 µm²). This was statistically anomalous and has been excluded from the statistical analysis.

In terms of area, the 105 gold grains associated with arsenopyrite account for 57.3% of the total gold, with those grains combined with arsenopyrite accounting for twice as much area as the grains enclosed in arsenopyrite, due to their greater mean size. The grains associated with pyrrhotite accounted for 13.2% of the total gold area. The grains associated with gangue accounted for 4.5% of the total and those grain combined with native bismuth accounted for 7.7% of the total area. The size distributions of gold are shown in Appendix A4.

The average size of gold grains in the LAB composite is much less than for the high grade ores (23 µm²). The contribution to total area by grains greater than 100µm² in size is 49.6%, from grains 20-100 µm², 34.1% and the smallest grains, less than 20 µm² in size contribute 16.3%.

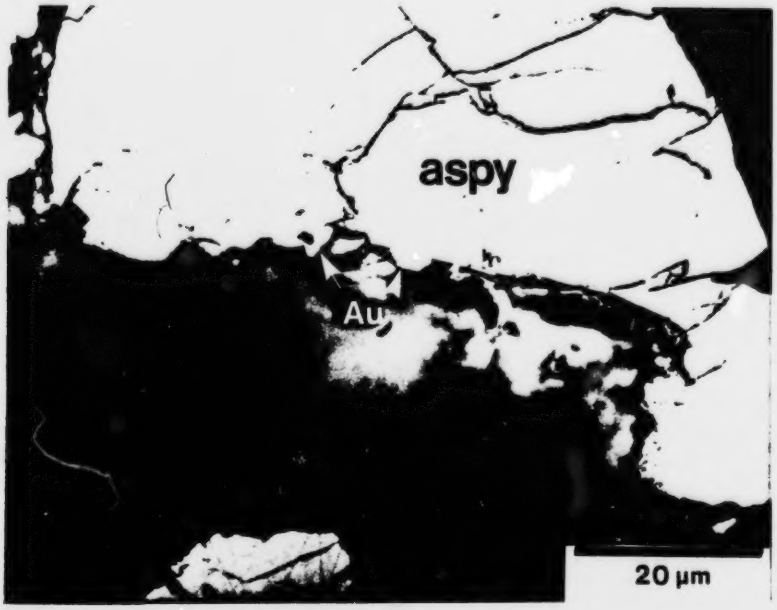
aspy
Au
20 µm

Plate 11 Typical occurence of gold in the **LAB zone composite**. Grains of native gold (Au) are combined with, and enclosed in fractures within arsenopyrite.

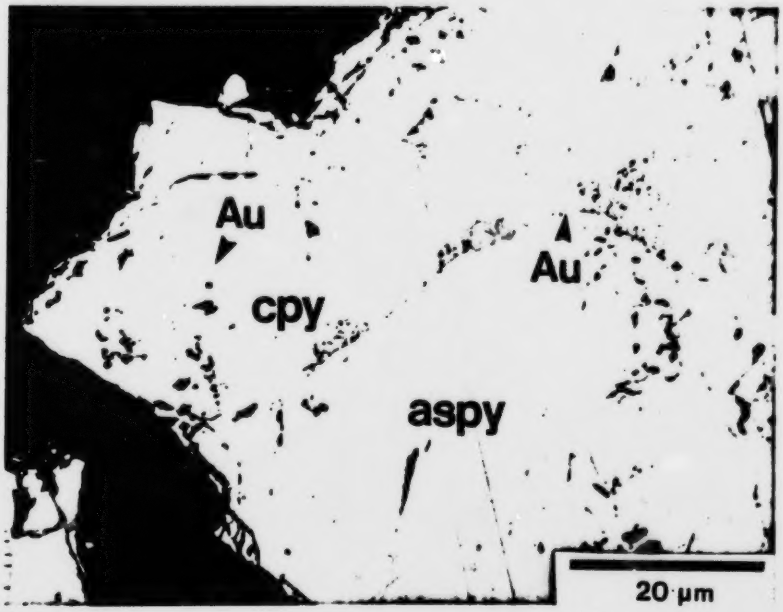
Au
Au
cpy
aspy
20 µm

Plate 12 Gold grains located at the boundary of chalcopyrite (cpy) and arsenopyrite (aspy), from LAB zone composite.

The LAB zone composite displays similarities with both the Peel zone composite AB and the previously tested composite (1) in average grain size and distribution of visible gold between the main minerals pyrrhotite and arsenopyrite. The calculations from the area measurement of visible gold in the LAB zone composite are summarized in Appendix A3.

11.4.0 DISCUSSION

On the Peel zone high grade composite:

Diagnostic cyanide leach testing of the high grade composite at a relatively coarse grind indicates that 91.9% of the gold can be recovered by cyanidation (Table 5). The lack of improvement in recovery at finer grinds was explained by image analysis of gold minerals. It has been demonstrated that fine grained gold (<100 μm^2) is of little significance in this ore and that it accounts for only 2.4% of the total gold (Figure 3). At a coarse grind, the coarse-grained gold becomes either exposed or liberated and is recoverable by cyanidation (Figure 4). It should be stressed that the average size of visible gold grains in the high grade composite is, greater by one order of magnitude, than the LAB zone composite, the Peel zone composite AB or the original composite (Figure 5). In addition, the proportion of visible gold associated with arsenopyrite is much less in the high grade ores than in the other ore types (Figures 4,6 and 7). This is because the coarse-grained gold particles are inter-crystalline, i.e. between pyrrhotite particles (Plates 13 and 14).

Direct measurements of solid solution gold with the ion microprobe have shown that only 2.9% of the gold in the composite is in the crystal lattices of the sulphide minerals. This balances with the gold content of the cyanide leach residue (Table 5). The other sulphides do not contribute significantly to the gold mineralogical balance.

Based on this distribution of gold in the high grade composite, a coarse grind, K_{80}: 100 µm, is proposed in order to liberate the coarse grained gold which can be recovered by gravity separation and expose the finer-grained gold which is recoverable by cyanidation of the gravity tailings. The invisible gold in arsenopyrite is minor and does not justify further treatment. The expected recovery is of the order of 93-95%, with a maximum recovery of 97% by the proposed scheme.

FIGURE 3

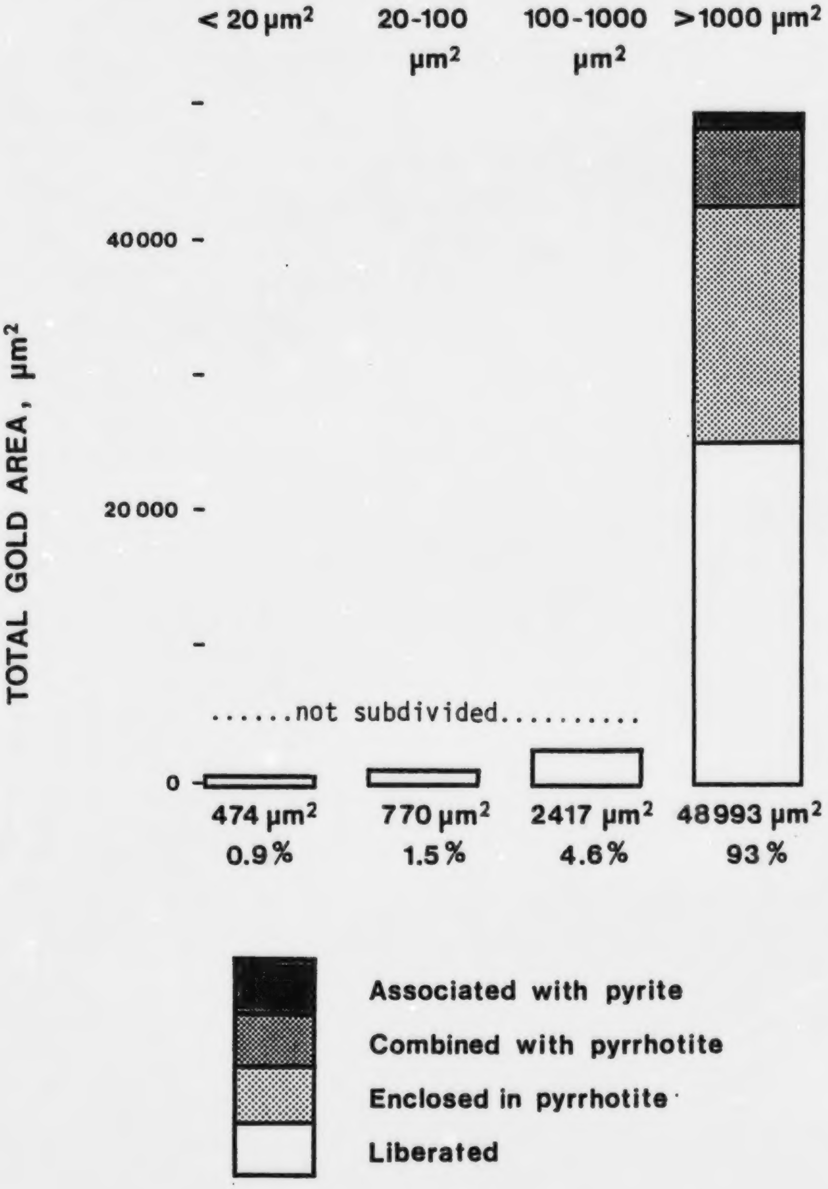

PEEL ZONE HIGH GRADE COMPOSITE

DIAGRAM SHOWING PROPORTIONS OF VISIBLE GOLD IN DIFFERENT MINERALOGICAL ASSOCIATIONS AT FOUR SIZE FRACTIONS, AS A PROPORTION OF THE TOTAL AREA

FIGURE 4

PEEL ZONE HIGH GRADE COMPOSITE

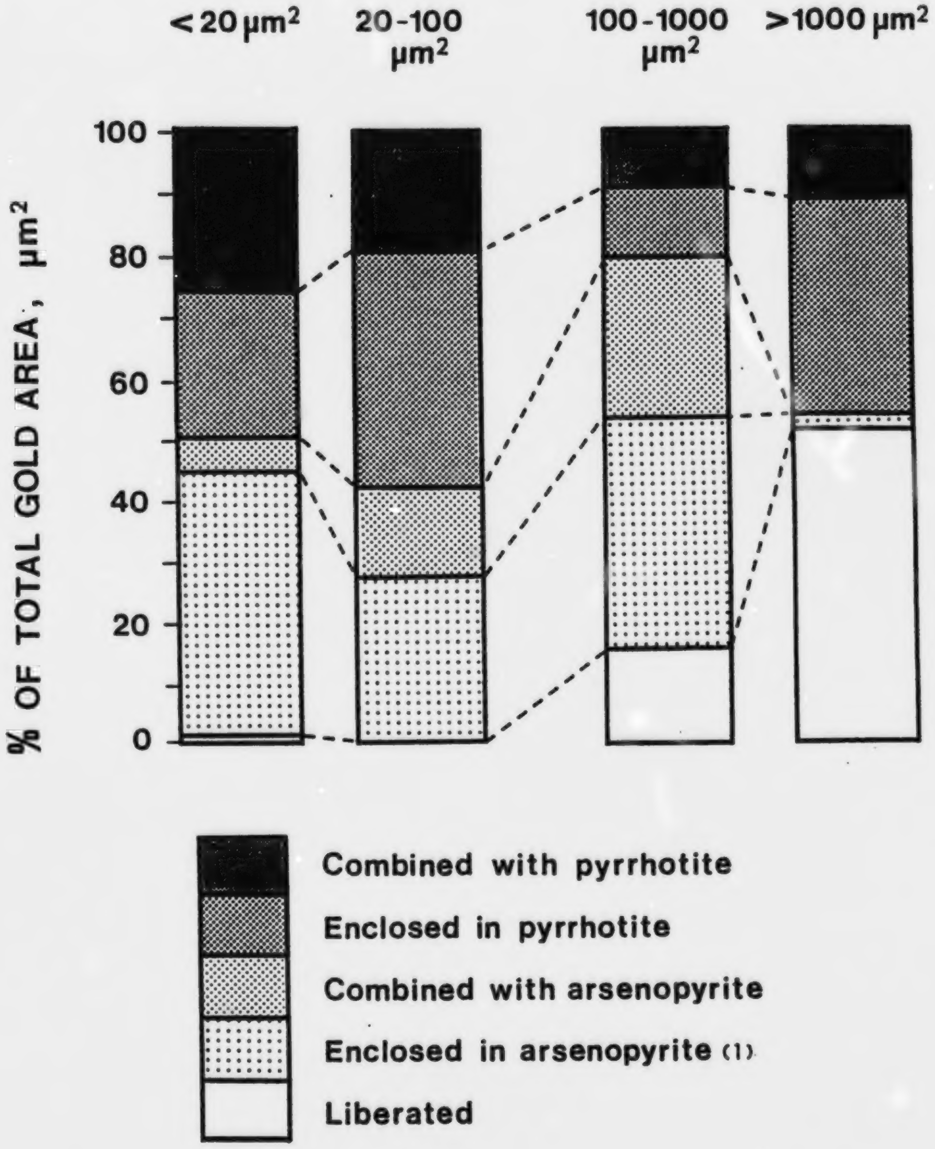

(1) including grains associated with pyrite and chalcopyrite

DIAGRAM SHOWING PROPORTIONS OF VISIBLE GOLD IN DIFFERENT MINERALOGICAL ASSOCIATIONS AT FOUR SIZE FRACTIONS, AS A PERCENTAGE OF THE TOTAL AREA OF VISIBLE GOLD AT THAT SIZE FRACTION.

FIGURE 5

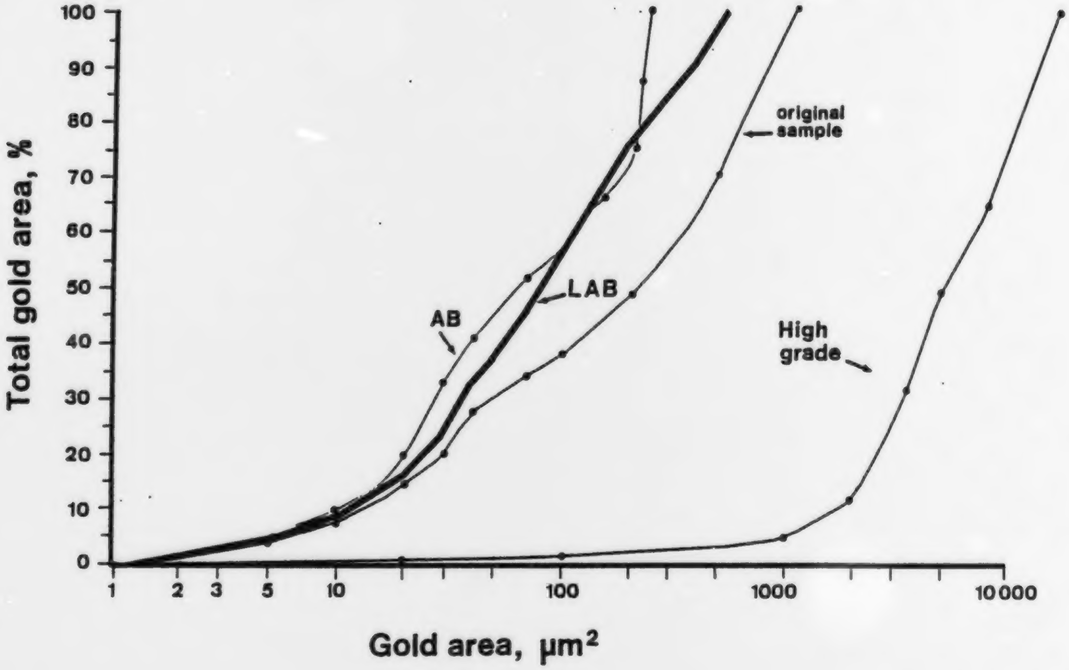

CUMULATIVE FREQUENCY PLOT OF GOLD PARTICLE SIZE DISTRIBUTION IN THE PEEL ZONE HIGH GRADE COMPOSITE, COMPOSITE AB, LAB ZONE COMPOSITE AND THE ORIGINAL SAMPLE.

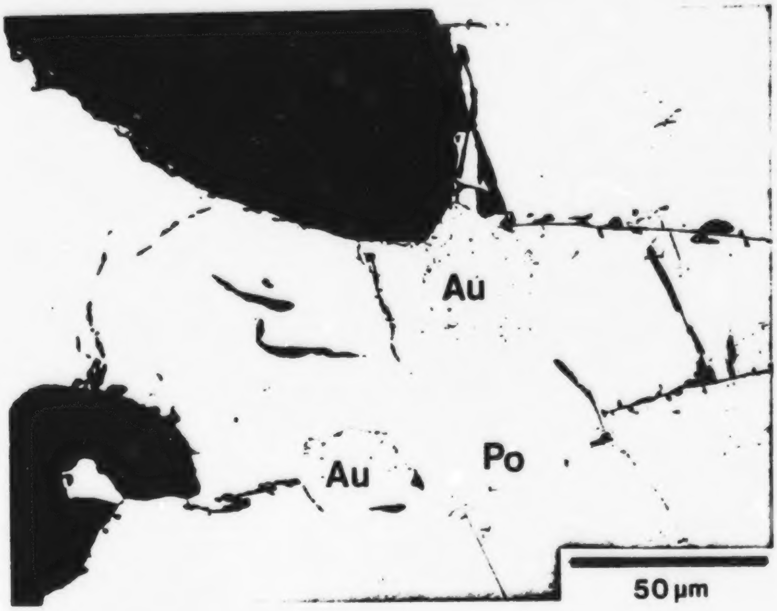

Plate 13 Coarse grained gold intercrystalline between pyrrhotite grains, under partly crossed nicols.

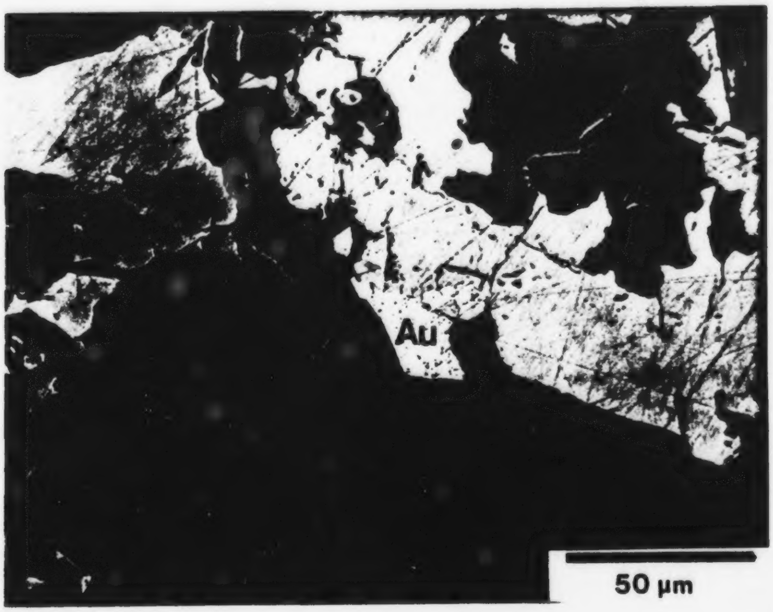

Plate 14 Coarse grained gold intercrystalline between pyrrhotite grains, under partly crossed nicols.

On the Peel zone composite AB:

Both image analysis of the visible gold and the cyanide leach tests have shown that a significant portion of the gold is fine-grained (Figs 5 and 6, Table 5). Fifty six percent is less than 100 µm² in size and twenty percent is less than 20 µm² in size. Only 25 percent of the gold grains which are less than 20 µm² is enclosed in pyrrhotite. This represents 4.8 percent of the AB composite head assay. Image analysis of gold indicated that 65% of the gold was visible, and this agrees well with the results of the cyanide tests. At K_{80} = 104 µm, 70.0% of the gold was recovered, which increased to 73.3% in a finely ground sample.

Ion probe microanalysis has shown that arsenopyrite contains significant amounts of invisible gold, 12.2 ± 4.1 g/t. Arsenopyrite accounts for 11% of the ore. Thus, invisible gold in arsenopyrite is clearly important in the AB ore and accounts for 1.3 ± 0.4 g/t, or 12.2 % of the head assay. No invisible gold was detected in either the pyrite or pyrrhotite.

The maximum recoverable gold by direct cyanidation of the AB sulphide composite is 88%. If the pyrrhotite is not overground to recover the fine grained gold, then the expected maximum recoverable gold is of the order of 84% from the AB zone.

On the LAB zone composite:

Image analysis of gold minerals and diagnostic cyanide testing have both shown that the LAB zone composite is comparable with the Peel zone AB composite in both size distribution and association of visible gold (Figs. 5 and 7, Table 5). The observed increase in recovery from 81.2% at K_{80} = 104 µm to 87.5% at K_{80} = 25 µm suggested the presence of approximately 13% of locked fine grained gold in the LAB composite. It was determined by image analysis that 16% of the visible gold is finer than 20 µm². Only 9% of the very fine grained gold is enclosed in pyrrhotite, which represents 1.4% of the head assay.

The balance of the gold is invisible. Ion probe microanalysis showed that arsenopyrite contained invisible gold at a concentration of 14.9 ± 4.6 g/t. Arsenopyrite accounted for 4.7% of the ore and the invisible gold in arsenopyrite accounts for 0.7 ± 0.2 g/t, or 5.9 % of the head assay. Minor amounts were accounted for by invisible

FIGURE 6

Peel zone composite A B

% of total area	20.4	36	43.6
no. of grains	62	19	4

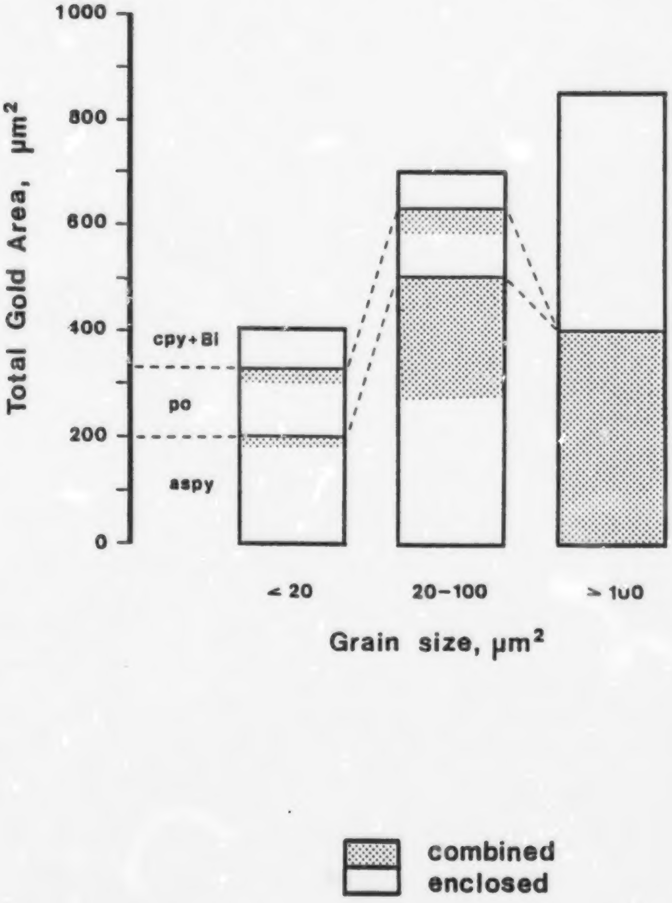

DIAGRAM SHOWING PROPORTIONS OF VISIBLE GOLD GRAINS IN DIFFERENT MINERALOGICAL ASSOCIATIONS AT THREE SIZE FRACTIONS, AS A PROPORTION OF THE TOTAL AREA OF VISIBLE GOLD GRAINS.

Lab zone composite

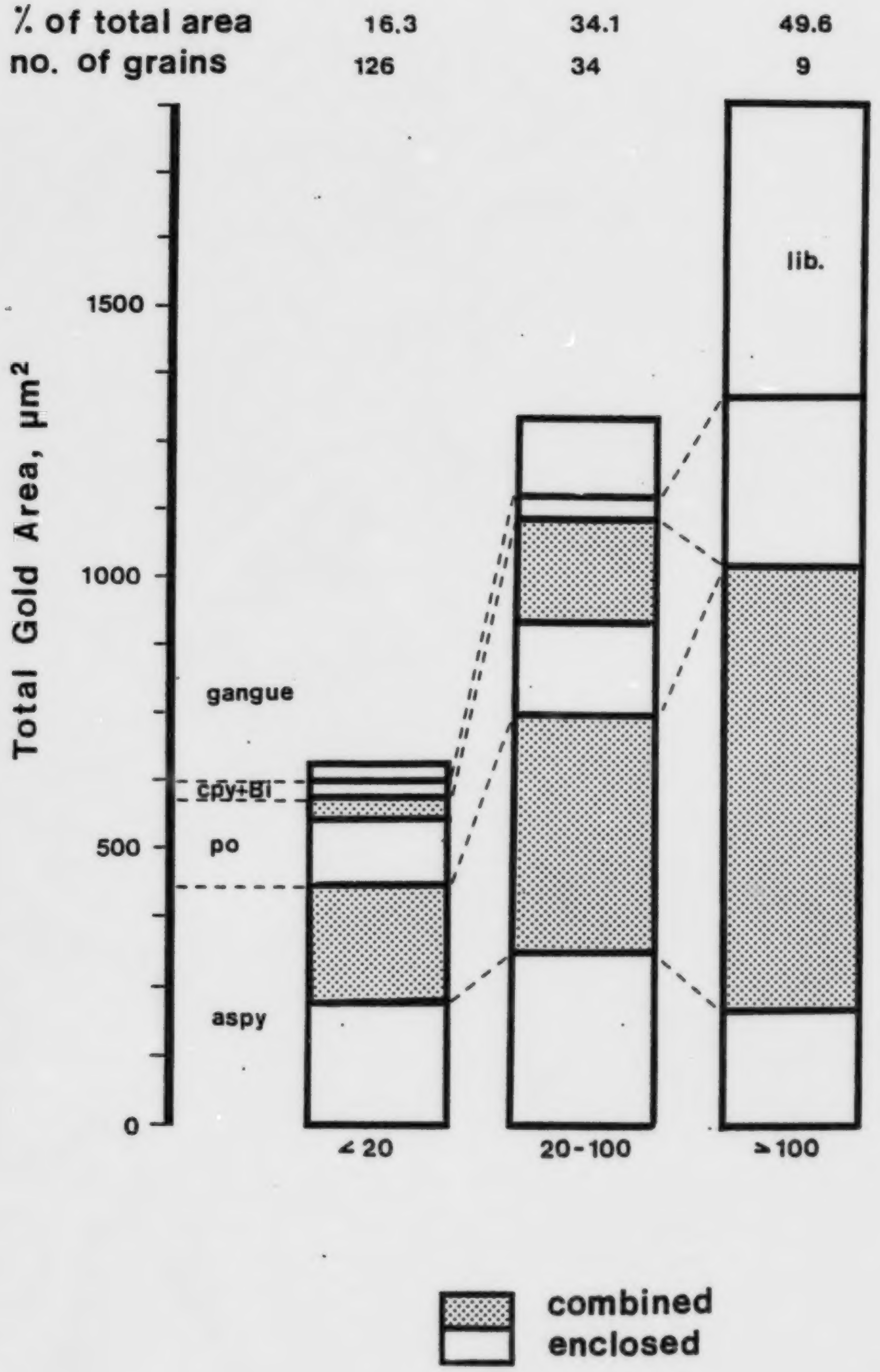

gold in pyrite, which is more abundant than arsenopyrite in the LAB zone composite. Pyrite has an invisible gold concentration of 1.4 ± 0.3 g/t Au and contributes 0.7% of the head assay.

Given the relatively small significance of arsenopyrite bound invisible gold and of the fine grained visible gold enclosed in pyrrhotite of the LAB zone composite, it is unlikely that both forms of gold can be recovered economically.

11.5.0 CONCLUSIONS

Based on the results of the gold mineralogical examination and the diagnostic metallurgical testing of the two composite samples representing the Peel and LAB zones and a high grade composite from the Peel zone, the following conclusions are made regarding the recovery of gold:

In the high grade sample, representing 20% of the confirmed reserves, coarse grained gold accounted for 90% of the head assay. With an average grain size of about 400 µm², the coarse grained gold may be recovered by gravity separation after a relatively coarse grind (K_{80} = 100 µm).

In the AB composite from the Peel zone and the composite from the LAB zone, which combined represent 80% of the reserves, the gold is fine grained. The average grain size is about 50 µm². The coarser gold is associated with pyrrhotite. Invariably, the majority of the finer grained gold is associated with arsenopyrite. Fine grinding of the entire sample have lead to unreasonably high cyanide consumptions. In order to take advantage of the specific size distribution of gold observed, it is proposed to separate the magnetic pyrrhotite with the coarser gold from the non-magnetic arsenopyrite etc., which hosts the finer grained gold. Then the non-magnetic fraction can be ground finer. The preaerated coarser pyrrhotite would then be combined with the fine-grained non-magnetic fraction for direct cyanidation. Thus, by avoiding to overgrind the pyrrhotite, reagant comsumption (cyanide and lime) and retention time will be maintained low. The unrecovered gold would be limited to the invisible gold in the arsenopyrite and the fine-grained gold which is enclosed in the pyrrhotite (Tables 2 and 3).

APPENDIX A1

IMAGE ANALYSIS OF GOLD PARTICLES IN THE THREE COMPOSITES

LIST OF GOLD GRAINS OBSERVD

SAMPLE: KR 85-85/68344

grain	size (μm^2)
Enclosed in arsenopyrite	
1	2
2	6
3	5
4	15
5	15
6	23
7	4
8	8
9	54
10	4
11	49
12	3
13	5
14	5
15	29
16	1
Combined with arsenopyrite	
17	114
18	5
19	2
Enclosed in pyrrhotite	
20	1
21	1
22	4
23	2
24	20
25	18
26	16
27	1
28	41
29	169
30	63
Combined with pyrrhotite	
31	9
32	4
33	2
34	3
35	1
36	1
37	6
38	1
39	12
40	1
41	11
42	227
43	3
44	5
45	7
46	3
47	5
48	2
49	4
50	4
51	3
52	1095
53	2438
54	4
Combined with pyrite	
55	13
Liberated	
56	6
57	2750
58	370
59	4820

LIST OF GOLD GRAINS OBSERVED

SAMPLE: KR 85-90/68364

grain	size (μm^2)
Combined with arsenopyrite	
1	37
Enclosed in pyrrhotite	
2	8457
3	1605
4	2500
5	4475
6	42
7	6
8	72
9	101
Liberated	
10	17280

LIST OF GOLD GRAINS OBSERVED

SAMPLE: KR 84-29/67213

grain	size (μm^2)
Enclosed in arsenopyrite	
1	17
2	3
3	14
4	13
5	4
6	12
7	2
8	8
9	3
10	11
11	26
Combined with arsenopyrite	
12	10
13	3
14	34
15	409
16	11
17	41
Enclosed in pyrrhotite	
18	31
19	6
20	8
21	3
22	11
23	31
24	6
Combined with pyrrhotite	
25	6
26	2488
Enclosed in pyrite	
27	25
28	1085

LIST OF GOLD GRAINS OBSERVED

SAMPLE: KR 85-90/68363

grain	size (μm^2)
Enclosed in arsenopyrite	
1	11
2	3
3	4
Combined with arsenopyrite	
4	108
Enclosed in pyrrhotite	
5	24
6	5
7	4
Combined with pyrrhotite	
8	76
Combined with chalcopyrite	
9	919
10	4
11	10
Combined with bismuthinite	
12	72
Liberated	
13	6
14	17

IMAGE ANALYSIS OF GOLD GRAINS

SAMPLE: PEEL ZONE COMPOSITE A B

Enclosed in arsenopyrite

grain	size (µm²)
1	1
2	32
3	4
4	1
5	3
6	17
7	43
8	38
9	2
10	2
11	24
12	7
13	5
14	13
15	3
16	2
17	3
18	6
19	4
20	3
21	8
22	9
23	2
24	1
25	14
26	12
27	1
28	4
29	11
30	48
31	19
32	36
33	7
34	4
35	2
36	23
37	27
38	4
39	2
40	5
41	4

Combined with arsenopyrite

42	59
43	2
44	2
45	4
46	221
47	78
48	171
49	27
50	54
51	31
52	2
53	3
54	3
55	6

Enclosed in pyrrhotite

56	13
57	9
58	12
59	5
60	29
61	13
62	10
63	27
64	15
65	12
66	26
67	4
68	12

Combined with pyrrhotite

69	37
70	17
71	3

Enclosed in chalcopyrite

72	29
73	3
74	15
75	22
76	2
77	2
78	3
79	16
80	15
81	2
82	1

Enclosed in pyrite

83	6

Combined with bismuthinite

84	204
85	246

IMAGE ANALYSIS OF GOLD GRAINS

SAMPLE: LAB ZONE COMPOSITE

grain	size (μm²)
Enclosed in arsenopyrite	
1	1
2	3
3	3
4	2
5	1
6	1
7	1
8	1
9	6
10	17
11	30
12	5
13	6
14	13
15	170
16	2
17	2
18	3
19	2
20	19
21	27
22	36
23	47
24	9
25	4
26	27
27	9
28	3
29	4
30	10
31	2
32	2
33	23
34	31
35	12
36	3
37	2
38	1
39	61
40	1
41	1
42	19
43	6
44	4
45	40
46	3
47	1
48	1
49	14
50	15
51	3
52	2
53	3
54	2
55	1
56	5
57	2
58	1
59	1
60	1
61	2
62	3
Combined with arsenopyrite	
63	37
64	5
65	2
66	2
67	19
68	11
69	116
70	27
71	262
72	10
73	1
74	5
75	45
76	16
77	39
78	187
79	5
80	14
81	35
82	26
83	5
84	24
85	7
86	54
87	163
88	9
89	1
90	8
91	23
92	17
93	29
94	7
95	126
96	2
97	3
98	87
99	5
100	5
101	6
102	17
103	4
104	18
105	3
Enclosed in pyrrhotite	
106	25
107	9
108	2
109	1
110	6
111	93
112	10
113	6
114	3
115	2
116	2
117	5
118	7
119	4
120	2
121	2
122	2
123	40
124	8
125	3
126	2
127	27
128	3
129	2
130	1
131	2
132	11
133	1
134	2
135	8
136	8
137	3
Combined with pyrrhotite	
138	17
139	2
140	47
141	76
142	5
143	21
144	4
145	36
Associated with chalcopyrite	
146	2
147	23
148	3
149	2
150	1
151	3
152	1
153	1
154	1
155	6
156	1
157	27
Associated with gangue	
159	68
160	32
161	17
162	21
163	2
164	2
165	34
Liberated	
166	12
167	584
Combined with bismuth	
168	193
169	107

APPENDIX A2

STATISTICAL ANALYSIS OF RESULTS FROM IMAGE ANALYSIS OF GOLD PARTICLES

APPENDIX

PEEL ZONE HIGH GRADE COMPOSITE

STATISTICAL ANALYSIS OF GOLD GRAINS (BY MODE)

Total area of gold observed = 52653 sq µm

Number of gold grains = 111

Number of polished sections studied = 20

Observed visible gold per sample = 2633 sq µm

= 70.2 ppm

Assay of sample (calc) = 25.6 ppm
Calc. Assay of sink fraction = 28.4 ppm

Association	# of grains	% of total
Enclosed in arsenopyrite	30	27
Combined with arsenopyrite	11	10
ASSOCIATED WITH ARSENOPYRITE	41	37
Enclosed in pyrrhotite	29	26
Combined with pyrrhotite	27	24
ASSOCIATED WITH PYRRHOTITE	56	50
Associated with chalcopyrite	3	3
Enclosed in pyrite	3	3
Enclosed in gangue	0	0
Liberated	7	6
Combined with bismuthinite	1	1
TOTAL	111	100

STATISTICAL ANALYSIS OF GOLD GRAINS (BY AREA)

		Σ AREA (µm²)	X (µm²)	%
1a	Grains enclosed in arsenopyrite	359	12	0.7
1b	Grains combined witharsenopyrite	774	70	1.5
1	Grains associate with arsenopyrite	1133	28	2.2
2	Grains enclosed in chalcopyrite	933	311	1.8
3	Grains enclosed in pyrite	1123	374	2.1
4	Liberated	25249	3607	47.9
5a	Grains enclosed in pyrrhotite	17722	611	33.7
5b	Grains combined with pyrrhotite	6421	238	12.2
5	Grains associated with pyrrhotite	24143	431	45.9
6	Grains enclosed in gangue	0	-	-
7	Combined with bismuthinite	72	72	0.1
	GRAND TOTAL	52653	474	100.0

APPENDIX

PEEL ZONE COMPOSITE A B

STATISTICAL ANALYSIS OF GOLD GRAINS (BY MODE)

Total area of gold observed = 1929 sq µm

Number of gold grains = 85

Number of polished sections studied = 12

Observed visible gold = 7.1 ppm

Assay of sample = 11.0 ppm
Calc. Assay of sink fraction = 12.7 ppm
Direct Assay of sink fraction = 11.4 ppm

Association	# of grains	% of total
Enclosed in arsenopyrite	41	49
Combined with arsenopyrite	14	16
ASSOCIATED WITH ARSENOPYRITE	55	65
Enclosed in pyrrhotite	13	15
Combined with pyrrhotite	3	4
ASSOCIATED WITH PYRRHOTITE	16	19
Associated with chalcopyrite	11	13
Enclosed in pyrite	1	1
Enclosed in gangue	0	0
Liberated	0	0
Combined with bismuthinite	2	2
TOTAL	85	100

STATISTICAL ANALYSIS OF GOLD GRAINS (BY AREA)

		Σ AREA (µm²)	X (µm²)	%
1a	Grains enclosed in arsenopyrite	456	11	23.6
1b	Grains combined witharsenopyrite	663	47	34.4
1	Grains associate with arsenopyrite	1119	20	58.0
2	Grains enclosed in chalcopyrite	110	10	5.7
3	Grains enclosed in pyrite	6	6	0.3
4	Liberated	0	-	-
A	Total flotable fraction	1235	18	64.0
5a	Grains enclosed in pyrrhotite	187	14	9.7
5b	Grains combined with pyrrhotite	57	19	3.0
5	Grains associated with pyrrhotite	244	15	12.7
6	Grains enclosed in gangue	0	-	-
7	Combined with bismuthinite	450	225	23.3
B	Total non-flotable fraction	694	39	36.0
	GRAND TOTAL	1929	23	100.0

APPENDIX

LAB ZONE COMPOSITE

STATISTICAL ANALYSIS OF GOLD GRAINS (BY MODE)

Total area of gold observed = 3872 sq μm
± 7.3

±21.7

Number of gold grains = 169

Number of polished sections studied = 20
± 0.8

Observed visible gold per sample = 7.74 ppm
± 1.98

Association	# of grains	% of total
Enclosed in arsenopyrite	62	37
Combined with arsenopyrite	43	25
ASSOCIATED WITH ARSENOPYRITE	105	62
Enclosed in pyrrhotite	32	22
Combined with pyrrhotite	8	6
ASSOCIATED WITH PYRRHOTITE	40	28
Associated with chalcopyrite	12	11
Enclosed in pyrite	0	0
Enclosed in gangue	7	6
Liberated	2*	1
Combined with bismuthinite	2	1
TOTAL	169	100

STATISTICAL ANALYSIS OF GOLD GRAINS (BY AREA)

		Σ AREA (μm²)	X (μm²)	%
1a 1a	Grains enclosed in arsenopyrite	732	12	18.9 ±7.3
1b 1b	Grains combined witharsenopyrite	1487	35	38.4 ±21.7
1	Grains associate with arsenopyrite	2219	21	57.3
2 2	Grains enclosed in chalcopyrite	71	6	1.8 ±0.8
3	Grains enclosed in pyrite	0	-	-
4	Liberated*	596	298	15.5
5a	Grains enclosed in pyrrhotite	302	9	7.8
5b	Grains combined with pyrrhotite	208	26	5.4
5	Grains associated with pyrrhotite	510	15	13.2
6	Grains enclosed in gangue	176	28	4.5
7	Combined with bismuthinite	300	150	7.7
	GRAND TOTAL	3872	23	100.0

* large liberated grain ignored

APPENDIX A3

CALCULATION OF VISIBLE GOLD IN THE THREE COMPOSITES

APPENDIX

CALCULATION OF VISIBLE GOLD IN PEEL ZONE HIGH GRADE COMPOSITE

Total area studied: (20 x 4.91 cm^2) = 98.20 cm^2

Coverage of sample = 28.0 %
(determined by point counting) +/- 1.2 %

Total sample area covered = 27.50 cm^2

Total sample weight (unit depth; 10^{-4} cm,
av. spec. grav., 4.90 g.cm^{-3}) = 134.73 x 10^{-4} g
(est. 80% p, 20% aspy)

Total gold area = 52653 µm^2
=5265.3 x 10^{-8} cm^2

Average gold content of grains (1) = 93 %

Total gold weight (unit depth; 10^{-4} cm
av. spec. grav.; 19.3 g.cm^{-3}) = 94.51 x 10^{-8} g

Total gold concentration relative to sulphide = 70.2 ppm (2)

'Visible' gold = 70.2 ppm

(1) from previous report

(2) due to sinking effect during sample mounting.

APPENDIX

CALCULATION OF VISIBLE GOLD IN PEEL ZONE COMPOSITE AB

Total area studied: (12 x 4.155 cm^2) = 29.46 cm^2

Coverage of sample = 20.6 %
(determined by point counting) +/- 1.4 %

Total sample area covered = 10.27 cm^2

Total sample weight (unit depth; 10^{-4} cm,
av. spec. grav., 4.75 $g.cm^{-3}$) = 48.79 x 10^{-4} g
(est. 80% p, 20% aspy)

Total gold area = 1929 μm^2
= 192.9 x 10^{-8} cm^2

Average gold content of grains (1) = 93 %

Total gold weight (unit depth; 10^{-4} cm
av. spec. grav.; 19.3 $g.cm^{-3}$) = 3.46 x 10^{-8} g

Total gold concentration relative to
sulphide = 7.1 ppm

'Visible' gold = 7.1 ppm

(1) from previous report

APPENDIX

CALCULATION OF VISIBLE GOLD IN LAB ZONE COMPOSITE

Total area studied: (10 x 4.155 cm^2) = 41.55 cm^2

Coverage of sample (determined by point counting) = 23.1 % +/- 2.2 %

Total sample area covered = 9.59 cm^2

Total sample weight (unit depth; 10^{-4} cm, av. spec. grav., 4.67 $g.cm^{-3}$) (est. 95% po, 5% aspy) = 44.83 x 10^{-4} g

---

Total gold area = 1936 μm^{2*}

Reproducibility = ± 495

= 193.6 x 10^{-8} cm^2

Average gold content of grains (1) = 93 %

Total gold weight (unit depth; 10^{-4} cm av. spec. grav.; 19.3 $g.cm^{-3}$) = 3.47 x 10^{-8} g

Total gold concentration relative to sulphide = 7.74 ppm ± 1.98

'Visible' gold = 7.74 ppm ± 1.98 ppm

(1) from previous report

* large liberated grain ignored

APPENDIX A4

HISTIGRAMS SHOWING THE SIZE DISTRIBUTION OF GOLD PARTICLES IN THE THREE COMPOSITES

APPENDIX

HISTOGRAM OF GRAIN SIZE OF GOLD PARTICLES IN THE PEEL ZONE HIGH GRADE COMPOSITE DIVIDED BY MINERALOGICAL ASSOCIATION

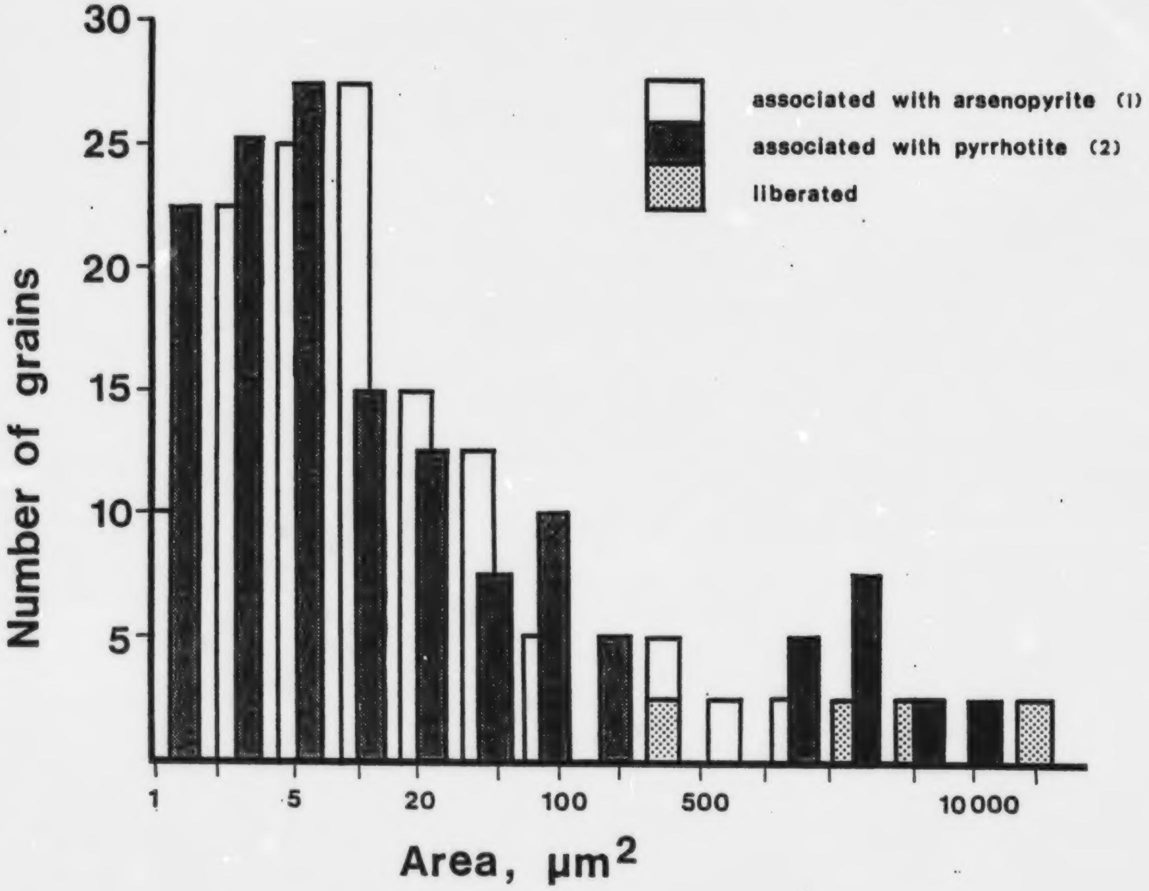

(1) also grains associated with pyrite and chalcopyrite

(2) also grains associated with bismuthinite/native bismuth

APPENDIX

HISTOGRAM OF GRAIN SIZE OF GOLD PARTICLES IN THE PEEL ZONE COMPOSITE A B DIVIDED BY MINERALOGICAL ASSOCIATION

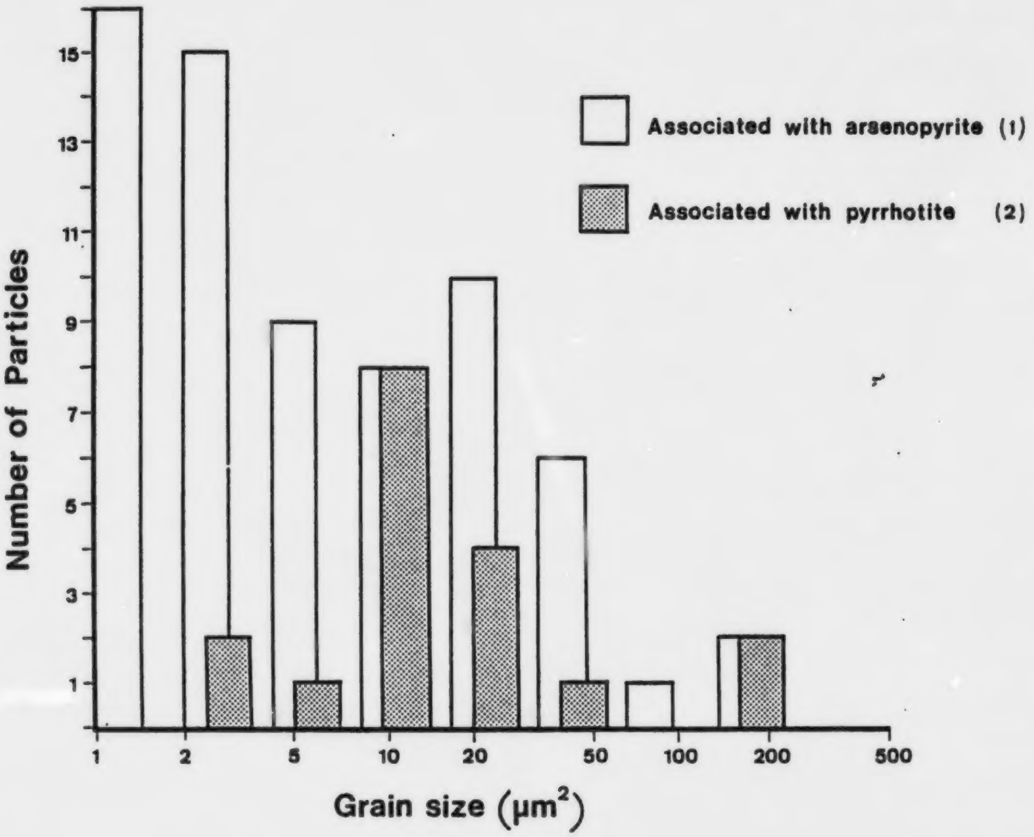

(1) also grains associated with pyrite and chalcopyrite

(2) also grains associated with bismuthinite/native bismuth

APPENDIX

HISTOGRAM OF GOLD PARTICLE GRAIN SIZE IN THE LAB ZONE COMPOSITE, DIVIDED BY MINERALOGICAL ASSOCIATION.

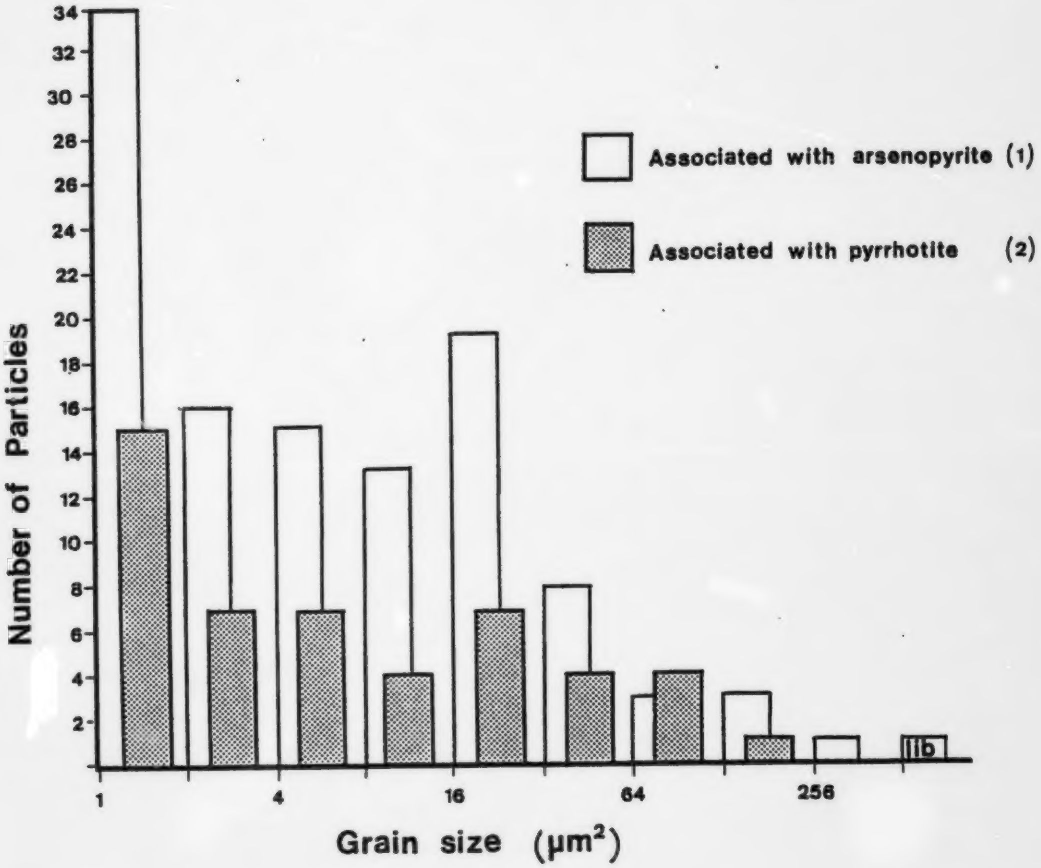

(1) also grains associated with pyrite and chalcopyrite.

(2) also grains associated with native bismuth and gangue.

APPENDIX A5

RESULTS OF ION PROBE ANALYSIS

APPENDIX

INVISIBLE GOLD CONCENTRATION IN SULPHIDES
Peel zone high grade composite

Arsenopyrite

KR84-29		KR85-85		KR85-90		KR85-90	
67213		68334		68364		68363	
particle #	Au, ppm	particle #	Au, ppm	particle #	Au, ppm	particle #	Au, ppm
1	10.	21	27.	36	13.	49	5.2
2	5.8	22	6.0	37	18.	50	9.6
3	13.	23	8.4	38	12.	51	8.0
4	8.5	24	4.7	39	13.	52	39.
5	40.	25	40.	40	12.	53	24.
6	5.2	26	2.8	41	13.	54	3.9
7	73.	27	4.2	43	7.2	55	270.(Au incs)
8	13.	28	8.2	44	67.	56	5.7
9	13.	29	4.0			57	6.2
10	15.	30	19.			58	27.
11	6.0	31	13.			59	17.
12	8.0	32	51.				
13	0.6	33	6.3				
14	140.(Au incs)	34	11.				
15	20.	35	16.				
16	39.						
17	62.						
18	48.						
19	0.6						
20	4.9						
N	: 19	N	: 15	N	: 8	N	: 10
$x \pm \lambda$	: 20.3 ± 9.8	$x \pm \lambda$	: 14.8 ± 7.4	$x \pm \lambda$	: 19.4 ± 13.8	$x \pm \lambda$	: 14.6 ± 7.5

N : 52 $x \pm \lambda$: 17.5 ± 4.8 ppm

Pyrite

particle #	Au, ppm
60	0.0
61	0.0

APPENDIX

INVISIBLE GOLD CONCENTRATION IN SULPHIDES
Peel zone composite A B

Arsenopyrite

particle #	Au, ppm	particle #	Au, ppm	particle #	Au, ppm
1	4.5	16	1.8	31	28.
2	13.	17	24.	32	5.5
3	45.	18	42.	33	6.8
4	5.8	19	2.4	34	1.8
5	6.6	20	7.0	35	9.8
6	52.	21	2.5	36	2.2
7	12.	22	3.7	37	6.0
8	10.	23	6.0	38	14.
9	0.8	24	0.4	39	11.
10	47.	25	4.0	40	23.
11	28.	26	13.	41	0.5
12	1.4	27	1.0	44	7.0
13	5.0	28	3.4	45	3.1
14	13.	29	4.7	46	5.5
15	15.	30	37.		

N : 44

$x \pm \lambda$: 12.2 ± 4.1

Pyrrhotite

particle #	Au, ppm
42	0.0
43	0.0

APPENDIX

INVISIBLE GOLD CONCENTRATION IN SULPHIDES
LAB zone composite

Arsenopyrite

particle #	Au, ppm	particle #	Au, ppm	particle #	Au, ppm
1	0.7	21	23.	65	3.4
2	16.3	22	5.8	66	5.4
3	8.4	23	19.	67	3.3
4	65.	24	0.7	68	14.
5	20.	25	0.5	69	8.
6	28.	26	2.2	70	4.3
7	51.	27	19.	71	7.2
8	25.	28	9.	72	39.
9	4.9	30	0.5	73	10.
10	1.9	31	1.2	74	1.1
11	49.	32	1.4	76	8.
12	3.0	33	38.	77	37.
16	9.3	62	17.	78	2.0
18	36.	63	28.	79	13.
19	0.4	64	8.8	80	11.

N : 46

$x \pm \lambda$: 14.9 ± 4.6

Pyrrhotite

particle #	Au, ppm
13	0.0
15	0.0

Pyrite

particle #	Au, ppm
14	1.5
20	1.2

N : 2

$x \pm \lambda$: 1.35 ± 0.3

Chalcopyrite

particle #	Au, ppm
17	0.3
29	0.3

N: 2

x: 0.3

APPENDIX A6

HISTOGRAMS SHOWING DISTRIBUTIONS OF INVISIBLE GOLD CONCENTRATION IN THE THREE COMPOSITES

Invisible gold in arsenopyrite

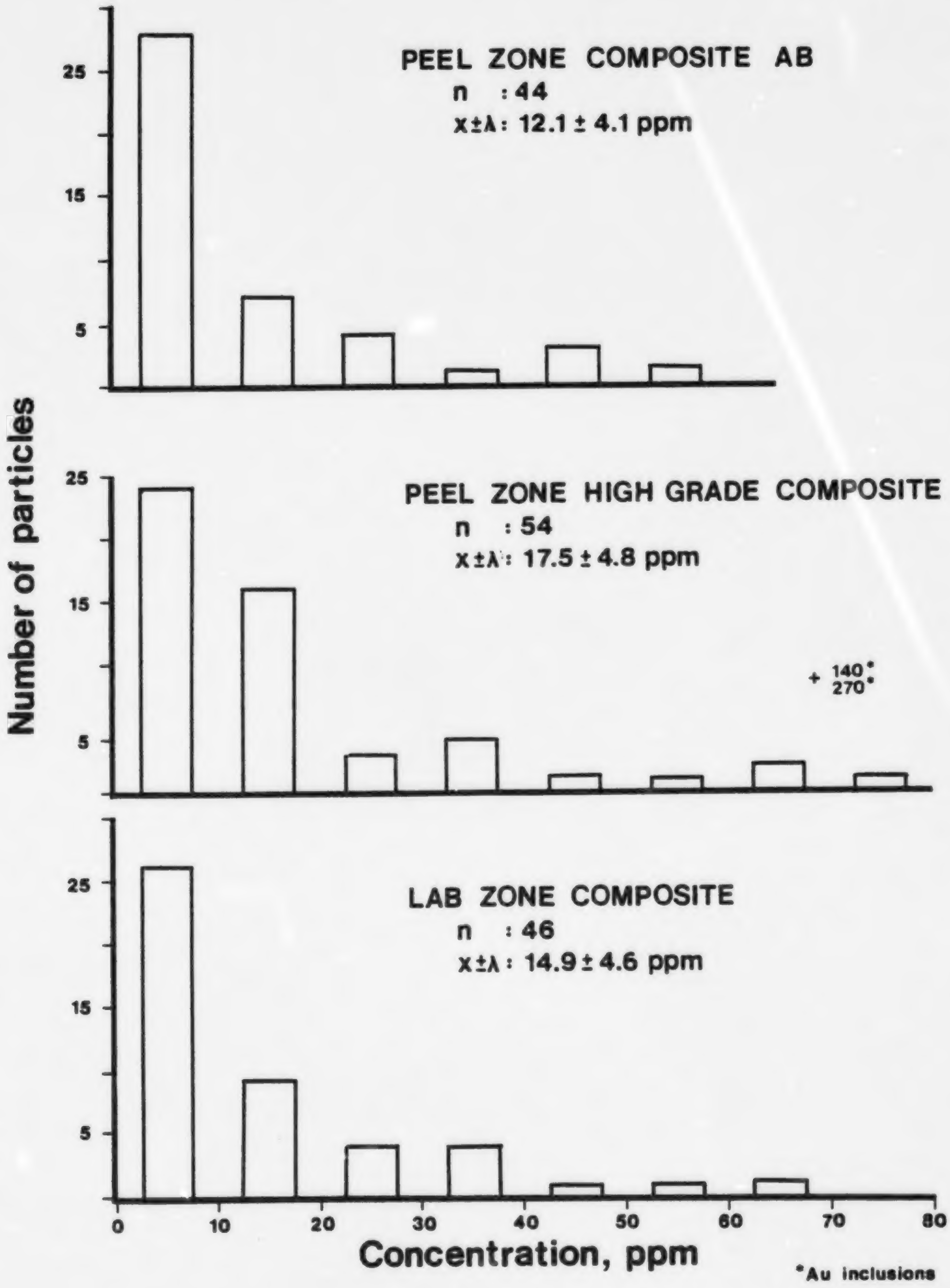

APPENDIX A7

RESULTS OF MODAL MINERALOGY AND SEPARATION TESTS

APPENDIX

Peel zone composite A+B

Area measurement of heavy fraction (20.25 µm², 1186 grains)

Pyrrhotite	85.1 ± 3.4 % vol.	82.1 ± 3.3 Wt. %
Arsenopyrite	10.6 ± 4.0 % vol.	13.5 ± 5.1 Wt. %
Pyrite	3.9 ± 1.1 % vol.	4.1 ± 1.2 Wt. %
Chalcopyrite	0.4 ± 0.3 % vol.	0.3 ± 0.2 Wt. %

HEAD SAMPLE

	Calc. from assay/separation	Image Analysis
Pyrrhotite	-	69.6 ± 2.8[1]
Arsenopyrite	11.0	11.4 ± 4.3[1]
Pyrite	-	3.5 ± 1.0[1]
Chalcopyrite		0.3 ± 0.2[1]
Gangue	15.2	-

---

[1] Balanced to 100% by difference

APPENDIX

LAB zone composite

Area measurement of heavy fraction (20.25 μm^2, 1332 grains)

Pyrrhotite	88.1 ± 2.0 % vol.	86.2 ± 2.0 Wt. %
Arsenopyrite	5.0 ± 0.5 % vol.	6.5 ± 0.7 Wt. %
Pyrite	6.8 ± 1.5 % vol.	7.2 ± 1.6 Wt. %
Chalcopyrite	<0.1 % vol.	-

HEAD SAMPLE

	Calc. from assay/separation	Image Analysis
Pyrrhotite	-	71.1 ± 1.6[1]
Arsenopyrite	4.7	5.4 ± 0.5[1]
Pyrite	-	5.9 ± 1.3[1]
Gangue	17.6	-

---

[1] Balanced to 100% by difference

APPENDIX

RESULTS OF SIEVE TESTING AND HEAVY LIQUID SEPARATION

	HIGH GRADE COMPOSITE			PEEL ZONE COMPOSITE A+B			LAB ZONE COMPOSITE		
FRACTION	mass split %	sink	float	mass split %	sink	float	mass split %	sink	float
-53 µm	0.6	--	--	6.4	--	--	4.7	--	--
53-300 µm	3.6	3.25	0.35	19.3	16.0	2.9	15.3	12.6	2.6
		(90.3%)	(9.7%)		(84.8%)	(15.2%)		(82.4%)	(17.6%)
+300 µm	95.8	--	--	73.4	--	--	80.0	--	--
TOTAL	100.0	--	--	100.0	--	--	100.0	--	--

CHAPTER 12

Quantification of gold in copper anodes by ion probe microanalysis

SSW/PMS/89/09

SUMMARY

The invisible gold concentration in the metallic phase of copper anodes from Kidd Creek, INCO, HBM and CCR (Noranda) was determined by ion probe microanalysis. Quantification was achieved by external standardization. Ion implantation was used to check the nominal concentration of the external standards. The average gold concentration determined in two Kidd Creek anodes were 7.9 ± 0.7 ppm and 22.1 ± 2.5 ppm. The gold concentration in the INCO anode is 5.7 ± 0.45 ppm; in the HBM anode 29.8 ± 2.5 ppm; and in the CCR anode is 52.0 ± 5.3 ppm. These data compare closely with bulk gold assays, which indicates that most of the gold is within the metallic copper. The absence of gold microinclusions larger than 0.03 µm was confirmed by the in-depth concentration profiling.

It has been documented in one Kidd Creek anode that the core is enriched in gold relative to the periphery.

LIST OF TABLES

Table 1 Operating conditions

Table 2 Ion probe microanalysis of implanted external standards

Table 3 Comparison of ion probe and bulk data on gold in copper anodes

Table A1 Raw ion probe data for Kidd Creek anodes

Table A2 Cross section of gold in Kidd Creek anode

Table A3 Raw ion probe data for Noranda, HBM, and INCO anodes

LIST OF FIGURES

Figure 1 Schematic diagram of IMS-3f ion microprobe

Figure 2 Depth profile of Au in copper

Figure 3 Calibration curve

Figure 4 Gold distribution in Kidd Creek copper anode

Figure 5 Gold distribution in INCO, HBM, and Noranda copper anodes

Figure 6 Gold concentration distribution in Cu anode cross section

LIST OF PLATES

Plate 1 Copper oxide inclusions in copper anode

LIST OF APPENDICES

A1 Raw ion probe data

A2 Selected representative in-depth Au & Se concentration profiles

12.1.0 INTRODUCTION

Gold is recovered as a by-product from many sulphide ores. In the processing of complex sulphide ores, every effort is made to float the gold minerals along with the copper minerals into the copper concentrate. This is because the copper smelter charges for the gold are the lowest. If a copper concentrate is not produced, gold is promoted into the lead concentrate. From the smelting of the lead ores a Cu-As speiss is produced which contains the gold. This is then sent to a copper smelter for further treatment. Gold mines not capable of producing a high grade gold concentrate that could be refined directly, produce a sulphide concentrate of some description that can be sold to a copper or lead smelter. Silica containing gold is used as a flux in copper smelters, resulting in the recovery of gold.

The blister copper is cast into copper anodes, which are used for the electrolytic refining of copper. The form in which gold is present in the copper anode has been debated for a long time. Gold in the anode is not visible even at high magnifications (5,000x or 10,000x) under the scanning electron microscope (Chen per. com., 1989).

The objectives of the present study were: (i) to detect and quantify the gold concentration in the metallic copper phase; and (ii) to determine the homogeneity of the gold concentration in the copper anodes. Anodes from the four Canadian copper refineries: Kidd Creek, HBM, INCO and CCR (Noranda) were analyzed. The study was financed by Kidd Creek, CANMET through a DSS unsolicited proposal (UP-W6-015), and Surface Science Western.

12.2.0 METHODOLOGY

12.2.1 Sample procurement and preparation

Kidd Creek provided an oriented sample from the 'ear' of a copper anode cast in March 1988. In this particular sample it was attempted to determine changes in the gold concentration from the outside to the core of the anode. Two pieces were sawn from the Kidd Creek anode and polished. One piece was used to determine the average gold concentration in the core and periphery of the anode, while the second piece was used to determine the variation in gold concentration along a cross section from the bottom side (base) to the upper side (top) of the anode. Unoriented sawn pieces of copper anodes from all four Canadian refineries were provided by CANMET in one polished mount.

12.2.2 Analytical

Ion probe microanalysis because of its sensitivity (150 counts/ppm Au), and its low minimum detection limit for gold in copper (< 100 ppb) was used for the detection and quantification of gold. The spot size used was from 40 to 60 µm in diameter depending on the primary current. The primary beam was rastered 150x150 µm on ion implanted samples. The analysis area ranged from 10 to 60 µm, as determined by an aperture in the secondary ion column (Fig. 1). The analysis area was selected based on the grain size of the metallic copper and the sensitivity required. Inclusions in the copper anodes are confined along grain boundaries (Plate 1). Interfering molecular ions, like CsCuH, were eliminated by energy offset (200 V), with the energy window fully open. Operating conditions are summarized in Table 1.

12.2.2.1 Standardization

Calibration of the ion microprobe is achieved by internal or external standardization (Chryssoulis and Cabri, 1989). Internal standardization involves gold ion implantation of the anode samples to be analyzed. Thus, in the same microvolume analyzed, both standard and unknown gold quantities reside (Chryssoulis et al., 1986). Gold has only one isotope ^{197}Au. Therefore after monitoring the characteristic implant concentration distribution with depth (ion probe microanalysis is a destructive microanalytical technique analyzing successively deeper layers with time), the original gold is monitored (Fig. 2). Quantification is obtained from the integrated implant and original gold counts, and the implant dose and depth of analysis (Chryssoulis et al., 1986).

External standardization involves the preparation of calibration curves using a series of standards. The curves convert secondary ion count ratios ($^{197}Au^-/^{63}Cu^-$) to concentration of gold in parts per million weight (ppm). The standards can be either synthetic homogeneously doped with gold, or copper implanted with different doses of gold, or implanted copper samples with different original gold contents (Chryssoulis and Cabri, 1989).

12.3.0 RESULTS

In this study a series of copper standards homogeneously doped with gold and silver were prepared by CANMET and used in conjunction with NBS standards C1251 and C1253. The nominal gold concentrations are: 10., 15., 50., 74.4, 100., 760., and 1,550. ppm. With the exception of NBS standard C1251 (15 ppm) and standards 660 (760 ppm), and 662 (50 ppm), the remainder were determined to be homogeneously doped with gold by ion probe and where possible electron probe microanalysis. A high purity

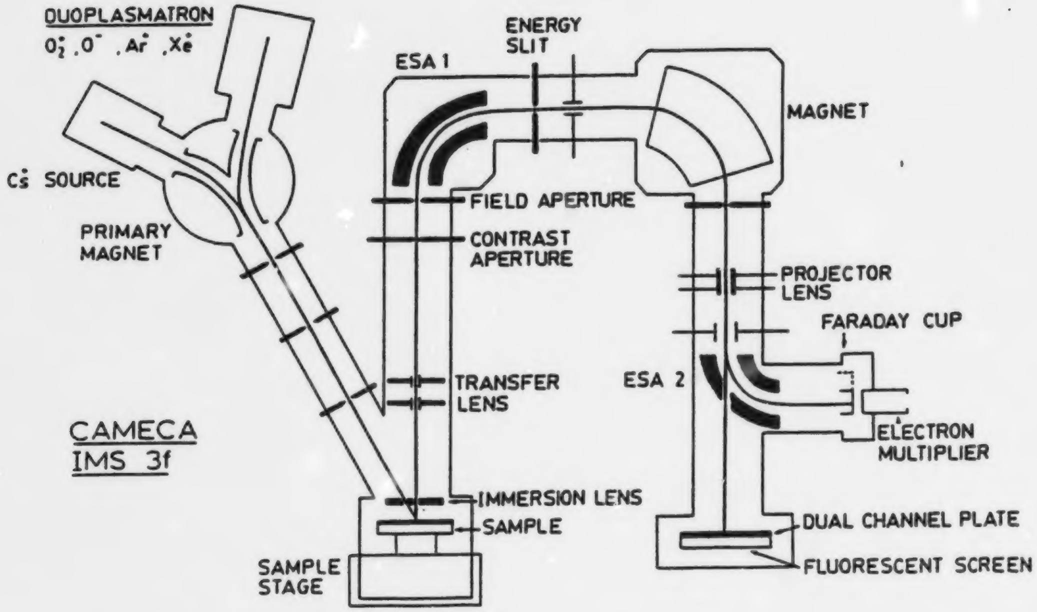
DUOPLASMATRON
O_2^+, O^-, Ar^+, Xe^+
ENERGY SLIT
ESA 1
MAGNET
Cs^+ SOURCE
FIELD APERTURE
PRIMARY MAGNET
CONTRAST APERTURE
PROJECTOR LENS
FARADAY CUP
ESA 2
TRANSFER LENS
ELECTRON MULTIPLIER
CAMECA IMS 3f
IMMERSION LENS
SAMPLE
DUAL CHANNEL PLATE
SAMPLE STAGE
FLUORESCENT SCREEN

FIGURE 1. Schematic diagram of IMS-3f ion microprobe.

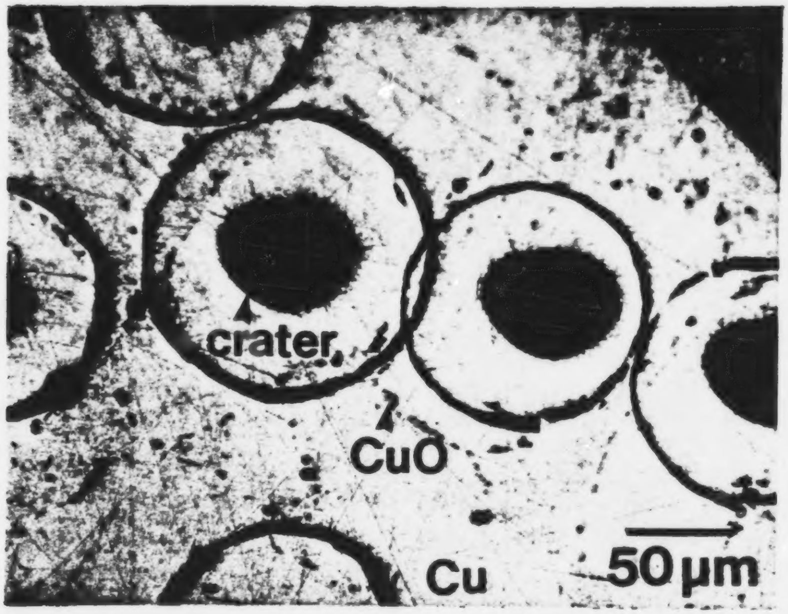
crater
CuO
Cu
50 µm

PLATE 1. Copper oxide inclusions in copper anode.

TABLE 1 Operating Conditions

Beam	Cs^+
Primary current	100 - 300 nÅ
Isotopes monitored	$^{197}\mathrm{Au}^-$, $^{63}\mathrm{Cu}^-$, $^{80}\mathrm{Se}^-$
Rastered area	150 x 150 µm
Analysis area	10 - 60 µm
Analysis time	7 - 10 min.
Depth of analysis	1 - 2 µm
External standardization	NBS, CANMET standards
Internal standardization	ion implantation
Interfering moleculars	200 V offset, 125 eV window

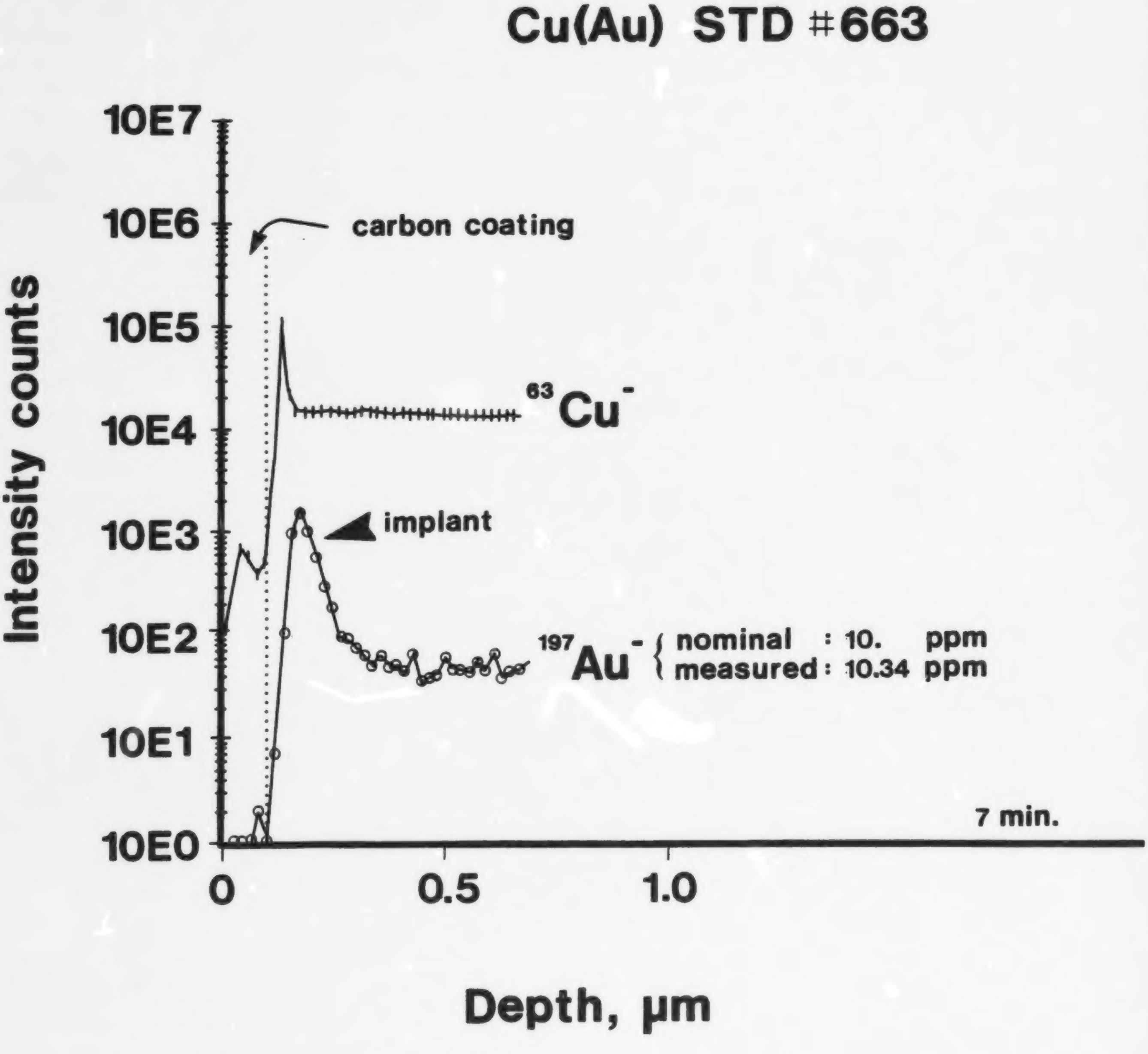

FIGURE 2. Depth profile of Au and Cu in copper standard #663. The spike on the ^{63}Cu profile is believed to have resulted from the lowering of the work function of Cu by the carbon coating (Storms et al. 1977).

Asarco copper cathode was used as a blank. The gold content of the Asarco cathode as determined by external standardization is less than 100 ppb. The calibration curve is given in Figure 3. Counting time for Au was 10 s compared to 0.1 s for Cu, thus the 100x multiplying factor. The precision as determined by the Thompson and Howarth method (1978) is 15%.

Internal standardization was used to determine independently the nominal gold concentration of the standards. Thus, all standards were implanted with $4x10^{13}$ Au atoms/cm^2. Results are given in Table 2. The gold concentration in the Asarco cathode is 32. ± 5. ppb.

The gold-poor Kidd Creek anode contains on average 7.9 ppm Au with a confidence interval of 0.7 ppm at the 95% significance level. The gold-rich anode contains 22.1 ± 2.5 ppm gold. This figure is probably less exact because of the oriented samples used. Invariably, the exterior of the anode was depleted in gold compared to the core. The differences as determined in two polished sections were statistically significant (Fig. 4). The average gold content in the cross section analyzed is slightly higher 29.2 ± 2.4 ppm.

The INCO anode contains the least gold of all four anodes analyzed. The average Au concentration as determined by ion probe microanalysis is 5.7 ± 0.45 ppm and compares closely with bulk assay data (Table 3).

The HBM anode has an average 29.8 ± 2.5 ppm gold with a moderate dispersion. The CCR (Noranda) anode is the most enriched in gold with an average concentration of 52.0 ± 5.3 ppm Au, and the greatest dispersion of data.

12.4.0 DISCUSSION

The average gold concentration as determined from approximately 50 ion microprobe analyses of the metallic copper phase per anode compares closely with published data on their bulk gold content (Table 3). This confirms the observation that visible gold, if present, is insignificant. In-depth concentration profiles have indicated the absence of gold microinclusions down to 300 Å in diameter. In the case of copper, the limiting factor in determining the size of sub-microinclusions with the ion probe is the roughness of the crater and not the sputtering rate, which is 17 $Ås^{-1}$ with a 200 nÅ beam.

Most probably gold is in solid solution in the metallic copper phase. The measure of scatter of gold spot assays around the mean was observed to increase with the average

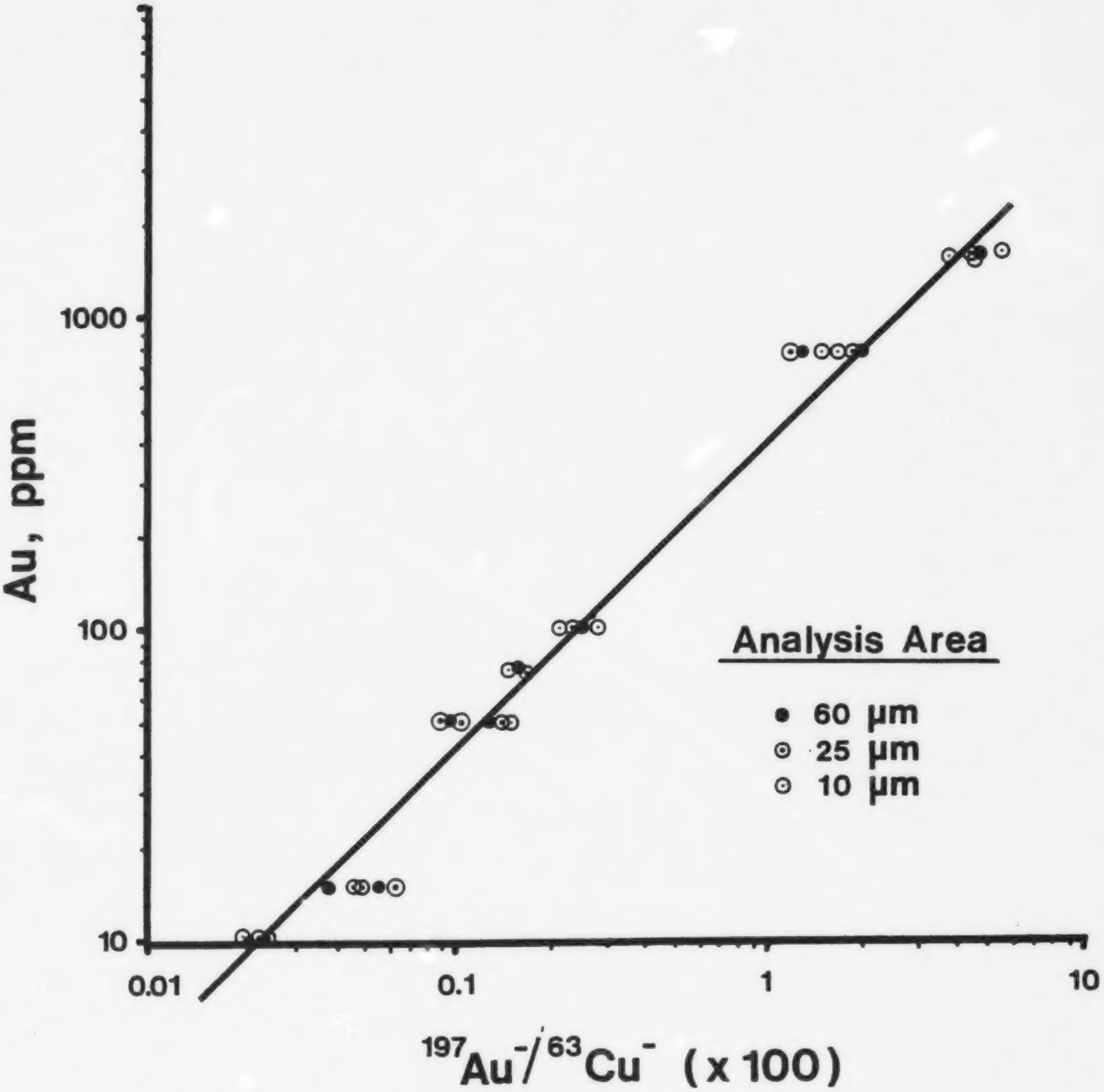

FIGURE 3. Calibration curve.

TABLE 2 Ion probe microanalysis of implanted external standards

Standard	Au, ppm nominal	Au, ppm SIMS
#659	1550.	1718. ; 1370.
#660[a]	760.	491. ; 601.
#661	100.	113. ; 99.
#662[a]	50.	34.6 ; 23.6 ; 23.5
#663	10.	10.3 ; 9.5
C1251[a]	15.0 ± 0.3	17.4 ; 22.7
C1253	74.4 ± 0.5	75.3 ; 73.2
Asarco	?	0.029 ; 0.034

a: inhomogeneous gold distribution; see calibration curve in Fig. 3.

The SIMS data quoted are from individual in-depth concentration profiles as the one shown in Fig. 2.

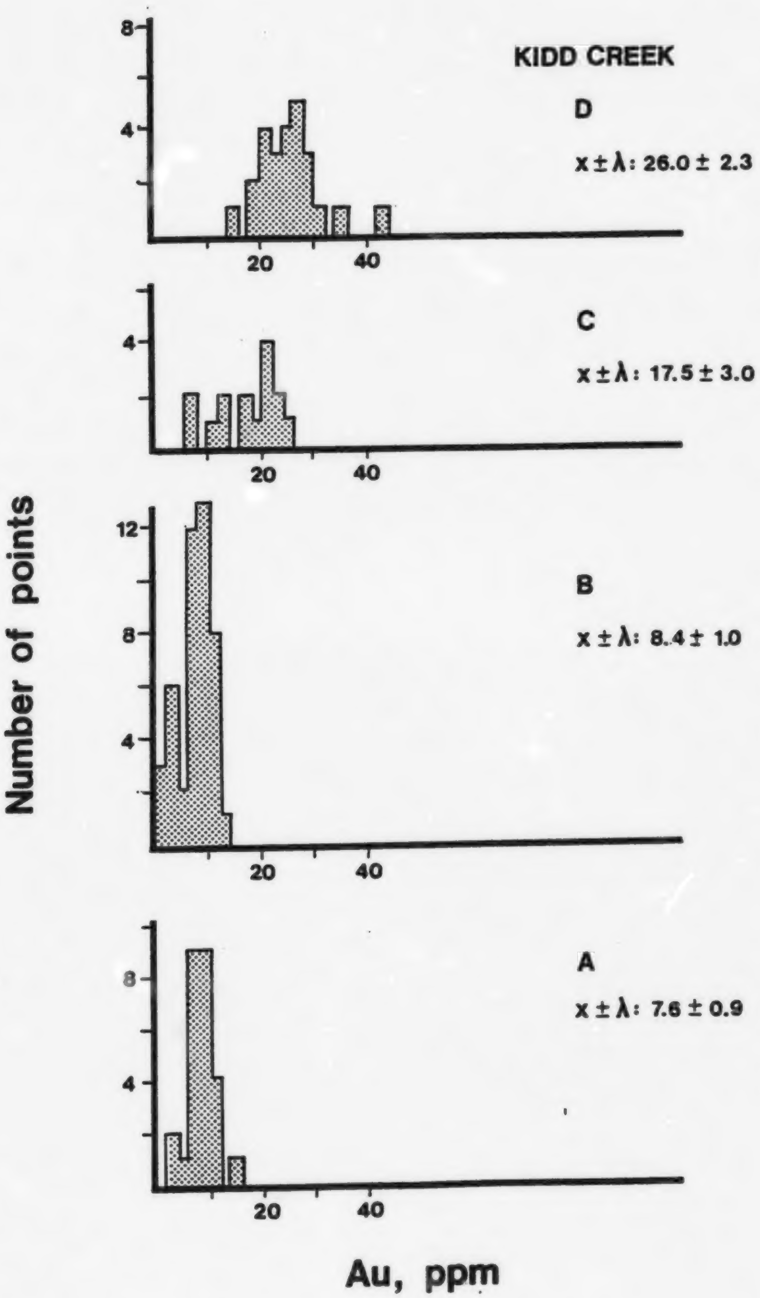

FIGURE 4. Gold distribution in Kidd Creek copper anode. Samples A, B not oriented, sample C periphery of anode and sample D core of the sample.

TABLE 3 **Gold concentration in Canadian copper anodes**

Smelter	Au, ppm	
	Bulk Assay	SIMS
Kidd Creek A	7.4	7.9
B	25.0	22.1
INCO	8.8	5.7
HBM	34.7	29.8
Noranda	65.8	52.0

content (Fig. 5). Thus, in the INCO anode with 5.7 ppm Au, the variance is 2.7 ppm, while in the CCR anode with a 52.7 ppm Au content the variance is 283 ppm or 500 % of the mean.

In the Kidd Creek anode statistically, the peripheral portion of the anode is depleted in gold compared to the core of the anode. The gold variation along the cross section of the anode (Fig. 6) is significant, with marginally more gold at the base (bottom side) of the anode, than at the top side. The copper to solidify last has the least gold, 2/3 up from the base. In the central portion of the cross section (corresponding to the core) the gold concentration is more homogeneous and on average slightly higher than on either side (peripheral portions). This has important implications in balancing the gold in the copper refinery since 30% of the anode (the core) is not dissolved and returns to the smelter.

12.5.0 CONCLUSIONS

Gold in the copper anodes is invisible, most probably in solid solution within the metallic copper. Gold dissolved in the copper accounts for the bulk gold assay. The gold concentration distribution in each case can be ascribed to one population. The variance of the population increases with the average gold content. The cooling history of the anode seems to have an effect on the gold concentration in the copper. In Hazelett cast anodes first-crystallized peripheral portions have higher amounts of gold, which eventually get lower. The core of the anode has a more homogeneous gold concentration distribution than the rim and the average gold content compared to the that of the periphery is higher.

The Kidd Creek copper anodes with 7.9 ± 0.7 and 22.1 ± 2.5 ppm gold are more enriched than the INCO anode with 5.7 ± 0.45 ppm gold, while they are poorer in gold compared to the HBM (29.8 ± 2.5 ppm) and CCR (52.0 ± 5.3 ppm) anodes.

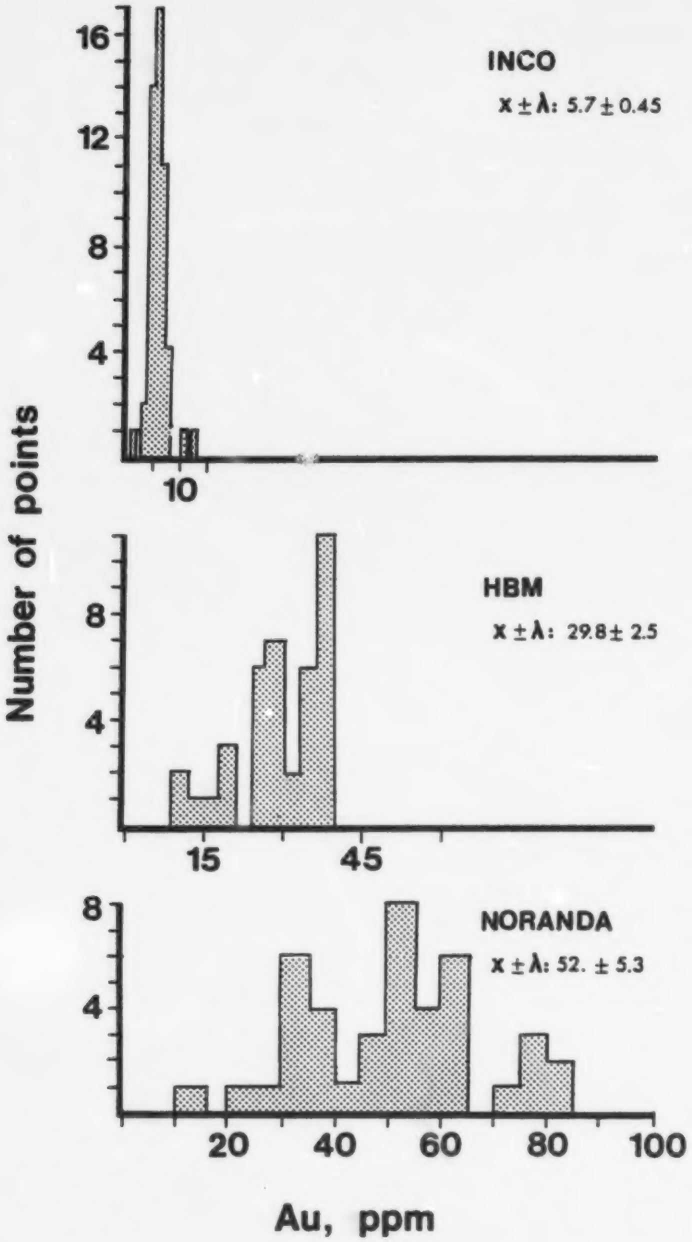

FIGURE 5. Gold distribution in INCO, HBM, Noranda copper anodes.

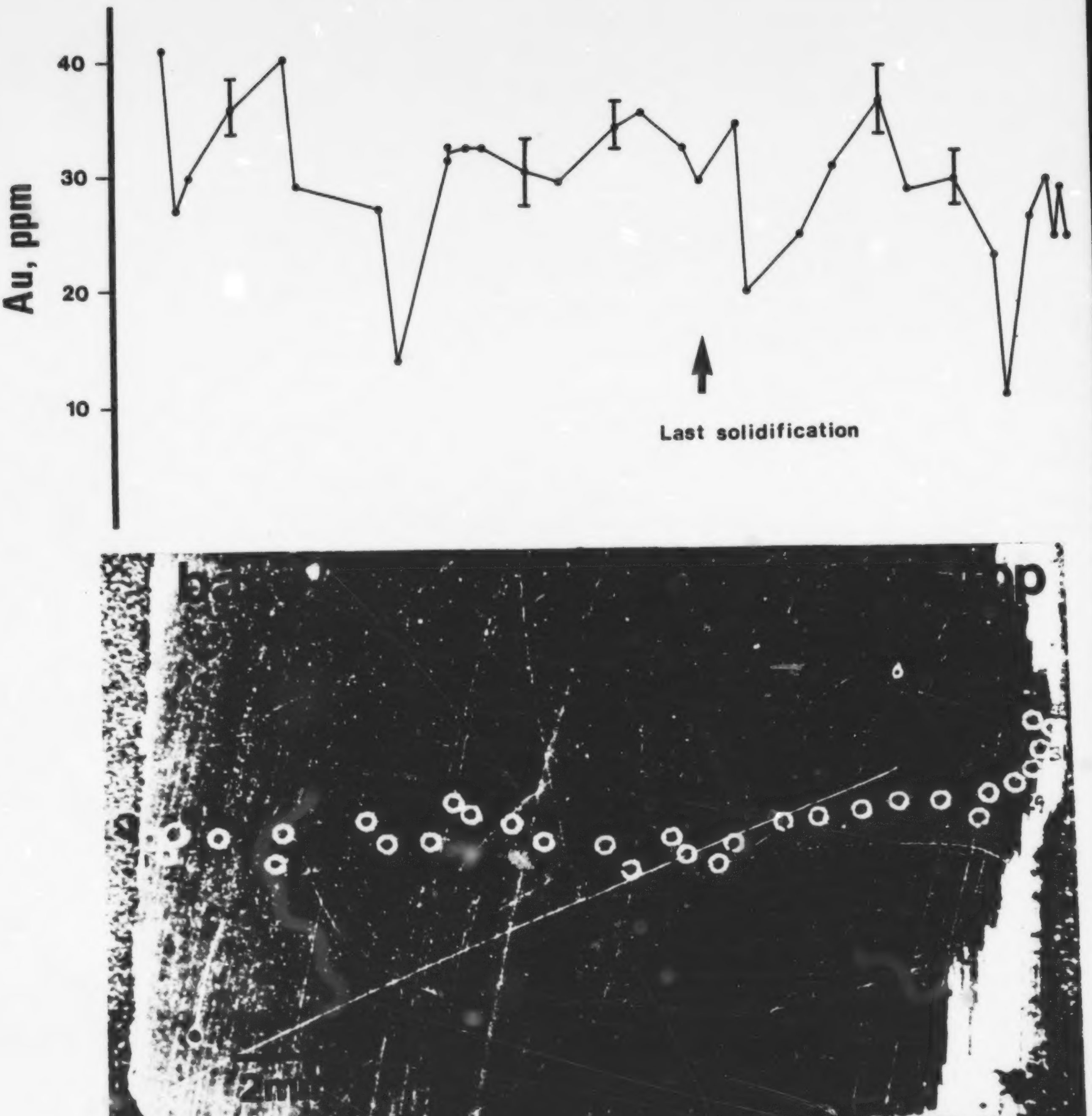

FIGURE 6. Gold concentration distribution in copper anode cross section.

APPENDIX A1

RAW ION PROBE DATA

TABLE A1 KIDD CREEK

A. Non-oriented sample

spot #	Au, ppm	spot #	Au, ppm
1	8.0	14	2.2
2	9.2	15	9.2
3	8.0	16	9.5
4	6.4	17	7.0
5	10.2	18	9.0
6	10.5	19	10.0
7	8.4	20	11.3
8	9.5	21	11.2
9	1.8	22	10.5
10	1.7	23	7.0
11	1.7	24	3.1
12	10.0	25	13.2
13	11.5	26	3.4

N = 26

x ± = 7.6 ± 0.9 ppm

B. Non-oriented sample

spot #	Au, ppm	spot #	Au, ppm	spot #	Au, ppm
27	2.7	42	8.6	57	9.0
28	2.8	43	8.6	58	8.2
29	8.8	44	4.6	59	9.5
30	11.0	45	5.9	60	6.6
31	7.4	46	7.7	61	6.6
32	11.0	47	7.6	62	9.8
33	9.3	48	7.4	63	9.2
34	2.8	49	6.0	64	11.0
35	8.0	50	6.4	65	10.5
36	7.0	51	7.2	66	2.2
37	7.2	52	8.4	66b	3.0
38	7.0	53	9.4	67	7.4
39	7.4	54	10.0	68	7.2
40	8.8	55	15.0	69	12.0
41	8.0	56	10.5	70	10.0

N = 44

x ± = 8.4 ± 1.0 ppm

b: beside

TABLE A1 (cont'd) **KIDD CREEK**

C. Periphery of anode

spot #	Au, ppm	spot #	Au, ppm
71	25.0	79	20.0
72	6.4	80	19.5
73	12.6	81	24.0
74	16.4	82	18.0
75	22.0	83	22.0
76	22.0	84	8.0
77	10.5	85	13.2
78	23.0		

N = 15

x ± = 17.5 ± 3.0 ppm

D. Core of anode

spot #	Au, ppm	spot #	Au, ppm
86	24.	99	23.
87	28.	100	25.
88	27.	101	44.
89	19.	102	27.
90	28.	103	22.
91	22.	104	21.
92	3.	105	26.
93	18.	106	25.
94	31.	107	28.
95	26.	108	36.
96	29.	109	30.
97	22.	110	14.5
98	24.		

N = 25

x ± = 26.0 ± 2.3 ppm

TABLE A2 Cross section of Kidd Creek anode

spot #	Au, ppm	
1	41.	Base
2	27.	
3	30.	
4	36. ± 2.4	
5	40.	
6	29.	
7	27.	
8	14.	
9	31.	
9 dupl	32.	
10	32.	
11	32.	
12	30. ± 3.0	
13	29.	
14	34. ± 1.9	
15	35.	
16	32.	
17	31.	
18	34.	
19	19.	
20	24.	
21	30.	
22	36. ± 3.2	
23	28.	
24	29. ± 2.4	
27	22.	
28	10.	
29	26.	
30	29.	
31	24.	
32	28.	
33	24.	Top (gravity up)

TABLE A3 **CCR (NORANDA)**

spot #	Au, ppm	spot #	Au, ppm
1	37	21	52
2	40	22	52
3	33	23	54
4	35	24	64
5	33	25	52
6	36	26	52
7	40	27	80
8	53	28	78
9	12	29	52
10	46	30	80
11	50	31	50
12	44	32	60
12d	33	33	56
13	65	34	38
14	65	35	56
15	32	36	84
16	72	37	62
17	63	38	58
18	54	39	82
19	24	40	62
20	29		

N = 40

x ± = 52.0 ± 5.3 ppm

HBM

spot #	Au, ppm	spot #	Au, ppm	spot #	Au, ppm
1	37	15	29	28	10
2	38	16	26	29	17
3	34	17	27	30	21
4	10	18	31	31	14
5	36	19	27	32	37.5
6	30	20	26	33	37
7	25	21	28	34	37
8	29	22	30	35	38
9	18.5	23	37	36	38
10	34	24	36	37	38
11	20	25	28	38	38
12	36	26	31	39	37
13	33	27	35		
14	30				

N = 39

x ± = 29.8 ± 2.5 ppm

d: duplicate

TABLE A3 (cont'd) **INCO**

spot #	Au, ppm	spot #	Au, ppm	spot #	Au, ppm
1	6.6	19	4.8	36	7.4
2	5.2	20	5.0	37	6.0
3	6.6	21	5.0	38	5.6
4	5.6	22	4.8	39	6.1
5	6.3	23	5.4	40	4.1
6	5.6	24	3.8	41	3.7
7	5.7	25	6.0	42	12.4
8	5.3	26	4.6	43	4.2
9	7.1	27	5.6	44	5.0
10	6.4	28	4.2	45	5.2
12	6.2	29	4.7	46	4.4
13	6.6	30	4.7	47	11.0
14	6.7	31	2.0	48	6.6
15	6.2	32	7.4	49	5.7
16	5.4	33	5.6	50	5.6
17	6.7	34	5.6	51	7.4
18	5.2	35	4.2		

N = 50

x ± = 5.7 ± 0.45 ppm

APPENDIX A2

SELECTED REPRESENTATIVE IN-DEPTH Au AND Se CONCENTRATION PROFILES

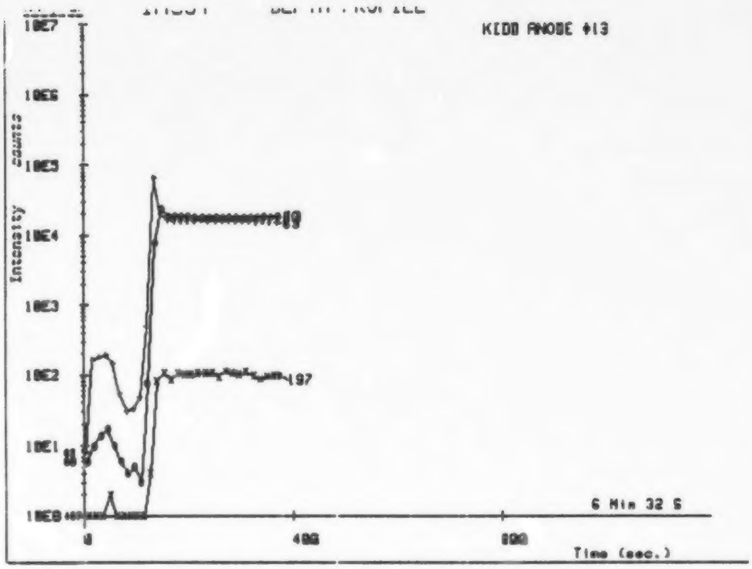

```
SAMPLE:KIDD ANODE #13
DATE:23/3/88
PRIMARY IONS :       CS           +
SECONDARY IONS :                  -
   DEAD TIME: 500.00E-10 sec.

PRIMARY CURRENT :     219 NANO AMP
HIGH VOLTAGE :       10.4 KILOVOLTS
RASTERING :             250 MICRONS
TRANSFER OPTICS :       150 MICRONS
FIELD APERTURE :    1  2  3
CONTRAST APERTURE :  4  3  2  :

Manual

 MASS NUMBER :   63.00   COLNT TIME :      .10   OFFSET VOLTAGE :    0.00
  M.F.P.: 29167   1

 TIME(SEC) COUNT   TIME(SEC) COUN"   TIME(SEC) COUNT   TIME(SEC) COUNT
       4       0         16    166         29    101         42    193
      35     144         68     55         81     30         94     33
     107      40        120    489        134  63663        147  20103
     160   16325        173  15000        186  15494        199  15787
     212   15770        225  16105        238  15964        252  15516
     265   15780        278  15707        291  15550        304  15465
     317   15673        330  14990        343  15310        356  15290
     369   15805        383  14640          0      0          0      0
 MASS NUMBER :   88.00   COLNT TIME :     1.00   OFFSET VOLTAGE :    0.00
  M.F.P.: 32990   0

 TIME(SEC) COUNT   TIME(SEC) COUN"   TIME(SEC) COUNT   TIME(SEC) COUNT
       7       6         19     10         32     14         45     17
      58      10         71      6         84      4         97      5
     110       3        123     75        137   7773        150  23299
     163   18640        176  18405        189  18015        202  18037
     215   17618        228  17471        241  17522        254  17743
     267   17615        281  17469        294  17679        307  17620
     320   17803        333  17533        346  17970        359  17929
     372   18194        385  18053          0      0          0      0
 MASS NUMBER :  197.00   COLNT TIME :     1.00   OFFSET VOLTAGE :    0.00
  M.F.P.: 52422   1

 TIME(SEC) COUNT   TIME(SEC) COUN"   TIME(SEC) COUNT   TIME(SEC) COUNT
      11       0         23      0         36      0         50      2
      63       0         76      1         89      1        102      1
     115       0        128      4        141     81        154    107
     167      85        181    104        194    101        207    108
     220     104        233    107        246    104        259     94
     272     112        285    104        298    100        311    109
     325      96        338     87        351     95        364     96
     377      97        391     85          0      0          0      0

.....TOTAL COUNTS IN PROFILE.....
  63               367380
  88               352546  >6.36E-3
 197                 1977

PROFILE TIME       392.000             SEC.
NUMBER CYCLES      30.000

TOTAL COUNTS CORRECTED FOR DUTY CYCLE                         29,

  MASS           TOTAL COUNT
   63           43939311
   88            4216422
  197              23645
```

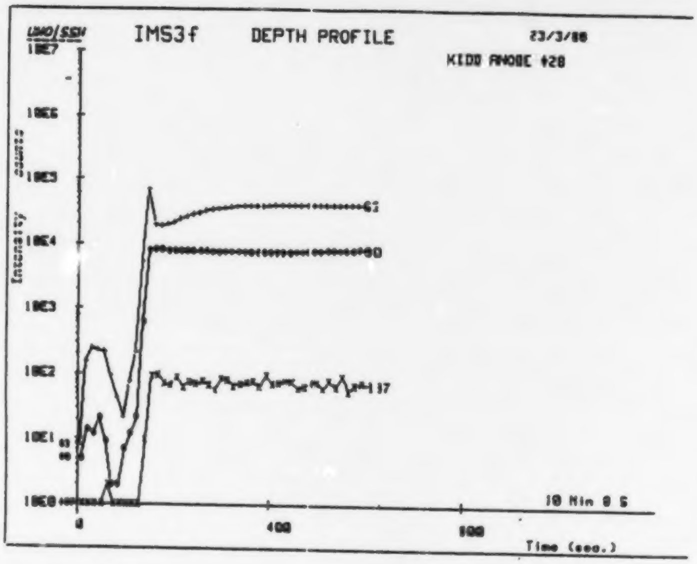

```
SAMPLE:KIDD ANODE #28
DATE:23/3/88
PRIMARY IONS :        CS          +
SECONDARY IONS :                  -
   DEAD TIME: 300.00E-10 sec.

PRIMARY CURRENT :      210 NANO AMP
HIGH VOLTAGE :       10.4 KILOVOLTS
RASTERING :             250 MICRONS
TRANSFER OPTICS :       150 MICRONS
FIELD APERTURE :    1  2  3
CONTRAST APERTURE :  4  3  2  :
Manual

 MASS NUMBER :   63.00   COUNT TIME :      .10   OFFSET VOLTAGE :    0.00
  M.F.P.: 29167    1

 TIME(SEC) COUNT   TIME(SEC) COUN"   TIME(SEC) COUNT   TIME(SEC) COUNT
      4        0        16     15:        29     237        42     224
     55      209        68     93         81      42        94      22
    108       77       121     21:       134    5170       147   67900
    160    19066       173   1004:       187   39766       200   21321
    213    23031       227   2591(       240   28211       253   29993
    266    31934       280   3377(       293   34630       306   35070
    319    37055       333   3771:       346   37935       359   38197
    373    38600       386   3832?       399   39026       412   39554
    426    39561       439   3954:       452   39406       465   39599
    479    39615       492   3968(       505   39664       519   39534
    532    39944       545   3994.       558   39700       572   39712
    585    39606       598   4010:         0       0         0       0
 MASS NUMBER :   80.00   COUNT TIME :     :.00   OFFSET VOLTAGE :    0.00
  M.F.P.: 32990    0

 TIME(SEC) COUNT   TIME(SEC) COUN"   TIME(SEC) COUN.   TIME(SEC) COUNT
      7        3        19     1.        32      12        45      21
     58        9        71     :         84       2        97       7
    110       12       123     2:       137      63       150    7974
    163     8136       176     818:      190    7891       203    7959
    216     7808       230     777"      243    7753       256    7764
    269     7723       283     759(      296    7630       309    7691
    322     7697       336     760.      349    7605       362    7559
    376     7533       389     741:      402    7410       415    7619
    429     7620       442     750.      455    7659       468    7659
    482     7832       495     783(      508    7976       521    8045
    535     8052       548     802:      561    8050       575    8241
    588     8401       601     826:        0       0         0       0
 MASS NUMBER :  197.00   COUNT TIME :     :.00   OFFSET VOLTAGE :    0.00
  M.F.P.: 52422    1

 TIME(SEC) COUNT   TIME(SEC) COUN"   TIME(SEC) COUNT   TIME(SEC) COUNT
     11        0        23     0         36       0        50       0
     63        2        76     0         89       1       102       1
    115        0       128     0        141      10       155      93
    168       97       181     7:       194      60       208      69
    221       64       234     7:       248      71       261      78
    274       70       287     50       301      84       314      83
    327       67       340     73       354      75       367      78
    380       65       394     9:       407      71       420      74
    433       80       447     7:       460      62       473      67
    486       75       500     76       513      62       526      81
    540       65       553     98       566      56       579      69
    593       74       607     70         0       0         0       0


.....TOTAL COUNTS IN PROFILE.....
   63              1239873
   80               274312
  197                 2625

PROFILE TIME          600.000             SEC.
NUMBER CYCLES          46.000

TOTAL COUNTS CORRECTED FOR DUTY CYCLE

  MASS            TOTAL COUNT
   63            152410620
   80              3310593
  197                31757
```

→ 2.17E-3

10.

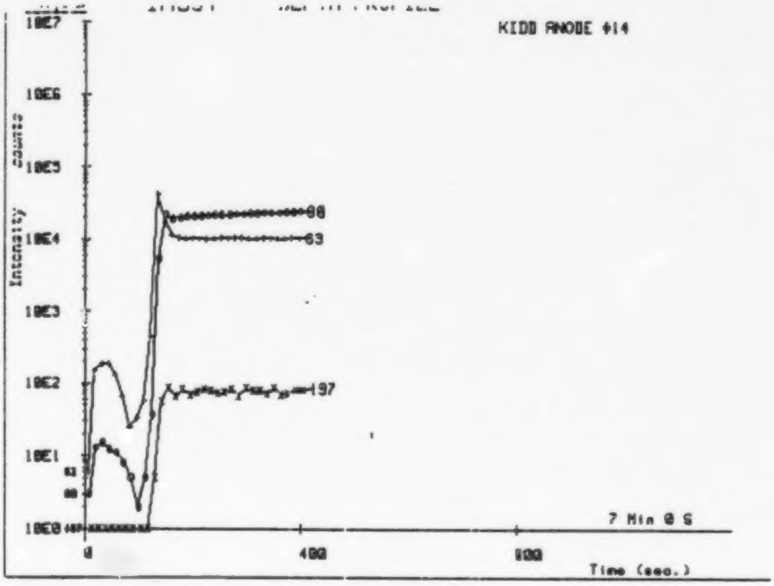

```
    SAMPLE:KIDD ANODE #14
    DATE:23/3/80
    PRIMARY IONS :        CS          +
    SECONDARY IONS :                  -
       DEAD TIME: 500.00E-10 sec.

    PRIMARY CURRENT :      215 NANO AMP
    HIGH VOLTAGE :      10.4 KILOVOLTS
    RASTERING :              250 MICRONS
    TRANSFER OPTICS :        150 MICRONS
    FIELD APERTURE :    1  2  3
    CONTRAST APERTURE :  4  1  2  :

Manual

  MASS NUMBER :   63.00   COUNT TIME :      .10   OFFSET VOLTAGE :     0.00
   M.F.P.: 29167   1

  TIME(SEC) COUNT   TIME(SEC) COUNT   TIME(SEC) COUNT   TIME(SEC) COUNT
       5        6        17     148        30     104        43     107
      56      120        69      66        82      25        95      33
     108       57       121     450       134   41204       148   17143
     161    11407       174   10460       187   10037       200   10147
     213    10164       226   10026       239   10047       253   10410
     266    10140       279   10337       292   10270       305   10069
     318    10004       331   10363       345   10161       358   10037
     371    10072       384   10213       397   10161       411   10221

  MASS NUMBER :   80.00   COUNT TIME :     1.00   OFFSET VOLTAGE :     0.00
   M.F.P.: 32990   0

  TIME(SEC) COUNT   TIME(SEC) COUNT   TIME(SEC) COUNT   TIME(SEC) COUNT
       8        3        20      13        33      15        46      12
      59       11        72       0        85       5        98       2
     111        5       124      37       137    5329       150   21799
     164    19071       177   20016       190   20509       203   20403
     216    20704       229   21129       242   21432       255   21424
     269    21620       282   22103       295   22164       308   22404
     321    22600       334   23072       347   23043       361   23116
     374    23611       387   23615       400   23997       414   24169

  MASS NUMBER :  197.00   COUNT TIME :     1.00   OFFSET VOLTAGE :     0.00
   M.F.P.: 52422   1

  TIME(SEC) COUNT   TIME(SEC) COUNT   TIME(SEC) COUNT   TIME(SEC) COUNT
      12        0        24       0        37       0        50       1
      63        0        77       0        90       0       103       0
     116        1       129       5       142      56       155      86
     168       66       181      80       195      69       208      74
     221       82       234      79       247      71       260      74
     273       82       286      67       300      85       313      70
     326       70       339      71       352      86       365      70
     378       73       391      80       405      80       419      83

.....TOTAL COUNTS IN PROFILE.....
  63              264533
  80              467521  >7.5E-3
 197                1670

PROFILE TIME          420.000              SEC.
NUMBER CYCLES          32.000

TOTAL COUNTS CORRECTED FOR DUTY CYCLE

  MASS          TOTAL COUNT
   63          31779176
   80           5616476
  197             20150
```

34,

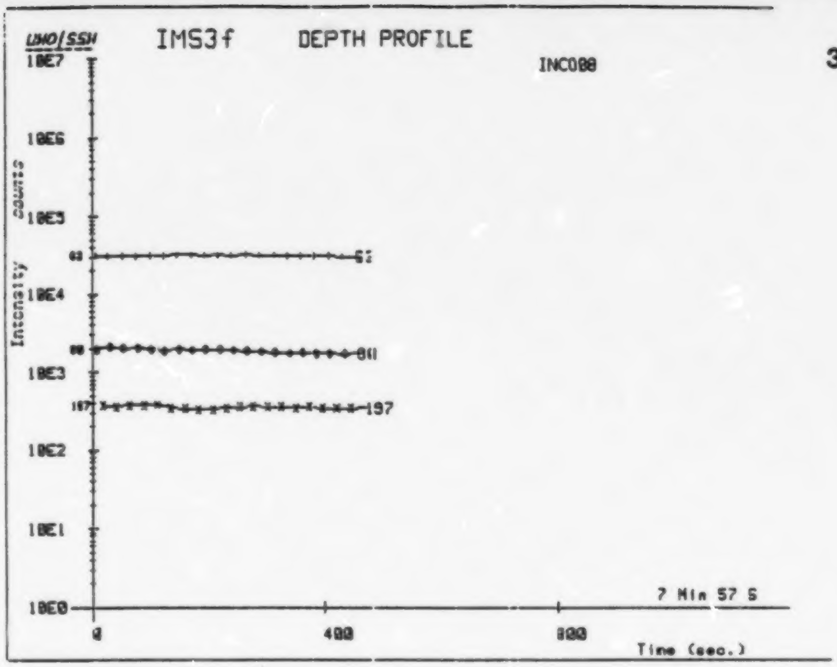

```
    SAMPLE:INC008
    DATE:
    PRIMARY IONS :      CESIUM      +
    SECONDARY IONS :                -
       DEAD TIME: 500.00E-10 sec.

    PRIMARY CURRENT :     101 NANO AMP
    HIGH VOLTAGE :      10.4 KILOVOLTS
    RASTERING :               50 MICRONS
    TRANSFER OPTICS :         25 MICRONS
    FIELD APERTURE :    1  2  3
    CONTRAST APERTURE :  4  3  2  :

Manual

   MASS NUMBER :   63.00   COUNT TIME :      .10   OFFSET VOLTAGE :    0.00
    M.F.P.: 31003   7

   TIME(SEC) COUNT    TIME(SEC) COUNT    TIME(SEC) COUNT    TIME(SEC) COUNT
        5     31526        27     30909       51     30782       75     31310
       99     31347       122     31230      146     31739      170     31667
      194     31430       218     31742      241     31507      265     31971
      289     31506       313     31425      337     31341      361     30940
      384     31026       408     30820      432     30313      456     30204

   MASS NUMBER :   80.00   COUNT TIME :     1.00   OFFSET VOLTAGE :    0.00
    M.F.P.: 35141   0

   TIME(SEC) COUNT    TIME(SEC) COUNT    TIME(SEC) COUNT    TIME(SEC) COUNT
        7      1964        30      2119       54      2024       78      2061
      101      1975       125      1875      149      1977      173      1900
      197      1938       221      1939      244      1904      268      1861
      292      1820       316      1780      340      1752      363      1760
      387      1736       411      1732      435      1712      460      1714

   MASS NUMBER :  197.00   COUNT TIME :    10.00   OFFSET VOLTAGE :    0.00
    M.F.P.: 35920   0

   TIME(SEC) COUNT    TIME(SEC) COUNT    TIME(SEC) COUNT    TIME(SEC) COUNT
       17       371        40       360       64       376       88       370
      112       381       135       344      159       340      183       333
      207       330       231       346      255       353      278       363
      302       355       326       354      350       344      374       355
      397       341       421       342      445       343      471       344

.....TOTAL COUNTS IN PROFILE.....
   63                625005
   80                 37551
  197                  7053

PROFILE TIME          477.000              SEC.
NUMBER CYCLES          20.000

TOTAL COUNTS CORRECTED FOR DUTY CYCLE

  MASS            TOTAL COUNT
   63           136437990
   80              819735
  197               15357


FILE  INC008  IS OPENED
```

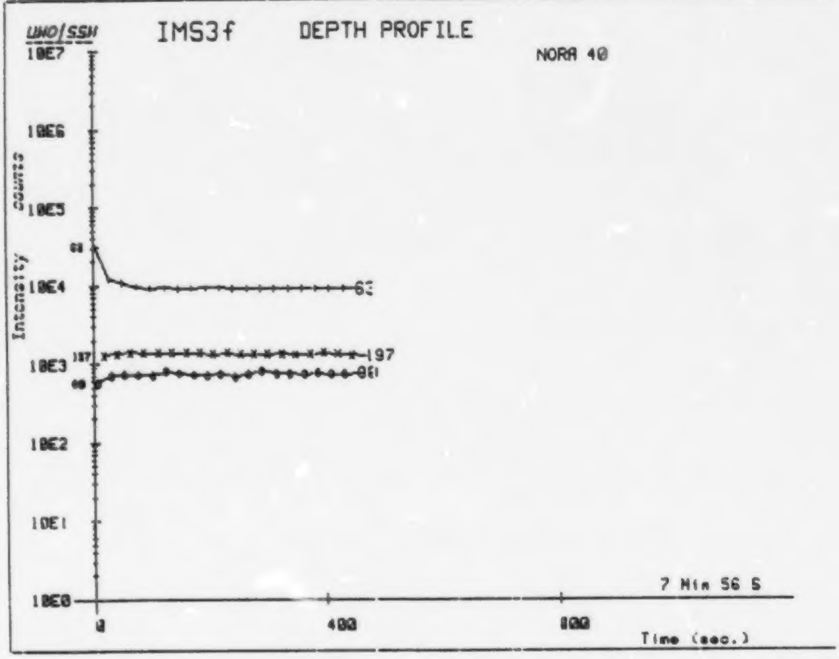

```
SAMPLE:NORA 40
DATE:
PRIMARY IONS :       CS           +
SECONDARY IONS :                  -
   DEAD TIME: 500.00E-10 sec.

PRIMARY CURRENT :     220 NANO AMP
HIGH VOLTAGE :      10.4 KILOVOLTS
RASTERING :              50 MICRONS
TRANSFER OPTICS :        25 MICRONS
FIELD APERTURE :   1  2  3
CONTRAST APERTURE :  4  3  2  1

M.F.P.

  MASS NUMBER :   63.00   COUNT TIME :     .10   OFFSET VOLTAGE :    0.00
   M.F.P.: 31001    5

  TIME(SEC) COUNT   TIME(SEC) COUNT | TIME(SEC) COUNT   TIME(SEC) COUNT
      4     31400       27    12262      50    10664       74     9674
     90      9237      122     9292     146     9214      169     9275
    193      9345      217     9325     241     9206      265     9116
    288      9154      312     9200     336     9161      360     9191
    384      9050      407     9134     431     9014      455     9090

  MASS NUMBER :   80.00   COUNT TIME :    1.00   OFFSET VOLTAGE :    0.00
   M.F.P.: 35132    3

  TIME(SEC) COUNT   TIME(SEC) COUNT   TIME(SEC) COUNT   TIME(SEC) COUNT
      7       573       30      707      53      724       77      710
    101       717      125      794     148      751      172      720
    196       710      220      737     244      603      267      729
    291       804      315      747     339      745      363      735
    386       757      410      731     434      726      458      762

  MASS NUMBER :  197.00   COUNT TIME :   10.00   OFFSET VOLTAGE :    0.00
   M.F.P.: 55927    5

  TIME(SEC) COUNT   TIME(SEC) COUNT | TIME(SEC) COUNT   TIME(SEC) COUNT
     16      1297       40     1353      63     1307       87     1381
    111      1376      135     1376     159     1370      182     1364
    206      1322      230     1364     254     1327      278     1317
    301      1322      325     1341     349     1299      373     1329
    397      1306      421     1316     444     1296      470     1263

.....TOTAL COUNTS IN PROFILE.....
  63              211092
  80               14570
 197               26794

PROFILE TIME        476.000            SEC.
NUMBER CYCLES        20.000

TOTAL COUNTS CORRECTED FOR DUTY CYCLE

  MASS           TOTAL COUNT
   63           45904577
   80             317395
  197              58360
```

0.144

29144

62

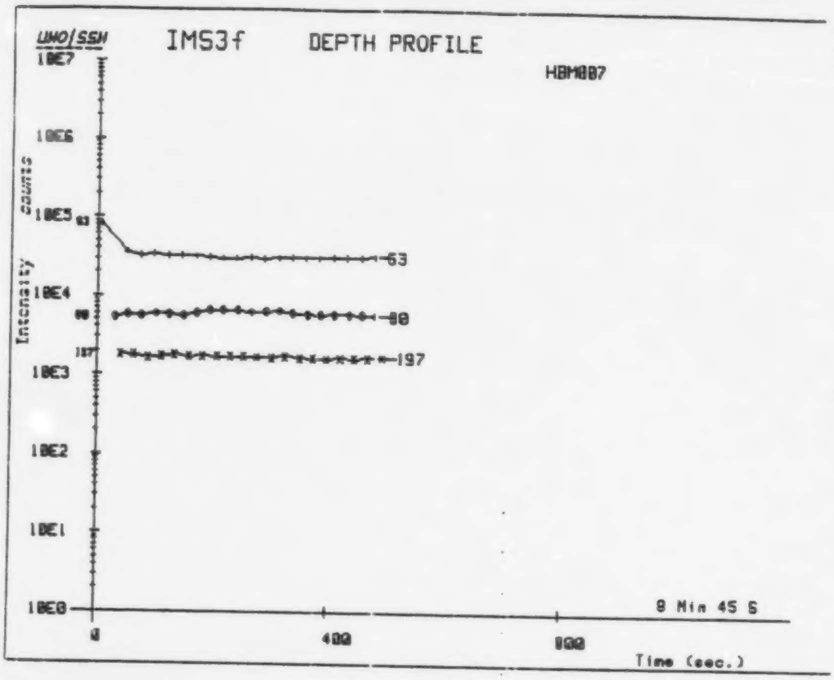

```
SAMPLE:HBM007
DATE:
PRIMARY IONS :       CESIUM      +
SECONDARY IONS :                 -
   DEAD TIME: 500.00E-10 sec.

PRIMARY CURRENT :     210 NANO AMP
HIGH VOLTAGE :      10.4 KILOVOLTS
RASTERING :             50 MICRONS
TRANSFER OPTICS :       25 MICRONS
FIELD APERTURE :   1  2  3
CONTRAST APERTURE :  4  3  2  :

M.F.P.

 MASS NUMBER :   63.00   COUNT TIME :      .10   OFFSET VOLTAGE :    0.00
  M.F.P.: 31001   4

 TIME(SEC) COUNT | TIME(SEC) COUNT   TIME(SEC) COUNT   TIME(SEC) COUNT
     5    82537  |    51     35922      75     32075      90     33682
   122    32256      146     32490     170     31016     194     30931
   217    30201      241     30100     265     31219     289     30065
   313    30406      337     30594     360     30471     384     30509
   408    31177      432     30843     456     30957     480     31704
   503    32037        0         0       0         0       0         0
 MASS NUMBER :   80.00   COUNT TIME :     1.00   OFFSET VOLTAGE :    0.00
  M.F.P.: 35130   5

 TIME(SEC) COUNT   TIME(SEC) COUNT   TIME(SEC) COUNT   TIME(SEC) COUNT
    31     5410       54      5750      77      5625     101      5952
   125     5869      149      5576     173      6093     196      6509
   220     6540      244      6564     268      6202     292      6334
   316     6404      339      6010     363      5905     387      5754
   411     5929      435      5940     459      5791     482      5710
   507     5643        0         0       0         0       0         0
 MASS NUMBER :  197.00   COUNT TIME :   10.00   OFFSET VOLTAGE :    0.00
  M.F.P.: 55934   2

 TIME(SEC) COUNT | TIME(SEC) COUNT   TIME(SEC) COUNT   TIME(SEC) COUNT
    40     1819  |    64      1770      88      1660     111      1712
   135     1790      159      1697     183      1739     207      1684
   230     1699      254      1690     278      1676     302      1654
   326     1736      350      1646     373      1610     397      1612
   421     1643      445      1633     469      1659     493      1601
   519     1693        0         0       0         0       0         0

.....TOTAL COUNTS IN PROFILE.....
  63              712000 -
  80              125606
 197               35517 -

PROFILE TIME        525.000         SEC.
NUMBER CYCLES        21.000

TOTAL COUNTS CORRECTED FOR DUTY CYCLE

 MASS          TOTAL COUNT
  63          162925231
  80            2074179
 197              81272
```

CONCLUSIONS

The present study has documented:

. the presence of invisible gold in sulphide and sulpharsenide minerals;

. that the principal carriers of invisible gold are: arsenopyrite and pyrite;

. that the gold is mostly concentrated in the arsenopyrite and to a lesser extent in pyrite;

. that the invisible gold concentration range in
arsenopyrite is < 0.2 (MDL) to 11,000 ppm
and in pyrite from <0.3 (MDL) to 108 ppm;

. the existence of an inverse relation between the grain size of arsenopyrite and its gold concentration;

. the presence of a positive correlation between gold and arsenic contents in pyrite;

. that the arsenian tetrahedrite-tennantite, fine-grained chalcopyrite, and bornite may contain invisible gold, but in lesser amounts;

. that the invisible gold is mostly refractory to direct cyanidation, accounting for the bulk of the non-recoverable gold in refractory carbon-free sulphide-bearing ores;

. that quantitative ion probe microanalysis provides unique information on the association and distribution of invisible gold, that is valuable to the mineral processor concerned with optimization of gold recovery;

. the presence of colloidal-size gold in sulphide oxidation products: iron-hydroxides and scorodite;

. that the gold in the copper anodes is invisible;

. and that the distribution of gold in the Hazelett cast anodes is inhomogeneous, with the core of the anode enriched relative to the rim.

REFERENCES

Aubert, G., Duong, P.K. and Geffroy, J. (1964) Sur la localisation de l'or dans le mineral du Chatelet (Creuse). Soc. Fr. Mineral. Cristallogr. Bulletin 87, p. 623-624.

Bakken, B.M., Hochella Jr, M.F., Marshall, A.F. and Turner, A.M. (1988) High resolution microscopy of gold in unoxidised ore from the Carlin Mine, Nevada. Economic Geology.

Boyle, R.W. (1979) The geochemistry of gold and its deposits. Geological Survey of Canada Bulletin 280.

Burg, G.H. (1935) Natur des in den Pyriten nicht sichtbar enthaltenen Goldes. Z. Prakt. Geol. v. 43, pt. 2, 17-26.

Cabri, L.J. (1987) The mineralogy of precious metals: new developments and metallurgical implications - Presidential Address. Canadian Metallurgist, v. 25, part 1, in press.

CANMET (1986) Mineralogical examination of drill core from the Lara property, Vancouver Island. Unpublished Report, 16 pp.

Chryssoulis, S.L. (1986) Trace element analysis by secondary ion mass spectrometry with particular reference to silver in the Brunswick Sphalerite. Canadian Metallurgical Quarterly, v. 25, p. 233-239.

Chryssoulis, S.L. (1986) Gold mineralogical balance in the cyanide leach residue from the Ketza River ore (Y.T.), RPC Report MDP/86/09, Research and productivity Council of New Brunswick.

Chryssoulis, S.L. (1988) Metallurgical testing of the Ketza River Massive Sulphide Ore. Surface Science Western Report SSW/PMS/88/10.

Chryssoulis, S.L. and Coleman, M. (1986) Gold mineralogical balance in samples from Lacana. RPC Report MDP/86/13, Research and Productivity Council of New Brunswick

Chryssoulis, S.L., Cabri, L.J. and Salter, R.S. (1987) Determination of invisible gold in refractory sulphide ores. In: Proc. International Symposium on Gold Metallurgy, Winnipeg, August 1987. Proc. Metall. Soc. of C.I.M.M Volume 1 (eds. S.S. Salter, D.M. Wyslouzil and G.W. McDonald).p. 235-244, Pergamon Press.

Chryssoulis, S.L., Cabri, L.J. and Lennard, W. (1989) Calibration of the ion microprobe for quantitative trace precious metal analyses of ore minerals. Accepted for publication in Economic Geology.

Coastech (1986) Various metallurgical test reports on the Lara ores.

Davies, J.A., and Howe L.M. (1980) Basic implantation processes. Site characterization and aggregation of implanted atoms in materials. Edited by A. Perez and R. Coussement.

Gasparrini, C. (1983) The mineralogy of gold and its significance in metal extraction. C.I.M. Bulletin, v. 76, p. 144-153.

Hackl, R.P. (1987) Preliminary evaluation of biotankleaching as a method to recover gold from Elmtree ore and concentrate. Report 6 pp.

Harris, D. (1986) Elmtree gold mineralogy, letter report, 3 pp.

Hawthorn, G. (1987/8) Various personal communications about the Congress deposit.

Haycock, M.H. (1937) The role of the microscope in the study of gold ores. C.I.M. Trans. 40, p. 405-414.

Healy, R.E. (1987) The mineral characteristics that affect metal recoveries from the Cu,Zn,Pb and Ag ores from Manitoba. Part 1: An investigation of the ore mineralogy of the Trout Lake deposit, with a view to predicting mineral liberation and metal recovery during ore dressing. Report; Canada-Manitoba Mineral Development Agreement, 1987.

Jackman, R. (1986) An investigation of the recovery of gold from samples submitted by CANAMAX Resources Inc., Lakefield Research Progress Report #1.

Jackman, R. (1987) An investigation of the recovery of gold from samples submitted by CANAMAX Resources Inc., Lakefield Research Progress Report #3.

Lakefield Research (1985) An investigation of the recovery of gold from Elmtree ore samples submitted by Lacana Exploration (1981) Inc. Progress Report #1.

Lakefield Research (1986) An investigation of the recovery of gold from Elmtree ore samples submitted by Lacana Exploration (1981) Inc. Progress Report #2.

Morrison, G.H. (1981) Quantifications of SIMS. Secondary ion mass spectrometry SIMS III. Editors: A. Benninghoven, J. Giber, J. Laszlo, M. Riedel, H.W. Werner, Springer-Verlag. Series in Chemical Physics # 14.

Mortimer, J.M. (1986) Elmtree gold project - Metallurgy. Review letter, 2 pp.

Palache, C., Berman, H. and Frondel, C. (1944) Dana's system of mineralogy. Volume 1, John Wiley and Sons.

Petruk, W. (1988) Recent progress in mineralogical investigations related to gold recovery. CANMET report MSL 88-145 (OP&J).

Storms, H.A., Brown, K.F., and Stein, J.D. (1977) Evaluation of a cesium positive ion source for secondary ion mass spectrometry: Anal. Chem. v. 49, B, 2023 - 2030.

Swash, P.M. (1988) A mineralogical investigation of refractory gold ores and their beneficiation, with special reference to arsenical ores. J.S. Afr. Inst. Min. Metall., Vol. 88, No. 5, pp 173-180.

Thompson, M. and Howarth, R.J. (1978) A new approach to the estimation of analytical precision. J. Geochem. Explor., 9: 23-30.

Tucker, R.J. (1987) Bioleaching- Elmtree, Review letter, 2 pp.

Wagner, F.E., Marion, P. and Reynard J.R. (1986) Mössbauer study of the chamical state of gold in gold ores. In Gold 100. Proc. Inter. Conf. on Gold. Vol. 2: Extr. Metall. of Gold, South African Institute of Mining and Metallurgy, pp 435 - 443.